

Panos Christakoglou[‡]

Lectures on Quantum Chromodynamics

Particle Physics II

February 6, 2024

^{*}P.Christakoglou@uu.nl - Utrecht University, Leonard S. Ornsteinlaboratorium Princetonplein 1, 3584CC Utrecht, The Netherlands

[‡]Panos.Christakoglou@nikhef.nl - Nikhef, Science Park 105, 1098XG Amsterdam, The Netherlands

Background material

The lectures are based on the following books:

- Griffiths** D. Griffiths, *Introduction to Elementary Particles*, Second Revised Edition, WILEY-VCH, (2008);
H&M F. Halzen and A.D. Martin, *Quarks and Leptons*, John Wiley & Sons, (1984).

You will need these books to supplement the lecture notes, and to successfully complete the exercises.

Some reference is also made to

- PP-I** W. Hulsbergen and M. Merk, *Lecture notes Particle Physics I*.

The following references were used in the preparation of these notes:

- A&H** I.J.R. Aitchison and A.J.G. Hey, *Gauge Theories in Particle Physics*, IOP Publishing Ltd, Volumes I and II, (2003);
DKS G. Dissertori, I. Knowles and M. Schmelling, *Quantum Chromodynamics*, Oxford University Press, (2003);
ESW R.K. Ellis, W.J. Stirling and B.R. Webber, *QCD and Collider Physics*, Cambridge University Press, (1996);
CTEQ CTEQ Collab. G. Sterman et al., *Handbook of Perturbative QCD*, Version 1.0 (2000), obtainable from <http://www.phys.psu.edu/~cteq>;
Soper D.E. Soper, *Basics of QCD Perturbation Theory*, hep-ph/9702203, (1997);
deWit B. de Wit and J. Smith, *Field Theory in Particle Physics*, Volume 1, North Holland, (1986);
Zee A. Zee, *Quantum Field Theory in a Nutshell*, Second Edition, Princeton University Press, (2010);
Ramond P. Ramond, *Group Theory*, Cambridge University Press, (2010);
Veltman M. Veltman, B. de Wit and G. 't Hooft, *Lie Groups in Physics*, Lecture notes, <http://www.staff.science.uu.nl/~h>
Schiff L.I. Schiff, *Quantum Mechanics*, Third Edition, McGraw-Hill, (1968);
Jackson J.D. Jackson, *Classical Electrodynamics*, Second Edition, John Wiley, (1975).

How is the final grade computed

The final grade of the Particle Physics 2 course is calculated as the average between the CP and the QCD parts. In order to pass the course the total grade needs to be larger than 5.5 e.g. if the average results into 5.49 your score will be downgraded to 5 and you will not pass, if it is 5.5 then it will be rounded up to 6 and you have succeeded.

For each individual part, you have the possibility to get maximum two extra bonus points by doing well with the homework assignments. The way to profit from the scheme is given below. However, it needs to be pointed out that you can take advantage of this bonus only if your grade for each individual exam (e.g. only the QCD exam for what concerns the QCD homework) is larger than 5.5.

If your QCD exam grade is larger than 5.5 then the grade of the QCD part (similarly for the CP part) is calculated as the maximum between the exam and the weighted average of the final exam and the weekly exercises. The relevant weight is 85 : 15 i.e. 85% of the grade comes from the final exam and 15% from the sum of the hand-in exercises. The formula based on which the grade of each individual part (i.e. here for QCD) is calculated is:

$$\text{grade} = \max \left(\left[0.85 \cdot (\text{exam}) + 0.15 \cdot \frac{1}{N} \sum_{i=1}^N (\text{homework})_i \right], [\text{exam}] \right)$$

where (exam) is the grade of the final exam, (homework)_i is the grade of each individual hand-in exercise set, and *N* is the total number of exercise sets you have to hand in. Please note that no matter if you handed in exercises one time or as many times as the number of lectures, the average of the grade related to the exercises will be computed over the total number of lectures (i.e. you should hand-in as many sets as the number of lectures to take advantage of the grading scheme).

If the grade of the QCD exam is lower than 5.5 then this reflects also the final QCD grade (similarly for the CP part).

If you fail the course then there is a retake exam which is announced well in advance to all students. You can participate in this retake exam even if you have succeeded in the initial attempt. However, this last grade of the retake exam will be considered in the final grade evaluation regardless of the score. The final QCD grade is calculated in an identical way as described before by replacing the grade of the exam with the grade of the retake.

After each lecture (with obviously the exception of the first one), you may hand-in the solution to the assigned homework exercises. The points are granted based on the correctness of the solution of each exercise. The value of each exercise is indicated clearly (i.e. the number under the square brackets). The final exercise sheet, may handed in before the final exam.

The exam is 'open book' so that you may consult the lecture notes and the books of Griffiths, Halzen & Martin and Aitchison & Hey, but not the worked-out exercises or any other material.

Some examples:

Example A: A student has a homework average of 9.5 in QCD. The same student scores 7.0 in the final exam. The final QCD grade is then the maximum between the grade of the exam (i.e. 7.0) and the weighted average between the exam and the homework i.e. $0.85 \cdot 7.0 + 0.15 \cdot 9.5 = 7.375 \rightarrow 7.4$. So in this case the final QCD grade will be 7.4.

Example B: A student has a homework average of 6.0 in QCD. The same student scores 8.7 in the final exam. The final QCD grade is then the maximum between the grade of the exam (i.e. 8.7) and the weighted average between the exam and the homework i.e. $0.85 \cdot 8.7 + 0.15 \cdot 6.0 = 8.295 \rightarrow 8.3$. So in this case the final QCD grade will be 8.7.

Example C: A student has a homework average of 9.5 in QCD. The same student scores 4.9 in the final exam. Note that the student in this case does not have the possibility to profit from his homework score, which would have raised the QCD grade $0.85 \cdot 4.9 + 0.15 \cdot 9.5 = 5.59 \rightarrow 5.6$. So in this case the final QCD grade will be the grade of the exam i.e. 4.9.

Contents

1	Introduction	1
1.1	The discovery of the electron	1
1.2	The atomic scale	3
1.3	The nucleus	4
1.4	The particles and forces of the Standard Model	4
1.4.1	Leptons of the Standard Model	5
1.4.2	Quarks of the Standard Model	6
1.4.3	The discovery of more particles	6
1.4.4	Interactions and mediators in the Standard Model	7
2	Symmetries and elements of group theory	15
2.1	Symmetries and conservation laws in physics	15
2.1.1	Discrete transformations	16
2.1.2	Continuous transformations	17
2.2	Introduction to groups	18
2.3	Lie groups	19
2.3.1	The $SO(3)$ group	20
2.3.2	The $SU(2)$ group	21
2.3.3	The $SU(3)$ group	22
2.4	Spin and angular momentum	23
2.4.1	Clebsch-Gordan coefficients	25
2.4.2	Isospin symmetry	27
2.5	The quark model	28
2.6	A new quantum number: colour	31
3	The Lagrangian formalism of Quantum Chromo Dynamics (QCD)	35
3.1	A small recap from QED	35
3.2	The free Dirac equation	36
3.2.1	Global gauge invariance	37

3.2.2	Local gauge invariance	37
3.2.3	The interaction term	39
3.3	The field kinetic term	40
3.4	Some comments	42
4	The Feynman calculus	45
4.1	Golden rule for decays and scattering	47
4.2	General Feynman rules	48
4.2.1	Feynman rules for QED and GWS	49
4.2.2	Feynman rules for QCD	49
4.2.3	A characteristic example: $e^- + \mu^- \rightarrow e^- + \mu^-$	52
5	Colour factors	55
5.1	Quark-Antiquark interactions	55
5.1.1	Colour factors for the octet configuration	56
5.1.2	Colour factors for the singlet configuration	58
5.2	Quark-Quark interactions	59
5.2.1	Colour factors for the sextet configuration	60
5.2.2	Colour factors for the triplet configuration	61
5.3	Colour interactions	62
6	Form factors	65
6.1	Evidence of colour	65
6.2	Elastic $e - p$ scattering	69
7	Deep inelastic scattering	75
7.1	Inelastic $e - p$ scattering	75
7.1.1	Kinematics of DIS	77
7.1.2	Bjorken scaling	78
7.2	The parton model	81
7.3	Probing the quark and gluon distributions in protons	84
8	Soft and Collinear Singularities	87
8.1	Can perturbative QCD predict anything?	87
8.1.1	The process $e^+e^- \rightarrow q\bar{q}g$	88
8.1.2	Singularities in the cross section	89
8.1.3	More kinematics	89
8.1.4	Phase space	90
8.1.5	Three-parton configurations	91
8.1.6	Origin of the singularities	92
8.1.7	Infrared singularities	92

8.1.8	Light cone coordinates	93
8.1.9	Space-time picture of the singularities	94
8.1.10	Infrared safe observables	94
8.2	The QCD improved Parton Model	97
8.2.1	The QCD factorisation theorem	97
8.2.2	Hadron-hadron cross sections I	97
8.2.3	Hadron-hadron cross sections II	98
8.2.4	Recap of the F_2 structure function	99
8.2.5	Scaling violation I	99
8.2.6	Scaling violation II	100
8.2.7	DGLAP evolution	101
8.2.8	Quark and gluon evolution	101
8.2.9	The leading order splitting functions	102
8.2.10	The coupled DGLAP equations	103
8.2.11	Singlet/gluon and non-singlet evolution	104
8.2.12	Higher orders ...	106
8.2.13	Intuitive picture	107
8.2.14	Scale breaking pattern of the F_2 structure function	108
8.2.15	Comparison of the F_2 data with the QCD prediction	109
8.2.16	The pdf set from the HERA QCD analysis	110
8.2.17	Scale dependence	110
9	Asymptotic freedom	113
9.1	Higher order corrections on $e - \mu$ scattering	114
9.1.1	Renormalisation	116
9.1.2	The running coupling constant of QED	117
9.2	The running coupling constant of QCD	121
9.2.1	Numerical results of α_s	122
10	Heavy-ion physics	127
10.1	The Bag model	127
10.2	Lattice QCD calculations	131
10.3	Probing the Quark-Gluon Plasma (QGP)	133
10.4	Kinematics	135
10.5	Centrality	136
10.6	Key observables	139
10.6.1	Collective flow	139
10.6.2	Jet quenching	142
	Units and conversion factors	149

Covariant notation ($c = 1$)	151
Vector calculus	153
Maxwell's equations in vacuum	155
The Lagrangian in classical mechanics	157
The Hamiltonian in classical mechanics	159
Dirac δ-function	161
Green functions	163
Non-relativistic scattering theory I	165
Non-relativistic scattering theory II	167
Non-relativistic scattering theory III	169
Dirac's bra-ket notation I	171
Dirac's bra-ket notation II	173
Dirac equation	175
Traces	177

Chapter 1

Introduction

Already from early days, humans tried to understand the world that surround us i.e. how it is formed, which are the basic constituents and what are the fundamental laws that govern our Cosmos. Although there is evidence that the theory of the atom was also developed in India, I can not help but mentioning the developments that took place in ancient Greece.

Greek atomism, the term originating from the Greek word *ατομο* i.e. uncuttable, was a response to problems in Greek philosophy. One aspect had to do with the problem of change – were we in a constant state of flux or was change illusory? How could one account for the seemingly endless multiplicity of Nature? Greek atomism was a means of answering philosophical difficulties and explaining the natural world. Around 440BC Leucippus of Miletus¹, in his lost book "The Greater World System," originated the atom concept. He and his pupil, Democritus² of Abdera, refined and extended it in future years. There are five major points to their atomic idea:

- All matter is composed of atoms, which are bits of matter too small to be seen. These atoms can not be further split into smaller portions.
- There is a void, which is empty space between atoms. In modern words, we would call this void *vacuum*.
- Atoms are completely solid objects. There can be no void inside the atom, otherwise it would be subject to changes from outside and would thus disintegrate i.e. it will no longer be an atom.
- Atoms are homogeneous, with no internal structure.
- Atoms are different in their sizes, their shapes and their weight, the latter property was added at a later stage by Epicurus³.

Almost all of the original writings of Leucippus and Democritus are lost. About the only sources we have for their atomistic ideas are found in quotations of other writers. The idea of the atom was strongly opposed by Aristotle and others. Because of this, the atom receded into the background. Although there is a fairly continuous pattern of atomistic thought through the ages, only a relative few scholars gave it much thought. It was not until 1897 and J. J. Thomson's discovery of the electron that the atom was shown to have an internal structure.

1.1 The discovery of the electron

The previous century was the period during which the idea that all matter is composed of a few types of elementary particles, that can no be further subdivided, has been established. The list of elementary particles has changed over time, as new particles have been discovered and some old ones were proven to be composed of elementary constituents. Through all these changes, the one particle type that has always remained on the list was the electron.

The electron was the first elementary particle to be ever identified. It is also by far the lightest of the elementary particles that have charge and one of the few that does not decay into other particles. The discovery of the electron is credited

¹ Leucippus of Miletus: Greek philosopher that lived in the early 5th century BC in Miletus

² Democritus: Greek pre-Socratic philosopher from Abdera, Thrace (460-371 BC)

³ Epicurus: Greek philosopher from Samos (341-270BC)

to J. J. Thomson⁴. Thomson was awarded the 1906 Nobel Prize in Physics for this discovery and for his work on the conduction of electricity in gases.

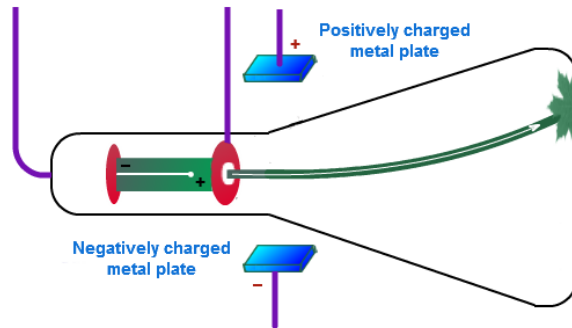


Fig. 1.1: One of the tubes that J. J. Thomson used to conduct his cathode-ray tubes experiments.

Thomson used Newton's second law of motion to obtain a general formula that would explain the measurements of the cathode-ray deflection, produced in his experiment by various electric or magnetic forces in terms of the properties of the cathode-ray particles. In the cathode-ray tube, shown in fig. 1.1, the particles pass through a region (i.e. the deflection region) in which they are subject to electric or magnetic forces acting at right angles to their original deflection and then through a force free region (i.e. the drift region) in which they travel freely until they hit the end of the tube. A glowing spot appears at the place where the ray particles hit the glass at the end of the tube. This made it easy for the observer to measure the displacement of the ray produced by the forces acting on it, by measuring the distance between the locations of the glowing spot when the forces were on and when they were switched off. The displacement could be calculated according to

$$d = \frac{F \times l_{deflection} \times l_{drift}}{m \times u^2}, \quad (1.1.1)$$

where d is the displacement of the ray-particles at the end of the tube, F is the force that acts upon the particles, $l_{deflection}$ and l_{drift} are the length that particles travel in the deflection and drift regions, respectively, m is the mass of the particles and u their velocity. The main idea behind the experiment is the way that the deflection is controlled via the external forces that are applied. These forces give an acceleration to the ray-particles with a component perpendicular to the original motion. In his experiment, Thomson measured the displacement produced by various electric and magnetic forces acting on the ray. Out of the quantities used in Eq. 1.1.1, the lengths of the deflection and drift regions are known quantities determined with high accuracy from the design of the cathode ray tube and the particle mass and velocity are the quantities that one would like to measure. The electric force acting on the particle is proportional to the charge of the particle itself. This makes the displacement measured with Eq. 1.1.1 a combination of different variables or parameters (i.e. mass and charge) of the ray-particles, but can not constrain them individually. To overcome this obstacle, Thomson measured the deflection induced by magnetic forces. A magnetic force is proportional to the the charge of a particle as well as, unlike electric forces, to its velocity. By measuring the deflections by both electric and magnetic forces, Thomson was able to determine at the same time the velocities and the ratio of electric charge to mass of the ray-particles.

The fact that the particles were 1000 times lighter than the known atoms suggested their elementary nature. Still, there were hints that led Thomson to further support his conclusion. One of the hints was given by the value of the charge to mass ratio that seemed not to depend on the circumstances under which the measurement was conducted (e.g. type of gas in the tube, type of cathode, even though the velocities were quite different). At first Thomson did not use any specific name for the particles that he discovered. The name was given by George Stoney⁵ as the fundamental unit quantity of electricity.

⁴ Sir Joseph John Thomson, (18 December 1856 ? 30 August 1940) was an English physicist who became a senior professor at the University of Cambridge.

⁵ George Johnstone Stoney (1826-1911) was an Anglo-Irish physicist.

1.2 The atomic scale

The concept of atoms was introduced in the early 1800s by John Dalton. He was the first to publish a table of relative atomic weights, containing six elements, namely: hydrogen, oxygen, nitrogen, carbon, sulfur, and phosphorus. The atom of hydrogen conventionally assumed to weight 1. A snapshot of one of Dalton's report where he was discussing his studies can be seen in 1.2. Dalton's theory of the atoms can be summarised by the following points:

- Elements are made of extremely small particles called atoms.
- Atoms of a given element are identical in size, mass, and other properties; atoms of different elements differ in size, mass, and other properties.
- Atoms cannot be subdivided, created, or destroyed.
- Atoms of different elements combine in simple whole-number ratios to form chemical compounds.
- In chemical reactions, atoms are combined, separated, or rearranged.

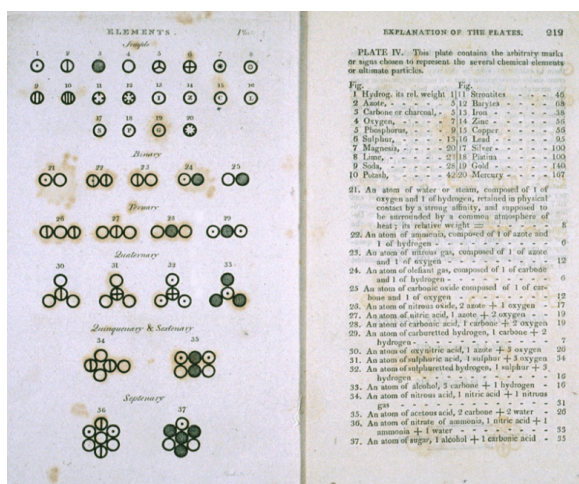


Fig. 1.2: One of the pages in a report from J. Dalton describing his studies on the atoms.

At a later stage, when Thomson discovered electrons, he also built one of the first atomic models. Thomson knew that electrons had a negative charge and thought that matter must have a positive charge. His model looked like raisins stuck on the surface of a lump of pudding.

In 1900 Max Planck, a professor of theoretical physics in Berlin showed that when you vibrate atoms strong enough, such as when you heat an object until it glows, you can measure the energy only in discrete units. He called these energy packets, quanta. Physicists at the time thought that light consisted of waves but, according to Albert Einstein, the quanta behaved like discrete particles. Physicists call Einstein's discrete light particle, a *photon*. Atoms not only emit photons, but they can also absorb them. In 1905, Albert Einstein wrote a ground-breaking paper that explained that light absorption can release electrons from atoms, a phenomenon called the "photoelectric effect." Einstein received his only Nobel Prize for physics in 1921 for his work on the photoelectric effect.

In 1911, Ernest Rutherford via his experiments probed the internal structure of the atom by discovering, as we will see in the next section, the nucleus, the positively charged core of the atom. In 1912 a Danish physicist, Niels Bohr came up with a theory that said the electrons do not spiral into the nucleus and came up with some rules for what does happen. Bohr introduced the idea that electrons can orbit only at certain allowed distances from the nucleus. He also suggested that atoms radiate energy when an electron jumps from a higher-energy orbit to a lower-energy orbit. Furthermore, an atom could absorb energy when an electron gets boosted from a low-energy orbit to a high-energy orbit.

1.3 The nucleus

The atomic model introduced by Thomson was quite popular until around 1913, when Geiger and Marsden, under the supervision of Rutherford, performed the well known by now gold foil experiments. They pointed a beam of α -particles at a thin foil of metal and measured the scattering pattern by using a fluorescent screen. The setup used is schematically depicted in fig. 1.3. They spotted α -particles bouncing off the metal foil in all directions, some right back at the source. This should have been impossible according to Thomson's model: the α -particles should have all gone straight through. Obviously, those particles had encountered an electrostatic force far greater than Thomson's model suggested they would, which in turn implied that the atom's positive charge was concentrated in a much tinier volume than Thomson imagined.

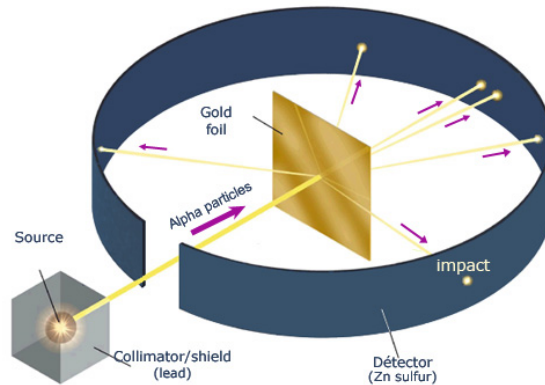


Fig. 1.3: A schematic representation of the experiment that Rutherford conducted.

Rutherford and his collaborator soon dismissed Thomson's model of the atom, and instead proposed a model where the atom consisted of mostly empty space, with all its positive charge concentrated in its center in a very tiny volume, the nucleus, surrounded by a cloud of electrons.

The discovery of the neutron by Chadwick (1932) showed that atomic nuclei are made up of protons and neutrons. It was also clear that, in addition to gravitation and the electromagnetic force, there should exist two short-range forces in nature: a strong force which binds the nucleons together and a weak force which is responsible for radioactive β -decay. These forces had to be short-range because they were not felt at atomic scales.

1.4 The particles and forces of the Standard Model

The traditional goal of particle physics has been to identify what appears to be structureless units of matter and to understand the nature of the forces acting upon and between them. The connection between fundamental matter and forces was made clear by Thomson's discovery of the electron and Maxwell's theory of the electromagnetic field, which together by many are considered to mark the birth of modern particle physics. In the last part of the previous century and in the beginning of the current one, significant progress has been made not only in the development of theories that describe three of the fundamental forces i.e. the electromagnetic, the weak and the strong forces, but there were also compelling and convincing experimental evidence of their applicability. This collection of theories is usually called the Standard Model.

It turns out that the units of matter are fermions i.e. particles with half-integer spin ($\hbar/2$). There are two types of fermions, the leptons and the quarks, which are both considered elementary particles. The leptons are a generalisation of the electrons and interact electromagnetically (i.e. charged and neutral leptons) and weakly (i.e. neutral leptons). On the other hand the quarks, are considered to be the constituents of hadrons and interact via all interactions i.e. electromagnetically, weakly and strongly. The weak and electromagnetic interactions of particles are described by the electroweak theory developed by Glashow, Weinberg and Salam⁶, which is in turns a generalisation of quantum electrodynamics or QED. The strong

⁶ Also known as GWS theory.

interactions however, which will be the main focus of these lectures, are described by the Quantum ChromoDynamics (QCD). All three interactions are types of gauge theories, though realised in different ways.

1.4.1 Leptons of the Standard Model

Forty years after the discovery of the electron by J. J. Thomson, the first member of another generation of leptons, the muon μ , was found independently by Street and Stevenson, and by Anderson and Neddermeyer. Following the convention of the electron, μ^- is the particle and μ^+ is the antiparticle. In 1975 Perl *et al.* discovered yet another replica of the electron. This particle was significantly heavier ($m \approx 1.78 \text{ GeV}/c^2$) than the electron and was the tau τ^- with its antiparticle τ^+ . Both particles behave quite similarly as the electrons and interact electromagnetically and weakly. These particles have half-integer spin of $1/2$.

An interesting observation about the behaviour of leptons is related to the fact that their decay into lighter leptons and a photon (e.g. $\tau^- \rightarrow \mu^- + \gamma$) is not observed. This indicated the necessity for a new conservation law which came in the form of a new additive quantum number called *lepton flavour*. We thus have the electron flavour number i.e. $L_e(e^-) = 1$ and $L_e(e^+) = -1$, the muon flavour number i.e. $L_\mu(\mu^-) = 1$ and $L_\mu(\mu^+) = -1$, and the tau flavour number i.e. $L_\tau(\tau^-) = 1$ and $L_\tau(\tau^+) = -1$. Each number is postulated to be conserved in all leptonic processes.

The electromagnetic interactions of these particles are the same, no matter what the flavour is. For the weak interactions, leptons are accompanied by their neutral partner, the neutrinos. The one emitted in the β decay of electrons was introduced by Pauli in 1930 as a last resort to restore the conservation laws of energy, momentum and angular momentum. These neutrinos are:

- ν_e with $L_e = 1$ and the antineutrino $\bar{\nu}_e$ with $L_e = -1$,
- ν_μ with $L_\mu = 1$ and the antineutrino $\bar{\nu}_\mu$ with $L_\mu = -1$,
- ν_τ with $L_\tau = 1$ and the antineutrino $\bar{\nu}_\tau$ with $L_\tau = -1$,

The realisation of the nature of antineutrinos came in 1956 by Cowan *et al.* by observing that they produce positrons via the inverse β decay:

$$\bar{\nu}_e + p \rightarrow n + e^+ \quad (1.4.1)$$

In addition, it was realised that the different neutrino flavours correspond indeed to different particles i.e. $\nu_e \neq \nu_\mu$ by observing the reaction $\bar{\nu}_\mu + p \rightarrow \mu^+ + n$ while at the same time the reaction $\bar{\nu}_\mu + p \rightarrow e^+ + n$ was not observed (i.e. an upper limit on the cross-section was given).

In summary there are three generations of leptons, grouped by flavour in charged and neutral: $(\nu_e, e^-, \nu_\mu, \mu^-)$ and (ν_τ, τ^-) . Some of the properties of these three generations are given in Table 1.1.

Particle	Mass (MeV)	Q/e	L_e	L_μ	L_τ
ν_e	$\leq 2 \times 10^{-6}$	0	1	0	0
$\bar{\nu}_e$	$\leq 2 \times 10^{-6}$	0	-1	0	0
e^-	0.511	-1	1	0	0
e^+	0.511	1	-1	0	0
ν_μ	≤ 0.19	0	0	1	0
$\bar{\nu}_\mu$	≤ 0.19	0	0	-1	0
μ^-	105.66	-1	0	1	0
μ^+	105.66	1	0	-1	0
ν_τ	≤ 18.2	0	0	0	1
$\bar{\nu}_\tau$	≤ 18.2	0	0	0	-1
τ^-	1777	-1	0	0	1
τ^+	1777	1	0	0	-1

Table 1.1: The basic properties of the Standard Model leptons.

1.4.2 Quarks of the Standard Model

Quarks are the constituents of hadrons, in which they are bound by the strong force. The quarks are grouped in three to form a baryon (e.g. p containing uud) or combined with antiquarks to form mesons (e.g. π^- containing $\bar{u}d$).

Evidence for the composite nature of hadrons was provided in the 60s and 70s. Elastic scattering of electrons from protons indicated that the latter was not point-like (we will see this later in Chapter 6), but had an approximately exponential distribution of charge with a root mean square value of 0.8 fm. In addition, in the field of baryon and meson spectroscopy, several excited states were revealed. The emerging picture resembled strongly the one associated to the atomic and nuclear physics. A proposal by Gell-Man and Zweig came in 1964 suggested that baryons are formed by the combination of three spin-1/2 constituents called quarks, while mesons contained a combination of a quark and its antiparticle.

When this proposal was put forward, three types of quarks were enough to account for the known (at that time) hadrons. These quarks were: u -quark (up) with a charge of $2/3$, d -quark (down) with a charge of $-1/3$ and the s -quark (strange) with a charge of $-1/3$. Soon later, and mainly based on arguments related to the quark-lepton symmetry, a fourth quark was proposed, which Glashow, Iliopoulos and Maiani in 1970 estimated to have a mass of about 3-4 GeV. At a later stage (i.e. in 1974) Gaillard and Lee performed more detailed calculations and predicted $m \approx 1.5 \text{ GeV}/c^2$. The prediction was confirmed in November of the same year with the discovery of the J/Ψ which was soon identified as a compound state of $c\bar{c}$, with c being the fourth quark called charm. The discovery of the third lepton generation hinted for the existence of a relevant third generation of quarks. The discovery of the b -quark (i.e. beauty) came shortly after, in 1977, from the observation of the heavy mesonic states known as Y , identified as a bound $b\bar{b}$ state. Finally, the three generations of quarks was completed with the discovery of the top quark by the CDF and D0 collaborations. A summary of the quarks and some of their basic properties can be seen in Table 1.2.

Particle	Mass (MeV)	Q/e	Strangeness	Charm	Beauty	Topness
u	2	$2/3$	0	0	0	0
\bar{u}	2	$-2/3$	0	0	0	0
d	5	$-1/3$	0	0	0	0
\bar{d}	5	$1/3$	0	0	0	0
c	1200	$2/3$	0	1	0	0
\bar{c}	1200	$-2/3$	0	-1	0	0
s	100	$-1/3$	-1	0	0	0
\bar{s}	100	$1/3$	1	0	0	0
t	174000	$2/3$	0	0	0	1
\bar{t}	174000	$-2/3$	0	0	0	-1
b	4200	$-1/3$	0	0	-1	0
\bar{b}	4200	$1/3$	0	0	1	0

Table 1.2: The basic properties of the quarks of the Standard Model.

1.4.3 The discovery of more particles

After the discovery of the proton, many more baryons were discovered, some of them seemed to behave strangely. These particles were produced in big numbers very fast (i.e. on a time scale of 10^{-23} sec) but they decayed very slowly, typically on a time scale of about 10^{-10} sec. This suggested that their creation process is governed by a different procedure as compared to their decay. The strange particles, that happened to contain also a strange quark, are produced by the strong interaction while they decay weakly. In 1953 Gell-Man and Nishijima suggested to assign a new property, a new quantum number to every particle that Gell-Man called *strangeness*. This new quantum number is conserved in strong interactions, contrary to weak interaction where this number is not preserved.

Soon enough, in 1961, Gell-Man introduced what is known as the *Eightfold Way*. Based on this, the mesons and baryons were arranged, initially, based on their charge and strangeness. An example is given in fig. 1.4, where the members of the meson octet are presented. In both cases the diagonal lines present the members of the group with the same charge.

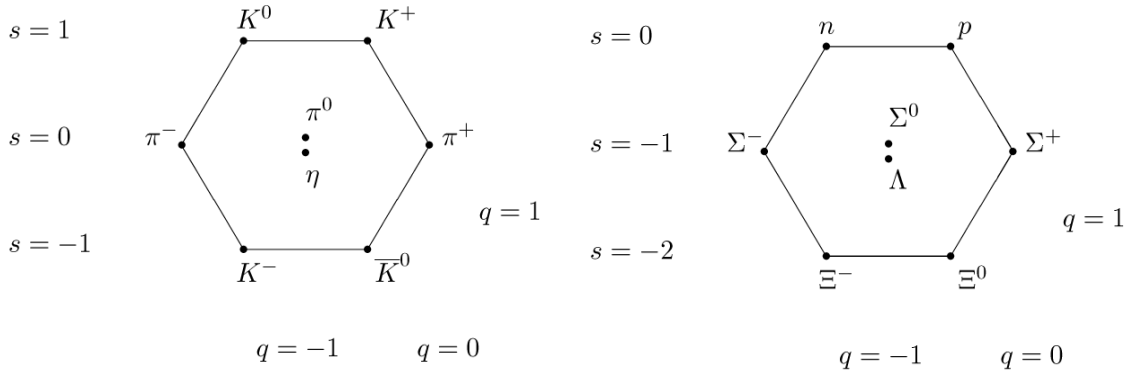


Fig. 1.4: The meson (left) and the baryon (right) octets.

Soon enough this classification illustrated its predicted power. Figure 1.5 presents the members of the baryon decuplet. At the time when this particles were positioned in the triangle, nine out of ten particles were already discovered. The remaining unknown particle had charge -1 and strangeness number -3 and it was expected to be positioned at the lower edge of the shape. Gell-Man went on to predict the existence of this multi-strange particle and suggested how this can be produced. Not long after, around 1964, the Ω^- was discovered.

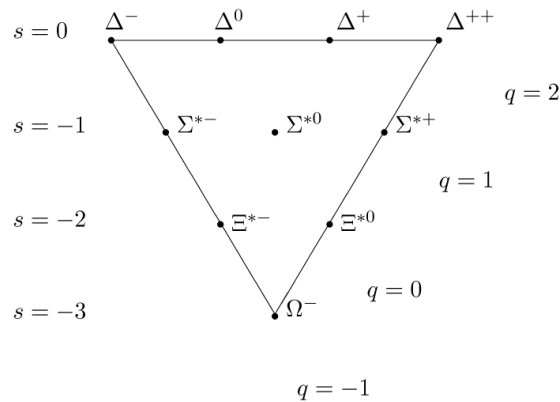


Fig. 1.5: The baryon octet (left) and decuplet (right).

1.4.4 Interactions and mediators in the Standard Model

According to the Standard Model of particle physics, there are four fundamental forces in nature: gravitational, weak, electromagnetic and strong. To each of these forces, a dedicated theory is developed and a relevant mediator, a particle carrier of the force is associated. The gravitational force is described by the general theory of relativity and its mediator which in many cases is referred to as the graviton. The weak force is described by the flavordynamic theory or better by the Glashow-Weinberg-Salam (GWS) theory. It accounts for the nuclear β decay, the decay of the pion, the muon and many strange particles. The mediators of the weak force are the W^\pm and Z bosons. The electromagnetic interaction is described in terms of Quantum ElectroDynamics or QED. Its classical representation was developed by Maxwell, while it was refined by people like Tomonaga, Feynman and Schwinger in around 1940-1950. The mediator in QED is the photon. Finally, the strong force is mediated by the gluons and is described by the theory that emerged last among all, around 1970, the Quantum ChromoDynamics, the topic of these lectures. Figure 1.6 summarise the three generations of matter in terms of leptons and quarks, the gauge bosons also known as force mediators and the Higgs boson. The latter

is the representation of the Higgs field which is believed to explain why some fundamental particles have mass while the symmetries controlling their interactions should require them to be massless, and why the weak force has a much shorter range than the electromagnetic force.

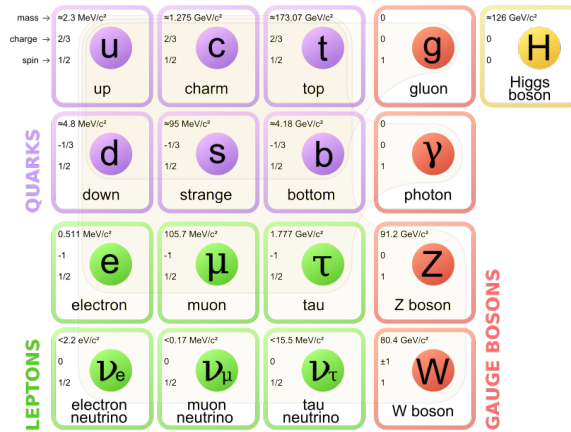


Fig. 1.6: The Standard Model of elementary particles, with the three generations of matter, gauge bosons in the fourth column, and the Higgs boson in the fifth.

1.4.4.1 Quantum ElectroDynamics - QED

Quantum ElectroDynamics or QED is the simplest of the dynamic theories of particle physics. It describes all electromagnetic phenomena, using one basic diagram that presents an elementary process and is shown in fig. 1.7. In this Feynman diagram time flows from left to right, horizontally. It can be read as follows: an electron (a lepton or even a quark in general) enters, emits a photon and exits.

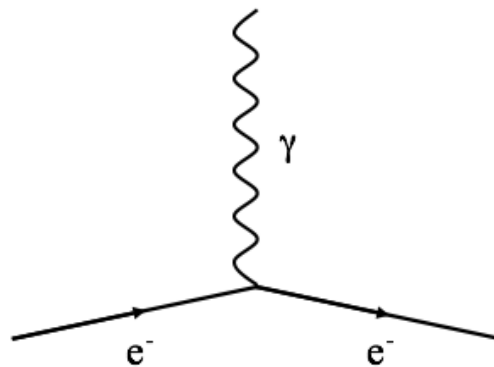


Fig. 1.7: The basic diagram that represents the most elementary process in QED.

Combining two of these elementary diagrams allows to describe more basic processes as the one presented in fig.1.8. This figure presents the scattering process between two electrons, also known as Møller scattering. It is seen that the process is mediated by a virtual photon and its cross-section is easy to be calculated using the Feynman rules that will be discussed in Chapter 4.

Particles decaying electromagnetically have a typical lifetime of 10^{-16} sec. The strength of the electromagnetic interaction is characterised by the coupling constant, known as the fine structure constant α ($\alpha = e^2/\hbar c$). The value of α is estimated

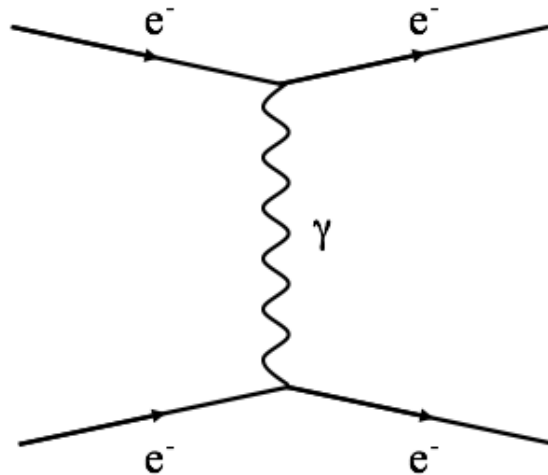


Fig. 1.8: The diagram describing the electron-electron scattering, known as Møller scattering.

to be $1/137$ with very high accuracy. It should be noted that it is believed that the fine structure constant is not a real constant but changes very slowly with energy, as we will see later in this chapter.

1.4.4.2 Weak interactions

Weak interactions are of fundamental significance in particle physics and are visible in processes involving leptons and quarks. The coupling constant is significantly smaller than the one of the electromagnetic force and it is of the order of 10^{-6} . Particles decaying weakly have a typical lifetime of $> 10^{-13}$ sec. There are two kinds of such interactions: the charged, mediated by the W-bosons, and the neutral, mediated by the Z-boson.

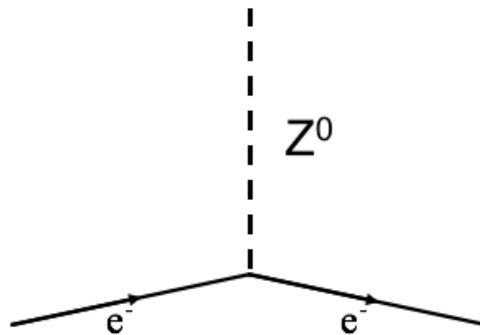


Fig. 1.9: The basic diagram that represents the most elementary neutral process in the GWS theory.

The diagram that is the basis of the neutral weak interactions is seen in fig. 1.9. It describes a Z-boson being emitted by an electron that enters and then exits. As in the case of QED, the combination of two of these diagrams can describe processes like the one that can be seen in fig. 1.10. The figure presents the scattering between an electron and a neutrino, which is mediated by there Z-boson.

On the other hand, the charged weak decay is mediated by the charged W-bosons and its fundamental diagram can be seen in fig. 1.11.

Charged weak decays can occur in the presence of leptons as illustrated in fig. 1.12-left. A simple inversion of the neutrino line in the bottom part allows to describe the muon decay process ($\mu^- \rightarrow \nu_\mu + e^- + \bar{\nu}_e$), presented in fig. 1.12-right.

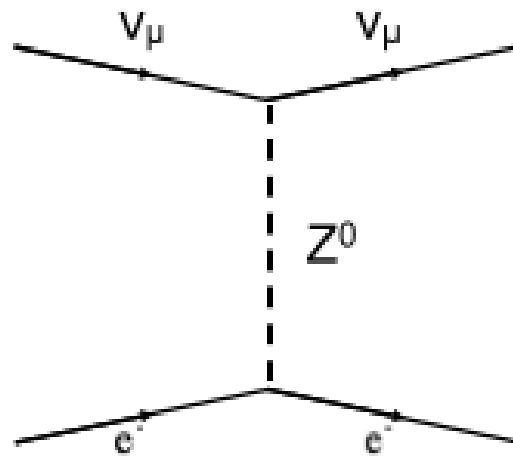


Fig. 1.10: The diagram describing the electron-neutrino scattering.

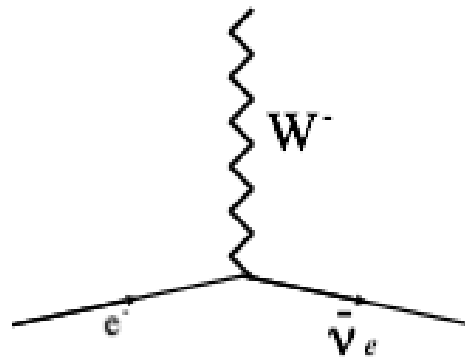


Fig. 1.11: The basic diagram that represents the most elementary charged process in the GWS theory.

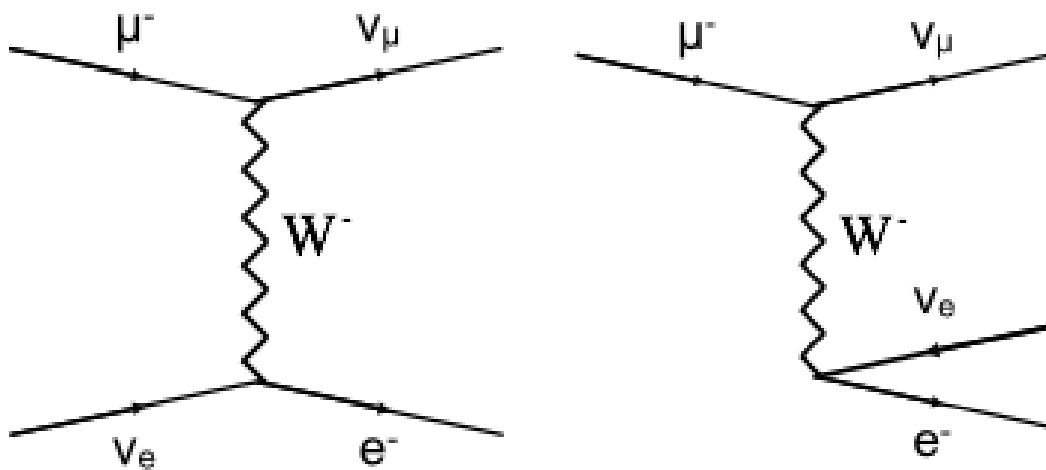


Fig. 1.12: The diagram describing the muon-neutrino charged scattering in the left plot. The right diagram results from the inversion of the line of the electron's neutrino and describes the muon decay.

The charged weak decays are the only ones where the flavour of a quark can change during the process. A perfect example is the decay of the neutron ($n \rightarrow p + e^- + \bar{\nu}_e$) that is described by the diagram of fig. 1.13-left.

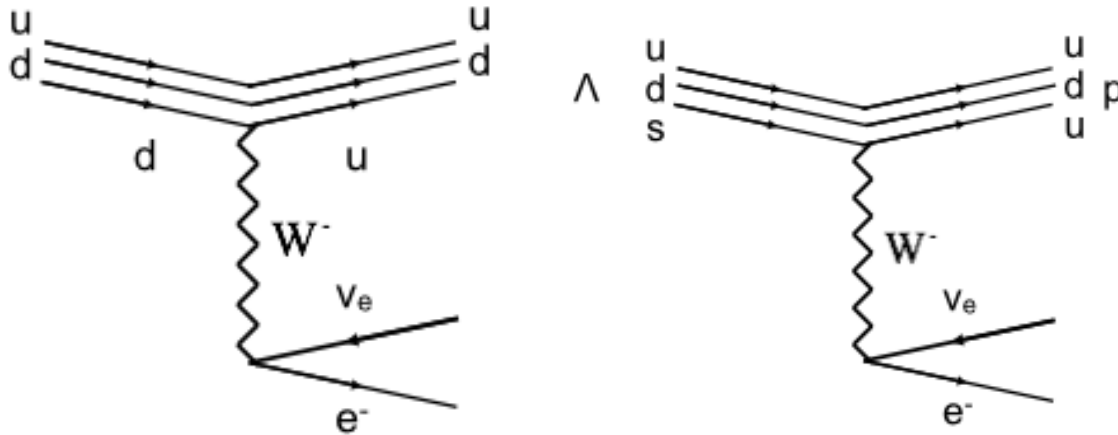


Fig. 1.13: The diagram describing the decay of the neutron (left) and of the Λ -baryon (right).

One interesting possibility though emerges by the observation of processes where strangeness changes, such as the decay of the Λ -baryon ($\Lambda \rightarrow p + \pi^-$). This process involves the conversion of a strange-quark to an up-quark, via the exchange of a W -boson as illustrated in fig. 1.13-right.

The solution to this was given by Cabbibo in 1963, and extended by Glashow, Iliopoulos and Maiani in 1970 and by Kobayashi and Maskawa in 1973. They suggested that the three quark generations have internal correlations and in particular that the d , s and b quarks are transformed to their respective prime particles that are linear combinations of the initial ones according to:

$$\begin{pmatrix} d' \\ s' \\ b' \end{pmatrix} = \begin{pmatrix} V_{ud} & V_{us} & V_{ub} \\ V_{cd} & V_{cs} & V_{cb} \\ V_{td} & V_{ts} & V_{tb} \end{pmatrix} \begin{pmatrix} d \\ s \\ b \end{pmatrix}$$

The 3×3 array is called the Kobayashi-Maskawa matrix and provides the coupling of u , c and t quarks to d , s and b .

1.4.4.3 Quantum Chromodynamics - QCD

Quantum chromodynamics or else QCD is the theory that describes the strong interaction. It describes all strong phenomena, using one basic diagram that presents an elementary process and is shown in fig. 1.14. The diagram can be read as follows: a quark enters, emits a gluon and exits.

QCD is quite similar in many ways to QED however, as we will see later, it has also distinct and fundamental differences. As in the case of QED, the combination of two similar diagrams as the one in fig. 1.14 can describe a known process i.e. the interactions between two quarks, as illustrated in fig. 1.15.

One of the fundamental differences of QCD with respect to QED is the fact that although in QED there is only one charge, in QCD the equivalent of the charge is the color. There are three kind of colors in QCD, that are conventionally called: red (R), green (G) and blue (B). Gluons have two colors, carrying one unit of color and one of anticolor. There are $3 \times 3 = 9$ possibilities for the gluons but as we will see in Chapter 2, there are only 8. Since the gluons carry color, they can also couple directly to other gluons making the existence of gluon-gluon vertices possible. Another difference comes from the fact that particles decaying strongly have typical lifetimes of 10^{-23} sec.

The coupling constant is denoted by α_s and as in the case of QED is not a constant. In contrast to QED though, we will see that the strong coupling constant changes quite rapidly as a function of the distance between the interacting particles. We will see in Chapter 9 that at large distance α_s is big, making the observation of quarks and gluons move as free particles

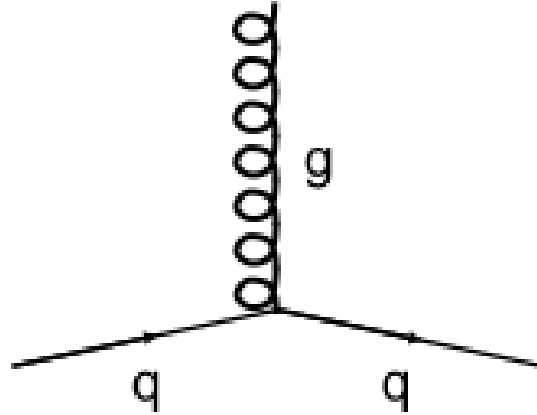


Fig. 1.14: The basic diagram that represents the most elementary process in QCD.

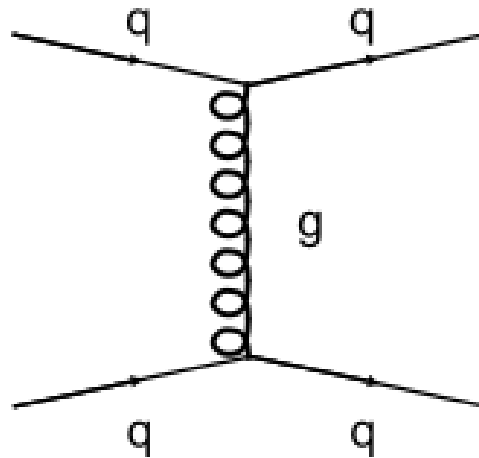


Fig. 1.15: The lower order diagram that describes the interaction between two quarks.

impossible. This phenomenon is called confinement. However, at short distances α_s becomes quite small, allowing the quarks e.g. within a proton to move freely without interacting much with their neighbouring quarks. This phenomenon is called asymptotic freedom and its existence was postulated in 1973 by Frank Wilczek, David Gross, and independently by David Politzer the same year. All three shared the Nobel Prize in physics in 2004.

In QED, a similar effect is observed which can be understood if one thinks that the vacuum itself behaves like a dielectric and creates electron-positron pairs as shown in the Feynman diagrams of fig. 1.16. The resulting vacuum polarisation screens the charge and reduces the field. This screening is reduced and eventually disappears if one approaches the charge.

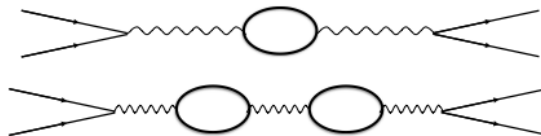


Fig. 1.16: The lower order diagrams that describe the vacuum polarisation in QED.

An analogous picture emerges in QCD, however with the addition of the gluon-gluon vertices that we saw before. The main difference now is that in QCD the effect is opposite i.e. there is a competition between the quark polarisation diagram that tends to increase α_s and the corresponding gluon diagram that decreases the coupling constant. What the effect will be depends on the number of flavours and colors according to

$$a = 2f - 11n, \tag{1.4.2}$$

where f is the number of flavours and n is the number of colors. It turns out that $f = 6$ and $n = 3$, resulting in a negative value of a of -21 . This means that the QCD coupling constant decreases at small distances.

Finally it is important to note that the particles that stream freely in nature, are colourless. Quarks are confined in colourless configurations of three (baryons) or together with an antiquark (forming the mesons).

1.4.4.4 Conservation laws

We already discussed about the lifetime of particles that decay electromagnetically, weakly or strongly. It is now time to look at some basic conservation laws. The first part of these laws is related to kinematics:

- Conservation of energy e.g. a particle can not decay spontaneously into particles heavier than itself
- Conservation of momentum
- Conservation of angular momentum

In addition to the previous constraints, there are also laws related to quantum numbers:

- All three interactions conserve the charge.
- Strong interactions conserve color.
- All three interactions conserve the baryon number.
- Lepton number is conserved in particle physics. Until recently there was no indication of a cross-talk or mixing between different leptons. However, neutrino oscillations make the previous statement not precise enough.
- Quark flavour is conserved in the strong and electromagnetic interactions.

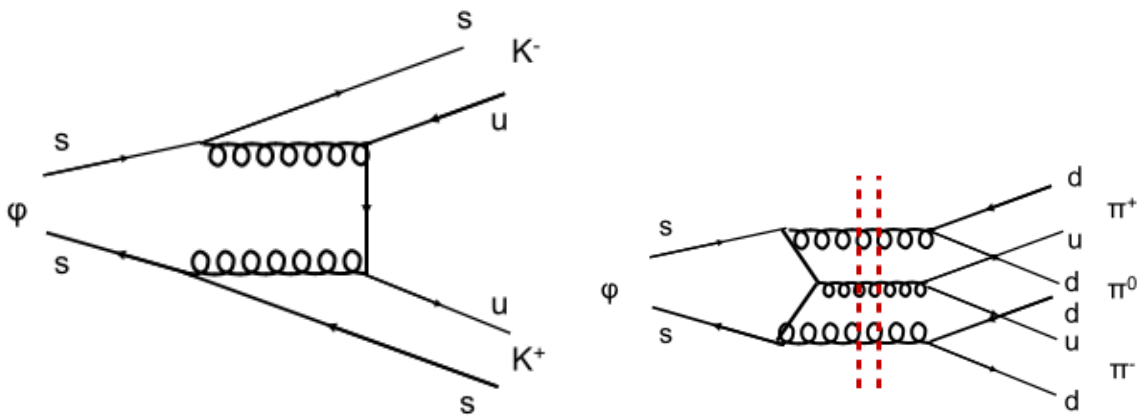


Fig. 1.17: The suppression of the decay of the ϕ -meson into three pions (right diagram) compared to the one into two kaons (left diagram) based on the OZI rule.

There is another law which is known as the *OZI rule*⁷ and was introduced to explain why the ψ -meson, consisting of a c-quark and a c-antiquark, decays strongly with a lifetime 10^3 more than the typical lifetime of a strong decay. The law states that if a diagram can be cut by snipping only gluon lines, then the relevant process is suppressed. The way this can be done is illustrated in fig. 1.17, where it is shown how by applying the OZI rule in the case of the ϕ -meson, the decay into three pions (right diagram) is suppressed as compared to the one into two kaons (left diagram).

⁷ OZI stands for Okubo, Zweig and Iizuka

Chapter 2

Symmetries and elements of group theory

A very important concept in physics is the symmetry or invariance of an equation describing a physical system under an operation. Imagine that one looks at a graph which has a repetitive pattern, without having any idea of what the functional form is. By simply observing the graph one could deduce if this is an odd or an even function i.e. $f(-x) = -f(x)$ or $f(-x) = f(x)$, respectively. The most obvious examples of symmetries is seen in shapes e.g. in crystals. But this is a static symmetry that we are not interested in studying, since we will rather focus on dynamical symmetries of motion.

2.1 Symmetries and conservation laws in physics

We can discuss about and describe a system by studying its Lagrangian. There are cases where the Lagrangian of a system is known from first principles. On the other hand there are cases where one can build a Lagrangian of a system profiting from the observed conservation laws. The connection between conservation laws and symmetries was illustrated by Emmy Noether in her famous theorem:

Every symmetry in nature yields a conservation law and inversely every conservation law reveals an underlying symmetry.

As we will see later, an invariance under spacial transformation yields the conservation of momentum. If the Lagrangian of the world would be fully known we could derive the equations of motion from it, and the symmetries of nature and the conservation laws would automatically follow. For instance the Maxwell Lagrangian yields, via the Maxwell equations, all the symmetries and conservation laws of electrodynamics. In subatomic physics the Lagrangians are not so obvious, and symmetry considerations provide essential clues to construct them.

Symmetries are represented by the respective operators. The operator acts on a wave function $|\psi\rangle$ of a system and transforms it to $|\psi'\rangle$. Operators are categorised in two groups: discrete and continuous. As will become clear later, it turns out that discrete symmetries lead to multiplicative conserved quantum numbers (e.g. reflection symmetry leads to parity conservation \rightarrow multiplication of parities) while continuous symmetries lead to additive conserved quantum numbers (e.g. rotation invariance leads to the angular momentum conservation \rightarrow addition of angular momentum quantum numbers).

Some examples of symmetry operators are given below:

- Reflection (parity): P which transforms $x \rightarrow x' = -x$, with the identity transformation $PP = I$ which transforms $x \rightarrow x' = -x$
- Rotation: in two dimensions it is performed around one point, while in three dimension around one axis (e.g. a rotation of a rectangular shape see fig. 2.1).
- Inversion: when performed around one point then this implies a combination of two operators i.e. reflection about a plane and a rotation of π in the plane.

A symmetry operation which leaves a physical system or shape invariant must satisfy the following requirements:

- a symmetry operation followed by another must be itself a symmetry operation,
- the symmetry operation must associate, although the order with which operations are performed is important,

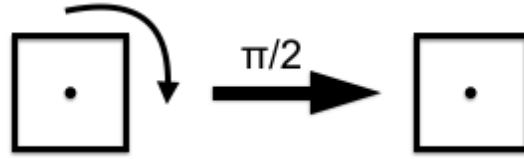


Fig. 2.1: Symmetry under rotations

- there must be an identify transformation that does nothing,
- whatever operation transforms a shape into itself must have an inverse operation

But when is an observable conserved? The expectation value of a quantum mechanical operator F is $\langle F \rangle \equiv \langle \psi | F | \psi \rangle$, with Hermitian conjugate $\langle F \rangle^* \equiv \langle \psi | F^\dagger | \psi \rangle$. The expectation value of an **observable** is a real number so that the operator of an observable should be Hermitian $F = F^\dagger$, if $\langle F \rangle$ is observable. Because energy is an observable the Hamiltonian H is Hermitian. We have for the Schrödinger equation and its Hermitian conjugate

$$i \frac{\partial |\psi\rangle}{\partial t} = H |\psi\rangle \quad \text{and} \quad -i \frac{\partial \langle \psi|}{\partial t} = \langle \psi| H^\dagger = \langle \psi| H$$

This immediately leads to $\frac{\partial \langle F \rangle}{\partial t} = i \langle \psi | HF - FH | \psi \rangle = 0 \Leftrightarrow HF - FH = 0$.

That, in turns, leads to the realisation that an observable constant of motion F is Hermitian and commutes with the Hamiltonian (or the Lagrangian). When H is known, we can find observable constants of motion by searching for Hermitian operators that commute with H . However, when H is not fully known, it is sufficient to establish (or postulate) the invariance of H , or the Lagrangian, under a symmetry operation, as we will now show.

Let a transformation operator U , that transforms one wave function into another: $|\psi'\rangle = U |\psi\rangle$ Wave functions are always normalized so that we must have: $\langle \psi' | \psi' \rangle = \langle \psi | U^\dagger U | \psi \rangle = 1$. This implies that the transformation operator must be unitary: $U^\dagger U = U U^\dagger = I$. We call U a symmetry operator when $|\psi'\rangle$ obeys the same Schrödinger equation as $|\psi\rangle$. Then, with U time independent,

$$i \frac{\partial U |\psi\rangle}{\partial t} = H U |\psi\rangle \quad \rightarrow \quad i \frac{\partial |\psi\rangle}{\partial t} = U^{-1} H U |\psi\rangle \stackrel{\text{I want}}{=} H |\psi\rangle$$

and thus

$$U^{-1} H U = H \quad \text{or} \quad [H, U] = 0$$

A symmetry operator U is unitary and commutes with the Hamiltonian. Thus U commutes with the Hamiltonian, as does a constant of motion. However, we cannot identify U with an observable since it is unitary, and not necessarily Hermitian.

2.1.1 Discrete transformations

There is a class of unitary transformations with the property $U^2 = I$. Multiplying from the right with U^\dagger and using $U U^\dagger = I$ we find that $U = U^\dagger$: the operator is both unitary and Hermitian. Thus if U is a symmetry of (commutes with) the Hamiltonian we can directly conclude that it is an observable constant of motion. Examples of this the are the charge conjugation operator C (exchange of particles and antiparticles) and the parity operator P (reflection of the spatial coordinates).¹

The C and P operators are not the only ones that are both unitary and Hermitian. This is, for instance, also true for the Pauli spin matrices, as is straight-forward to check.

¹ The time reversal operator T also has $T^2 = I$ but it is antiunitary, and not unitary.

$$\sigma_x = \begin{pmatrix} 0 & 1 \\ 1 & 0 \end{pmatrix}, \quad \sigma_y = \begin{pmatrix} 0 & -i \\ i & 0 \end{pmatrix}, \quad \sigma_z = \begin{pmatrix} 1 & 0 \\ 0 & -1 \end{pmatrix}$$

If $|\psi\rangle$ is an eigenvector of both U_1 and U_2 then

$$U_{1,2}|\psi\rangle = \lambda_{1,2}|\psi\rangle \quad \text{and} \quad U_1U_2|\psi\rangle = U_2U_1|\psi\rangle = \lambda_1\lambda_2|\psi\rangle$$

The quantum numbers of a discrete symmetry are multiplicative.

In these lectures we are not so much interested in discrete transformations (like C , P , T) but, instead, in continuous transformations. These transformations are unitary (by definition), but not necessarily Hermitian. But the generator of a unitary continuous transformation is Hermitian, as we will see.

2.1.2 Continuous transformations

There is a large class of continuous transformations that depend on one or more continuous parameters, say α such that $|\psi'\rangle = U(\alpha)|\psi\rangle$. An example is the transformation induced by a rotation over an angle α of the coordinate system (passive rotation), or of the wave function (active rotation). Such transformations have the property that they can be written as a succession of infinitesimal deviations from the identity

$$U(\alpha) = \lim_{n \rightarrow \infty} \left(I + \frac{i\alpha}{n} F \right)^n = \exp(i\alpha F)$$

The factor ‘ i ’ is a matter of definition but important (see below). In the above, F is called the generator of U .² Now if U is unitary we have, to first order in α ,

$$U^\dagger U = (I - i\alpha F^\dagger)(I + i\alpha F) = I + i\alpha(F - F^\dagger) = I$$

so that $F = F^\dagger$. In other words, **the generator of a unitary operator is Hermitian**. We now also understand the factor ‘ i ’ in the definition of a generator: without it the generator $G \equiv iF$ of a unitary operator would not be Hermitian but **anti-Hermitian**: $G = -G^\dagger$.

We have seen that a symmetry operator U commutes with the Hamiltonian so it remains to show that its generator will then also commute with H . The proof is very simple and starts with $U(\alpha)$, a symmetry operator. The infinitesimal transformation $U(\varepsilon)$ will also be a symmetry operator. Expanding to the first order in ε obtains:

$$[H, U] \doteq [H, I + i\varepsilon F] = \underbrace{[H, I]}_0 + i\varepsilon [H, F] = 0 \quad \rightarrow \quad [H, F] = 0$$

It is seen that if U is a unitary operator that commutes with the Hamiltonian, then its generator F is a Hermitian operator that also commutes with the Hamiltonian. A multiplication of continuous symmetry operators corresponds to the addition of their generators in the exponent. The conserved quantum numbers, which are related to F and not to U , are therefore additive.

² Exponentiation of an operator F should be interpreted as $\exp(i\alpha F) = I + i\alpha F + \frac{1}{2!}(i\alpha F)^2 + \dots$. However, the familiar relation $e^A e^B = e^{A+B}$ is *only* true when A and B commute.

2.2 Introduction to groups

Group theory is a branch of mathematics that underlies the treatment of symmetry. A group G is a collection of elements (or operators), say (a_1, a_2, \dots, a_n) , with well defined laws that describe how one can combine any two of the elements with an operator (let's indicate it with \times) so as to form the product such that the following four conditions are fulfilled:

- **Closure:** For every element a_i and a_j of the group G , their product (or in general an operator \times) $a_i \times a_j$ is also a member of the group G , such that $a_i \times a_j = a_k$.
- **Associativity:** The law of combination is associative i.e. $(a_i \times a_j) \times a_k = a_i \times (a_j \times a_k)$.
- **Identity element:** Every group G contains an identity element e such that for all a_i in G $a_i \times e = e \times a_i = a_i$.
- **Inverse element:** For all a_i of a group G there is a unique inverse element a_i^{-1} such that $a_i \times (a_i)^{-1} = (a_i)^{-1} \times a_i = e$.

The associativity requirement does not imply that the elements of the group commute. **A group for which any of the two elements commute is called Abelian, otherwise the group is called non-Abelian.** When a group contains a finite number of elements, let's say n , then the group is called **finite group of order n**.

Example A

The elements $(\dots, -2, -1, 0, 1, 2, \dots)$ form an infinite group of integer numbers. The addition operation (i.e. in this case $\times \equiv +$) allows to go from one element to the other and thus satisfy the four relations presented above:

- $1 + 2 = 3$, also a member of the same group (closure),
- $(1 + 2) + 3 = 1 + (2 + 3)$ (associativity),
- $1 + 0 = 0 + 1 = 1$ (identity element with $e \equiv 0$),
- $1 + (-1) = (-1) + 1 = 0$ (inverse element $(a_i)^{-1} \equiv -1$ and in general all negative integers).

Example B

The elements $(1, i, -1, -i)$ form a finite group of order 4. The multiplication operation (i.e. in this case $\times \equiv \cdot$) allows to go from one element to the other and thus satisfy the four relations presented above:

- $i \cdot (-1) = -i$, also a member of the same group (closure),
- $(1 \cdot i) \cdot (-i) = 1 \cdot (i \cdot (-i))$ (associativity),
- $1 \cdot i = i \cdot 1 = i$ (identity element with $e \equiv 1$),
- $i \cdot (-i) = (-i) \cdot i = 1$ (inverse element $(a_i)^{-1} \equiv (-i)$ and in general the algebraic reciprocal).

Example C

The matrices

$$d_1 = \begin{pmatrix} 1 & 0 \\ 0 & 1 \end{pmatrix}, \quad d_2 = \begin{pmatrix} 0 & 1 \\ -1 & 0 \end{pmatrix}, \quad d_3 = \begin{pmatrix} -1 & 0 \\ 0 & -1 \end{pmatrix}, \quad d_4 = \begin{pmatrix} 0 & -1 \\ 1 & 0 \end{pmatrix}$$

form a finite group of order 4. The matrix multiplication operation takes the place of \times in the general description, the identity element is the unit matrix (i.e. d_1) and the inverse being the usual inverse matrices.

These last two examples are indicative of another property of groups. The matrices multiply together in exactly the same way (and order) the four elements of the second example did. In addition, the correspondence between the elements of the group is *one-to-one* i.e. if we label the four elements of these two groups as (e, a_1, a_2, a_3) and (e', a'_1, a'_2, a'_3) , then $e \Leftrightarrow e'$, $a_1 \Leftrightarrow a'_1$, $a_2 \Leftrightarrow a'_2$, $a_3 \Leftrightarrow a'_3$. **Two groups with the same multiplication scheme and with an one-to-one correspondence between their elements are called isomorphic. If they have the same multiplication scheme but the correspondence between the elements is not one-to-one, the groups are called homomorphic.**

2.3 Lie groups

As stated before, in these lectures we are not interested so much in discrete but rather in continuous transformations. These are described in terms of continuous groups, whose elements are labelled by a number of continuously variable real parameters, say a_1, a_2, \dots, a_n , and by the relevant operators $g(a_1, a_2, \dots, a_n) \equiv g(\mathbf{a})$. In particular we are interested in coordinate transformations that, as we will see later, are not only of space-time origin but can also be internal e.g. colour in SU(3). The following examples are indicative of these type of transformations which are usually represented by matrices:

- Rotations in three dimensions form the SO(3) group (i.e. special orthogonal group in three dimensions), whose elements are specified by three real numbers (i.e. two defining the axis of rotation and one the angle for the angle of rotation about the axis).
- Lorenz transformations form the group with six real variables i.e. three for the rotations and the other three for the velocity transformations.

By convention, parameterisations are arranged in such a way so that $g(0)$ is the identity element of the group. For a continuous group, the first group condition takes the form $g(\alpha) \times g(\beta) = g[\gamma(\alpha, \beta)]$, where the parameters γ are continuous functions of the parameters α and β . If the parameters γ are analytic functions of α and β the group is called a **Lie group**.

Let us consider a group of transformations defined by $x'_i = f_i(x_1, x_2, \dots, x_n; \alpha_1, \alpha_2, \dots, \alpha_n)$, where x_i with $i = 1, 2, \dots, n$ are the coordinates on which the transformation acts and α_i are the real parameters of the transformation. By convention, $\alpha = \mathbf{0}$ is the identity transformation, such that $x_i = f_i(\mathbf{x}, \mathbf{0})$.

A transformation in the neighbourhood of the identity is then given by

$$dx_i = \sum_{v=1}^r \frac{\partial f_i}{\partial \alpha_v} d\alpha_v,$$

where the $d\alpha_v$ are infinitesimal parameters and the partial derivative is evaluated at the point $\mathbf{x}, \mathbf{0}$.

Let's now consider the change in a function $F(\mathbf{x})$ under the previous infinitesimal transformation. This reads:

$$F \rightarrow F + dF = F + \sum_{i=1}^N \frac{\partial F}{\partial x_i} dx_i = F + \sum_{i=1}^N \left[\sum_{v=1}^r \frac{\partial f_i}{\partial \alpha_v} d\alpha_v \right] \frac{\partial F}{\partial x_i} \equiv \left[1 - \sum_{v=1}^r d\alpha_v i\hat{X}_v \right] F \quad (2.3.1)$$

where in Eq. 2.3.1,

$$\hat{X}_v \equiv i \sum_{i=1}^N \frac{\partial f_i}{\partial \alpha_v} \frac{\partial}{\partial x_i} \quad (2.3.2)$$

is a generator of infinitesimal transformations. Finite transformations are obtained by:

$$U(\alpha) = \lim_{n \rightarrow \infty} [1 + i(\alpha/n) \cdot X]^n = \exp(i\alpha \cdot X) \quad (2.3.3)$$

where we have written $\sum_{v=1}^r \alpha_v \hat{X}_v = \alpha \hat{X}$.

There is a theorem which states that the commutator of two generators is always a linear combination of the generators

$$[\hat{X}_i, \hat{X}_j] = f_{ij}^k \hat{X}_k \quad (\text{summation over } k \text{ implied})$$

These commutation relations are called the algebra, and the complex numbers f_{ij}^k are called the structure constants of the group. It can be shown that these structure constants fully characterise the multiplication structure of a Lie group.

2.3.1 The $SO(3)$ group

Rotations in three dimensions are usually represented by a matrix R which is 3×3 :

$$\vec{x}' = R\vec{x}$$

It follows that the length is invariant under such transformations, such that $\vec{x}' \cdot \vec{x}' = \vec{x} \cdot \vec{x}$. This in turns implies that $R^\dagger R = I$ so that the matrix R is orthogonal. Based on the previous:

$$1 = \det(R^\dagger R) = \det(R^\dagger) \cdot \det(R) = [\det(R)]^2,$$

which needs $\det(R) = \pm 1$. The matrices with a negative determinant include a parity transformation which is not continuous and thus not connected with the identity of the transformation. This leaves only the matrices with $\det(R) = 1$ to form the elements of the $SO(3)$ group i.e. the *Special Orthogonal group in three dimensions*.

An expansion of R close to the identity matrix I can be written as $R = I + \delta R$, where

$$(I + \delta R)^\dagger (I + \delta R) = I$$

Expanding this expression and keeping terms out to first order one gets:

$$\delta R^\dagger = -\delta R$$

so that δR is an anti-symmetric 3×3 matrix that can be parameterised as

$$\delta R = \begin{pmatrix} 0 & \varepsilon_3 & -\varepsilon_2 \\ -\varepsilon_3 & 0 & \varepsilon_1 \\ \varepsilon_2 & -\varepsilon_1 & 0 \end{pmatrix}$$

An infinitesimal rotation, that transforms x to x' can be written as

$$x' = x + \delta R \times x$$

from where one gets $dx_1 = -\varepsilon_2 x_3 + \varepsilon_3 x_2$, $dx_2 = -\varepsilon_3 x_1 + \varepsilon_1 x_3$ and $dx_3 = -\varepsilon_1 x_2 + \varepsilon_2 x_1$.

Since the transformation in the neighbourhood of the identity is then given by

$$dx_i = \sum_{v=1}^3 \frac{\partial f_i}{\partial \alpha_v} d\alpha_v,$$

it is easy to see that $d\alpha_1 \equiv \varepsilon_1$, $d\alpha_2 \equiv \varepsilon_2$ and $d\alpha_3 \equiv \varepsilon_3$. It follows that

$$\frac{\partial f_1}{\partial \alpha_1} = 0$$

$$\frac{\partial f_1}{\partial \alpha_2} = -x_3$$

$$\frac{\partial f_1}{\partial \alpha_3} = x_2$$

$$\frac{\partial f_2}{\partial \alpha_1} = x_3$$

$$\frac{\partial f_2}{\partial \alpha_2} = 0$$

$$\frac{\partial f_2}{\partial \alpha_3} = -x_1$$

$$\frac{\partial f_3}{\partial \alpha_1} = -x_2$$

$$\frac{\partial f_3}{\partial \alpha_2} = x_1$$

$$\frac{\partial f_3}{\partial \alpha_3} = 0$$

The generators, as we have seen before, are generally given by $\hat{X}_v \equiv i \sum_{i=1}^N \frac{\partial f_i}{\partial \alpha_v} \frac{\partial}{\partial x_i}$ (see Eq. 2.3.2). This gives the generators of the SO(3) group:

$$\hat{X}_1 = ix_3 \frac{\partial}{\partial x_2} - ix_2 \frac{\partial}{\partial x_3}$$

$$\hat{X}_2 = ix_1 \frac{\partial}{\partial x_3} - ix_3 \frac{\partial}{\partial x_1}$$

$$\hat{X}_3 = ix_2 \frac{\partial}{\partial x_1} - ix_1 \frac{\partial}{\partial x_2}$$

These generators are easily recognised as the quantum mechanical angular momentum operators:

$$\hat{X} = x \times (-i)\nabla$$

which satisfies the SO(3) algebra $[\hat{X}_i, \hat{X}_j] = i\epsilon_{ijk}\hat{X}_k$.

2.3.2 The SU(2) group

For the SU(2) group, the infinitesimal transformation acting on a general complex two-component column vector as

$$\begin{pmatrix} q_1' \\ q_2' \end{pmatrix} = (1 + i\epsilon\tau/2) \begin{pmatrix} q_1 \\ q_2 \end{pmatrix}$$

so that from

$$dx_i = \sum_{v=1}^r \frac{\partial f_i}{\partial \alpha_v} d\alpha_v,$$

we get

$$dq_1 = \frac{i\epsilon_3}{2}q_1 + \left(\frac{i\epsilon_1}{2} + \frac{\epsilon_2}{2}\right)q_2$$

$$dq_2 = \frac{-i\varepsilon_3}{2}q_2 + \left(\frac{i\varepsilon_1}{2} - \frac{\varepsilon_2}{2}\right)q_1$$

and that $d\alpha_1 \equiv \varepsilon_1$, $d\alpha_2 \equiv \varepsilon_2$ and $d\alpha_3 \equiv \varepsilon_3$. It follows that

$$\frac{\partial f_1}{\partial \alpha_1} = \frac{iq_2}{2}$$

$$\frac{\partial f_1}{\partial \alpha_2} = \frac{q_2}{2}$$

$$\frac{\partial f_1}{\partial \alpha_3} = \frac{iq_1}{2}$$

$$\frac{\partial f_2}{\partial \alpha_1} = \frac{iq_1}{2}$$

$$\frac{\partial f_2}{\partial \alpha_2} = \frac{-q_1}{2}$$

$$\frac{\partial f_2}{\partial \alpha_3} = \frac{-iq_2}{2}$$

The generators that are given by Eq. 2.3.2, are in this case:

$$\hat{X}_1 = -\frac{1}{2} \left[q_2 \frac{\partial}{\partial q_1} + q_1 \frac{\partial}{\partial q_2} \right]$$

$$\hat{X}_2 = \frac{i}{2} \left[q_2 \frac{\partial}{\partial q_1} - q_1 \frac{\partial}{\partial q_2} \right]$$

$$\hat{X}_3 = \frac{1}{2} \left[-q_1 \frac{\partial}{\partial q_1} + q_2 \frac{\partial}{\partial q_2} \right]$$

It is interesting to see that the commutation relation of these generators is the same as the one we saw for the generators of the SO(3) group.

2.3.3 The SU(3) group

For the SU(3) group, the infinitesimal transformation acting on a general three-component column vector as

$$\begin{pmatrix} q_1' \\ q_2' \\ q_3' \end{pmatrix} = (1 + i\eta\lambda/2) \begin{pmatrix} q_1 \\ q_2 \\ q_3 \end{pmatrix}$$

where the η -matrices are 8 (i.e. η_1, \dots, η_8) and λ are the Gell-Mann matrices:

$$\begin{array}{cccc}
\underbrace{\begin{pmatrix} 0 & 1 & 0 \\ 1 & 0 & 0 \\ 0 & 0 & 0 \end{pmatrix}}_{\lambda_1} & \underbrace{\begin{pmatrix} 0 & -i & 0 \\ i & 0 & 0 \\ 0 & 0 & 0 \end{pmatrix}}_{\lambda_2} & \underbrace{\begin{pmatrix} 1 & 0 & 0 \\ 0 & -1 & 0 \\ 0 & 0 & 0 \end{pmatrix}}_{\lambda_3} & \underbrace{\begin{pmatrix} 0 & 0 & 1 \\ 0 & 0 & 0 \\ 1 & 0 & 0 \end{pmatrix}}_{\lambda_4} \\
\underbrace{\begin{pmatrix} 0 & 0 & -i \\ 0 & 0 & 0 \\ i & 0 & 0 \end{pmatrix}}_{\lambda_5} & \underbrace{\begin{pmatrix} 0 & 0 & 0 \\ 0 & 0 & 1 \\ 0 & 1 & 0 \end{pmatrix}}_{\lambda_6} & \underbrace{\begin{pmatrix} 0 & 0 & 0 \\ 0 & 0 & -i \\ 0 & i & 0 \end{pmatrix}}_{\lambda_7} & \underbrace{\frac{1}{\sqrt{3}} \begin{pmatrix} 1 & 0 & 0 \\ 0 & 1 & 0 \\ 0 & 0 & -2 \end{pmatrix}}_{\lambda_8}
\end{array}$$

The first three generators of the SU(3) group are the same as the ones of the SU(2):

$$\hat{G}_1 = -\frac{1}{2} \left[q_2 \frac{\partial}{\partial q_1} + q_1 \frac{\partial}{\partial q_2} \right]$$

$$\hat{G}_2 = \frac{i}{2} \left[q_2 \frac{\partial}{\partial q_1} - q_1 \frac{\partial}{\partial q_2} \right]$$

$$\hat{G}_3 = \frac{1}{2} \left[-q_1 \frac{\partial}{\partial q_1} + q_2 \frac{\partial}{\partial q_2} \right]$$

The remaining of the generators can be constructed by Eq. 2.3.2 and they respect the algebra:

$$[\hat{G}_i, \hat{G}_j] = i f_{ijk} \hat{G}_k$$

where i, j, k run from 1 to 8 and the constants f_{ijk} are known as the structure constants.

2.4 Spin and angular momentum

In quantum mechanics we can not measure all three components of the angular momentum. What is normally done is to measure the magnitude L^2 and the third component L_z which is allowed to have only certain values due to the quantisation. In particular the magnitude L^2 takes always values of the form:

$$L^2 \rightarrow l(l+1)\hbar,$$

where l is a non-negative integer $l : 0, 1, 2, \dots$. For a given value of l a measurement of the third component yields a value of the form $m_l \hbar$, where m_l is an integer in the range $[-l, l]$ i.e. $m_l : -l, -l+1, \dots, 0, \dots, l-1, l$. Figure 2.2 presents the possible orientations of the angular momentum vector for $l = 2$.

Similarly for the spin of a particle, one can measure its magnitude S^2 and the third component S_z . The value of S^2 can be of the form:

$$S^2 \rightarrow s(s+1)\hbar$$

In the case of the spin though, the quantum number s can take half-integer values as well as integer ones i.e. $s : 0, 1/2, 1, 3/2, 2, 5/2, 3, 7/2, \dots$. For a given value of s , its third component S_z can have values of the form $m_s \hbar$, where m_s is an integer or half integer in the range of $[-s, s]$ i.e. $m_s : -s, -s+1, \dots, 0, \dots, s-1, s$. Both L_z and S_z can take $2k+1$ values, where k is either l or s , respectively.

Every particle can have any value of angular momentum but their spin is fixed. We call particles with half integer spin fermions (e.g. leptons, quarks, baryons) and the ones with integer spin bosons (e.g. mesons and force mediators).

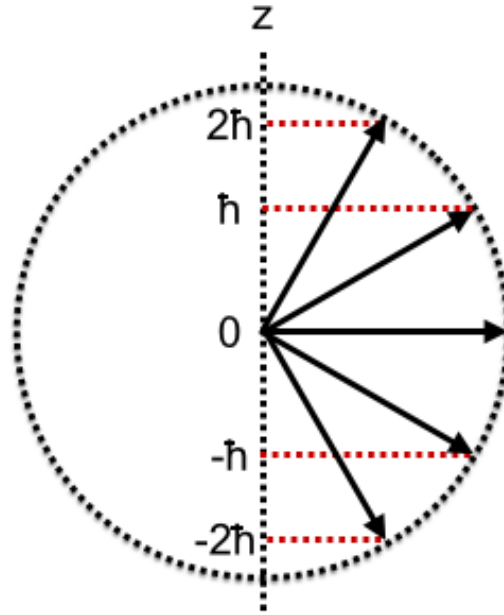


Fig. 2.2: Possible orientations of the angular momentum vector for $l = 2$.

Angular momentum and spin states are usually represented with a 'ket' i.e. $|l, m_l\rangle$ and $|s, m_s\rangle$. It can be that we are not interested in the value of the angular momentum or the spin separately but rather in the value of the total angular momentum $\vec{J} = \vec{L} + \vec{S}$. It can also be that we are interested in the relevant values of the total momentum of a particle, composed by e.g. a quark and an anti-quark that, as we will see later, is called a meson. Combining angular momenta of two particles implies combining two states $|j_1, m_1\rangle$ and $|j_2, m_2\rangle$. Adding the third component is done naturally by

$$m = m_1 + m_2$$

But for the magnitude, it turns out that the quantum number j can take any value from $|j_1 - j_2|$ up to $|j_1 + j_2|$ in integer steps:

$$j = |j_1 - j_2|, |j_1 - j_2| + 1, \dots, (j_1 + j_2) - 1, (j_1 + j_2)$$

Example A: What are the possible spin states of a meson, composed from a quark and an anti-quark in a state of 0 angular momentum?

Every quark carries spin of $1/2$, which means that the meson will carry a value of $|s_1 - s_2|$ or $s_1 + s_2$ i.e. 0 or 1. Mesons with spin-0 are called **pseudo-scalar mesons**, while the ones with spin-1 are called **vector mesons**.

Example B: What are the possible spin states of a baryon, composed from three quarks in a state of 0 angular momentum?

Combining two quarks, one gets a state with values $s_{12} : |s_1 - s_2|, s_1 + s_2$, which means that $s_{12} = 0$ or $s_{12} = 1$. Adding the third quark, one gets:

- For $s_{12} = 0$: $s_{123} : |s_{12} - s_3|, s_{12} + s_3 = |s_3|$ which means that $s = 1/2$.
- For $s_{12} = 1$: $s_{123} : |s_{12} - s_3|, \dots, s_{12} + s_3$ which means that $s = 1/2$ or $s = 3/2$.

2.4.1 Clebsch-Gordan coefficients

There are cases where instead of the total angular momentum, one requires the knowledge of the decomposition into the two different states $|j_1, m_1\rangle|j_2, m_2\rangle$ into states of total angular momentum $|j, m\rangle$:

$$|j_1, m_1\rangle|j_2, m_2\rangle = \sum_{j=|j_1-j_2|}^{(j_1+j_2)} C_{mm_1m_2}^{jj_1j_2} |j, m\rangle, \quad (2.4.1)$$

where $m = m_1 + m_2$. The numbers $C_{mm_1m_2}^{jj_1j_2}$ are called the Clebsch-Gordan coefficients. These numbers give the probability of getting a value of $j \cdot (j+1)\hbar$ for any allowed j if we measure J^2 on a system consisting of two angular momentum states $|j_1, m_1\rangle$ and $|j_2, m_2\rangle$. Figure 2.3 presents part of the Clebsch-Gordan coefficients extracted from the Particle Data Group (PDG). The square of the coefficients is given, which means that the reader should take the square root.

Example C: The electron in the hydrogen atom occupies the orbital status $|2, -1\rangle$ and the spin state $|1/2, 1/2\rangle$. What are the values of J^2 and what is the probability of each one of them?

The z-component of the angular momentum is $m = m_1 + m_2 = -1/2$. The possible states of the total angular momentum j are $j = l - s = 3/2$ and $j = l + s = 5/2$. Thus the two different states can be $|3/2, -1/2\rangle$ and $|5/2, -1/2\rangle$. We now need to extract the Clebsch-Gordan coefficients for the following final decomposition:

$$|2, -1\rangle|1/2, 1/2\rangle = a \cdot |3/2, -1/2\rangle + b \cdot |5/2, -1/2\rangle$$

The coefficients can be found in fig. 2.3 by looking at the table labeled $2 \times 1/2$ (i.e. combining a $j_1 = 2$ with a $j_2 = 1/2$ states) and finding the the horizontal row labeled $-1, 1/2$ (i.e. combining a $m_1 = -1$ with a $m_2 = 1/2$ states). The relevant values are $2/5$ and $-3/5$, which means that $a = -\sqrt{3/5}$ and $b = \sqrt{2/5}$. The final decomposition can thus be written as

$$|2, -1\rangle|1/2, 1/2\rangle = -\sqrt{3/5} \cdot |3/2, -1/2\rangle + \sqrt{2/5} \cdot |5/2, -1/2\rangle$$

The probability of getting $j = 3/2$ is $3/5$ and the relevant value for $j = 5/2$ is $2/5$.

Example D: The combination of a quark and an antiquark (see example-A) gives spin-0 and spin-1 states. What is the Clebsch-Gordan decomposition of these states?

The angular momentum states of the two quarks are:

- $|1/2, 1/2\rangle|1/2, 1/2\rangle$
- $|1/2, -1/2\rangle|1/2, 1/2\rangle$
- $|1/2, 1/2\rangle|1/2, -1/2\rangle$
- $|1/2, -1/2\rangle|1/2, -1/2\rangle$

Consulting the $1/2 \times 1/2$ table one gets the following decomposition:

$$|1/2, 1/2\rangle|1/2, 1/2\rangle = |1, 1\rangle$$

$$|1/2, -1/2\rangle|1/2, 1/2\rangle = \frac{1}{\sqrt{2}}|1, 0\rangle - \frac{1}{\sqrt{2}}|0, 0\rangle$$

$$|1/2, 1/2\rangle|1/2, -1/2\rangle = \frac{1}{\sqrt{2}}|1, 0\rangle + \frac{1}{\sqrt{2}}|0, 0\rangle$$

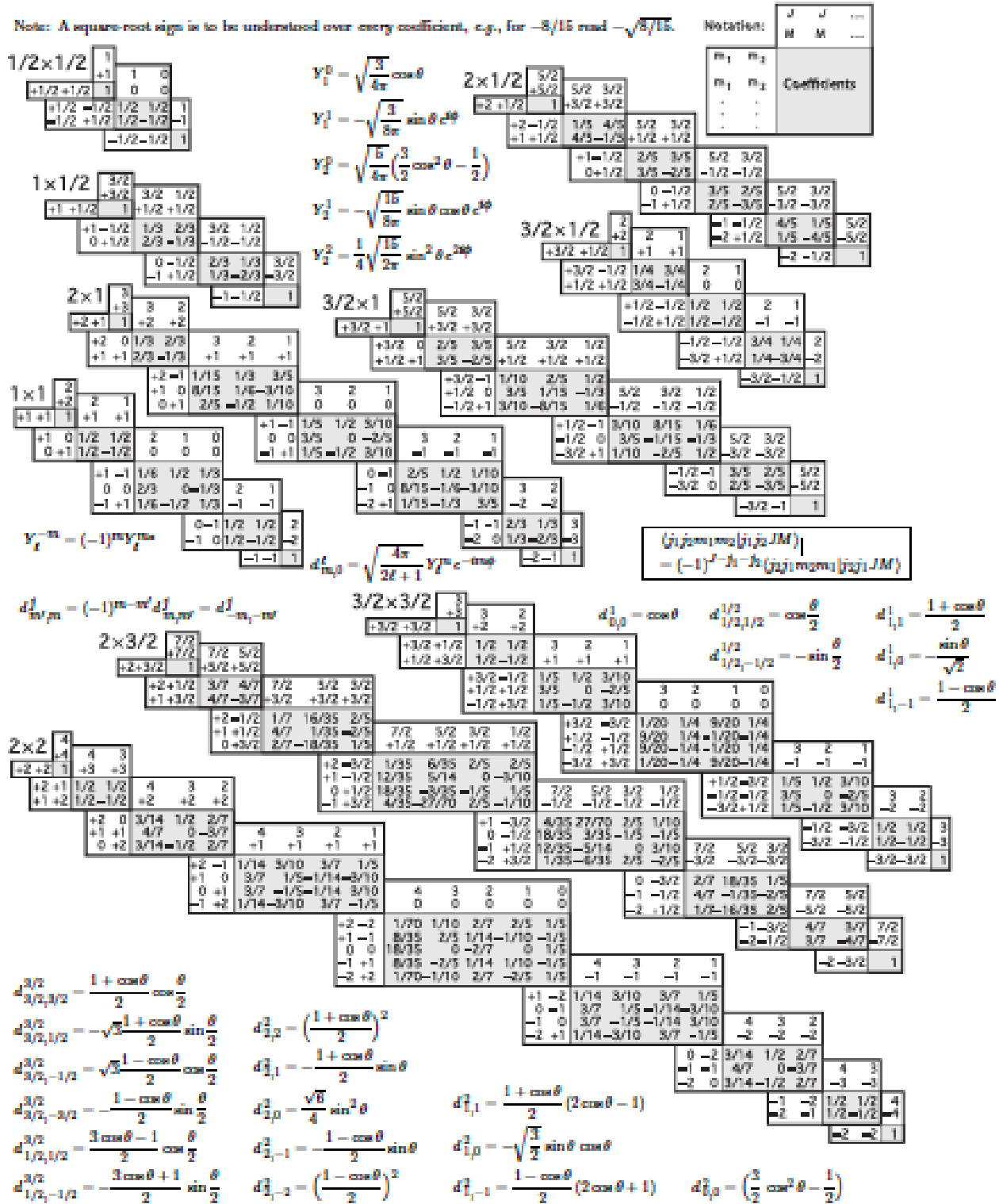


Fig. 2.3: The Clebsch-Gordan coefficients extracted from the Particle Data Group (PDG). The square of the coefficients is given, which means that the reader should take the square root.

$$|1/2, -1/2\rangle|1/2, -1/2\rangle = |1, -1\rangle$$

Inversely, the spin-0 final state can be written as:

$$|0, 0\rangle = \frac{1}{\sqrt{2}} [|1/2, 1/2\rangle|1/2, -1/2\rangle - |1/2, -1/2\rangle|1/2, 1/2\rangle]$$

The spin-1 states are written as:

$$|1, 1\rangle = |1/2, 1/2\rangle|1/2, 1/2\rangle$$

$$|1, 0\rangle = \frac{1}{\sqrt{2}} [|1/2, 1/2\rangle|1/2, -1/2\rangle + |1/2, -1/2\rangle|1/2, 1/2\rangle]$$

$$|1, -1\rangle = |1/2, -1/2\rangle|1/2, -1/2\rangle$$

2.4.2 Isospin symmetry

After the discovery of the neutron by Chadwick in 1932, the near equality of its mass (939.5 MeV) to that of the proton (938.3 MeV) suggested to Heisenberg that, as far as the strong interactions are concerned, these are two nearly degenerate states of one particle: the nucleon.

This ‘isospin symmetry’ of the strong force is further supported by, for instance, the observation of very similar energy levels in mirror nuclei (the number of protons in one, is equal to number of neutrons in the other, and *vice versa*, like in ${}^{13}_7\text{N}$ and ${}^{13}_6\text{C}$).

In addition, apart from the p-n doublet, there are other particles that are nearly degenerate in mass, like the pion triplet (~ 140 MeV) and the quadruplet of Δ resonances (~ 1.23 GeV). This looks like the doublet, triplet and quadruplet structure of spin- $\frac{1}{2}$, spin-1 and spin- $\frac{3}{2}$ systems built from spin- $\frac{1}{2}$ states, and is thus strongly suggestive of hadronic substructure.

We know today that hadrons are built up from quarks and we can explain isospin symmetry from the fact that the strong interaction is insensitive to the quark flavour. The mass differences within the nucleon, π and Δ multiplets are, after electromagnetic correction, believed to be due to the difference in the u and d quark masses.

The invariance for p to n transitions obeys the mathematics of ordinary spin, hence the term ‘isospin’. The reason is that transitions in any 2-state quantum mechanical system are described by the special unitary group SU(2), as will become clear next.

We work in a 2-dim Hilbert space spanned by the basis vectors³

$$|p\rangle = \begin{pmatrix} 1 \\ 0 \end{pmatrix} \quad \text{and} \quad |n\rangle = \begin{pmatrix} 0 \\ 1 \end{pmatrix}$$

The Hermitian conjugates are $\langle p| = (1, 0)$ and $\langle n| = (0, 1)$. An arbitrary state is written as the linear combination

$$|\psi\rangle = \alpha |p\rangle + \beta |n\rangle$$

Because $|\alpha|^2$ is the probability to find the system in a $|p\rangle$ state and $|\beta|^2$ the same for the $|n\rangle$ state we must have, for any state $|\psi\rangle$,

$$\langle \psi | \psi \rangle = |\alpha|^2 + |\beta|^2 = 1$$

³ When we talk about quarks we will use the notation $|u\rangle$ and $|d\rangle$ instead.

We have seen already that a transformation $|\psi'\rangle = U|\psi\rangle$ must preserve the norm so that U must be unitary: $U^\dagger U = 1$.

Taking determinants we find

$$\det(U^\dagger U) = \det(U^\dagger) \det(U) = \det(U)^* \det(U) = 1$$

Therefore $\det(U) = e^{i\phi}$ with ϕ some arbitrary phase factor.

So we may set $U = e^{i\phi} V$ with $\det(V) = 1$. Invariance for phase shifts is called a U(1) invariance and leads to charge conservation, as we will see later. The charge conserved in the p-n case here is not electrical charge, but **baryon number**

$$A = (N_p - N_{\bar{p}}) + (N_n - N_{\bar{n}})$$

Putting U(1) invariance aside, we have to deal with unitary 2×2 matrices V with unit determinant, that is, with the group SU(2).

2.5 The quark model

During the decade of 1960, a number of new states i.e. baryon and meson resonances were discovered. The pattern of the multiplets that these particles form was accounted for in terms of quark constituents. This was the basis of the so-called quark model that we are going to discuss in this paragraph.

According to the quark model all hadrons are formed from a combination of quarks bound together by the strong force. The fundamental representation of SU(3) is a triplet which is the multiplet from which every other multiplet can be deduced. Figure 2.4 presents the quark (left) and antiquark (right) multiplets in SU(3). The two axis of the figure present the isospin I_3 (i.e. x-axis) and hyper charge $Y \equiv B + S$, where B and S are the baryon and strangeness numbers, respectively. Each quark is assigned spin-1/2 and baryon number $B = 1/3$. Baryons consist of three quarks and mesons of a combination of one quark and one anti-quark. The charge of each quark is given by

$$Q = I_3 + \frac{Y}{2}$$

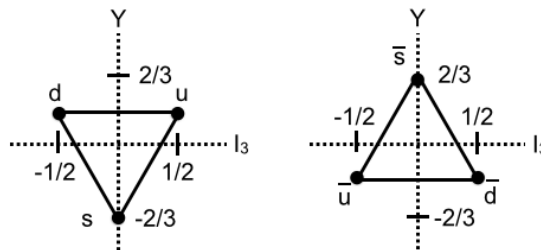


Fig. 2.4: The SU(3) quark (left) and antiquark (right) multiplets.

Mesons consist of a combination of one quark with one anti-quark. In terms of group theory, and for three quark flavours, the quarks are represented by the triplet, fundamental representation of SU(3) denoted as 3 , whereas the anti-quarks form the conjugate representation $\bar{3}$. For these three quark flavours, we have nine combinations of $q\bar{q}$. These nine states divide into an SU(3) octet and singlet as can be seen in fig. 2.5:

$$3 \otimes \bar{3} = 8 \oplus 1$$

The combinations of quarks and anti-quarks that have $Y = 0$ and $I_3 = 0$ consist of combinations of $u\bar{u}$, $d\bar{d}$ and $s\bar{s}$ states. One of them is taken to be the member of the isospin triplet π^-, X_1, π^+ and thus is identified as the neutral pion (π^0). The

other is the singlet and contains all combinations on equal footing and is identified as the η' : $(u\bar{u} + d\bar{d} + s\bar{s})/\sqrt{3}$. Finally the remaining particle is the η -meson which contains η : $(u\bar{u} + d\bar{d} - 2s\bar{s})/\sqrt{6}$.

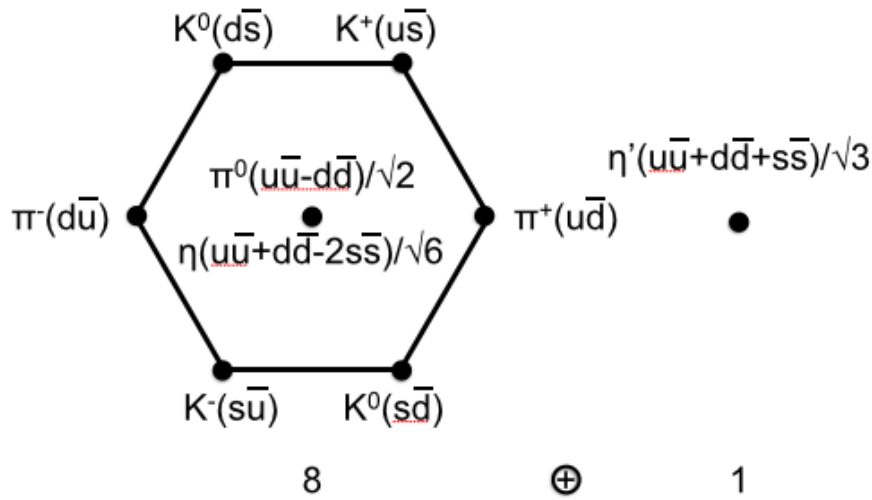


Fig. 2.5: The SU(3) octet (left) and singlet (right) that form the lightest pseudo-scalar meson multiplet.

For the same three quark flavours, we have 27 possible qqq combinations that form the lightest baryon multiplets. In order to discover these multiplets we first need to combine two quarks that form nine different states i.e. six symmetric (interchange of two quarks leaves the state untouched) and 3 antisymmetric (interchange of two quarks changes the sign of the wave function):

$$3 \otimes 3 = 6 \oplus \bar{3}$$

The resulting multiplets of the two-quark states are illustrated in fig.2.6

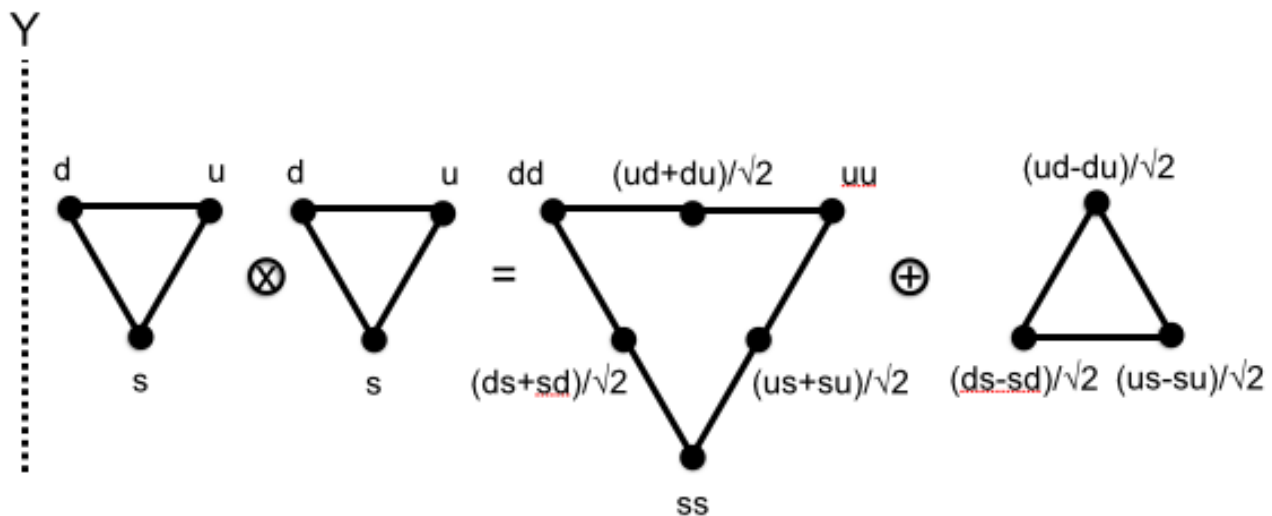


Fig. 2.6: The SU(3) lightest baryon multiplets.

What remains to be done is to combine another quark which leads to

$$3 \otimes 3 \otimes 3 = (3 \otimes 3) \otimes 3 = (6 \oplus \bar{3}) \otimes 3 = (6 \otimes 3) \oplus (\bar{3} \otimes 3) = 10 \oplus 8 \oplus 8 \oplus \bar{1}$$

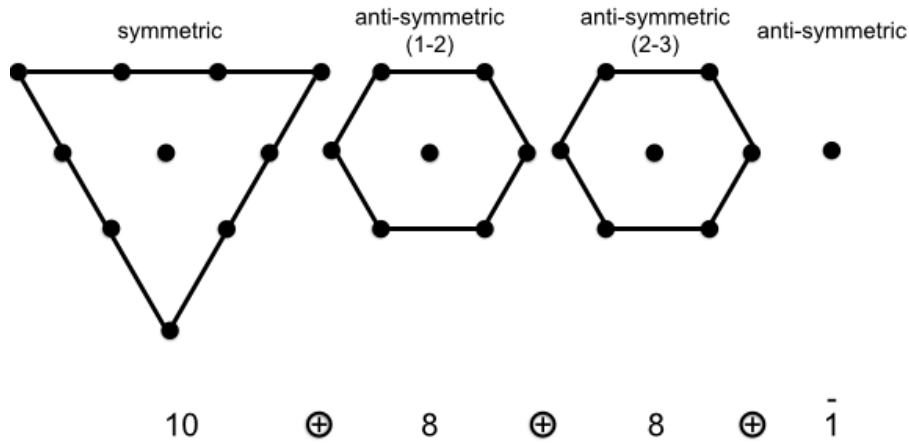


Fig. 2.7: The SU(3) lightest baryon multiplets.

The singlet state is completely anti-symmetric and consists of the linear combination:

$$(uds - usd + dsu - dus + sud - sdu)/\sqrt{6}$$

The second multiplet (i.e. octet) is partially anti-symmetric i.e. it is anti-symmetric under the interchange of the first and the second quark and can be seen in fig. 2.8.

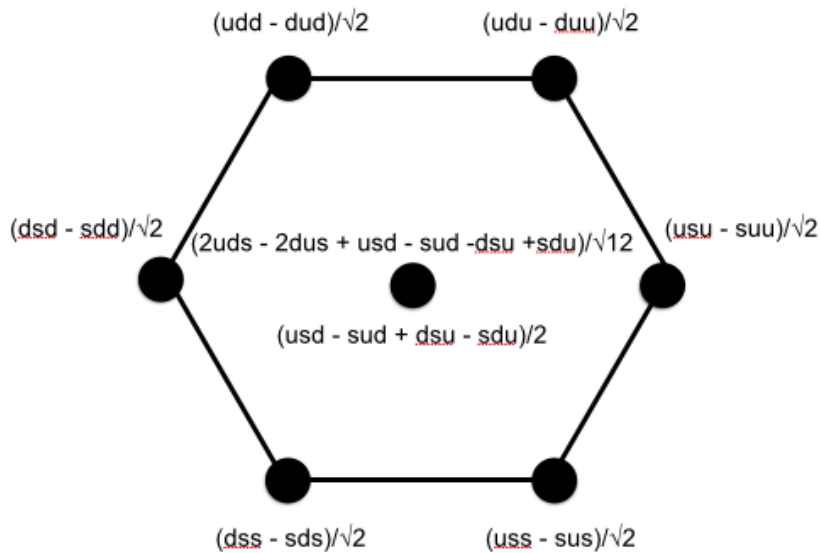


Fig. 2.8: The first anti-symmetric baryon octet.

The third multiplet (i.e. octet) is also partially anti-symmetric i.e. it is anti-symmetric under the interchange of the second and the third quark and can be seen in fig. 2.9. We can also construct one octet which is anti-symmetric under the interchange of the first and the third quarks but this will not be independent.

Finally the first multiplet (i.e. 10) is completely symmetric under any interchange of quarks and can be seen in fig. 2.10.

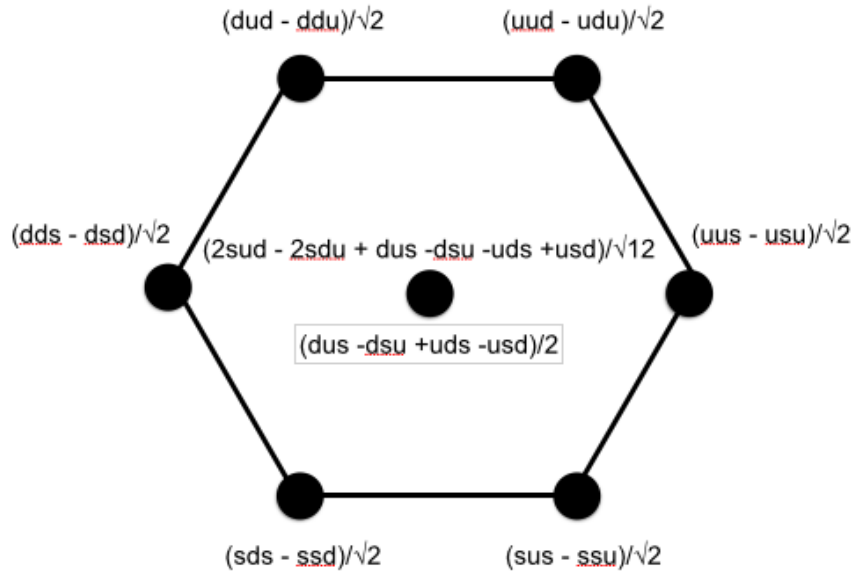


Fig. 2.9: The second anti-symmetric baryon octet.

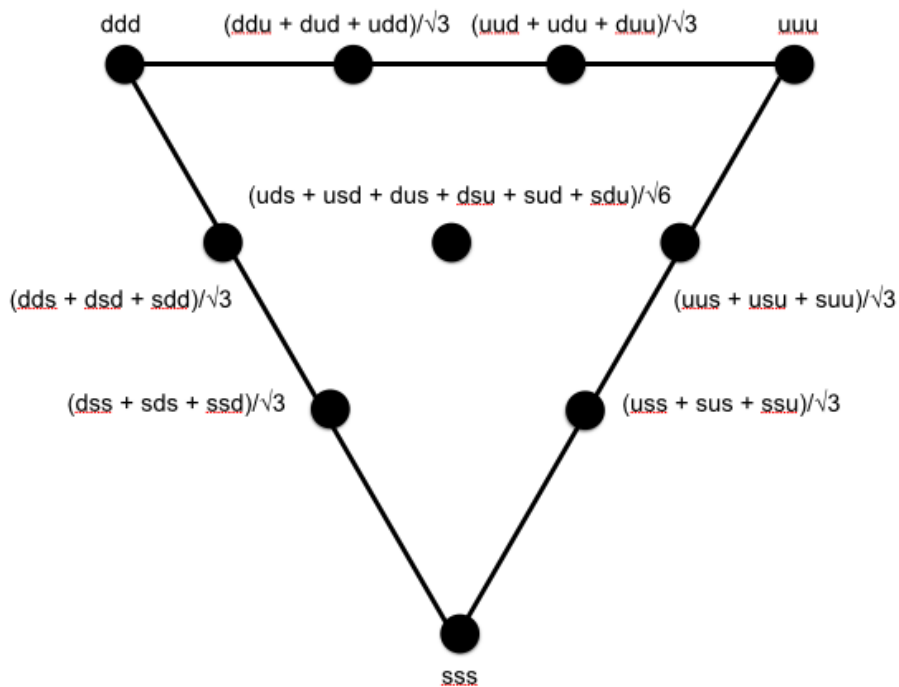


Fig. 2.10: The fully symmetric baryon multiplet.

2.6 A new quantum number: colour

One of the major achievements of quantum field theory was the proof of the connection between spin and statistics:

- bosons, described by the Bose-Einstein statistics, have integer spin and have symmetric wave functions i.e. $\psi(1,2) = \psi(2,1)$,
- fermions, (described by the Fermi-Dirac statistics, have half-integer spin and have anti-symmetric wave functions i.e. $\psi(1,2) = -\psi(2,1)$.

Suppose that we have two particles and one is in state ψ_α and the other in ψ_β . If these two particles are different (e.g. an electron and a muon), then one can discuss about which of the two is in which state. Depending on the answer, we can have $\psi(1,2) = \psi_\alpha(1)\psi_\beta(2)$ or $\psi(1,2) = \psi_\alpha(2)\psi_\beta(1)$. However, if the particles are identical, then if they are bosons then the wave function is a symmetric combination of ψ_α and ψ_β :

$$\psi(1,2) = \frac{1}{\sqrt{2}}[\psi_\alpha(1)\psi_\beta(2) + \psi_\alpha(2)\psi_\beta(1)]$$

On the other hand, if the two particles are identical fermions then the wave function is anti-symmetric:

$$\psi(1,2) = \frac{1}{\sqrt{2}}[\psi_\alpha(1)\psi_\beta(2) - \psi_\alpha(2)\psi_\beta(1)]$$

That implies that if one tries to put two identical fermions in the same state then the final wave function collapses to 0 i.e. 0 probability for this state to exist. This is another manifestation of the Pauli exclusion principle.

The wave functions of particles up to this moment consist of the part that describe space and time ($\psi(\vec{r},t)$), the part that describe the spin ($\psi(s)$) and the part that describe the flavour ($\psi(flavour)$), such that ($\psi = \psi(\vec{r},t) \cdot \psi(s) \cdot \psi(flavour)$). This representation seems to be problematic if one considers e.g. the *uuu* baryon state (the so-called Δ^{++}). This baryon that consists of three identical fermions, should have an anti-symmetric wave function, however the function at this stage seems to be symmetric. To cure this, a new quantum number is introduced, the one of colour, with three possible values: red (*R*), green (*G*) and blue (*B*). The combination of quarks with different colours is done in such a way so that all hadrons are colourless particles. Thus, the wave function now reads

$$\psi = \psi(\vec{r},t) \cdot \psi(s) \cdot \psi(flavour) \cdot \psi(colour)$$

The colour quantum number can be represented by a single column matrix:

$$\begin{pmatrix} 1 \\ 0 \\ 0 \end{pmatrix} \text{ for R}$$

$$\begin{pmatrix} 0 \\ 1 \\ 0 \end{pmatrix} \text{ for B}$$

$$\begin{pmatrix} 0 \\ 0 \\ 1 \end{pmatrix} \text{ for G}$$

The quarks interact with each other, with the possibility to change the relevant colour. This is usually done at the quark-gluon vertex as we will see in the next chapters. This interaction is mediated by the gluons that carry the supplementary colour (and anti-colour). There are nine gluon species which are described by the SU(3) color symmetry:

$$3 \otimes 3 = 8 \oplus \bar{1}$$

The octet consists of the following states:

$$|1\rangle = \frac{1}{\sqrt{2}}(R\bar{B} + B\bar{R})$$

$$|2\rangle = \frac{1}{\sqrt{2}}[-i(R\bar{B} - B\bar{R})]$$

$$|3\rangle = \frac{1}{\sqrt{2}}(R\bar{R} - B\bar{B})$$

$$|4\rangle = \frac{1}{\sqrt{2}}(R\bar{G} + G\bar{R})$$

$$|5\rangle = \frac{1}{\sqrt{2}}[-i(R\bar{G} - G\bar{R})]$$

$$|6\rangle = \frac{1}{\sqrt{2}}(B\bar{G} + G\bar{B})$$

$$|7\rangle = \frac{1}{\sqrt{2}}[-i(B\bar{G} - G\bar{B})]$$

$$|8\rangle = \frac{1}{\sqrt{6}}(R\bar{R} + B\bar{B} - 2G\bar{G})$$

The colour singlet is formed by $|9\rangle = \frac{1}{\sqrt{3}}(R\bar{R} + B\bar{B} + G\bar{G})$. This last configuration is not physical. As we will see in Chapter 9, confinement requires that all naturally occurring particles are colour singlet states. This explains why the colour octet states can not be seen in nature. But $|9\rangle$ is also a colour singlet, and thus would have been easy to detect in nature, as a free particle. In addition, being a state of a mediator it could be exchanged by e.g. a proton and a neutron (i.e. colour singlet states) which would imply that the strong force is long range, while we know that it is short range. All these indicates that the colour singlet $|9\rangle$ does not occur in our world.

Finally, like in the (iso)spin case we can write a unitary transformation as

$$|\psi'\rangle = U|\psi\rangle = \exp(ia \cdot \lambda/2)|\psi\rangle \equiv \exp(ia \cdot T)|\psi\rangle$$

The generators λ are now Hermitian 3×3 matrices. A complex 3×3 matrix is characterised by 18 numbers but only 8 are independent because the matrices are Hermitian, and traceless since $\det U = 1$. Thus there are 8 independent generators. The 8 Gell-Mann matrices (with Pauli matrices inside!) are

$$\begin{array}{cccc} \underbrace{\begin{pmatrix} 0 & 1 & 0 \\ 1 & 0 & 0 \\ 0 & 0 & 0 \end{pmatrix}}_{\lambda_1} & \underbrace{\begin{pmatrix} 0 & -i & 0 \\ i & 0 & 0 \\ 0 & 0 & 0 \end{pmatrix}}_{\lambda_2} & \underbrace{\begin{pmatrix} 1 & 0 & 0 \\ 0 & -1 & 0 \\ 0 & 0 & 0 \end{pmatrix}}_{\lambda_3} & \underbrace{\begin{pmatrix} 0 & 0 & 1 \\ 0 & 0 & 0 \\ 1 & 0 & 0 \end{pmatrix}}_{\lambda_4} \\ \underbrace{\begin{pmatrix} 0 & 0 & -i \\ 0 & 0 & 0 \\ i & 0 & 0 \end{pmatrix}}_{\lambda_5} & \underbrace{\begin{pmatrix} 0 & 0 & 0 \\ 0 & 0 & 1 \\ 0 & 1 & 0 \end{pmatrix}}_{\lambda_6} & \underbrace{\begin{pmatrix} 0 & 0 & 0 \\ 0 & 0 & -i \\ 0 & i & 0 \end{pmatrix}}_{\lambda_7} & \underbrace{\frac{1}{\sqrt{3}} \begin{pmatrix} 1 & 0 & 0 \\ 0 & 1 & 0 \\ 0 & 0 & -2 \end{pmatrix}}_{\lambda_8} \end{array}$$

The algebra of the SU(3) group is given by the commutation relation of the matrices $T_a = \lambda_a/2$: $[T_a, T_b] = if_{ab}^c T_c$. The parameters f_{ab}^c are called **structure constants**. These structure constants f_{ab}^c are antisymmetric in the exchange of two indices. The non-zero ones are:

$$\begin{aligned} f_{12}^3 &= 1 \\ f_{14}^7 &= f_{16}^5 = f_{24}^6 = f_{25}^7 = f_{34}^5 = f_{37}^6 = \frac{1}{2} \\ f_{45}^8 &= f_{67}^8 = \frac{1}{2}\sqrt{3} \end{aligned}$$

Chapter 3

The Lagrangian formalism of Quantum Chromo Dynamics (QCD)

The next pillar of the Standard Model that will be briefly presented is the one that describes the strong interactions. The gauge theory is called Quantum Chromo Dynamics or QCD and explains how the world of the smallest building blocks of ordinary matter, the quarks and the gluons, works. QCD shares a number of similarities with QED and thus we will profit from the experience that we gained from previous courses (e.g. PP1) to explore the fundamental properties of our theory. However, it is essential to point out that QCD, being by far more complicated than QED, has a number of fundamental differences compared to the theory that is based on U(1) transformations. Thus a large part of the current chapter will be devoted to highlighting these differences.

Once again, we will start by the Dirac Lagrangian that describes the dynamics of a free particle, this time a quark. We will then impose a more complicated transformation described by the SU(3) group, the underlying group of QCD. The requirement of local gauge invariance will automatically lead us to the term of the QCD Lagrangian that reflects the interactions between the free particle and the field. The kinetic term of this field will be derived again from the Proca Lagrangian. Requiring local gauge invariance also for this term, will reveal the nature of the QCD field: eight massless fields, the gluons.

We will then proceed by looking at a number of QCD processes with the help of the, known to us by now, Feynman diagrams. After a small recap of the similarities and the differences between QED and QCD we will focus on one of the main, fundamental differences between the two gauge theories: we will see how the strong coupling constant behaves depending on how “soft“ or “hard“ a process is (reflected by the momentum transfer). This discussion will naturally lead to the introduction of two of the main characteristics of QCD: confinement and asymptotic freedom.

We will conclude the chapter by briefly discussing about QCD processes known as deep inelastic scattering. Through this discussion we are going to see how one can probe the distribution functions of valence and sea quarks inside nucleons. Finally, we will talk about the remaining part inside nucleons: the gluon distribution functions.

3.1 A small recap from QED

Let us briefly summarise the steps we followed in QED to derive the overall Lagrangian density of the gauge theory:

- We started off with the Dirac Lagrangian that describes a free particle (e.g. a lepton) of the form:

$$\mathcal{L} = i\bar{\Psi}\gamma_{\mu}\partial^{\mu}\Psi - m\bar{\Psi}\Psi$$

- We then made a transformation of the form $U = e^{ig\Lambda}$, that transforms the eigenfunction as $\Psi' = e^{ig\Lambda}\Psi$, where g is a constant and Λ is a scalar. This is, as we saw, a U(1) transformation, a rotation with a phase $g\Lambda$.
- We then promoted the transformation from global to local by adding a dependence of Λ on space and/or time such that $\Lambda = \Lambda(\vec{x}, t) = \Lambda(x^{\mu})$.
- Applying this local transformation to the Lagrangian density, we saw that

$$\mathcal{L}' = i\bar{\Psi}\gamma_\mu\partial^\mu\Psi + i\bar{\Psi}\gamma_\mu\left(ig\partial^\mu\Lambda\right)\Psi - m\bar{\Psi}\Psi \neq \mathcal{L}$$

- The second term of the previous equation is responsible for breaking the invariance. Why is the invariance broken? Because of the dependence of the scalar Λ on space and time (note that now $\Lambda = \Lambda(\vec{x}, t) = \Lambda(x^\mu)$), which leads to

$$\partial^\mu\Psi' = \partial^\mu\left(e^{ig\Lambda}\Psi\right) = e^{ig\Lambda}\partial^\mu\Psi + ig e^{ig\Lambda}\left(\partial^\mu\Lambda\right)\Psi = e^{ig\Lambda}\left[\partial^\mu + ig\left(\partial^\mu\Lambda\right)\right]\Psi \neq e^{ig\Lambda}\partial^\mu\Psi$$

- How do we cure this? We tried to absorb the term that breaks the invariance, $\partial^\mu + ig\left(\partial^\mu\Lambda\right)$, by introducing a covariant derivative $D^\mu = \partial^\mu + ig\left(\partial^\mu\Lambda\right)$ in the place of the partial derivative ∂^μ .
- This automatically leads to the introduction of a new vector field A^μ , such that $D^\mu = \partial^\mu + igA^\mu$.
- We then request local gauge invariance. Since this can't be achieved with the partial derivative, we use the newly introduced covariant derivative, such that after the U(1) transformation we demand that

$$D'_\mu\Psi' = e^{ig\Lambda}D_\mu\Psi$$

- It turned out that in order to have local gauge invariance the external vector field A^μ should transform with a given rule, namely

$$A'_\mu = A_\mu - \partial_\mu\Lambda$$

- Adding then the covariant derivative D^μ in the place of the partial derivative ∂^μ in the free Dirac Lagrangian gives:

$$\mathcal{L} = i\bar{\Psi}\gamma_\mu D^\mu\Psi - m\bar{\Psi}\Psi = \bar{\Psi}\left(i\gamma_\mu\partial^\mu\Psi - m\right)\Psi - g\bar{\Psi}\gamma_\mu A^\mu\Psi$$

- The first term in the previous equation (i.e. $\bar{\Psi}\left(i\gamma_\mu\partial^\mu\Psi - m\right)\Psi$) describes the free Dirac Lagrangian density for a lepton or a quark. The second term (i.e. $g\bar{\Psi}\gamma_\mu A^\mu\Psi$) is the interaction term.
- To get the full Lagrangian density of the gauge theory we then added the Proca Lagrangian that describes the field itself:

$$\mathcal{L} = -\frac{1}{4}F_{\mu\nu}F^{\mu\nu} + \frac{1}{2}m^2 A_\mu A^\mu$$

- Applying the same U(1) transformation as before also for this term and requesting local gauge invariance leads to $\mathcal{L}' = \mathcal{L} \Rightarrow m = 0$. This implies that the gauge field is massless i.e. the photon.
- Finally, we also saw that the electromagnetic tensor $F_{\mu\nu} = \partial_\mu A_\nu - \partial_\nu A_\mu$ can be derived by its gauge invariant form: $[D_\mu, D_\nu] = igF_{\mu\nu}$.

3.2 The free Dirac equation

For the case of QCD, we will start again with the Dirac Lagrangian that describes, this time, a free quark:

$$\mathcal{L} = i\bar{\Psi}\gamma_\mu\partial^\mu\Psi - m\bar{\Psi}\Psi \tag{3.2.1}$$

As in the case of QED, also here, we are going to act on it with a transformation. The underlying group that describes the relevant transformations in QCD is not as simple as U(1). These transformations are now described by 3×3 matrices, described by the generators of the SU(3) group. The SU(3) transformation is not of the form

$$U = e^{ig\frac{\lambda}{2}\Lambda}, \quad (3.2.2)$$

where Λ are eight parameters associated with the eight gauge bosons of the theory i.e. the gluons. The matrices λ are all 3×3 matrices also known as Gell-Mann matrices with the form:

$$\begin{aligned} \lambda_1 &= \begin{pmatrix} 0 & 1 & 0 \\ 1 & 0 & 0 \\ 0 & 0 & 0 \end{pmatrix}, \quad \lambda_2 = \begin{pmatrix} 0 & -i & 0 \\ i & 0 & 0 \\ 0 & 0 & 0 \end{pmatrix}, \quad \lambda_3 = \begin{pmatrix} 1 & 0 & 0 \\ 0 & -1 & 0 \\ 0 & 0 & 0 \end{pmatrix}, \quad \lambda_4 = \begin{pmatrix} 0 & 0 & 1 \\ 0 & 0 & 0 \\ 1 & 0 & 0 \end{pmatrix}, \\ \lambda_5 &= \begin{pmatrix} 0 & 0 & -i \\ 0 & 0 & 0 \\ i & 0 & 0 \end{pmatrix}, \quad \lambda_6 = \begin{pmatrix} 0 & 0 & 0 \\ 0 & 0 & 1 \\ 0 & 1 & 0 \end{pmatrix}, \quad \lambda_7 = \begin{pmatrix} 0 & 0 & 0 \\ 0 & 0 & -i \\ 0 & i & 0 \end{pmatrix}, \quad \lambda_8 = \frac{1}{\sqrt{3}} \begin{pmatrix} 1 & 0 & 0 \\ 0 & 1 & 0 \\ 0 & 0 & -2 \end{pmatrix} \end{aligned}$$

3.2.1 Global gauge invariance

Let us again first discuss the case where the transformation is global i.e. the parameters Λ are not a function of space and time but rather a constant. Is the Lagrangian density of Eq. 3.2.1 invariant under these types of transformations?

$$\begin{aligned} \mathcal{L}' &= i\bar{\Psi}' \gamma_\mu \partial^\mu \Psi' - m\bar{\Psi}' \Psi' \\ &= ie^{-ig\frac{\lambda}{2}\Lambda} \bar{\Psi} \gamma_\mu \partial^\mu (e^{ig\frac{\lambda}{2}\Lambda} \Psi) - me^{-ig\frac{\lambda}{2}\Lambda} \bar{\Psi} e^{ig\frac{\lambda}{2}\Lambda} \Psi \end{aligned}$$

Since Λ does not depend on space and time, it can be taken out from the partial derivative in the first term, such that:

$$\begin{aligned} \mathcal{L}' &= ie^{-ig\frac{\lambda}{2}\Lambda} e^{ig\frac{\lambda}{2}\Lambda} \bar{\Psi} \gamma_\mu \partial^\mu \Psi - me^{-ig\frac{\lambda}{2}\Lambda} e^{ig\frac{\lambda}{2}\Lambda} \bar{\Psi} \Psi \\ &= i\bar{\Psi} \gamma_\mu \partial^\mu \Psi - m\bar{\Psi} \Psi \Rightarrow \\ \mathcal{L}' &= \mathcal{L} \end{aligned}$$

We thus reach again the conclusion that our system, described by the Lagrangian density of Eq. 3.2.1, is invariant under global SU(3) transformations.

3.2.2 Local gauge invariance

We will now promote the transformation of Eq. 3.2.2 into a local one, by adding a dependence of Λ on space and/or time i.e. $\Lambda = \Lambda(\vec{x}, t) = \Lambda(x^\mu)$:

$$U = e^{ig\frac{\lambda}{2}\Lambda(x^\mu)}, \quad (3.2.3)$$

where g is still a constant and Λ this time is a scalar field. Let's look at how this transformation alters the Lagrangian density of Eq. 3.2.1 (note that I suppress in the lines below the dependence of Λ on x^μ , however the reader should not misinterpret it as if the dependence is not there!!!):

$$\begin{aligned}\mathcal{L}' &= i\bar{\Psi}' \gamma_\mu \partial^\mu \Psi' - m\bar{\Psi}' \Psi' \\ &= ie^{-ig\Lambda} \bar{\Psi} \gamma_\mu \partial^\mu \left(e^{ig\Lambda} \Psi \right) - me^{-ig\Lambda} \bar{\Psi} e^{ig\Lambda} \Psi\end{aligned}$$

Note that Λ is not a constant but a scalar field i.e. a field whose value depends on space and time. That means that we can not just take it out from the partial derivative of the first term, but instead the derivative has to act on $\Lambda(x^\mu)$:

$$\begin{aligned}\mathcal{L}' &= ie^{-ig\frac{\lambda}{2}\Lambda} \bar{\Psi} \gamma_\mu \left(\partial^\mu e^{ig\frac{\lambda}{2}\Lambda} \right) \Psi + ie^{-ig\frac{\lambda}{2}\Lambda} \bar{\Psi} \gamma_\mu e^{ig\frac{\lambda}{2}\Lambda} \left(\partial^\mu \Psi \right) - me^{-ig\frac{\lambda}{2}\Lambda} e^{ig\frac{\lambda}{2}\Lambda} \bar{\Psi} \Psi \\ &= ie^{-ig\frac{\lambda}{2}\Lambda} \bar{\Psi} \gamma_\mu \left(ig\frac{\lambda}{2} \right) e^{ig\frac{\lambda}{2}\Lambda} \left(\partial^\mu \Lambda \right) \Psi + i\bar{\Psi} \gamma_\mu \partial^\mu \Psi - m\bar{\Psi} \Psi \\ &= -g\frac{\lambda}{2} \bar{\Psi} \gamma_\mu \left(\partial^\mu \Lambda \right) \Psi + i\bar{\Psi} \gamma_\mu \partial^\mu \Psi - m\bar{\Psi} \Psi \\ &= -g\frac{\lambda}{2} \bar{\Psi} \gamma_\mu \left(\partial^\mu \Lambda \right) \Psi + \mathcal{L} \neq \mathcal{L}\end{aligned}$$

It is thus clear that the Lagrangian does not remain invariant under this local gauge transformation. The first term in the equation above is responsible for this, with the underlying reason being that the exponent that describes the transformation can not be taken out from the partial derivative: ∂^μ has to act on $e^{ig\Lambda(x^\mu)}$ since now Λ is not a constant but a scalar field that depends on x^μ .

Let's look again a bit closer at the responsible term:

$$\partial^\mu \Psi' = \partial^\mu \left(e^{ig\frac{\lambda}{2}\Lambda} \Psi \right) = e^{ig\frac{\lambda}{2}\Lambda} \partial^\mu \Psi + ig\frac{\lambda}{2} \left(\partial^\mu \Lambda \right) \Psi = e^{ig\frac{\lambda}{2}\Lambda} \left[\partial^\mu + ig\frac{\lambda}{2} \left(\partial^\mu \Lambda \right) \right] \Psi \neq e^{ig\frac{\lambda}{2}\Lambda} \partial^\mu \Psi$$

The idea is the same as in the case of QED, it is just the term that needs to be absorbed is a bit more complicated since it involves the λ -matrices. So how about trying to absorb the term $\left[\partial^\mu + ig\frac{\lambda}{2} \left(\partial^\mu \Lambda \right) \right]$ which is responsible for breaking the invariance into a new quantity that will be built for the exact purpose of restoring the desired invariance of the Lagrangian density?

For this reason we introduce the covariant derivative $D^{\mu\mu}$ constructed in a way to have the desired property:

$$D^{\mu'} \Psi' = e^{ig\frac{\lambda}{2}\Lambda} D^\mu \Psi$$

The term responsible for breaking the invariance of the Lagrangian density, $\left[\partial^\mu + ig\frac{\lambda}{2} \left(\partial^\mu \Lambda \right) \right]$, once again motivates the form of the covariant derivative:

$$D^\mu = \partial^\mu + ig\frac{\lambda}{2} A^\mu, \quad (3.2.4)$$

where A^μ are eight external vector fields. So from now on, we need to replace in the Lagrangian density the term $\partial^\mu \Psi$ with $D^\mu \Psi$. The latter provides us with the feature of $D^{\mu'} \Psi' = e^{ig\frac{\lambda}{2}\Lambda} D^\mu \Psi$ we need. Here comes another complication: due to the fact that A^μ are eight gauge fields, we need to introduce another index to keep track of this:

$$D^\mu \equiv \partial^\mu + ig\frac{\lambda^\alpha}{2} A^{\mu\alpha}, \quad (3.2.5)$$

We now investigate how the external fields should transform to ensure that local gauge invariance is preserved. For this we need $D^{\mu'} \Psi' = e^{ig\frac{\lambda^\alpha}{2}\Lambda^\alpha} D^\mu \Psi$. Let us look at the different terms one by one:

- Let us first look at the term $D^{\mu'}\Psi'$:

$$\begin{aligned} D^{\mu'}\Psi' &= \left(\partial^\mu + ig\frac{\lambda^\alpha}{2}A^{\mu\alpha}\right)\left(e^{ig\frac{\lambda^\alpha}{2}A^{\mu\alpha}}\Psi\right) = \\ &= \partial^\mu\left(e^{ig\frac{\lambda^\alpha}{2}A^{\mu\alpha}}\Psi\right) + ig\frac{\lambda^\alpha}{2}A^{\mu\alpha'}e^{ig\frac{\lambda^\alpha}{2}A^{\mu\alpha}}\Psi = \\ &= e^{ig\frac{\lambda^\alpha}{2}A^{\mu\alpha}}\left(\partial^\mu\Psi\right) + ig\frac{\lambda^\alpha}{2}e^{ig\frac{\lambda^\alpha}{2}A^{\mu\alpha}}\left(\partial^\mu A^\alpha\right)\Psi + ig\frac{\lambda^\alpha}{2}A^{\mu\alpha'}e^{ig\frac{\lambda^\alpha}{2}A^{\mu\alpha}}\Psi \end{aligned}$$

- Next, we look at the term $e^{ig\frac{\lambda^\alpha}{2}A^{\mu\alpha}}D^\mu\Psi$:

$$\begin{aligned} e^{ig\frac{\lambda^\alpha}{2}A^{\mu\alpha}}D^\mu\Psi &= e^{ig\frac{\lambda^\alpha}{2}A^{\mu\alpha}}\left(\partial^\mu + ig\frac{\lambda^\alpha}{2}A^{\mu\alpha}\right)\Psi = \\ &= e^{ig\frac{\lambda^\alpha}{2}A^{\mu\alpha}}\left(\partial^\mu\Psi\right) + ig\frac{\lambda^\alpha}{2}A^{\mu\alpha}e^{ig\frac{\lambda^\alpha}{2}A^{\mu\alpha}}\Psi \end{aligned}$$

Comparing those two terms, it turns out that the external fields should transform in a rather complicated manner, given by:

$$e^{ig\frac{\lambda^\alpha}{2}A^{\mu\alpha}}\lambda^\alpha A^{\mu\alpha} = \lambda^\alpha A^{\mu\alpha'}e^{ig\frac{\lambda^\alpha}{2}A^{\mu\alpha}} + \lambda^\alpha e^{ig\frac{\lambda^\alpha}{2}A^{\mu\alpha}}\left(\partial^\mu A^\alpha\right) \quad (3.2.6)$$

This complicated transformation that the external fields need to obey stems from the fact that, contrary to the U(1) case, in SU(3) the matrices λ^α and the gauge fields $A^{\mu\alpha}$ do not commute. In the vocabulary of group theory, this means that SU(3) is not Abelian.

3.2.3 The interaction term

With the previous requirement we have ensured that local gauge invariance is preserved and we can safely write down the QCD Lagrangian density of the free quark field:

$$\begin{aligned} \mathcal{L}_{\text{QCD}} &= i\bar{\Psi}\gamma_\mu D^\mu\Psi - m\bar{\Psi}\Psi = \\ &= i\bar{\Psi}\gamma_\mu\left(\partial^\mu + ig\frac{\lambda^\alpha}{2}A^{\mu\alpha}\right)\Psi - m\bar{\Psi}\Psi = \\ &= i\bar{\Psi}\gamma_\mu\partial^\mu\Psi - m\bar{\Psi}\Psi - g\bar{\Psi}\gamma_\mu\frac{\lambda^\alpha}{2}A^{\mu\alpha}\Psi \rightarrow \\ \mathcal{L}_{\text{QCD}}^{\text{partial}} &= \bar{\Psi}(i\gamma_\mu\partial^\mu - m)\Psi - g\bar{\Psi}\gamma_\mu\frac{\lambda^\alpha}{2}A^{\mu\alpha}\Psi \quad (3.2.7) \end{aligned}$$

The first term of Eq. 3.2.7 is the standard Lagrangian density of the free particle i.e. the quark. The second term that was introduced, involves both the spinors $\bar{\Psi}$ and Ψ but also the external vector fields $A^{\mu\alpha}$. This is the interaction term! This term introduced by the requirement of local gauge invariance, reflects the interactions between the particles (i.e. quarks in this case) with the external field.

3.3 The field kinetic term

So far our theory consists of the term that describes the free particle with mass m (i.e. the free quark) and the term that describes the interaction of the particle with the vector fields (i.e. the interaction term). To complete our theory we need to include also the term that describes the field itself. This term comes once again from the Proca Lagrangian:

$$\mathcal{L} = -\frac{1}{4}F_{\mu\nu}F^{\mu\nu} + \frac{1}{2}M^2A_\mu A^\mu, \quad (3.3.1)$$

where $F_{\mu\nu}$ is the field tensor of the theory. Let us note again that in this equation, M is the mass of the vector fields, whereas in Eq. 3.2.1 m corresponds to the mass of the particle that feels the field i.e. the quark in this case.

We now apply the transformation of Eq. 3.2.3 in Eq. 3.3.1:

$$\mathcal{L}' = -\frac{1}{4}F'_{\mu\nu}F'^{\mu\nu} + \frac{1}{2}m^2A'_\mu A'^\mu$$

At this point, I will not repeat the same tedious mathematical steps that we did in the relevant part of the QED Lagrangian density. In addition to the fact that the procedure is practically the same, the vector fields in QCD have a highly not trivial transformation they need to obey (see Eq. 3.2.6). This fact adds some additional number of lines of algebraic actions that one needs to follow. Nevertheless, if one completes all the steps we will once again reach the conclusion that in order for local gauge invariance to be preserved also for the field term, then the fields need to be massless (i.e. $M = 0$). So we have eight (since our theory is described by SU(3) that has eight generators) massless fields: the eight physical gluons!!!

After setting the mass of the vector fields to zero, the term that remains is the one that has the tensor “squared“: i.e. $-\frac{1}{4}F_{\mu\nu}F^{\mu\nu}$. In the case of QED, where the underlying group was the one of U(1), the tensor was simply given by $F_{\mu\nu} = \partial_\mu A_\nu - \partial_\nu A_\mu$. But this term in QCD, described by SU(3), is not anymore gauge invariant! However we know very well how to construct such a term in a way that local gauge invariant is not at question: we will use the equation

$$[D_\mu, D_\nu] = igF_{\mu\nu} \rightarrow F_{\mu\nu} = \frac{-i}{g}[D_\mu, D_\nu]$$

The advantage is obvious: the field tensor is constructed from the commutator of the covariant derivatives. Remember that the covariant derivatives were introduced in a way to absorb the terms that were breaking local gauge invariance. Therefore, preserving local gauge invariance is in that way guaranteed. In what follows, we will derive the form of the field tensor. For that, it is easier (i.e. it will make the place where different partial derivatives act more clear) if we let the previous equation act on a spinor field, such that $F_{\mu\nu}\Psi = \frac{-i}{g}[D_\mu, D_\nu]\Psi$.

$$\begin{aligned} \frac{-i}{g}[D_\mu, D_\nu]\Psi &= -\frac{i}{g}\left(\partial_\mu + ig\frac{\lambda^\alpha}{2}A_\mu^\alpha\right)\left(\partial_\nu + ig\frac{\lambda^\beta}{2}A_\nu^\beta\right)\Psi + \frac{i}{g}\left(\partial_\nu + ig\frac{\lambda^\beta}{2}A_\nu^\beta\right)\left(\partial_\mu + ig\frac{\lambda^\alpha}{2}A_\mu^\alpha\right)\Psi = \\ &= -\frac{i}{g}\partial_\mu\left(\partial_\nu\Psi\right) + \frac{\lambda^\alpha}{2}A_\mu^\alpha\left(\partial_\nu\Psi\right) + \frac{\lambda^\beta}{2}A_\nu^\beta\left(\partial_\mu\Psi\right) + ig\frac{\lambda^\alpha}{2}A_\mu^\alpha\frac{\lambda^\beta}{2}A_\nu^\beta\Psi - \frac{i}{g}\partial_\mu\left(ig\frac{\lambda^\beta}{2}A_\nu^\beta\right)\Psi \\ &+ \frac{i}{g}\partial_\nu\left(\partial_\mu\Psi\right) - \frac{\lambda^\beta}{2}A_\nu^\beta\left(\partial_\mu\Psi\right) - \frac{\lambda^\alpha}{2}A_\mu^\alpha\left(\partial_\nu\Psi\right) - ig\frac{\lambda^\beta}{2}A_\nu^\beta\frac{\lambda^\alpha}{2}A_\mu^\alpha\Psi + \frac{i}{g}\partial_\nu\left(ig\frac{\lambda^\alpha}{2}A_\mu^\alpha\right)\Psi = \\ &= \frac{ig}{4}\left(\lambda^\alpha A_\mu^\alpha\lambda^\beta A_\nu^\beta - \lambda^\beta A_\nu^\beta\lambda^\alpha A_\mu^\alpha\right) + \frac{1}{2}\partial_\mu\left(\lambda^\beta A_\nu^\beta\right)\Psi - \frac{1}{2}\partial_\nu\left(\lambda^\alpha A_\mu^\alpha\right)\Psi = \\ &= \frac{ig}{4}\left[\lambda^\alpha A_\mu^\alpha, \lambda^\beta A_\nu^\beta\right] + \frac{1}{2}\left[\lambda^\beta\left(\partial_\mu A_\nu^\beta\right) - \lambda^\alpha\left(\partial_\nu A_\mu^\alpha\right)\right] = \\ &= \frac{ig}{4}\left[\lambda^\alpha A_\mu^\alpha, \lambda^\beta A_\nu^\beta\right] + \frac{1}{2}\lambda^\alpha\left(\partial_\mu A_\nu^\alpha - \partial_\nu A_\mu^\alpha\right) \end{aligned}$$

In the last two lines, the last terms imply using the summation rule for indices with indices α and β . But the λ -matrices can be considered the same i.e. both their indices run from 1 to 8 at the same time, and thus can factorise. As for the commutator, the first term of the previous equation, we have to use again the summation rule for indices. We can then pull out of the commutator the vector fields A_μ and A_ν such that:

$$[\lambda^\alpha A_\mu^\alpha, \lambda^\beta A_\nu^\beta] = [\lambda^\alpha, \lambda^\beta] A_\mu^\alpha A_\nu^\beta$$

The commutator is not zero due to the Gell-Mann matrices! The generators of SU(3) respect the following Algebra:

$$[\lambda^\alpha, \lambda^\beta] = if^{\alpha\beta\gamma} \lambda^\gamma, \quad (3.3.2)$$

where the variables $f^{\alpha\beta\gamma}$ are real numbers, called the structure constants of SU(3).

Let's now identify the final form of the field tensor (note that we will interchange the indices α , β and γ compared to what we followed before to make the final expression more convenient in writing; there is no essential change with this action):

$$\begin{aligned} F_{\mu\nu} &= \frac{ig}{4} [\lambda^\beta, \lambda^\gamma] A_\mu^\beta A_\nu^\gamma + \frac{1}{2} \lambda^\alpha (\partial_\mu A_\nu^\alpha - \partial_\nu A_\mu^\alpha) = \frac{ig}{4} f^{\alpha\beta\gamma} \lambda^\alpha A_\mu^\beta A_\nu^\gamma + \frac{1}{2} \lambda^\alpha (\partial_\mu A_\nu^\alpha - \partial_\nu A_\mu^\alpha) \Rightarrow \\ F_{\mu\nu} &= \frac{1}{2} \lambda^\alpha (\partial_\mu A_\nu^\alpha - \partial_\nu A_\mu^\alpha) - \frac{g}{4} f^{\alpha\beta\gamma} \lambda^\alpha A_\mu^\beta A_\nu^\gamma \end{aligned} \quad (3.3.3)$$

Once again, we can pull out the λ^α matrices so that the field tensor can take the following form:

$$F_{\mu\nu} = \lambda^\alpha F_{\mu\nu}^\alpha, \quad (3.3.4)$$

where $F_{\mu\nu}^\alpha = \frac{1}{2} (\partial_\mu A_\nu^\alpha - \partial_\nu A_\mu^\alpha) - \frac{g}{4} f^{\alpha\beta\gamma} A_\mu^\beta A_\nu^\gamma$.

We are not done since the final QCD Lagrangian density had the field tensor ‘‘squared’’. It is enough to see what kind of complications this brings by simply looking at the ‘‘square’’ of the $F_{\mu\nu}^\alpha$ part:

$$\begin{aligned} F_{\mu\nu}^\alpha F^{\mu\nu\alpha} &= \left[\frac{1}{2} (\partial_\mu A_\nu^\alpha - \partial_\nu A_\mu^\alpha) - \frac{g}{4} f^{\alpha\beta\gamma} A_\mu^\beta A_\nu^\gamma \right] \left[\frac{1}{2} (\partial^\mu A^{\nu\alpha} - \partial^\nu A^{\mu\alpha}) - \frac{g}{4} f^{\alpha\delta\epsilon} A^{\mu\delta} A^{\nu\epsilon} \right] = \\ &= \frac{1}{4} (\partial_\mu A_\nu^\alpha - \partial_\nu A_\mu^\alpha) (\partial^\mu A^{\nu\alpha} - \partial^\nu A^{\mu\alpha}) \\ &\quad - \frac{g}{8} f^{\alpha\beta\gamma} A_\mu^\beta A_\nu^\gamma (\partial_\mu A_\nu^\alpha - \partial_\nu A_\mu^\alpha) \\ &\quad - \frac{g}{8} f^{\alpha\delta\epsilon} (\partial_\mu A_\nu^\alpha - \partial_\nu A_\mu^\alpha) A^{\mu\delta} A^{\nu\epsilon} \\ &\quad - \frac{g^2}{16} f^{\alpha\beta\gamma} f^{\alpha\delta\epsilon} A_\mu^\beta A_\nu^\gamma A^{\mu\delta} A^{\nu\epsilon} \end{aligned}$$

Let us try to understand what each term brings:

- $\frac{1}{4} (\partial_\mu A_\nu^\alpha - \partial_\nu A_\mu^\alpha) (\partial^\mu A^{\nu\alpha} - \partial^\nu A^{\mu\alpha})$: This first term of the previous equation is the standard term for the field we encountered also in QED (modulo the factor 1/4 which is not relevant).
- $\frac{g}{8} f^{\alpha\beta\gamma} A_\mu^\beta A_\nu^\gamma (\partial_\mu A_\nu^\alpha - \partial_\nu A_\mu^\alpha)$: This term contains ‘‘interactions’’ between three vector fields e.g. $A_\mu^\beta A_\nu^\gamma \partial_\mu A_\nu^\alpha$. These terms reveal one of the main differences between QED and QCD which have to do with vertices involving three gluons.

- $\frac{g}{8} f^{\alpha\delta\epsilon} (\partial_\mu A_\nu^\alpha - \partial_\nu A_\mu^\alpha) A^{\mu\delta} A^{\nu\epsilon}$: Similarly to the term before, also this term contains “interactions“ between three vector fields e.g. $\partial_\mu A_\nu^\alpha A^{\mu\delta} A^{\nu\epsilon}$. These terms describe again vertices that involve three gluons.
- $\frac{g^2}{16} f^{\alpha\beta\gamma} f^{\alpha\delta\epsilon} A_\mu^\beta A_\nu^\gamma A^{\mu\delta} A^{\nu\epsilon}$: This term clearly involves “interactions“ between four vector fields and describe vertices that involve four gluons.

These last elements, which are characteristic of QCD are shown in fig. 3.1.

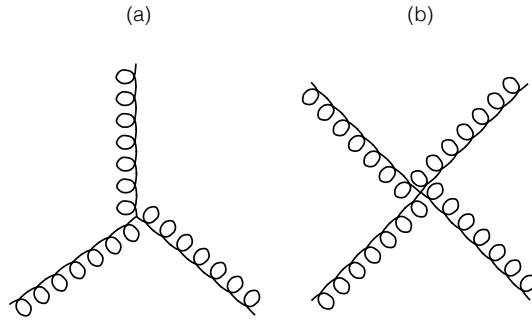


Fig. 3.1: One of the main characteristic QCD feature: the self coupling of the gauge bosons of the theory originating from its non-Abelian nature i.e. the three and four gluon vertices.

3.4 Some comments

At this stage it is once again essential to take a break and reflect on a few things. Let me guide you through with the following comments:

- As in the case of QED, also in QCD, we acted on the Dirac Lagrangian of the free particle with a transformation. The underlying group that describes the relevant transformations in QCD is not as simple as $U(1)$. These transformations are now described by 3×3 matrices, described by the generators of the $SU(3)$ group.

But how do we act on the eigenfunction Ψ with such a complicated transformation that obeys the properties and rules of the $SU(3)$ group? The answer is that we have to make Ψ a bit more complicated as well: the eigenfunction needs to have this time three additional elements:

$$\Psi = (\Psi_R, \Psi_B, \Psi_G) \quad (3.4.1)$$

where each component of the new array corresponds to the new quantum number associated with the strong interaction i.e. the colour: Ψ_R for red, Ψ_B for blue and Ψ_G for green.

Remember though that that Ψ in the Dirac equations was a 4–component vector representing two particles with spin $\pm 1/2$ and two antiparticles with similar as before spin orientation of $\pm 1/2$. That means that this new 3–component spinor comes on top of the existing four components! These three components are different colour charges of each element of the 4–component Dirac spinor!!! An extra dimension on the existing spinor, but this time explicitly for quarks.

- A few words about the “charge“ and its nature in QED and in QCD. In QED the word “charge“ was associated to the electric charge. It had two possible values ± 1 : a positive and a negative charge always an integer multiple of the charge of the electron.

In QCD on the other had, the word “charge“ is associated to the colour charge. We have seen that we have three charges: red, blue and green. Note that as in the case of QED, also in QCD, each of these charges have two possible values: R and \bar{R} , B and \bar{B} , G and \bar{G} .

Overall, it looks as if QCD contains three times the QED fundamental structure. In the language of group theory, people say that the maximum commuting subgroup of $SU(3)$ is $U(1) \times U(1) \times U(1)$.

- Each quark has a colour chosen between the three available i.e. R, B and G. Each antiquark has an anticolour chosen between the three available i.e. \bar{R} , \bar{B} and \bar{G} . Gluons have one colour and one anticolour.

The basis vectors in colour space are

$$C_1 = |R\rangle = \begin{pmatrix} 1 \\ 0 \\ 0 \end{pmatrix}$$

$$C_2 = |B\rangle = \begin{pmatrix} 0 \\ 1 \\ 0 \end{pmatrix}$$

$$C_3 = |G\rangle = \begin{pmatrix} 0 \\ 0 \\ 1 \end{pmatrix}$$

Their Hermitian conjugates are:

$$C_1^\dagger = \langle R| = (1 \ 0 \ 0)$$

$$C_2^\dagger = \langle B| = (0 \ 1 \ 0)$$

$$C_3^\dagger = \langle G| = (0 \ 0 \ 1)$$

- There are eight physical gauge bosons in QCD, as expected by the fact that the underlying group that describes the strong interactions is $SU(3)$ that has eight generators. Each gluon contains one colour and one anticolour. The physical states are written as follows:

$$\begin{aligned} |1\rangle &= \frac{1}{\sqrt{2}} \begin{pmatrix} R\bar{B} + B\bar{R} \end{pmatrix} & |2\rangle &= \frac{-i}{\sqrt{2}} \begin{pmatrix} R\bar{B} - B\bar{R} \end{pmatrix} \\ |3\rangle &= \frac{1}{\sqrt{2}} \begin{pmatrix} R\bar{R} + B\bar{B} \end{pmatrix} & |4\rangle &= \frac{1}{\sqrt{2}} \begin{pmatrix} R\bar{G} + G\bar{R} \end{pmatrix} \\ |5\rangle &= \frac{-i}{\sqrt{2}} \begin{pmatrix} R\bar{G} - G\bar{R} \end{pmatrix} & |6\rangle &= \frac{1}{\sqrt{2}} \begin{pmatrix} B\bar{G} + G\bar{B} \end{pmatrix} \\ |7\rangle &= \frac{-i}{\sqrt{2}} \begin{pmatrix} B\bar{G} - G\bar{B} \end{pmatrix} & |8\rangle &= \frac{1}{\sqrt{6}} \begin{pmatrix} R\bar{R} + B\bar{B} - 2G\bar{G} \end{pmatrix} \end{aligned}$$

- The $SU(3)$ transformation that is applied is, as we have seen, of the form $U = e^{ig\frac{\lambda}{2}A}$. The matrices λ are all 3×3 matrices also known as Gell-Mann matrices with the form:

$$\begin{array}{cccc}
\underbrace{\begin{pmatrix} 0 & 1 & 0 \\ 1 & 0 & 0 \\ 0 & 0 & 0 \end{pmatrix}}_{\lambda_1} & \underbrace{\begin{pmatrix} 0 & -i & 0 \\ i & 0 & 0 \\ 0 & 0 & 0 \end{pmatrix}}_{\lambda_2} & \underbrace{\begin{pmatrix} 1 & 0 & 0 \\ 0 & -1 & 0 \\ 0 & 0 & 0 \end{pmatrix}}_{\lambda_3} & \underbrace{\begin{pmatrix} 0 & 0 & 1 \\ 0 & 0 & 0 \\ 1 & 0 & 0 \end{pmatrix}}_{\lambda_4} \\
\underbrace{\begin{pmatrix} 0 & 0 & -i \\ 0 & 0 & 0 \\ i & 0 & 0 \end{pmatrix}}_{\lambda_5} & \underbrace{\begin{pmatrix} 0 & 0 & 0 \\ 0 & 0 & 1 \\ 0 & 1 & 0 \end{pmatrix}}_{\lambda_6} & \underbrace{\begin{pmatrix} 0 & 0 & 0 \\ 0 & 0 & -i \\ 0 & i & 0 \end{pmatrix}}_{\lambda_7} & \frac{1}{\sqrt{3}} \underbrace{\begin{pmatrix} 1 & 0 & 0 \\ 0 & 1 & 0 \\ 0 & 0 & -2 \end{pmatrix}}_{\lambda_8}
\end{array}$$

- There are, as we have seen, eight physical gluon states. These states are in fact reflected in the Gell-Mann matrices if one writes the general form of the matrix as

$$\begin{pmatrix} \overline{R}R & \overline{R}B & \overline{R}G \\ \overline{B}R & \overline{B}B & \overline{B}G \\ \overline{G}R & \overline{G}B & \overline{G}G \end{pmatrix}$$

The Gell-Mann matrices have the colours of each gluon state embedded in them!

- Why is the underline group of QCD the one of $SU(3)$ and not the one of $U(3)$? After all, the generators of $U(3)$ are also 3×3 matrices. The reason is that in that case there would be a ninth gluon whose form would be

$$|9\rangle = \frac{1}{\sqrt{3}} (\overline{R}R + \overline{B}B + \overline{G}G)$$

Note that this is a colour singlet state. Remember that all naturally observed particles are in a colour singlet state and thus the ninth gluon would qualify as one i.e. we would be able to see gluons flying free in nature!!! Since this is not observed, then this means that this gluon state does not exist, it is not physical!

- We have seen in Section 3.3 how the fact that $SU(3)$ is a non-Abelian group leads to additional terms in the QCD Lagrangian density revealed by the introduction of the field kinetic term. These three and four gluon vertices highlight the self-coupling nature of the gauge bosons of QCD.

Chapter 4

The Feynman calculus

In this chapter we are going to describe the Feynman rules for the electromagnetic, electroweak and strong interactions. Before doing so, let's review a couple of important ingredients that we are going to encounter when dealing with particle interactions.

Let's imagine that we have N_0 particles that decay and after dt the relevant number becomes N . We define as decay rate Γ the probability that a particle will decay per unit time:

$$\frac{dN}{dt} = -\Gamma N$$

$$\frac{1}{N}dN = -\Gamma dt$$

$$\int_{N_0}^{N(t)} \frac{1}{N'} dN' = -\Gamma \int_{t_0}^t dt'$$

$$[\ln N]_{N_0}^{N(t)} = -\Gamma(t - t_0)$$

$$\ln N(t) - \ln N_0 = -\Gamma \Delta t$$

$$\ln \frac{N(t)}{N_0} = -\Gamma \Delta t$$

$$N(t) = N_0 e^{-\Gamma \Delta t}$$

We define as mean (or average) lifetime τ , the time it takes for a sample of particles to reach the value of $N(\tau) = N_0/e$. It turns out that:

$$\tau = \frac{1}{\Gamma}$$

If a particle has more than one decay mode, then

$$\Gamma_{tot} = \sum_{i=1}^n \Gamma_i$$

$$\tau = \frac{1}{\Gamma_{tot}}$$

In the case of a decay, an important property is the so-called branching ratio that defines the fraction of particles of a given type that decay by each mode. This is defined by

$$B.R. = \frac{\Gamma_i}{\Gamma_{tot}}$$

A different category of particle interactions is related to scattering. The relevant quantity that reflects the probability of such an interaction is the so-called cross-section. The cross-section depends on the nature of the interaction e.g. we can speak about elastic, inelastic, total or inclusive cross-section. This latter is calculated as the sum of every individual contribution, such that

$$\sigma_{tot} = \sum_{i=1}^n \sigma_i$$

In the following, we are going to study some basic examples, while at the end of this chapter we are going to calculate the cross-section for an indicative process (i.e. $e^- + \mu^- \rightarrow e^- + \mu^-$) which although being of electromagnetic nature, will assist us in calculating cross-sections in QCD.

Example A: Extract the differential cross-section for a particle that bounces elastically off a hard sphere of radius R

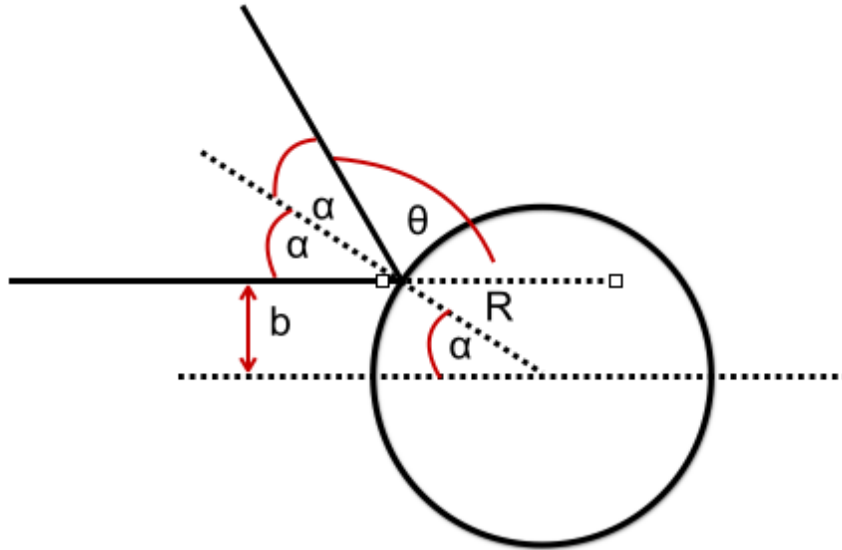


Fig. 4.1: Scattering of a particle on a hard sphere.

$$\frac{b}{R} = \sin(\alpha) \Leftrightarrow b = R \sin(\alpha)$$

But $2\alpha + \theta = \pi$, which means that

$$b = R \sin\left(\frac{\pi}{2} - \frac{\theta}{2}\right) \Leftrightarrow b = R \cos\left(\frac{\theta}{2}\right) \quad (4.0.1)$$

If one considers the azimuthal (φ) and polar (θ) angles, the differential cross-section is defined as $d\sigma/d\Omega$:

$$d\sigma = |b \cdot db \cdot d\varphi|$$

$$d\Omega = |\sin(\theta) \cdot d\theta \cdot d\varphi|$$

$$\frac{d\sigma}{d\Omega} = \left| \frac{b \cdot db}{\sin(\theta) \cdot d\theta} \right| \quad (4.0.2)$$

Equation 4.0.2 with the help of Eq. 4.0.1 can be written as:

$$\begin{aligned} \frac{d\sigma}{d\Omega} &= \left| \frac{b}{\sin(\theta)} \cdot \frac{R}{2} \cdot \sin\left(\frac{\theta}{2}\right) \right| \\ \Leftrightarrow \frac{d\sigma}{d\Omega} &= \left| \frac{R^2}{2} \cdot \frac{\cos\left(\frac{\theta}{2}\right) \cdot \sin\left(\frac{\theta}{2}\right)}{\sin(\theta)} \right| \\ \Leftrightarrow \frac{d\sigma}{d\Omega} &= \left| \frac{R^2}{2} \cdot \frac{\sin(\theta)/2}{\sin(\theta)} \right| \\ \Leftrightarrow \frac{d\sigma}{d\Omega} &= \frac{R^2}{4} \end{aligned}$$

The total integrated cross-section is then given by

$$\sigma = \int \frac{R^2}{4} d\Omega = \frac{R^2}{4} \int_0^\pi \sin(\theta) d\theta \int_0^{2\pi} d\varphi = \pi R^2$$

Finally, let's define as luminosity the number of particles per unit time and per unit area, such that:

$$dN = L \cdot d\sigma$$

4.1 Golden rule for decays and scattering

To calculate the previous quantities one uses the golden rule for decays and scattering that states that a transition rate is given by the product of the amplitude or matrix element M_{if} squared and the phase space factor, the latter being purely kinematic:

$$(\text{transition rate}) = \frac{2\pi}{\hbar} |M_{if}|^2 \times (\text{phase space factor})$$

Decays: Assume that we have the following decay mode $|1\rangle \rightarrow |2\rangle + |3\rangle + \dots + |n\rangle$. The decay rate is then given by

$$\Gamma = \frac{S}{2 \cdot \hbar \cdot m_1} \int |M_{if}|^2 (2\pi)^4 \delta^4(\vec{P}_1 - \vec{P}_2 - \vec{P}_3 - \dots - \vec{P}_n) \times \prod_{j=2}^n 2\pi \delta(p_j^2 - m_j^2 c^2) \theta(p_j) \frac{d^4 \vec{P}_j}{(2\pi)^4}, \quad (4.1.1)$$

where S is a statistical factor that reflects the number of states accessible to distinguishable particles. The $(1/k!)$ (for each group of k identical particles in the final state) factor divides out the number of equivalent states for identical particles.

Scattering: Assume that we have the following scattering process mode $|1\rangle + |2\rangle \rightarrow |3\rangle + \dots + |n\rangle$. The interaction rate is then given by

$$\Gamma = \frac{S}{2 \cdot \hbar \cdot m_1} \int |M_{if}|^2 (2\pi)^4 \delta^4(\vec{P}_1 + \vec{P}_2 - \vec{P}_3 - \dots - \vec{P}_n) \times \prod_{j=3}^n 2\pi \delta(p_j^2 - m_j^2 c^2) \theta(p_j) \frac{d^4 \vec{P}_j}{(2\pi)^4}, \quad (4.1.2)$$

4.2 General Feynman rules

We will first start by giving the general Feynman rules, no matter what the underlying theory is. In the subsequent sections we will review how these rules are modified for the case of the electromagnetic and weak interactions in Sections 4.2.1 and for the case of strong interactions in Section 4.2.2. In what follows we will be working in natural units i.e. $\hbar = c = 1$.

A characteristic diagram describing any kind of interaction of the type $A + B \rightarrow C + D$ is given in fig. 4.2.

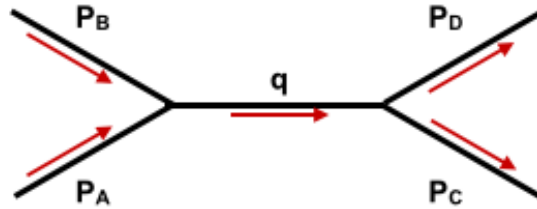


Fig. 4.2: A diagram describing the process $A + B \rightarrow C + D$.

The general rules that one needs to follow in order to calculate the matrix element M_{if} are given below:

- **Labeling:** We first label the incoming and outgoing four-momenta \vec{P}_A , \vec{P}_B , \vec{P}_C and \vec{P}_D . For each external line we add an arrow which indicates the positive (i.e. along the time axis) direction for particles. We then label all internal lines e.g. in fig. 4.2 we label the four-momentum of the propagator as \vec{q} and give an arbitrary direction to the relevant arrow.
- **Vertices:** For each vertex we note down in the diagram the coupling constant factor $-ig\gamma^\mu$.
- **Propagators:** For each internal line, we give a factor of

$$\frac{i}{\vec{q}^2 - m^2}$$

where $\vec{q}^2 = q_\nu q^\nu$ the invariant mass of the propagator.

- **δ -functions:** For each vertex we should add a δ -function of the form

$$(2\pi)^4 \delta^4(\vec{P}_A + \vec{P}_B - \vec{q})$$

where depending on the direction of the arrow of the relevant line in the diagram, we give a positive or negative sign to the 4-momentum symbol. This function guarantees the conservation of energy and momentum at the vertex.

- **Integrate:** For each internal line we should be writing down a factor

$$\frac{1}{(2\pi)^4} d^4\vec{q}$$

and we should integrate over all internal momenta.

- **Cancelation of δ -functions:** The result will contain a factor of

$$(2\pi)^4 \delta^4(\vec{P}_A + \vec{P}_B - \vec{P}_C - \vec{P}_D)$$

If this factor is cancelled, what remains is $-i\mathbf{M}_{if}$.

4.2.1 Feynman rules for QED and GWS

Let's now review how these general rules described before change in the case of an electromagnetic or weak interaction.

- **Labeling:** We label every external line with the ingoing and outgoing momenta $\vec{P}_1, \dots, \vec{P}_n$, adding also an arrow indicating whether a particle is approaching or moving away from the vertex. If the diagram includes antiparticles, we still label them as particles but with the reverse direction of the arrow. We then label the 4-momenta for all internal lines $\vec{q}_1, \dots, \vec{q}_j$ and we give an arbitrary direction to the relevant arrow.
- **External lines:** Each external line contributes the following factors:

Incoming electron $\rightarrow u$

Outgoing electron $\rightarrow \bar{u}$

Incoming positron $\rightarrow \bar{v}$

Outgoing positron $\rightarrow v$

Incoming photon $\rightarrow \epsilon_\mu$

Outgoing photon $\rightarrow \epsilon_\mu^*$

where u and v are the relevant Dirac spinors and ϵ_μ are the photon polarisation vectors which are orthogonal to the 4-momentum $\vec{P}_\nu \epsilon^\nu = 0$.

- **Vertices:** For each vertex we note down in the diagram the coupling constant factor $-ig_\epsilon \gamma^\mu$ or $-ig_w \gamma^\mu$, if the interaction is electromagnetic or weak, respectively. These factors are connected to the coupling constants via the equations

$$g_\epsilon = \sqrt{4\pi\alpha}$$

and

$$g_w = \sqrt{4\pi\alpha_w}$$

- **Propagators:** For each internal line, we give a factor of

$$e^\pm : \frac{i(\gamma_\mu \vec{q}^\mu + m)}{\vec{q}^2 - m^2}$$

$$\gamma : \frac{-ig_{\mu\nu}}{\vec{q}^2}$$

- **δ -functions and integration:** The remaining steps are identical as in the general rules described before.

Figure 4.3 presents the lines for the basic particles and anti-particles but also the propagators for both the electromagnetic and weak interactions.

4.2.2 Feynman rules for QCD

Let's now review how these general rules described before change in the case of a strong interaction.

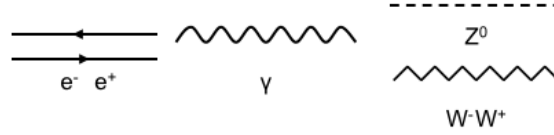


Fig. 4.3: The most characteristic lines for the Feynman diagrams in electromagnetic and weak interactions.

- **Labeling:** We label every external line with the ingoing and outgoing momenta $\vec{P}_1, \dots, \vec{P}_n$, adding also an arrow indicating whether a particle is approaching or moving away from the vertex. If the diagram includes antiparticles, we still label them as particles but with the reverse direction of the arrow. We then label the 4-momenta for all internal slash lines $\vec{q}_1, \dots, \vec{q}_j$ and we give an arbitrary direction to the relevant arrow.
- **External lines:** Each external line contribute the following factors:

$$\text{Incoming quark} \rightarrow u^s \cdot c$$

$$\text{Outgoing quark} \rightarrow \bar{u}^s \cdot c^\dagger$$

$$\text{Incoming anti-quark} \rightarrow \bar{v}^s \cdot c^\dagger$$

$$\text{Outgoing anti-quark} \rightarrow v \cdot c$$

$$\text{Incoming gluon} \rightarrow \varepsilon_\mu \cdot a^\alpha$$

$$\text{Outgoing gluon} \rightarrow \varepsilon_\mu^* \cdot a^{\alpha*}$$

where u and v are the relevant Dirac spinors. In the previous c are the matrices that represent the colour:

$$\begin{pmatrix} 1 \\ 0 \\ 0 \end{pmatrix} \text{ for R, } \begin{pmatrix} 0 \\ 1 \\ 0 \end{pmatrix} \text{ for B, } \begin{pmatrix} 0 \\ 0 \\ 1 \end{pmatrix} \text{ for G}$$

and a are the 8-element column matrices, one for each gluon state (i.e. α goes from 1 to 8):

$$|1\rangle \equiv \begin{pmatrix} 1 \\ 0 \\ 0 \\ 0 \\ 0 \\ 0 \\ 0 \\ 0 \end{pmatrix}, |2\rangle \equiv \begin{pmatrix} 0 \\ 1 \\ 0 \\ 0 \\ 0 \\ 0 \\ 0 \\ 0 \end{pmatrix}, |3\rangle \equiv \begin{pmatrix} 0 \\ 0 \\ 1 \\ 0 \\ 0 \\ 0 \\ 0 \\ 0 \end{pmatrix}, |4\rangle \equiv \begin{pmatrix} 0 \\ 0 \\ 0 \\ 1 \\ 0 \\ 0 \\ 0 \\ 0 \end{pmatrix}, |5\rangle \equiv \begin{pmatrix} 0 \\ 0 \\ 0 \\ 0 \\ 1 \\ 0 \\ 0 \\ 0 \end{pmatrix}, |6\rangle \equiv \begin{pmatrix} 0 \\ 0 \\ 0 \\ 0 \\ 0 \\ 1 \\ 0 \\ 0 \end{pmatrix}, |7\rangle \equiv \begin{pmatrix} 0 \\ 0 \\ 0 \\ 0 \\ 0 \\ 0 \\ 1 \\ 0 \end{pmatrix}, |8\rangle \equiv \begin{pmatrix} 0 \\ 0 \\ 0 \\ 0 \\ 0 \\ 0 \\ 0 \\ 1 \end{pmatrix}$$

- **Vertices:** For each vertex we note down in the diagram the coupling constant factor $\approx g_s$. This factor is connected to the coupling constant via the equation

$$g_s = \sqrt{4\pi\alpha_s}$$

For a quark-gluon vertex (see fig. 4.4) the factor is of the form:

$$\frac{-ig_s}{2} \lambda^\alpha \gamma^\mu$$

where the parameters λ^α are the Gell-Mann λ -matrices of SU(3).

For a 3-gluon vertex (see fig. 4.4) the factor is of the form:

$$-g_s f^{\alpha\beta\gamma} [g_{\mu\nu}(\vec{k}_1 - \vec{k}_2)_\rho + g_{\nu\rho}(\vec{k}_2 - \vec{k}_3)_\mu + g_{\rho\mu}(\vec{k}_3 - \vec{k}_1)_\nu]$$

where the factors $f^{\alpha\beta\gamma}$ are the structure constants of SU(3) and \vec{k}_i are the 4-momenta of each internal line (with $i = 1, 2, 3$).

Finally, for a 4-gluon vertex (see fig. 4.4) the factor is of the form:

$$-ig_s^2 [f^{\alpha\beta\eta} f^{\gamma\delta\eta} (g_{\mu\sigma} g_{\nu\rho} - g_{\mu\rho} g_{\nu\sigma}) + f^{\alpha\delta\eta} f^{\beta\gamma\eta} (g_{\mu\nu} g_{\sigma\rho} - g_{\mu\sigma} g_{\nu\rho}) + f^{\alpha\gamma\eta} f^{\delta\beta\eta} (g_{\mu\rho} g_{\nu\sigma} - g_{\mu\nu} g_{\sigma\rho})]$$

- **Propagators:** For each internal line, we give a factor of

$$q - \bar{q} : \frac{i(\not{q} + m)}{\not{q}^2 - m^2}$$

$$\text{gluon} : -ig_{\mu\nu} \delta^{\alpha\beta}$$

where $\not{q} \equiv \gamma_\nu q^\nu$.

- **δ -functions and integration:** The remaining steps are identical as in the general rules described before.

Figure 4.4 presents the lines for the basic particles and anti-particles but also the propagators for the strong interactions.

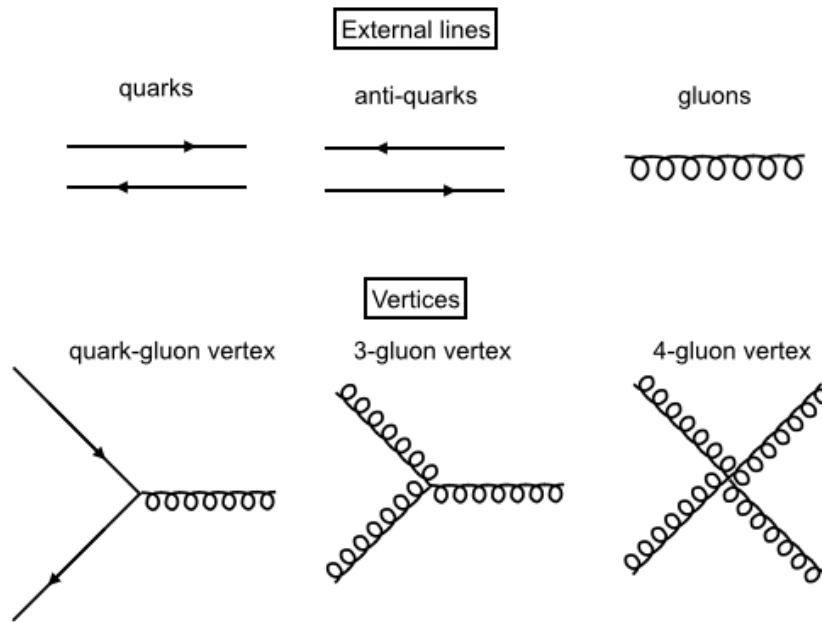


Fig. 4.4: The most characteristic lines for the Feynman diagrams in strong interactions.

4.2.3 A characteristic example: $e^- + \mu^- \rightarrow e^- + \mu^-$

In this section we are going to calculate the matrix element of a characteristic electromagnetic process i.e. the electron-muon scattering (also known as Møtt scattering). We will find this calculation convenient for QCD processes that we are going to encounter in the following chapters.

Figure 4.5 presents the basic Feynman diagram of the Møtt scattering. It is seen that an electron and a muon enter from the left, they interact by exchanging a photon and scatter.

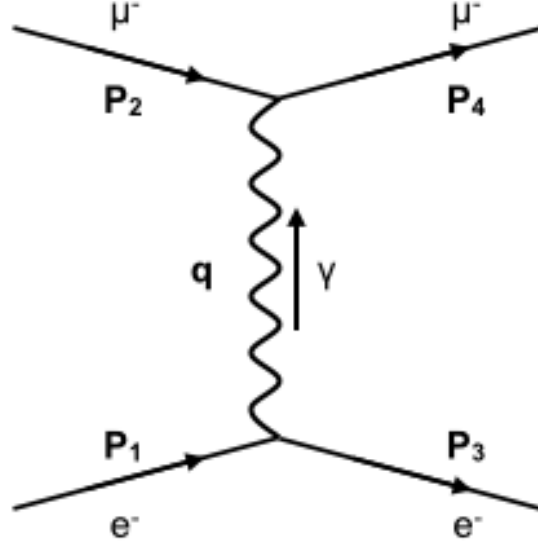


Fig. 4.5: The Feynman diagram for the process $e^- + \mu^- \rightarrow e^- + \mu^-$.

Following the Feynman rules for QED we have:

$$\int \left[\bar{u}(\vec{P}_3) (ig_e \gamma^\mu) u(\vec{P}_1) \right] \left(\frac{-ig_{\mu\nu}}{q^2} \right) \left[\bar{u}(\vec{P}_4) (ig_e \gamma^\nu) u(\vec{P}_2) \right] \cdot \left[(2\pi)^4 \delta^4(\vec{P}_1 - \vec{P}_3 - \vec{q}) \right] \cdot \left[(2\pi)^4 \delta^4(\vec{P}_2 - \vec{P}_4 + \vec{q}) \right] \cdot \frac{d^4 q}{(2\pi)^4}$$

$$= ig_e^2 (2\pi)^4 \int \bar{u}(\vec{P}_3) \gamma^\mu u(\vec{P}_1) \cdot \frac{g_{\mu\nu}}{q^2} \cdot \bar{u}(\vec{P}_4) \gamma^\nu u(\vec{P}_2) \cdot \delta^4(\vec{P}_1 - \vec{P}_3 - \vec{q}) \cdot \delta^4(\vec{P}_2 - \vec{P}_4 + \vec{q}) d^4 q$$

But $\vec{P}_1 - \vec{P}_3 = \vec{q}$ and the previous can be written:

$$ig_e^2 (2\pi)^4 \bar{u}(\vec{P}_3) \gamma^\mu u(\vec{P}_1) \cdot \frac{g_{\mu\nu}}{(\vec{P}_1 - \vec{P}_3)^2} \cdot \bar{u}(\vec{P}_4) \gamma^\nu u(\vec{P}_2) \cdot \delta^4(\vec{P}_1 + \vec{P}_2 - \vec{P}_3 - \vec{P}_4) d^4 q$$

To get the matrix element, one simply cancels the δ -function and gets rid of the imaginary factor:

$$M_{if} = \frac{-g_e^2}{(\vec{P}_1 - \vec{P}_3)^2} \left[\bar{u}(\vec{P}_3) \gamma^\mu u(\vec{P}_1) g_{\mu\nu} \bar{u}(\vec{P}_4) \gamma^\nu u(\vec{P}_2) \right] \Leftrightarrow$$

$$M_{if} = \frac{-g_e^2}{(\vec{P}_1 - \vec{P}_3)^2} \left[\bar{u}(\vec{P}_3) \gamma^\mu u(\vec{P}_1) \bar{u}(\vec{P}_4) \gamma_\mu u(\vec{P}_2) \right] \quad (4.2.1)$$

We now need to compute $\langle |M_{if}|^2 \rangle$, where the brackets denote an average over all initial and final spin configurations. This can be done by taking the average of Eq. 4.2.1 and using the so-called Casimir identity which makes usage of traces of matrices.

$$|M_{if}|^2 = \frac{g_e^4}{(\vec{P}_1 - \vec{P}_3)^4} \left[\bar{u}(\vec{P}_3) \gamma^\mu u(\vec{P}_1) \right] \cdot \left[\bar{u}(\vec{P}_4) \gamma_\mu u(\vec{P}_2) \right] \cdot \left[\bar{u}(\vec{P}_3) \gamma^\nu u(\vec{P}_1) \right]^* \cdot \left[\bar{u}(\vec{P}_4) \gamma_\nu u(\vec{P}_2) \right]^*$$

where the brackets with the 'star' are the complex conjugates.

The average of the previous equation over all spin configurations leads to the identity:

$$\begin{aligned} \langle |M_{if}|^2 \rangle &= \frac{1}{4} \sum_{all\ spins} |M_{if}|^2 = \frac{g_e^4}{4(\vec{P}_1 - \vec{P}_3)^4} \sum_{all\ spins} \left[\bar{u}(\vec{P}_3) \gamma^\mu u(\vec{P}_1) \right] \cdot \left[\bar{u}(\vec{P}_4) \gamma_\mu u(\vec{P}_2) \right] \cdot \left[\bar{u}(\vec{P}_3) \gamma^\nu u(\vec{P}_1) \right]^* \cdot \left[\bar{u}(\vec{P}_4) \gamma_\nu u(\vec{P}_2) \right]^* \Leftrightarrow \\ \langle |M_{if}|^2 \rangle &= \frac{g_e^4}{4(\vec{P}_1 - \vec{P}_3)^4} \cdot \text{Tr} \left[\gamma^\mu (\vec{\not{P}}_1 + m) \cdot \gamma^\nu (\vec{\not{P}}_3 + m) \right] \cdot \text{Tr} \left[\gamma_\mu (\vec{\not{P}}_2 + M) \cdot \gamma_\nu (\vec{\not{P}}_4 + M) \right] \end{aligned}$$

where m and M are the electron and muon masses, respectively. Let us now calculate the first of the two traces:

$$\begin{aligned} \text{Tr} \left[\gamma^\mu (\vec{\not{P}}_1 + m) \cdot \gamma^\nu (\vec{\not{P}}_3 + m) \right] &= \\ \text{Tr}(\gamma^\mu \vec{\not{P}}_1 \gamma^\nu \vec{\not{P}}_3) + m \left[\text{Tr}(\gamma^\mu \vec{\not{P}}_1 \gamma^\nu) \right] + m \left[\text{Tr}(\gamma^\mu \gamma^\nu \vec{\not{P}}_3) \right] + m^2 \text{Tr}(\gamma^\mu \gamma^\nu) \end{aligned}$$

Consulting the theorems for traces, the trace of odd number of matrices is 0, which reduces the workload in the previous equation to calculating the trace of the first and the fourth term:

First trace:

$$\text{Tr}(\gamma^\mu \vec{\not{P}}_1 \gamma^\nu \vec{\not{P}}_3) = (\vec{P}_1)_\rho \cdot (\vec{P}_3)_\sigma \cdot \text{Tr}(\gamma^\mu \gamma^\rho \gamma^\nu \gamma^\sigma) = (\vec{P}_1)_\rho \cdot (\vec{P}_3)_\sigma \cdot 4 \left(g^{\mu\rho} g^{\nu\sigma} - g^{\mu\nu} g^{\rho\sigma} + g^{\mu\sigma} g^{\rho\nu} \right) = 4 \left(\vec{P}_1^\mu \vec{P}_3^\nu - g^{\mu\nu} \vec{P}_1^\mu \vec{P}_3^\mu + \vec{P}_3^\mu \vec{P}_1^\nu \right)$$

Fourth trace:

$$m^2 \text{Tr}(\gamma^\mu \gamma^\nu) = m^2 g^{\mu\nu}$$

The initial first trace is then:

$$\text{Tr} \left[\gamma^\mu (\vec{\not{P}}_1 + m) \cdot \gamma^\nu (\vec{\not{P}}_3 + m) \right] = 4 \left[\vec{P}_1^\mu \vec{P}_3^\nu + \vec{P}_3^\mu \vec{P}_1^\nu + g^{\mu\nu} \left(m^2 - \vec{P}_1^\mu \vec{P}_3^\mu \right) \right]$$

The second trace is nothing else than the above calculation after replacing M for m and exchanging $1 \rightarrow 2$ and $3 \rightarrow 4$. This results in

$$\langle |M_{if}|^2 \rangle = \frac{4g_e^4}{(\vec{P}_1 - \vec{P}_3)^4} \cdot \left[\vec{P}_1^\mu \vec{P}_3^\nu + \vec{P}_3^\mu \vec{P}_1^\nu + g^{\mu\nu} \left(m^2 - \vec{P}_1^\mu \vec{P}_3^\mu \right) \right] \cdot \left[\vec{P}_2^\mu \vec{P}_4^\nu + \vec{P}_4^\mu \vec{P}_2^\nu + g_{\mu\nu} \left(M^2 - \vec{P}_2^\mu \vec{P}_4^\mu \right) \right] \Leftrightarrow$$

$$\langle |M_{if}|^2 \rangle = \frac{4g_e^4}{(\vec{P}_1 - \vec{P}_3)^4} \cdot \left[\left(\vec{P}_1^\mu \vec{P}_2^\mu \right) \left(\vec{P}_3^\mu \vec{P}_4^\mu \right) + \left(\vec{P}_1^\mu \vec{P}_4^\mu \right) \left(\vec{P}_2^\mu \vec{P}_3^\mu \right) - M^2 \left(\vec{P}_1^\mu \vec{P}_3^\mu \right) - m^2 \left(\vec{P}_2^\mu \vec{P}_4^\mu \right) + 2 \left(mM \right)^2 \right] \quad (4.2.2)$$

Let's now assume that the initial muon is at rest and that $m \ll M$. The 4-momenta of the particles participating in the process can be written:

$$\vec{P}_{1\mu} = (E_1, \vec{P}_1)$$

$$\vec{P}_{2\mu} = (M, \vec{0})$$

$$\vec{P}_{3\mu} = (E_3, \vec{P}_3)$$

$$\vec{P}_{4\mu} = (E_4, \vec{P}_4)$$

Let's now calculate each term of Eq. 4.2.2:

- $(\vec{P}_1 - \vec{P}_3)^2$:

$$(\vec{P}_1 - \vec{P}_3)^2 = (E_1 - E_3)^2 - (\vec{P}_1 - \vec{P}_3)^2 = E_1^2 + E_3^2 - 2E_1E_3 - P_1^2 - P_3^2 - 2P_1P_3 \cos(\theta)$$

Assuming that $P_1 \approx P_3 = P$ the previous equation is written:

$$(\vec{P}_1 - \vec{P}_3)^2 = 2m^2 - 2(P^2 + m^2) + 2P^2 \cos(\theta) = -2P^2(1 - \cos(\theta))$$

- $(\vec{P}_{1\mu} \vec{P}_{2\mu}) (\vec{P}_{3\mu} \vec{P}_{4\mu}) \approx ME_1ME_3 = M^2E^2$
- $(\vec{P}_{1\mu} \vec{P}_{4\mu}) (\vec{P}_{2\mu} \vec{P}_{3\mu}) \approx ME_1ME_3 = M^2E^2$
- $(\vec{P}_{1\mu} \vec{P}_{3\mu}) = E_1E_3 - P^2 \cos(\theta)$
- $(\vec{P}_{2\mu} \vec{P}_{4\mu}) \approx M^2$

The square of the matrix element can thus be written as¹:

$$\langle |M_{if}|^2 \rangle = \frac{4g_e^4}{[2P^2(1 - \cos(\theta))]^2} \cdot [M^2E^2 + M^2E^2 - (m^2 + P^2(1 - \cos(\theta)))M^2 - m^2M^2 + 2m^2M^2] \Leftrightarrow$$

$$\langle |M_{if}|^2 \rangle = \frac{g_e^4}{P^4 \sin^4(\theta/2)} \cdot (2M^2E^2 - M^2P^2 \sin^2(\theta/2) + m^2M^2 - m^2M^2) \Leftrightarrow$$

$$\langle |M_{if}|^2 \rangle = \frac{g_e^4 M^2}{P^4 \sin^4(\theta/2)} \cdot (m^2 + P^2 \cos^2(\theta/2))$$

The differential cross-section, considering also that $g_e = \sqrt{4\pi\alpha}$ can be written:

$$\frac{d\sigma}{d\Omega} = \frac{\alpha^2}{4P^4 \sin^4(\theta/2)} (m^2 + P^2 \cos^2(\theta/2)) \quad (4.2.3)$$

¹ Remember that $1 - \cos(\theta) = \sin^2(\theta/2)$

Chapter 5

Colour factors

In this chapter we are going to review the interactions between quarks and anti-quarks. This is something that obviously we can not observe in nature since quarks are confined within hadrons. However it will be instructive to look at the effective potentials. We will start from the effective potential between two charges e.g. electrons and positrons, that are attracted or repulsed by the potential

$$V(r) = -\frac{e^2}{r} = -\frac{\alpha\hbar c}{r} \quad (5.0.1)$$

where α is the fine structure constant and at this stage we decided not to drop \hbar and c by working with natural units.

5.1 Quark-Antiquark interactions

Let's try to calculate the matrix element for the interaction between a quark (e.g. u) and an anti-quark (e.g. \bar{d}) as illustrated in fig. 5.1. We consider the interaction of quarks of different flavour in order to avoid calculating extra diagrams that involve crossing of the outgoing external lines.

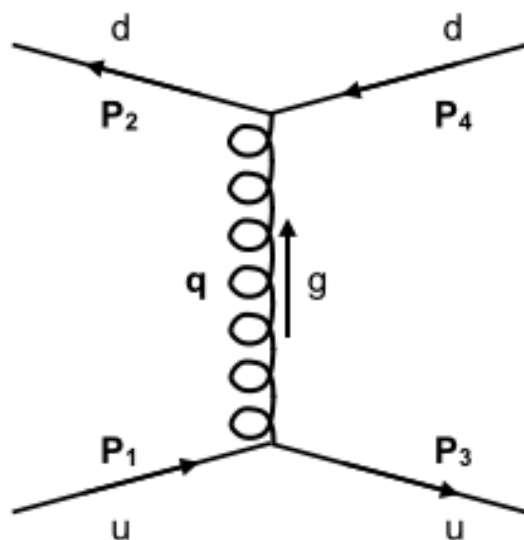


Fig. 5.1: The diagram describing the interaction between a quark and an anti-quark. In this particular case the quark and the anti-quark do not have the same flavour thus avoiding the extra diagram that involves crossing output lines.

$$\begin{aligned}
& \int [\bar{u}(3)c_3^\dagger] \cdot \left[\frac{-ig_s}{2} \lambda^\alpha \gamma^\mu \right] \cdot [u(1)c_1] \cdot \left[\frac{-ig_{\mu\nu}\delta^{\alpha\beta}}{\bar{q}^2} \right] \cdot [\bar{v}(2)c_2^\dagger] \cdot \left[\frac{-ig_s}{2} \lambda^\beta \gamma^\nu \right] \cdot [v(4)c_4] \cdot \\
& \quad [(2\pi)^4 \delta^4(\vec{P}_1 - \vec{P}_3 - \vec{q})] \cdot [(2\pi)^4 \delta^4(\vec{P}_2 - \vec{P}_4 + \vec{q})] \cdot \frac{d^4q}{(2\pi)^4} = \\
& \frac{ig_s^2(2\pi)^4}{4} \cdot [\bar{u}(3)c_3^\dagger] \cdot [\lambda^\alpha \gamma^\mu] \cdot [u(1)c_1] \cdot \left[\frac{g_{\mu\nu}\delta^{\alpha\beta}}{\bar{q}^2} \right] \cdot [\bar{v}(2)c_2^\dagger] \cdot [\lambda^\beta \gamma^\nu] \cdot [v(4)c_4] \cdot \delta^4(\vec{P}_1 + \vec{P}_2 - \vec{P}_3 - \vec{P}_4) \Leftrightarrow \\
& M_{if} = \frac{g_s^2}{4\bar{q}^2} \cdot [\bar{u}(3)c_3^\dagger] \cdot [\lambda^\alpha \gamma^\mu] \cdot [u(1)c_1] \cdot [g_{\mu\nu}\delta^{\alpha\beta}] \cdot [\bar{v}(2)c_2^\dagger] \cdot [\lambda^\beta \gamma^\nu] \cdot [v(4)c_4] \Leftrightarrow \\
& M_{if} = \frac{g_s^2}{4\bar{q}^2} \cdot [\bar{u}(3)\gamma^\mu u(1)] \cdot [\bar{v}(2)\gamma_\mu v(4)] \cdot \left[[c_3^\dagger \lambda^\alpha c_1] \cdot (\delta^{\alpha\beta}) \cdot [c_2^\dagger \lambda^\beta c_4] \right] \Leftrightarrow \\
& M_{if} = \frac{g_s^2}{\bar{q}^2} \cdot (\bar{u}(3)\gamma^\mu u(1)\bar{v}(2)\gamma_\mu v(4)) \cdot \left[\frac{1}{4} \cdot (c_3^\dagger \lambda^\alpha c_1) \cdot (c_2^\dagger \lambda^\alpha c_4) \right] \tag{5.1.1}
\end{aligned}$$

The first part of Eq. 5.1.1 i.e. $\frac{g_s^2}{\bar{q}^2} \cdot (\bar{u}(3)\gamma^\mu u(1)\bar{v}(2)\gamma_\mu v(4))$, is the same as in QED (e.g. scattering of an electron off a positive muon) with the strong coupling constant g_s taking the place of g_e . The second part i.e. $\left[\frac{1}{4} \cdot (c_3^\dagger \lambda^\alpha c_1) \cdot (c_2^\dagger \lambda^\alpha c_4) \right]$ is better known as **colour factors**.

The colour factor depends on the colour state of the interacting quarks. For a quark and an anti-quark, as we have seen in Chapter 2 and in particular in Section 2.5, we can form an octet and a singlet state. We will now calculate the colour factors separately for each state.

5.1.1 Colour factors for the octet configuration

Let's take one typical octet colour state e.g. $R\bar{B}$ with the relevant diagram of fig. 5.1 being transformed into fig.5.2. The diagram reads: an incoming red u quark interacts with another incoming antigreen d antiquark and produce a red u quark and an antigreen d antiquark. In order for the interaction to take place they have to exchange a gluon (colour-anticolour combination) that preserves the colour on every vertex. That would then be any of the $R\bar{R}$, $G\bar{G}$ or $B\bar{B}$ combinations.

For this choice of colours the matrices c_1 , c_2 , c_3 and c_4 are written as:

$$\begin{aligned}
c_1 = c_3 &= \begin{pmatrix} 1 \\ 0 \\ 0 \end{pmatrix} \\
c_2 = c_4 &= \begin{pmatrix} 0 \\ 1 \\ 0 \end{pmatrix}
\end{aligned}$$

It follows that

$$f = \frac{1}{4} \left[(1 \ 0 \ 0) \lambda^\alpha \begin{pmatrix} 1 \\ 0 \\ 0 \end{pmatrix} \right] \left[\begin{pmatrix} 1 \\ 0 \\ 0 \end{pmatrix} \lambda^\alpha \begin{pmatrix} 0 \\ 1 \\ 0 \end{pmatrix} \right]$$

The index α runs over all the Gell-Mann matrices i.e. $\alpha = 1, \dots, 8$:

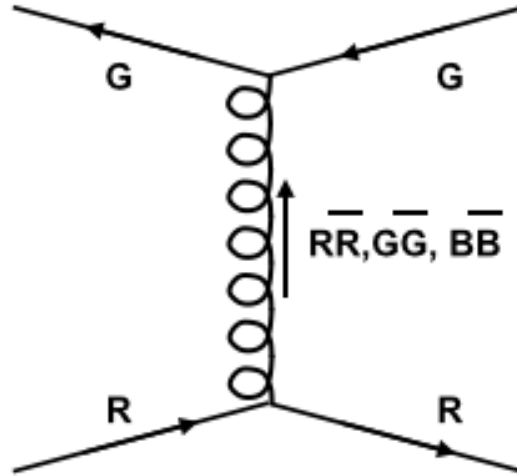


Fig. 5.2: The colour representation of one colour octet state of fig. 5.1.

$$\begin{aligned}
 & \cdot \left[(1\ 0\ 0) \lambda^1 \begin{pmatrix} 1 \\ 0 \\ 0 \end{pmatrix} \right] \left[(0\ 1\ 0) \lambda^1 \begin{pmatrix} 0 \\ 1 \\ 0 \end{pmatrix} \right] = \left[(1\ 0\ 0) \begin{pmatrix} 0 & 1 & 0 \\ 1 & 0 & 0 \\ 0 & 0 & 0 \end{pmatrix} \begin{pmatrix} 1 \\ 0 \\ 0 \end{pmatrix} \right] \left[(0\ 1\ 0) \begin{pmatrix} 0 & 1 & 0 \\ 1 & 0 & 0 \\ 0 & 0 & 0 \end{pmatrix} \begin{pmatrix} 0 \\ 1 \\ 0 \end{pmatrix} \right] = 0 \\
 & \cdot \left[(1\ 0\ 0) \lambda^2 \begin{pmatrix} 1 \\ 0 \\ 0 \end{pmatrix} \right] \left[(0\ 1\ 0) \lambda^2 \begin{pmatrix} 0 \\ 1 \\ 0 \end{pmatrix} \right] = \left[(1\ 0\ 0) \begin{pmatrix} 0 & -i & 0 \\ i & 0 & 0 \\ 0 & 0 & 0 \end{pmatrix} \begin{pmatrix} 1 \\ 0 \\ 0 \end{pmatrix} \right] \left[(0\ 1\ 0) \begin{pmatrix} 0 & -i & 0 \\ i & 0 & 0 \\ 0 & 0 & 0 \end{pmatrix} \begin{pmatrix} 0 \\ 1 \\ 0 \end{pmatrix} \right] = 0 \\
 & \cdot \left[(1\ 0\ 0) \lambda^3 \begin{pmatrix} 1 \\ 0 \\ 0 \end{pmatrix} \right] \left[(0\ 1\ 0) \lambda^3 \begin{pmatrix} 0 \\ 1 \\ 0 \end{pmatrix} \right] = \left[(1\ 0\ 0) \begin{pmatrix} 1 & 0 & 0 \\ 0 & -1 & 0 \\ 0 & 0 & 0 \end{pmatrix} \begin{pmatrix} 1 \\ 0 \\ 0 \end{pmatrix} \right] \left[(0\ 1\ 0) \begin{pmatrix} 1 & 0 & 0 \\ 0 & -1 & 0 \\ 0 & 0 & 0 \end{pmatrix} \begin{pmatrix} 0 \\ 1 \\ 0 \end{pmatrix} \right] = 1 \cdot (-1) = -1 \\
 & \cdot \left[(1\ 0\ 0) \lambda^4 \begin{pmatrix} 1 \\ 0 \\ 0 \end{pmatrix} \right] \left[(0\ 1\ 0) \lambda^4 \begin{pmatrix} 0 \\ 1 \\ 0 \end{pmatrix} \right] = \left[(1\ 0\ 0) \begin{pmatrix} 0 & 0 & 1 \\ 0 & 0 & 0 \\ 1 & 0 & 0 \end{pmatrix} \begin{pmatrix} 1 \\ 0 \\ 0 \end{pmatrix} \right] \left[(0\ 1\ 0) \begin{pmatrix} 0 & 0 & 1 \\ 0 & 0 & 0 \\ 1 & 0 & 0 \end{pmatrix} \begin{pmatrix} 0 \\ 1 \\ 0 \end{pmatrix} \right] = 0 \\
 & \cdot \left[(1\ 0\ 0) \lambda^5 \begin{pmatrix} 1 \\ 0 \\ 0 \end{pmatrix} \right] \left[(0\ 1\ 0) \lambda^5 \begin{pmatrix} 0 \\ 1 \\ 0 \end{pmatrix} \right] = \left[(1\ 0\ 0) \begin{pmatrix} 0 & 0 & -i \\ 0 & 0 & 0 \\ i & 0 & 0 \end{pmatrix} \begin{pmatrix} 1 \\ 0 \\ 0 \end{pmatrix} \right] \left[(0\ 1\ 0) \begin{pmatrix} 0 & 0 & -i \\ 0 & 0 & 0 \\ i & 0 & 0 \end{pmatrix} \begin{pmatrix} 0 \\ 1 \\ 0 \end{pmatrix} \right] = 0 \\
 & \cdot \left[(1\ 0\ 0) \lambda^6 \begin{pmatrix} 1 \\ 0 \\ 0 \end{pmatrix} \right] \left[(0\ 1\ 0) \lambda^6 \begin{pmatrix} 0 \\ 1 \\ 0 \end{pmatrix} \right] = \left[(1\ 0\ 0) \begin{pmatrix} 0 & 0 & 0 \\ 0 & 0 & 1 \\ 0 & 1 & 0 \end{pmatrix} \begin{pmatrix} 1 \\ 0 \\ 0 \end{pmatrix} \right] \left[(0\ 1\ 0) \begin{pmatrix} 0 & 0 & 0 \\ 0 & 0 & 1 \\ 0 & 1 & 0 \end{pmatrix} \begin{pmatrix} 0 \\ 1 \\ 0 \end{pmatrix} \right] = 0 \\
 & \cdot \left[(1\ 0\ 0) \lambda^7 \begin{pmatrix} 1 \\ 0 \\ 0 \end{pmatrix} \right] \left[(0\ 1\ 0) \lambda^7 \begin{pmatrix} 0 \\ 1 \\ 0 \end{pmatrix} \right] = \left[(1\ 0\ 0) \begin{pmatrix} 0 & 0 & 0 \\ 0 & 0 & -i \\ 0 & i & 0 \end{pmatrix} \begin{pmatrix} 1 \\ 0 \\ 0 \end{pmatrix} \right] \left[(0\ 1\ 0) \begin{pmatrix} 0 & 0 & 0 \\ 0 & 0 & -i \\ 0 & i & 0 \end{pmatrix} \begin{pmatrix} 0 \\ 1 \\ 0 \end{pmatrix} \right] = 0 \\
 & \cdot \left[(1\ 0\ 0) \lambda^8 \begin{pmatrix} 1 \\ 0 \\ 0 \end{pmatrix} \right] \left[(0\ 1\ 0) \lambda^8 \begin{pmatrix} 0 \\ 1 \\ 0 \end{pmatrix} \right] = \left[(1\ 0\ 0) \frac{1}{\sqrt{3}} \begin{pmatrix} 1 & 0 & 0 \\ 0 & 1 & 0 \\ 0 & 0 & -2 \end{pmatrix} \begin{pmatrix} 1 \\ 0 \\ 0 \end{pmatrix} \right] \left[(0\ 1\ 0) \frac{1}{\sqrt{3}} \begin{pmatrix} 1 & 0 & 0 \\ 0 & 1 & 0 \\ 0 & 0 & -2 \end{pmatrix} \begin{pmatrix} 0 \\ 1 \\ 0 \end{pmatrix} \right] = \frac{1}{\sqrt{3}} \cdot \frac{1}{\sqrt{3}} = \frac{1}{3}
 \end{aligned}$$

The colour factor is then:

$$f = \frac{1}{4} \left(-1 + \frac{1}{3} \right) = -\frac{1}{6}$$

Hint: Only the matrices with non-zero points at ii contribute!

5.1.2 Colour factors for the singlet configuration

If the incoming quarks are in the colour singlet state $\frac{1}{\sqrt{3}}(R\bar{R} + G\bar{G} + B\bar{B})$ then there are three terms in the colour factor:

$$f = \frac{1}{4} \frac{1}{\sqrt{3}} \left[\cdot \left[c_3^\dagger \lambda^\alpha \begin{pmatrix} 1 \\ 0 \\ 0 \end{pmatrix} \right] \cdot \left[(1 \ 0 \ 0) \lambda^\alpha c_4 \right] + \left[c_3^\dagger \lambda^\alpha \begin{pmatrix} 0 \\ 1 \\ 0 \end{pmatrix} \right] \cdot \left[(0 \ 1 \ 0) \lambda^\alpha c_4 \right] + \left[c_3^\dagger \lambda^\alpha \begin{pmatrix} 0 \\ 0 \\ 1 \end{pmatrix} \right] \cdot \left[(0 \ 0 \ 1) \lambda^\alpha c_4 \right] \right]$$

Similarly the outgoing quarks, represented by the matrices c_3 and c_4 , are in the colour singlet state, resulting into calculating nine terms:

$$\begin{aligned} f = \frac{1}{4} \frac{1}{\sqrt{3}} \cdot & \left[\left[(1 \ 0 \ 0) \lambda^\alpha \begin{pmatrix} 1 \\ 0 \\ 0 \end{pmatrix} \right] \cdot \left[(1 \ 0 \ 0) \lambda^\alpha \begin{pmatrix} 1 \\ 0 \\ 0 \end{pmatrix} \right] + \right. \\ & \left[(0 \ 1 \ 0) \lambda^\alpha \begin{pmatrix} 1 \\ 0 \\ 0 \end{pmatrix} \right] \cdot \left[(1 \ 0 \ 0) \lambda^\alpha \begin{pmatrix} 0 \\ 1 \\ 0 \end{pmatrix} \right] + \\ & \left[(0 \ 0 \ 1) \lambda^\alpha \begin{pmatrix} 1 \\ 0 \\ 0 \end{pmatrix} \right] \cdot \left[(1 \ 0 \ 0) \lambda^\alpha \begin{pmatrix} 0 \\ 0 \\ 1 \end{pmatrix} \right] + \\ & \left[(1 \ 0 \ 0) \lambda^\alpha \begin{pmatrix} 0 \\ 1 \\ 0 \end{pmatrix} \right] \cdot \left[(0 \ 1 \ 0) \lambda^\alpha \begin{pmatrix} 1 \\ 0 \\ 0 \end{pmatrix} \right] + \\ & \left[(0 \ 1 \ 0) \lambda^\alpha \begin{pmatrix} 0 \\ 1 \\ 0 \end{pmatrix} \right] \cdot \left[(0 \ 1 \ 0) \lambda^\alpha \begin{pmatrix} 0 \\ 1 \\ 0 \end{pmatrix} \right] + \\ & \left[(0 \ 0 \ 1) \lambda^\alpha \begin{pmatrix} 0 \\ 1 \\ 0 \end{pmatrix} \right] \cdot \left[(0 \ 1 \ 0) \lambda^\alpha \begin{pmatrix} 0 \\ 0 \\ 1 \end{pmatrix} \right] + \\ & \left[(1 \ 0 \ 0) \lambda^\alpha \begin{pmatrix} 0 \\ 0 \\ 1 \end{pmatrix} \right] \cdot \left[(0 \ 0 \ 1) \lambda^\alpha \begin{pmatrix} 1 \\ 0 \\ 0 \end{pmatrix} \right] + \\ & \left[(0 \ 1 \ 0) \lambda^\alpha \begin{pmatrix} 0 \\ 0 \\ 1 \end{pmatrix} \right] \cdot \left[(0 \ 0 \ 1) \lambda^\alpha \begin{pmatrix} 0 \\ 1 \\ 0 \end{pmatrix} \right] + \\ & \left. \left[(0 \ 0 \ 1) \lambda^\alpha \begin{pmatrix} 0 \\ 0 \\ 1 \end{pmatrix} \right] \cdot \left[(0 \ 0 \ 1) \lambda^\alpha \begin{pmatrix} 0 \\ 0 \\ 1 \end{pmatrix} \right] \right] \end{aligned}$$

The first term is non-zero for the non-zero elements of λ^α at 11 i.e. it gives rise to $\lambda_{11}^\alpha \cdot \lambda_{11}^\alpha$, the second term gives rise to $\lambda_{21}^\alpha \cdot \lambda_{12}^\alpha$, the third $\lambda_{31}^\alpha \cdot \lambda_{13}^\alpha, \dots$. The end product is:

$$f = \frac{1}{12} \sum_{\alpha=1}^8 \sum_{i=1}^3 \sum_{j=1}^3 \lambda_{ij}^\alpha \cdot \lambda_{ji}^\alpha = \frac{1}{12} \text{Tr}(\lambda^\alpha \cdot \lambda^\alpha)$$

It can be shown that $\text{Tr}(\lambda^\alpha \cdot \lambda^\beta) = 2\delta^{\alpha\beta}$, which means that with the summation over α : $\text{Tr}(\lambda^\alpha \cdot \lambda^\alpha) = 16$, which in turns lead to:

$$f = \frac{4}{3}$$

5.2 Quark-Quark interactions

Let's try to calculate the matrix element for the interaction between two quarks (e.g. u and a d) as illustrated in fig. 5.3. Once again, we consider the interaction of quarks of different flavour in order to avoid calculating extra diagrams that involve crossing of the outgoing external lines.

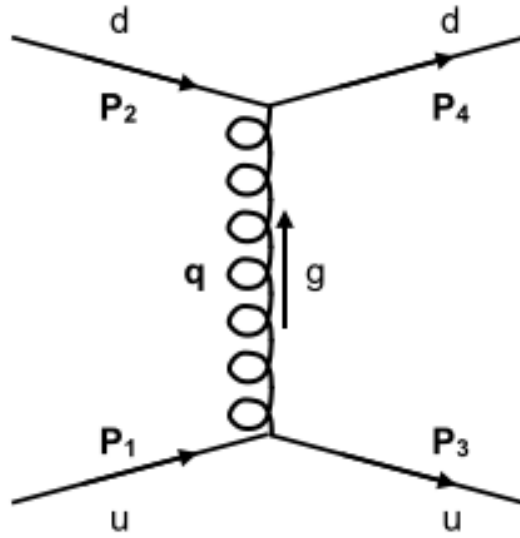


Fig. 5.3: The diagram describing the interaction between two quarks.

$$\begin{aligned}
 & \int [\bar{u}(3)c_3^\dagger] \cdot \left[\frac{-ig_s}{2} \lambda^\alpha \gamma^\mu \right] \cdot [u(1)c_1] \cdot \left[\frac{-ig_{\mu\nu}\delta^{\alpha\beta}}{\vec{q}^2} \right] \cdot [\bar{u}(4)c_4^\dagger] \cdot \left[\frac{-ig_s}{2} \lambda^\beta \gamma^\nu \right] \cdot [u(2)c_2] \cdot \\
 & \quad [(2\pi)^4 \delta^4(\vec{P}_1 - \vec{P}_3 - \vec{q})] \cdot [(2\pi)^4 \delta^4(\vec{P}_2 - \vec{P}_4 + \vec{q})] \cdot \frac{d^4q}{(2\pi)^4} = \\
 & \frac{ig_s^2(2\pi)^4}{4} \cdot [\bar{u}(3)c_3^\dagger] \cdot [\lambda^\alpha \gamma^\mu] \cdot [u(1)c_1] \cdot \left[\frac{g_{\mu\nu}\delta^{\alpha\beta}}{\vec{q}^2} \right] \cdot [\bar{u}(4)c_4^\dagger] \cdot [\lambda^\beta \gamma^\nu] \cdot [u(2)c_2] \cdot \delta^4(\vec{P}_1 + \vec{P}_2 - \vec{P}_3 - \vec{P}_4) \Leftrightarrow \\
 & M_{if} = \frac{g_s^2}{4\vec{q}^2} \cdot [\bar{u}(3)c_3^\dagger] \cdot [\lambda^\alpha \gamma^\mu] \cdot [u(1)c_1] \cdot [g_{\mu\nu}\delta^{\alpha\beta}] \cdot [\bar{u}(4)c_4^\dagger] \cdot [\lambda^\beta \gamma^\nu] \cdot [u(2)c_2] \Leftrightarrow \\
 & M_{if} = \frac{g_s^2}{4\vec{q}^2} \cdot [\bar{u}(3)\gamma^\mu u(1)] \cdot [\bar{u}(4)\gamma_\nu u(2)] \cdot \left[[c_3^\dagger \lambda^\alpha c_1] \cdot (\delta^{\alpha\beta}) \cdot [c_4^\dagger \lambda^\beta c_2] \right] \Leftrightarrow \\
 & M_{if} = \frac{g_s^2}{\vec{q}^2} \cdot (\bar{u}(3)\gamma^\mu u(1)\bar{u}(4)\gamma_\nu u(2)) \cdot \left[\frac{1}{4} \cdot (c_3^\dagger \lambda^\alpha c_1) \cdot (c_4^\dagger \lambda^\alpha c_2) \right] \tag{5.2.1}
 \end{aligned}$$

The first part of Eq. 5.2.1 i.e. $\frac{g_s^2}{q^2} \cdot (\bar{u}(3)\gamma^\mu u(1)\bar{u}(4)\gamma_\mu u(2))$, is the same as in QED (e.g. scattering of an electron off a muon) with the strong coupling constant g_s taking the place of g_e . The second part i.e. $\left[\frac{1}{4} \cdot (c_3^\dagger \lambda^\alpha c_1) \cdot (c_4^\dagger \lambda^\alpha c_2)\right]$ gives the relevant colour factors for the $q-q$ interactions.

The colour factor depends on the colour state of the interacting quarks. For two quarks, as we have seen in Chapter 2 and in particular in Section 2.5, we can form a symmetric sextet and an anti-symmetric triplet state. We will now calculate the colour factors separately for each state.

5.2.1 Colour factors for the sextet configuration

The sextet consists of the following combinations: RR , GG , BB , $(RB + BR)/\sqrt{2}$, $(GB + BG)/\sqrt{2}$, and $(RG + GR)/\sqrt{2}$. Let's take one typical octet colour state e.g. RR with the relevant diagram of fig. 5.3 being transformed into fig.5.4. The diagram reads: an incoming red u quark interacts with another incoming red d quark and produce a red u quark and another red d quark. In order for the interaction to take place they have to exchange a gluon (colour-anticolour combination) that preserves the colour on every vertex. That would then be any of the \overline{RR} , \overline{GG} or \overline{BB} combinations.

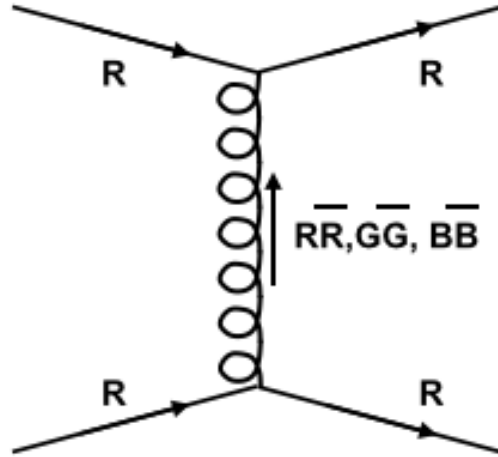


Fig. 5.4: The colour representation of one colour sextet state of fig. 5.1.

For this choice of colours the matrices c_1 , c_2 , c_3 and c_4 are written as:

$$c_1 = c_2 = c_3 = c_4 = \begin{pmatrix} 1 \\ 0 \\ 0 \end{pmatrix}$$

It follows that

$$f = \frac{1}{4} \left[(1 \ 0 \ 0) \lambda^\alpha \begin{pmatrix} 1 \\ 0 \\ 0 \end{pmatrix} \right] \left[(1 \ 0 \ 0) \lambda^\alpha \begin{pmatrix} 1 \\ 0 \\ 0 \end{pmatrix} \right]$$

The index α runs over all the Gell-Man matrices i.e. $\alpha = 1, \dots, 8$:

$$\bullet \left[(1 \ 0 \ 0) \lambda^1 \begin{pmatrix} 1 \\ 0 \\ 0 \end{pmatrix} \right] \left[(1 \ 0 \ 0) \lambda^1 \begin{pmatrix} 1 \\ 0 \\ 0 \end{pmatrix} \right] = \left[(1 \ 0 \ 0) \begin{pmatrix} 0 & 1 & 0 \\ 1 & 0 & 0 \\ 0 & 0 & 0 \end{pmatrix} \begin{pmatrix} 1 \\ 0 \\ 0 \end{pmatrix} \right] \left[(1 \ 0 \ 0) \begin{pmatrix} 0 & 1 & 0 \\ 1 & 0 & 0 \\ 0 & 0 & 0 \end{pmatrix} \begin{pmatrix} 1 \\ 0 \\ 0 \end{pmatrix} \right] = 0$$

$$\begin{aligned}
& \bullet \left[(1\ 0\ 0) \lambda^2 \begin{pmatrix} 1 \\ 0 \\ 0 \end{pmatrix} \right] \left[(1\ 0\ 0) \lambda^2 \begin{pmatrix} 1 \\ 0 \\ 0 \end{pmatrix} \right] = \left[(1\ 0\ 0) \begin{pmatrix} 0 & -i & 0 \\ i & 0 & 0 \\ 0 & 0 & 0 \end{pmatrix} \begin{pmatrix} 1 \\ 0 \\ 0 \end{pmatrix} \right] \left[(1\ 0\ 0) \begin{pmatrix} 0 & -i & 0 \\ i & 0 & 0 \\ 0 & 0 & 0 \end{pmatrix} \begin{pmatrix} 1 \\ 0 \\ 0 \end{pmatrix} \right] = 0 \\
& \bullet \left[(1\ 0\ 0) \lambda^3 \begin{pmatrix} 1 \\ 0 \\ 0 \end{pmatrix} \right] \left[(1\ 0\ 0) \lambda^3 \begin{pmatrix} 1 \\ 0 \\ 0 \end{pmatrix} \right] = \left[(1\ 0\ 0) \begin{pmatrix} 1 & 0 & 0 \\ 0 & -1 & 0 \\ 0 & 0 & 0 \end{pmatrix} \begin{pmatrix} 1 \\ 0 \\ 0 \end{pmatrix} \right] \left[(1\ 0\ 0) \begin{pmatrix} 1 & 0 & 0 \\ 0 & -1 & 0 \\ 0 & 0 & 0 \end{pmatrix} \begin{pmatrix} 1 \\ 0 \\ 0 \end{pmatrix} \right] = 1 \cdot 1 = 1 \\
& \bullet \left[(1\ 0\ 0) \lambda^4 \begin{pmatrix} 1 \\ 0 \\ 0 \end{pmatrix} \right] \left[(1\ 0\ 0) \lambda^4 \begin{pmatrix} 1 \\ 0 \\ 0 \end{pmatrix} \right] = \left[(1\ 0\ 0) \begin{pmatrix} 0 & 0 & 1 \\ 0 & 0 & 0 \\ 1 & 0 & 0 \end{pmatrix} \begin{pmatrix} 1 \\ 0 \\ 0 \end{pmatrix} \right] \left[(1\ 0\ 0) \begin{pmatrix} 0 & 0 & 1 \\ 0 & 0 & 0 \\ 1 & 0 & 0 \end{pmatrix} \begin{pmatrix} 1 \\ 0 \\ 0 \end{pmatrix} \right] = 0 \\
& \bullet \left[(1\ 0\ 0) \lambda^5 \begin{pmatrix} 1 \\ 0 \\ 0 \end{pmatrix} \right] \left[(1\ 0\ 0) \lambda^5 \begin{pmatrix} 1 \\ 0 \\ 0 \end{pmatrix} \right] = \left[(1\ 0\ 0) \begin{pmatrix} 0 & 0 & -i \\ 0 & 0 & 0 \\ i & 0 & 0 \end{pmatrix} \begin{pmatrix} 1 \\ 0 \\ 0 \end{pmatrix} \right] \left[(1\ 0\ 0) \begin{pmatrix} 0 & 0 & -i \\ 0 & 0 & 0 \\ i & 0 & 0 \end{pmatrix} \begin{pmatrix} 1 \\ 0 \\ 0 \end{pmatrix} \right] = 0 \\
& \bullet \left[(1\ 0\ 0) \lambda^6 \begin{pmatrix} 1 \\ 0 \\ 0 \end{pmatrix} \right] \left[(1\ 0\ 0) \lambda^6 \begin{pmatrix} 1 \\ 0 \\ 0 \end{pmatrix} \right] = \left[(1\ 0\ 0) \begin{pmatrix} 0 & 0 & 0 \\ 0 & 0 & 1 \\ 0 & 1 & 0 \end{pmatrix} \begin{pmatrix} 1 \\ 0 \\ 0 \end{pmatrix} \right] \left[(1\ 0\ 0) \begin{pmatrix} 0 & 0 & 0 \\ 0 & 0 & 1 \\ 0 & 1 & 0 \end{pmatrix} \begin{pmatrix} 1 \\ 0 \\ 0 \end{pmatrix} \right] = 0 \\
& \bullet \left[(1\ 0\ 0) \lambda^7 \begin{pmatrix} 1 \\ 0 \\ 0 \end{pmatrix} \right] \left[(1\ 0\ 0) \lambda^7 \begin{pmatrix} 1 \\ 0 \\ 0 \end{pmatrix} \right] = \left[(1\ 0\ 0) \begin{pmatrix} 0 & 0 & 0 \\ 0 & 0 & -i \\ 0 & i & 0 \end{pmatrix} \begin{pmatrix} 1 \\ 0 \\ 0 \end{pmatrix} \right] \left[(1\ 0\ 0) \begin{pmatrix} 0 & 0 & 0 \\ 0 & 0 & -i \\ 0 & i & 0 \end{pmatrix} \begin{pmatrix} 1 \\ 0 \\ 0 \end{pmatrix} \right] = 0 \\
& \bullet \left[(1\ 0\ 0) \lambda^8 \begin{pmatrix} 1 \\ 0 \\ 0 \end{pmatrix} \right] \left[(1\ 0\ 0) \lambda^8 \begin{pmatrix} 1 \\ 0 \\ 0 \end{pmatrix} \right] = \left[(1\ 0\ 0) \frac{1}{\sqrt{3}} \begin{pmatrix} 1 & 0 & 0 \\ 0 & 1 & 0 \\ 0 & 0 & -2 \end{pmatrix} \begin{pmatrix} 1 \\ 0 \\ 0 \end{pmatrix} \right] \left[(1\ 0\ 0) \frac{1}{\sqrt{3}} \begin{pmatrix} 1 & 0 & 0 \\ 0 & 1 & 0 \\ 0 & 0 & -2 \end{pmatrix} \begin{pmatrix} 1 \\ 0 \\ 0 \end{pmatrix} \right] = \frac{1}{\sqrt{3}} \cdot \frac{1}{\sqrt{3}} = \frac{1}{3}
\end{aligned}$$

The colour factor is then:

$$f = \frac{1}{4} \left(1 + \frac{1}{3} \right) = \frac{1}{3}$$

Although we followed all the steps, it is important to realise that only the matrices with non-zero points at ii contribute!

5.2.2 Colour factors for the triplet configuration

The triplet configuration is an anti-symmetric one with elements $(RB - BR)/\sqrt{2}$, $(BG - GB)/\sqrt{2}$, and $(GR - RG)/\sqrt{2}$. Let's now take the last colour state i.e. $(RG - GR)/\sqrt{2}$, and calculate the colour factors:

$$\begin{aligned}
f &= \frac{1}{4} \frac{1}{\sqrt{2}} \frac{1}{\sqrt{2}} \cdot \left[(1\ 0\ 0) \lambda^\alpha \begin{pmatrix} 1 \\ 0 \\ 0 \end{pmatrix} \right] \cdot \left[(0\ 1\ 0) \lambda^\alpha \begin{pmatrix} 0 \\ 1 \\ 0 \end{pmatrix} \right] \\
&\quad + \left[(0\ 1\ 0) \lambda^\alpha \begin{pmatrix} 0 \\ 1 \\ 0 \end{pmatrix} \right] \cdot \left[(1\ 0\ 0) \lambda^\alpha \begin{pmatrix} 1 \\ 0 \\ 0 \end{pmatrix} \right] \\
&\quad - \left[(1\ 0\ 0) \lambda^\alpha \begin{pmatrix} 0 \\ 1 \\ 0 \end{pmatrix} \right] \cdot \left[(0\ 1\ 0) \lambda^\alpha \begin{pmatrix} 1 \\ 0 \\ 0 \end{pmatrix} \right] \\
&\quad - \left[(0\ 1\ 0) \lambda^\alpha \begin{pmatrix} 1 \\ 0 \\ 0 \end{pmatrix} \right] \cdot \left[(1\ 0\ 0) \lambda^\alpha \begin{pmatrix} 0 \\ 1 \\ 0 \end{pmatrix} \right] =
\end{aligned}$$

$$\begin{aligned}
& \frac{1}{8} \left[\left(\lambda_{11}^\alpha \cdot \lambda_{22}^\alpha \right) + \left(\lambda_{22}^\alpha \cdot \lambda_{11}^\alpha \right) - \left(\lambda_{12}^\alpha \cdot \lambda_{21}^\alpha \right) - \left(\lambda_{21}^\alpha \cdot \lambda_{12}^\alpha \right) \right] = \\
& \frac{1}{4} \left[\left(\lambda_{11}^\alpha \cdot \lambda_{22}^\alpha \right) - \left(\lambda_{12}^\alpha \cdot \lambda_{21}^\alpha \right) \right] = \\
& \frac{1}{4} \left[\left(\lambda_{11}^3 \cdot \lambda_{22}^3 \right) + \left(\lambda_{11}^8 \cdot \lambda_{22}^8 \right) - \left(\lambda_{12}^1 \cdot \lambda_{21}^1 \right) - \left(\lambda_{12}^2 \cdot \lambda_{21}^2 \right) \right] \Leftrightarrow \\
& f = \frac{-2}{3}
\end{aligned}$$

5.3 Colour interactions

Let us now calculate the effective potentials for the two cases i.e. the $q-\bar{q}$ and $q-q$ interactions. Equation 5.0.1 is modified in such a way so that it takes into account both the strong coupling constant and the colour factors. For what concerns the $q-\bar{q}$ case, we have:

$$V(r) = -f \frac{\alpha_s \hbar c}{r} \quad (5.3.1)$$

The relevant potentials for the different multiplets are:

- Colour octet: $V(r) = \frac{1}{6} \frac{\alpha_s \hbar c}{r}$
- Colour singlet: $V(r) = -\frac{4}{3} \frac{\alpha_s \hbar c}{r}$

This clearly indicates that the force is attractive for the colour singlet state and repulsive for the colour octet. This gives another explanation on how the $q-\bar{q}$ binding occurs in the colour singlet state, resulting into coloured neutral mesons.

For what concerns the $q-q$ case, we have:

$$V(r) = f \frac{\alpha_s \hbar c}{r} \quad (5.3.2)$$

Note that the negative sign is removed due to the same charges of the two quarks. The relevant potentials for the different multiplets are:

- Colour sextet: $V(r) = \frac{1}{3} \frac{\alpha_s \hbar c}{r}$
- Colour triplet: $V(r) = -\frac{2}{3} \frac{\alpha_s \hbar c}{r}$

This clearly indicates that the force is attractive for the colour triplet state and repulsive for the colour sextet. However one needs to add another quark in the mix to form a baryon. As we have seen in Section 2.5 one can form a completely anti-symmetric singlet state, a symmetric decuplet, and two semi-anti-symmetric octets.

As pointed out before, these potentials are valid in case of short scales. QCD is formally very reminiscent of QED but there are important differences because, unlike photons, the gluons interact among themselves. In QED, the electric field of two oppositely charged particles permeates all space and diminishes quickly when the charges are separated. On the other hand, when one tries to separate a colour charge the gluon self-interaction causes the colour field between these charges to organise itself into a so-called flux tube or colour string. When stretched, the behaviour of such a string is very much like that of a rubber band. This behaviour of the gluon field leads to a force which is constant between the colour charges, regardless of their distance. The strength of this force is huge, about 16×10^4 N, or 16 tons. It follows that the colour charges cannot be fully separated since that would cost an infinite amount of energy. Instead, it will be energetically

more favourable to pull a quark-antiquark pair out of the vacuum and this causes the string to break. QED-like behaviour at small distance, and string behaviour at large distance leads to a QCD potential that behaves roughly as:

$$V(r) \sim \frac{\alpha}{r} + kr$$

Chapter 6

Form factors

In this chapter, we will discuss about the experimental evidence of the colour quantum number and we will get a first glimpse about the internal structure of protons.

6.1 Evidence of colour

So far we have discussed about colour as a new quantum number that characterises quarks and gluons. We have not discussed how the existence of colour was established. To do this, we need to go back to a QED process we should be by now familiar with i.e. the electron-positron scattering described by the interaction $e^- + e^+ \rightarrow \mu^- + \mu^+$ and by the diagram 6.1.

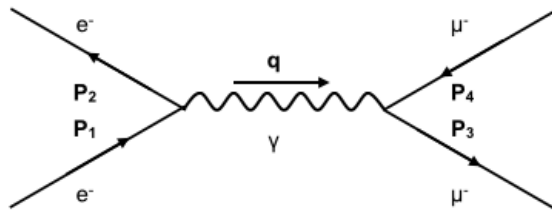


Fig. 6.1: The diagram describing the electron-positron scattering into a pair of muons $e^- + e^+ \rightarrow \mu^- + \mu^+$.

Similarly to this figure, one can as well create a pair of quarks i.e. more precise a $q - \bar{q}$ pair that for a brief moment fly apart until they are separated by a distance of the size of the hadron ($\approx 10^{-15}$ m). The relevant diagram for this process is given in fig. 6.2. As we have seen in Chapter 5 and in particular in Section 5.3, beyond this distance it is energetically favourable to form new $q - \bar{q}$ pairs that eventually lead to the creation of hadrons. It turns out though that the initial $q - \bar{q}$ pair leaves a footprint in the final state hadron production since these hadrons usually emerge as two back-to-back sprays, known as jets. In some cases it happens that a gluon emerges with a substantial fraction of the initial energy. This gluon then fragments, creating a third jet, a topology known as a three-jet event. Examples of a two- and three-jet events are shown in the left and right plot of fig. 6.3, respectively.

At the Large Hadron Collider (LHC), where the energy compared to the previous colliders has increased significantly i.e. by orders of magnitude, we are able to detect event topologies that involve more than three jets. That implies that more than one gluon carries enough energy, fragment and produce additional jets. An example of a five jet event topology from the ATLAS experiment is given in fig. 6.4

Let us now try to calculate the cross-section for the process $e^- + e^+ \rightarrow \text{hadrons}$ and compare it to the one of $e^- + e^+ \rightarrow \mu^- + \mu^+$. For this we will rely on the QED Feynman rules and we will first calculate the matrix element as follows:

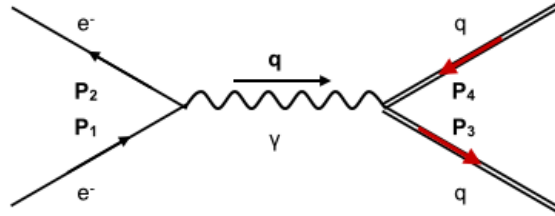


Fig. 6.2: The diagram describing the electron-positron scattering into a pair of quarks $e^- + e^+ \rightarrow q + \bar{q}$.

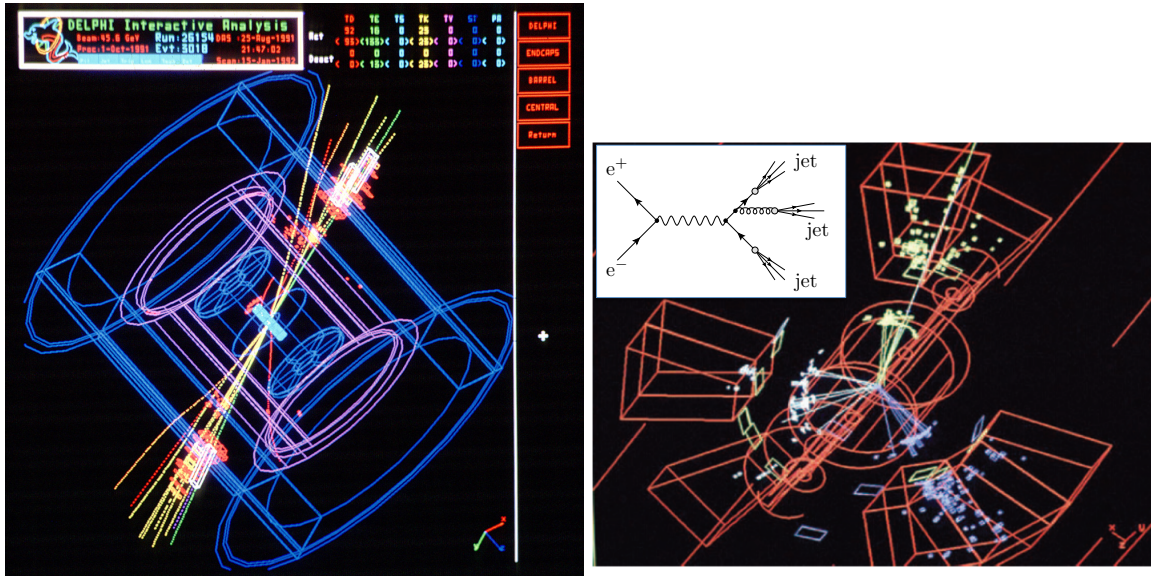


Fig. 6.3: A typical two- and three-jet topology in the left and right plot, respectively.

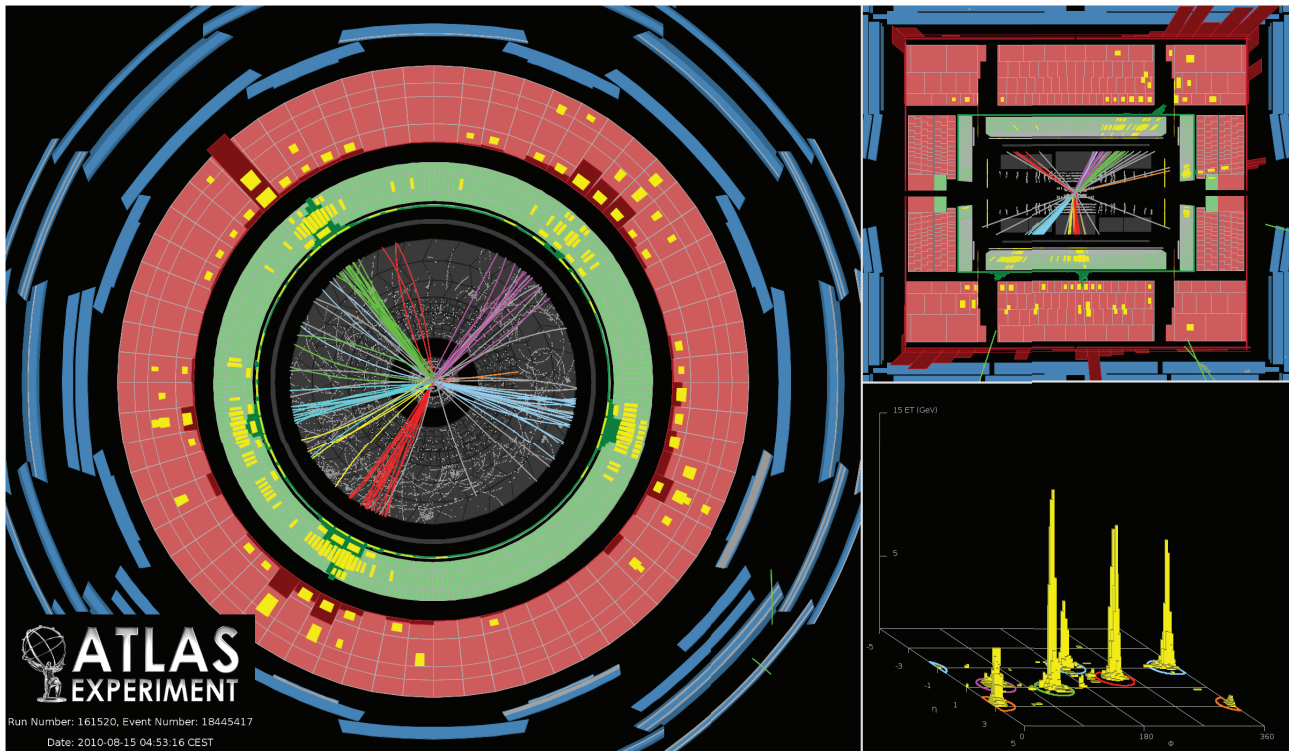


Fig. 6.4: A typical five-jet topology as recorded by the ATLAS experiment at the LHC.

$$\begin{aligned}
& \int \left[\bar{u}(\vec{P}_3)(ig_e\gamma^\mu)v(\vec{P}_4) \right] \left(\frac{-ig_{\mu\nu}}{q^2} \right) \left[\bar{v}(\vec{P}_2)(ig_e\gamma^\nu)u(\vec{P}_1) \right] \cdot \left[(2\pi)^4 \delta^4(\vec{P}_1 + \vec{P}_2 - \vec{q}) \right] \cdot \left[(2\pi)^4 \delta^4(-\vec{P}_3 - \vec{P}_4 + \vec{q}) \right] \cdot \frac{d^4q}{(2\pi)^4} = \\
& \int -i^3 g_e^2 (2\pi)^4 \left[\bar{u}(\vec{P}_3)\gamma^\mu v(\vec{P}_4) \right] \left(\frac{g_{\mu\nu}}{q^2} \right) \left[\bar{v}(\vec{P}_2)\gamma^\nu u(\vec{P}_1) \right] \cdot \left[\delta^4(\vec{P}_1 + \vec{P}_2 - \vec{q}) \right] \cdot \left[\delta^4(-\vec{P}_3 - \vec{P}_4 + \vec{q}) \right] \cdot d^4q = \\
& \frac{ig_e^2 (2\pi)^4}{(\vec{P}_1 + \vec{P}_2)^2} \left[\bar{u}(\vec{P}_3)\gamma^\mu v(\vec{P}_4) \right] \left[\bar{v}(\vec{P}_2)\gamma_\mu u(\vec{P}_1) \right] \cdot \left[\delta^4(\vec{P}_1 + \vec{P}_2 - \vec{P}_3 - \vec{P}_4) \right] \cdot d^4q = \\
& M_{if} = \frac{g_e^2}{(\vec{P}_1 + \vec{P}_2)^2} \left[\bar{u}(\vec{P}_3)\gamma^\mu v(\vec{P}_4) \right] \left[\bar{v}(\vec{P}_2)\gamma_\mu u(\vec{P}_1) \right] \tag{6.1.1}
\end{aligned}$$

For the case of quarks instead of muons, we only have to add the relevant charge of the quark Q :

$$M_{if} = \frac{Qg_e^2}{(\vec{P}_1 + \vec{P}_2)^2} \left[\bar{u}(\vec{P}_3)\gamma^\mu v(\vec{P}_4) \right] \left[\bar{v}(\vec{P}_2)\gamma_\mu u(\vec{P}_1) \right] \tag{6.1.2}$$

The square of the matrix element of Eq. 6.1.2 is then:

$$|M_{if}|^2 = \frac{Q^2 g_e^4}{(\vec{P}_1 + \vec{P}_2)^4} \left[\bar{u}(\vec{P}_3)\gamma^\mu v(\vec{P}_4) \right] \left[\bar{v}(\vec{P}_2)\gamma_\mu u(\vec{P}_1) \right] \left[\bar{u}(\vec{P}_3)\gamma^\mu v(\vec{P}_4) \right]^* \left[\bar{v}(\vec{P}_2)\gamma_\mu u(\vec{P}_1) \right]^* \tag{6.1.3}$$

One has to take the sum over all initial and final spin states:

$$\begin{aligned}
& \sum_{spin} \left[\bar{v}(\vec{P}_2)\gamma_\mu u(\vec{P}_1) \right] \cdot \left[\bar{v}(\vec{P}_2)\gamma_\mu u(\vec{P}_1) \right]^* = \text{Tr} \left(\gamma_\mu (\vec{\not{P}}_1 + m) \gamma_\nu (\vec{\not{P}}_2 - m) \right) \\
& \sum_{spin} \left[\bar{u}(\vec{P}_3)\gamma^\mu v(\vec{P}_4) \right] \cdot \left[\bar{u}(\vec{P}_3)\gamma^\mu v(\vec{P}_4) \right]^* = \text{Tr} \left(\gamma_\mu (\vec{\not{P}}_4 - M) \gamma_\nu (\vec{\not{P}}_3 + M) \right)
\end{aligned}$$

The average over all spin states of Eq. 6.1.3 is then:

$$\langle |M_{if}|^2 \rangle = \frac{1}{4} \frac{Q^2 g_e^4}{(\vec{P}_1 + \vec{P}_2)^4} \cdot \text{Tr} \left(\gamma_\mu (\vec{\not{P}}_1 + m) \gamma_\nu (\vec{\not{P}}_2 - m) \right) \cdot \text{Tr} \left(\gamma_\mu (\vec{\not{P}}_4 - M) \gamma_\nu (\vec{\not{P}}_3 + M) \right) \tag{6.1.4}$$

We will now calculate each trace separately:

- $\text{Tr} \left(\gamma_\mu (\vec{\not{P}}_1 + m) \gamma_\nu (\vec{\not{P}}_2 - m) \right) = \text{Tr}(\gamma_\mu \vec{\not{P}}_1 \gamma_\nu \vec{\not{P}}_2) + m \text{Tr}(\gamma_\mu \gamma_\nu \vec{\not{P}}_2) - m \text{Tr}(\gamma_\mu \vec{\not{P}}_1 \gamma_\nu) - m^2 \text{Tr}(\gamma_\mu \gamma_\nu)$

The first trace is: $\text{Tr}(\gamma_\mu \vec{\not{P}}_1 \gamma_\nu \vec{\not{P}}_2) = 4 \left[P_{1\mu} P_{2\nu} - g_{\mu\nu} (P_{1\lambda} P_2^\lambda) + P_{2\mu} P_{1\nu} \right]$

The second and third traces give 0:

$m \text{Tr}(\gamma_\mu \gamma_\nu \vec{\not{P}}_2) = 0$ i.e. odd number of γ -matrices,

$m \text{Tr}(\gamma_\mu \vec{\not{P}}_1 \gamma_\nu) = 0$ i.e. odd number of γ -matrices.

Finally, the last trace is $m^2 \text{Tr}(\gamma_\mu \gamma_\nu) = 4m^2 g_{\mu\nu}$.

The trace is then:

$$\text{Tr} \left(\gamma_\mu (\vec{\not{P}}_1 + m) \gamma_\nu (\vec{\not{P}}_2 - m) \right) = 4 \left[P_{1\mu} P_{2\nu} + P_{2\mu} P_{1\nu} - g_{\mu\nu} \left((P_{1\lambda} P_2^\lambda) + m^2 \right) \right]$$

- Similarly for the other trace of Eq. 6.1.4 we have:

$$\text{Tr}\left(\gamma^\mu(\vec{p}_4 - M)\gamma^\nu(\vec{p}_3 + M)\right) = 4\left[\vec{p}_4^\mu\vec{p}_3^\nu + \vec{p}_3^\mu\vec{p}_4^\nu - g^{\mu\nu}\left((\vec{p}_{4\lambda}\vec{p}_3^\lambda) + M^2\right)\right]$$

It then follows that Eq. 6.1.4 is written as:

$$\langle|M_{if}|^2\rangle = \frac{1}{4}\frac{Q^2g_e^4}{(\vec{P}_1 + \vec{P}_2)^4} \cdot 4\left[\vec{P}_{1\mu}\vec{P}_{2\nu} + \vec{P}_{2\mu}\vec{P}_{1\nu} - g_{\mu\nu}\left((\vec{P}_{1\lambda}\vec{P}_2^\lambda) + m^2\right)\right] \cdot 4\left[\vec{P}_4^\mu\vec{P}_3^\nu + \vec{P}_3^\mu\vec{P}_4^\nu - g^{\mu\nu}\left((\vec{P}_{4\lambda}\vec{P}_3^\lambda) + M^2\right)\right] \Leftrightarrow$$

$$\langle|M_{if}|^2\rangle = 8\left[\frac{Qg_e^2}{(\vec{P}_1 + \vec{P}_2)^2}\right]^2 \cdot \left[\left(\vec{P}_{1\mu}\vec{P}_4^\mu\right) \cdot \left(\vec{P}_{2\nu}\vec{P}_3^\nu\right) + \left(\vec{P}_{1\mu}\vec{P}_3^\mu\right) \cdot \left(\vec{P}_{2\nu}\vec{P}_4^\nu\right) + M^2\left(\vec{P}_{1\lambda}\vec{P}_2^\lambda\right) + m^2\left(\vec{P}_{4\lambda}\vec{P}_3^\lambda\right) + 2(mM)^2\right]$$

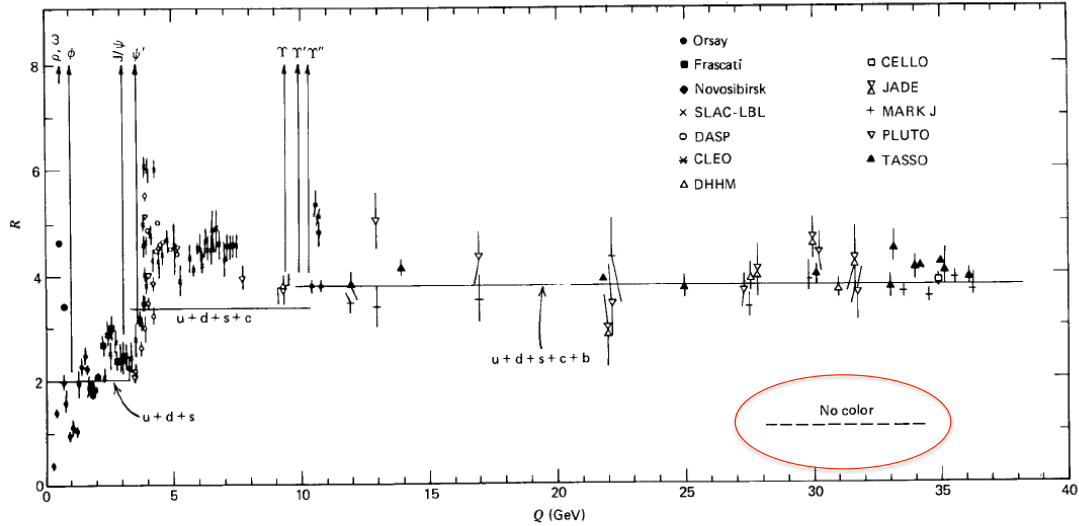


Fig. 11.3 Ratio R of (11.6) as a function of the total e^-e^+ center-of-mass energy. (The sharp peaks correspond to the production of narrow 1^- resonances just below or near the flavor thresholds.)

Fig. 6.5: The energy evolution of R as measured in experiments.

In terms of the incident energy E of the electron (positron) and the scattering angle θ between the electron and the quark, the previous formula is written as:

$$\langle|M_{if}|^2\rangle = Q^2g_e^4\left[1 + \left(\frac{m}{E}\right)^2 + \left(\frac{M}{E}\right)^2 + \left(1 - \left(\frac{m}{E}\right)^2\right) \cdot \left(1 - \left(\frac{M}{E}\right)^2\right) \cos^2(\theta)\right]$$

It is obvious that there is a threshold for this interaction to occur: $E \geq M$, below which the process is kinematically forbidden. The final integrated cross-section for the case where $E > M \gg m$ is

$$\sigma = \frac{\pi}{3} \left[\frac{Q\alpha}{E} \right]^2 \quad (6.1.5)$$

As the energy increases, new quarks are allowed to be created e.g. at about 1.5 GeV the charm quark.

Through the comparison between the cross-sections for the processes $e^- + e^+ \rightarrow q + \bar{q}$ and $e^- + e^+ \rightarrow \mu^- + \mu^+$, one can probe the number of colours via the ratio

$$R = \frac{\sigma(e^- + e^+ \rightarrow \text{hadrons})}{\sigma(e^- + e^+ \rightarrow \mu^- + \mu^+)} \quad (6.1.6)$$

Since the numerator includes all possible $q - \bar{q}$ pairs, Eq. 6.1.5 gives:

$$R(E) = 3 \sum Q_i^2,$$

where the sum is over all quark flavours with threshold below E and the factor 3 in front of the summation reflects the fact that there are three colours for each flavour. For u , d , and s quarks one expects to have:

$$R = 3 \left[\left(\frac{2}{3} \right)^2 + \left(\frac{-1}{3} \right)^2 + \left(\frac{-1}{3} \right)^2 \right] = 2$$

Above the threshold for the c -quark: $R = 2 + 3(2/3)^2 = 10/3$, above the threshold for the b -quark $R = 10/3 + 3(-1/3)^2 = 11/3$. One expects a staircase evolution, depending on the threshold and certainly something that reflects the existence of three colours. Figure 6.5 present the energy evolution of R as measured in experiments.

6.2 Elastic $e - p$ scattering

Scattering of electrons off a proton is one of the cleanest probes of the internal structure of the latter. In order to study the relevant interaction, one simply has to go back to Section 4.2.3 since the diagrams are quite similar. This is indicated in the left diagram of fig. 6.6. However, we need to point out that we do not really know how the virtual photon interacts with the proton which is not seen as an elementary particle anymore. As a result we have the right diagram of fig. 6.6, where this unknown interaction is covered by the red blob. Let us now compute the matrix element for such a process. While doing so, we will describe the proton part with the unknown factor A .

$$\int \left[\bar{u}(\vec{P}_3)(ig_e\gamma^\mu)u(\vec{P}_1) \right] \cdot \left[\frac{-ig_{\mu\nu}}{q^2} \right] \cdot \left[A(\vec{P}_4)(ig_e\gamma^\nu)A(\vec{P}_2) \right] \cdot \left[(2\pi)^4 \delta^4(\vec{P}_1 - \vec{P}_3 - \vec{q}) \right] \cdot \left[(2\pi)^4 \delta^4(\vec{P}_2 - \vec{P}_4 + \vec{q}) \right] \cdot \frac{d^4q}{(2\pi)^4} =$$

$$\frac{ig_e^2(2\pi)^4}{(\vec{P}_1 - \vec{P}_3)^2} \left[\bar{u}(\vec{P}_3)\gamma^\mu u(\vec{P}_1) \right] \cdot \left[A(\vec{P}_4)\gamma_\mu A(\vec{P}_2) \right] \cdot \delta^4(\vec{P}_1 + \vec{P}_2 - \vec{P}_3 - \vec{P}_4) \Leftrightarrow$$

$$M_{if} = \frac{g_e^2}{\vec{q}^2} \cdot \left[\bar{u}(\vec{P}_3)\gamma^\mu u(\vec{P}_1) \right] \cdot \left[A(\vec{P}_4)\gamma_\mu A(\vec{P}_2) \right]$$

The spin averaged matrix element is then:

$$\langle |M_{if}|^2 \rangle = \frac{g_e^4}{4\vec{q}^4} \cdot \left[\bar{u}(\vec{P}_3)\gamma^\mu u(\vec{P}_1) \right] \cdot \left[A(\vec{P}_4)\gamma_\mu A(\vec{P}_2) \right] \cdot \left[\bar{u}(\vec{P}_3)\gamma^\nu u(\vec{P}_1) \right]^* \cdot \left[A(\vec{P}_4)\gamma_\nu A(\vec{P}_2) \right]^*$$

The previous can thus be written as a product of two tensors, one for the electron and one for the proton:

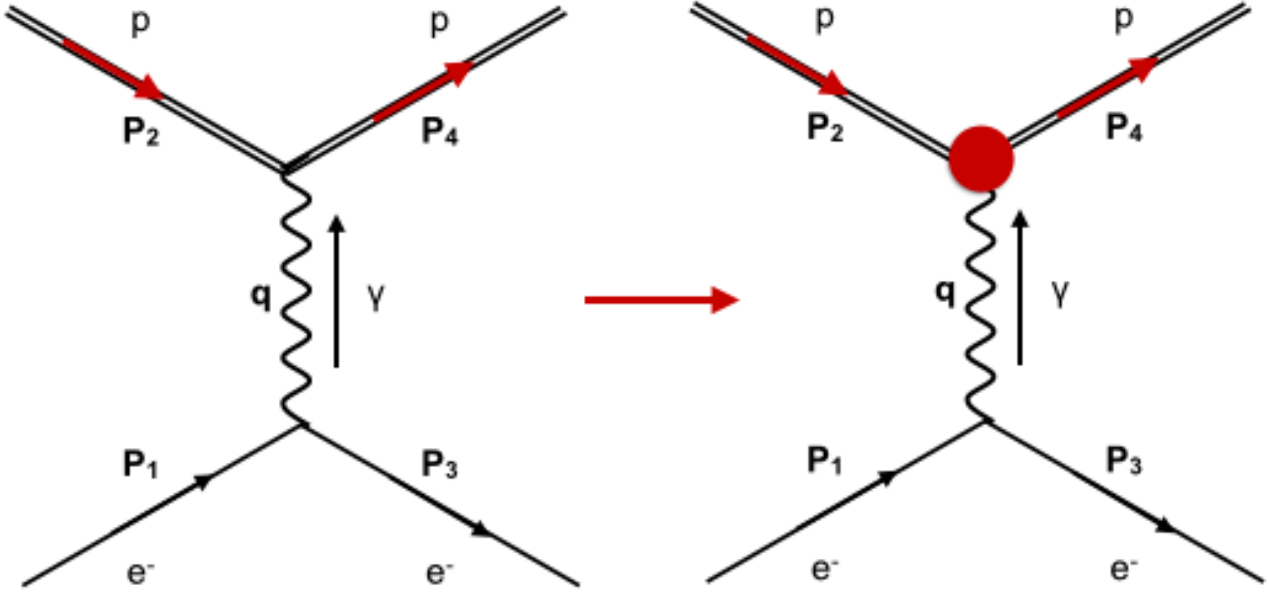


Fig. 6.6: The scattering of an electron off a proton. The blob on the right hand side diagram indicates that we do not really know how the virtual photon interacts with a complex, non-elementary object as the proton.

$$\langle |M_{if}|^2 \rangle = \frac{g_e^4}{4\vec{q}^4} \cdot K_{\mu\nu}(p) \cdot L^{\mu\nu}(e) \quad (6.2.1)$$

The tensor describing the proton states is unknown, however there are a couple of elements that we can use in order to constrain its form: $K_{\mu\nu}(p)$ is obviously a second rank tensor that depends on \vec{P}_2 , \vec{P}_4 and possibly on \vec{q} . However, these three 4-vectors are not independent since $\vec{P}_2 + \vec{q} = \vec{P}_4$. For the relevant representation we will choose two of them e.g. $\vec{P}_2 \equiv \vec{P}$ and \vec{q} :

$$K_{\mu\nu} = -K_1 g_{\mu\nu} + \frac{K_2}{M^2} \vec{P}_\mu \vec{P}_\nu + \frac{K_4}{M^2} \vec{q}_\mu \vec{q}_\nu + \frac{K_5}{M^2} (\vec{P}_\mu \vec{q}_\nu + \vec{P}_\nu \vec{q}_\mu),$$

where K_i are unknown functions of \vec{q}^2 and the division by the square of the proton mass is done to allow all K_i to have the same dimensions. It is important to note that we could have added the anti-symmetric combination $\vec{P}_\mu \vec{q}_\nu - \vec{P}_\nu \vec{q}_\mu$, however this would not contribute since the other tensor i.e. $L^{\mu\nu}(e)$ is symmetric.

The form of $L^{\mu\nu}(e)$ is known already from the electron-muon scattering discussed in Section 4.2.3:

$$\begin{aligned} L^{\mu\nu}(e) &= 2 \left[\vec{P}_1^\mu \vec{P}_3^\nu + \vec{P}_3^\mu \vec{P}_1^\nu + g^{\mu\nu} (m^2 - (\vec{P}_1)_\mu (\vec{P}_3)^\mu) \right] \\ \vec{q}_\mu L^{\mu\nu} &= 2 \left[(\vec{q}_\mu \vec{P}_1^\mu) \vec{P}_3^\nu + (\vec{q}_\mu \vec{P}_3^\mu) \vec{P}_1^\nu + \vec{q}_\mu g^{\mu\nu} (m^2 - (\vec{P}_1)_\mu (\vec{P}_3)^\mu) \right] = \\ \vec{q}_\mu L^{\mu\nu} &= 2 \left[(\vec{q}_\mu \vec{P}_1^\mu) \vec{P}_3^\nu + (\vec{q}_\mu \vec{P}_3^\mu) \vec{P}_1^\nu + m^2 \vec{q}^\mu - \vec{q}^\mu (\vec{P}_1)_\mu (\vec{P}_3)^\mu \right] \end{aligned} \quad (6.2.2)$$

We will now calculate each individual term of Eq. 6.2.2:

- $\vec{P}_1)_\mu (\vec{P}_1)^\mu = \vec{P}_3)_\mu (\vec{P}_3)^\mu = m^2$
- $\vec{q}_\mu \vec{P}_1^\mu$:

$$\vec{P}_1)_\mu - \vec{q}_\mu = \vec{P}_3)_\mu \Leftrightarrow \vec{P}_3)_\mu (\vec{P}_3)^\mu = (\vec{P}_1 - \vec{q})_\mu (\vec{P}_1 - \vec{q})^\mu \Leftrightarrow$$

$$m^2 = \vec{q}_\mu \vec{q}^\mu + \vec{P}_{1\mu} \vec{P}_1^\mu - 2\vec{q}_\mu \vec{P}_1^\mu \Leftrightarrow \vec{q}^2 = 2\vec{q}_\mu \vec{P}_1^\mu$$

• $\vec{q}_\mu \vec{P}_3^\mu$:

$$\vec{P}_{1\mu} = \vec{q}_\mu + \vec{P}_{3\mu} \Leftrightarrow \vec{P}_{1\mu} \vec{P}_1^\mu = (\vec{q} + \vec{P}_3)_\mu (\vec{q} + \vec{P}_3)^\mu \Leftrightarrow$$

$$m^2 = \vec{q}_\mu \vec{q}^\mu + \vec{P}_{3\mu} \vec{P}_3^\mu + 2\vec{q}_\mu \vec{P}_3^\mu \Leftrightarrow \vec{q}^2 = -2\vec{q}_\mu \vec{P}_3^\mu$$

• $\vec{P}_{1\mu} \vec{P}_3^\mu$:

$$\vec{P}_{1\mu} - \vec{P}_{3\mu} = \vec{q}_\mu \Leftrightarrow \vec{q}_\mu \vec{q}^\mu = (\vec{P}_1 - \vec{P}_3)_\mu (\vec{P}_1 - \vec{P}_3)^\mu \Leftrightarrow$$

$$\vec{q}^2 = \vec{P}_{1\mu} \vec{P}_1^\mu + \vec{P}_{3\mu} \vec{P}_3^\mu - 2\vec{P}_{1\mu} \vec{P}_3^\mu \Leftrightarrow \vec{P}_{1\mu} \vec{P}_3^\mu = \frac{2m^2 - \vec{q}^2}{2}$$

Equation 6.2.2 can thus be written as:

$$\vec{q}_\mu L^{\mu\nu} = 2 \left[\frac{\vec{q}^2}{2} \vec{P}_3^\nu - \frac{\vec{q}^2}{2} \vec{P}_1^\nu + m^2 \vec{q}^\nu - \frac{2m^2 - \vec{q}^2}{2} \vec{q}^\nu \right] =$$

$$2 \left[\frac{\vec{q}^2}{2} (\vec{P}_3^\nu - \vec{P}_1^\nu) + m^2 \vec{q}^\nu - m^2 \vec{q}^\nu - \frac{\vec{q}^2}{2} \vec{q}^\nu \right] =$$

$$2\vec{q}^\nu \left[\frac{\vec{q}^2}{2} - \frac{\vec{q}^2}{2} \right] = 0$$

It can also be shown that $\vec{q}_\nu \vec{P}^\nu = -\vec{q}^2/2$:

$$\vec{P}_{2\mu} + \vec{q}_\mu = \vec{P}_{4\mu} \Leftrightarrow (\vec{P} + \vec{q})_\mu (\vec{P} + \vec{q})^\mu = \vec{P}_{4\mu} \vec{P}_4^\mu \Leftrightarrow$$

$$\vec{q}_\mu \vec{q}^\mu + \vec{P}_\mu \vec{P}^\mu + 2\vec{q}_\mu \vec{P}^\mu = M^2 \Leftrightarrow \vec{q}_\mu \vec{P}^\mu = -\frac{\vec{q}^2}{2}$$

The same equation applies for the other tensor i.e. $\vec{q}_\mu K^{\mu\nu} = 0$

$$\vec{q}_\mu K^{\mu\nu} = -K_1 \vec{q}_\mu g^{\mu\nu} + \frac{K_2}{M^2} \vec{q}_\mu \vec{P}^\mu \vec{P}^\nu + \frac{K_4}{M^2} \vec{q}_\mu \vec{q}^\mu \vec{q}^\nu + \frac{K_5}{M^2} \vec{q}_\mu (\vec{P}^\mu \vec{q}^\nu + \vec{P}^\nu \vec{q}^\mu) \Leftrightarrow$$

$$0 = -K_1 \vec{q}^\nu + \frac{K_2}{M^2} (\vec{q}_\mu \vec{P}^\mu) \vec{P}^\nu + \frac{K_4}{M^2} \vec{q}^2 \vec{q}^\nu + \frac{K_5}{M^2} [(\vec{q}_\mu \vec{P}^\mu) \vec{q}^\nu + \vec{q}^2 \vec{P}^\nu] \Leftrightarrow$$

$$0 = \left[-K_1 + \frac{K_4}{M^2} \vec{q}^2 + \frac{K_5}{M^2} (\vec{q}_\mu \vec{P}^\mu) \right] \vec{q}^\nu + \left[\frac{K_2}{M^2} (\vec{q}_\mu \vec{P}^\mu) + \frac{K_5}{M^2} \vec{q}^2 \right] \vec{P}^\nu$$

Contracting with

$$\vec{P}^\nu$$

from the left leads to the realisation that the coefficients of \vec{q}^ν and \vec{P}^ν must be 0 at the same time:

$$\begin{aligned} \frac{K_2}{M^2} (\vec{q}_\mu \vec{P}^\mu) + \frac{K_5}{M^2} \vec{q}^2 = 0 &\Leftrightarrow K_5 = -K_2 \frac{(\vec{q}_\mu \vec{P}^\mu)}{\vec{q}^2} \\ -K_1 + \frac{K_4}{M^2} \vec{q}^2 + \frac{K_5}{M^2} (\vec{q}_\mu \vec{P}^\mu) = 0 &\Leftrightarrow \\ K_4 = \frac{M^2}{\vec{q}^2} K_1 + \frac{(\vec{q}_\mu \vec{P}^\mu)}{\vec{q}^4} K_2 & \end{aligned}$$

The proton tensor can thus be written as:

$$\begin{aligned} K_{\mu\nu} = -K_1 g_{\mu\nu} + \frac{K_2}{M^2} \vec{P}_\mu \vec{P}_\nu + \frac{K_1 M^2}{\vec{q}^2 M^2} \vec{q}_\mu \vec{q}_\nu + \frac{K_2}{4M^2} \vec{q}_\mu \vec{q}_\nu + \frac{K_2}{2M^2} (\vec{P}_\mu \vec{q}_\nu + \vec{P}_\nu \vec{q}_\mu) = \\ K_1 \left[-g_{\mu\nu} + \frac{1}{\vec{q}^2} \vec{q}_\mu \vec{q}_\nu \right] + \frac{K_2}{M^2} \left[\vec{P}_\mu \vec{P}_\nu + \frac{1}{4} \vec{q}_\mu \vec{q}_\nu + \frac{1}{2} (\vec{P}_\mu \vec{q}_\nu + \vec{P}_\nu \vec{q}_\mu) \right] \Leftrightarrow \\ K_{\mu\nu} = \left[-g_{\mu\nu} + \frac{1}{\vec{q}^2} \vec{q}_\mu \vec{q}_\nu \right] K_1 + \left(\vec{P}_\mu + \frac{1}{2} \vec{q}_\mu \right) \left(\vec{P}_\nu + \frac{1}{2} \vec{q}_\nu \right) K_2 \end{aligned} \quad (6.2.3)$$

The two remaining factors in Eq. 6.2.3 i.e. K_1 and K_2 are called **form factors**. These factors describe the proton structure in terms of its constituents i.e. the quarks and gluons. They are easily measured experimentally, since they are directly connected to the elastic $e - p$ cross-section. To compute this cross-section, one has to compute the average over all spin states of the squared matrix element of Eq. 6.2.1:

$$\langle |M_{if}|^2 \rangle = \frac{4g_e^4}{\vec{q}^4} \left[K_1 \left((\vec{P}_{1\mu} \vec{P}_3^\mu) - 2m^2 \right) + K_2 \left(\frac{(\vec{P}_{1\mu} \vec{P}^\mu)(\vec{P}_{3\nu} \vec{P}^\nu)}{M^2} + \frac{\vec{q}^2}{4} \right) \right]$$

In the lab frame, the target proton has a 4-momentum of $\vec{P}_\mu = (M, \vec{0})$. The electron scatters off the proton, having an initial energy E and is emitted with a final one of E' at an angle θ . If $E, E' \gg m$, we can safely put $m = 0$ with the 4-momenta of the incoming and outgoing electrons being $\vec{P}_{1\mu} = (E, \vec{P}_1)$ and $\vec{P}_{3\mu} = (E', \vec{P}_3)$, respectively (note that $\vec{P}_1 \cdot \vec{P}_3 = P_1 P_3 \cos(\theta)$). The matrix element can then be written as:

$$\langle |M_{if}|^2 \rangle = \frac{g_e^4}{4EE' \sin^4(\theta/2)} \left(2K_1 \sin^2(\theta/2) + K_2 \cos^2(\theta/2) \right)$$

It can be shown that:

$$E' = \frac{ME}{M + E(1 - \cos(\theta))} \Leftrightarrow E' = \frac{E}{1 + \frac{2E}{M} \sin^2(\theta/2)}$$

The differential cross-section can then be written as:

$$\frac{d\sigma}{d\Omega} = \left[\frac{\alpha}{4ME \sin^2(\theta/2)} \right]^2 \frac{E'}{E} \left(2K_1 \sin^2(\theta/2) + K_2 \cos^2(\theta/2) \right) \quad (6.2.4)$$

The form factors are connected to the electric G_E and magnetic G_M moment distributions of the proton via the equations:

$$K_1 = -\vec{q}^2 G_M^2$$

$$K_2 = (2M)^2 \frac{G_E^2 - [\bar{q}^2/(2M)^2] G_M^2}{1 - \bar{q}^2/(2M)^2}$$

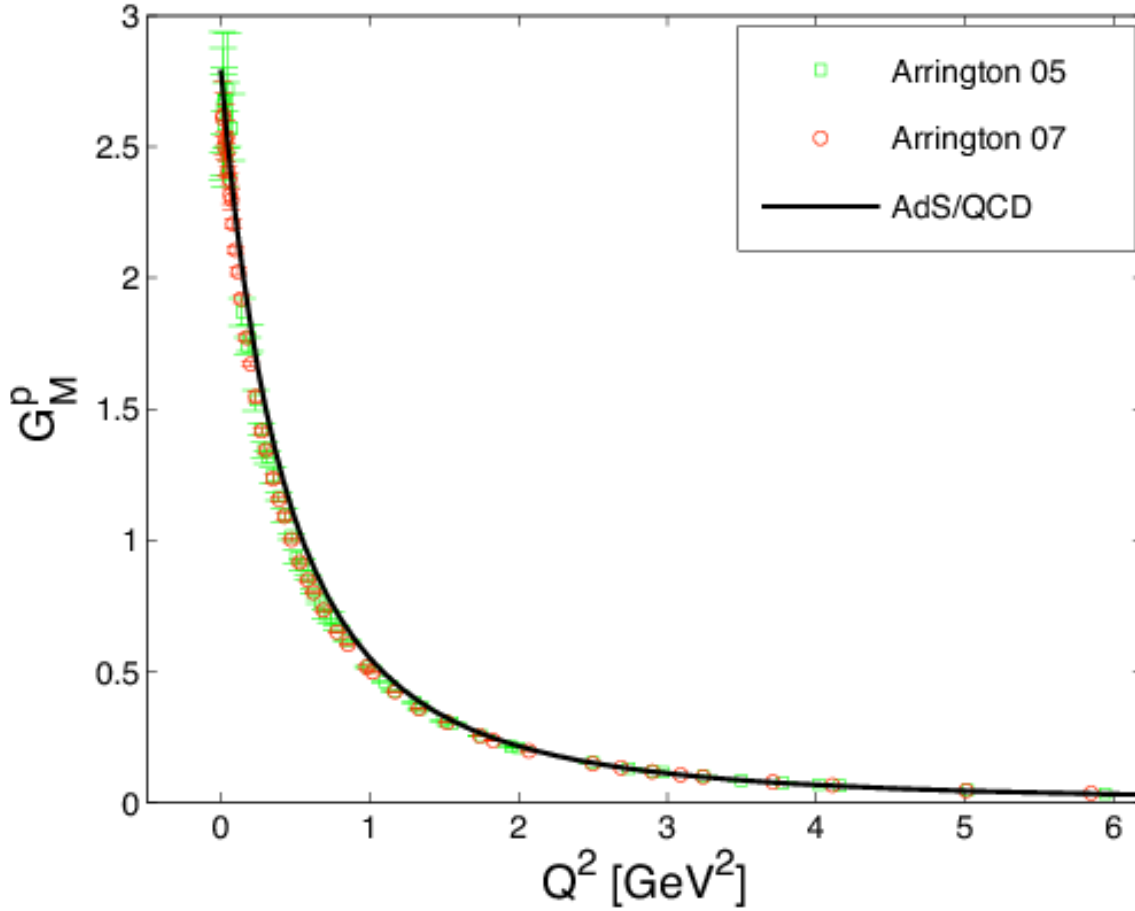


Fig. 6.7: The proton electric and magnetic moments as a function of \bar{q}^2 .

Figure 6.7 presents the experimentally measured \bar{q}^2 dependence of G_E and G_M . It turns out that they both follow a specific \bar{q}^2 dependence:

$$G_E(q^2) = \left(1 - \frac{q^2}{0.71}\right)^{-2}$$

in GeV^2

The behavior at small values of q^2 can be used to determine the mean square proton charge radius:

$$\langle r^2 \rangle = 6 \left(\frac{dG_E(q^2)}{dq^2} \right)_{q^2=0} = (0.81 \cdot 10^{-13} \text{ cm})^2$$

This radius of about 0.8 fm is obtained for both the charge and magnetic proton distributions.

Chapter 7

Deep inelastic scattering

One way to probe the internal structure of matter is to bombard it with high energy particles, and then see what happens. For instance, in the Rutherford experiment (1911), alpha particles (helium nuclei) were deflected on a thin gold foil. Rutherford found that the deflections followed his famous inverse $\sin^4(\theta/2)$ law, and concluded that the alpha particles were scattered from electrically charged point-like nuclei inside the gold atoms. Experiments using probes of higher energy later revealed that the point-like scattering distributions were damped by form factors which are essentially the Fourier transform of a charge distribution. This clearly showed that nuclei are not point-like and indeed, after the discovery of the neutron by Chadwick (1932), it became clear that nuclei are bound states of protons and neutrons. Also the protons and neutrons were found not to be point-like and a real breakthrough came with a series of deep inelastic scattering experiments in the 1960's at SLAC, where electron beams were scattered on proton targets at energies of about 20 GeV, large enough to reveal the proton's internal structure. The SLAC experiments showed that the electrons were scattering off quasi-free point-like constituents inside the proton which were soon identified with quarks. This was the first time that quarks were shown to be dynamical entities, instead of bookkeeping devices to classify the hadrons (Gell-Mann's eightfold way). The Nobel prize was awarded in 1990 for this spectacular discovery.

The pioneering SLAC experiments were followed by a series of other fixed-target experiments¹ with larger energies at CERN (Geneva) and at Fermilab (Chicago), using electrons, muons, neutrino's and anti-neutrinos as probes. The largest centre-of-mass energies were reached at the HERA collider in Hamburg (1992–2007) with counter rotating beams of 27 GeV electrons and 800 GeV protons. Deep inelastic scattering (DIS) data are very important since they provide detailed information on the momentum distributions of the partons (quarks and gluons) inside the proton. Parton distributions are crucial ingredients in theoretical predictions of scattering cross-sections at hadron colliders like the Tevatron (Fermilab, proton-antiproton at 2 TeV) or the LHC (CERN, proton-proton at 5–14 TeV). The reason for this is simple: the colliding (anti)protons have a fixed centre-of-mass energy but not the colliding partons, since their momenta are distributed inside the (anti)proton. Clearly one has to fold-in this momentum spread to compare theoretical predictions with the data. Apart from providing parton distributions, DIS is also an important testing ground for perturbative QCD, as we will see.

7.1 Inelastic $e - p$ scattering

Elastic scattering $e - p$ scattering dominates at relevant low energies. During this process, the proton still interacts but emerges as a proton. Once we crank up the energy, the interaction becomes inelastic and many more particles emerge from the $\gamma - p$ blob as indicated in fig. 7.1.

The lepton vertex is still unaffected which allows us to write the matrix element in a similar way as in the previous chapter in Eq. 6.2.1:

$$\langle |M_{if}|^2 \rangle = \frac{g_e^4}{\bar{q}^4} \cdot K_{\mu\nu}(pX) \cdot L^{\mu\nu}(e) \quad (7.1.1)$$

¹ In a fixed-target experiment, beam particles interact with a stationary target in the laboratory, and the debris is recorded in a downstream detector. In a collider experiment, on the other hand, counter-rotating beams collide in the centre of a detector, which is built around the interaction region.

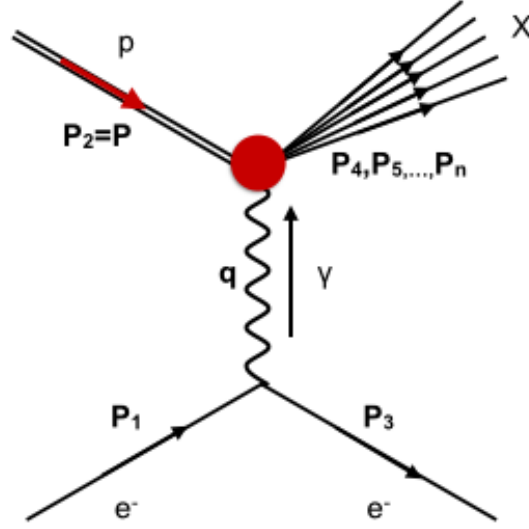


Fig. 7.1: The inelastic scattering of an electron off a proton.

In a similar way as before, the proton tensor is unknown (but not completely) and depends on \vec{q} , $\vec{P}_2 \equiv \vec{P}$ and the 4-momenta of the outgoing particles $\vec{P}_4, \vec{P}_5, \dots, \vec{P}_n$. The scattering cross-section is given by the golden rule described in Section 4.1:

$$d\sigma = \frac{\langle |M_{if}|^2 \rangle}{4\sqrt{(P_1 P_2)^2 - (mM)^2}} \cdot \left[\frac{d^3 \vec{P}_3}{(2\pi)^3 2E_3} \right] \cdot \left[\frac{d^3 \vec{P}_4}{(2\pi)^3 2E_4} \right] \cdot \dots \cdot \left[\frac{d^3 \vec{P}_n}{(2\pi)^3 2E_n} \right] \cdot (2\pi)^4 \delta^4(\vec{P}_1 + \vec{P}_2 - \vec{P}_3 - \vec{P}_4 - \dots - \vec{P}_n)$$

In experiments, we normally record the momentum of the scattered electron and what is measured is the so-called inclusive cross-section, in which all available final states are included. This is done by summing over all final X-states and integrating the previous equation over the outgoing momenta of the proton blob:

$$d\sigma = \frac{g_e^4 W_{\mu\nu} L^{\mu\nu}}{4\vec{q}^2 \sqrt{(P_1 P_2)^2 - (mM)^2}} \cdot \left[\frac{d^3 \vec{P}_3}{(2\pi)^3 2E_3} \right] \cdot 4\pi M,$$

where

$$W_{\mu\nu} \equiv \frac{1}{4\pi M} \sum_X \int \dots \int K_{\mu\nu}(X) \left[\frac{d^3 \vec{P}_4}{(2\pi)^3 2E_4} \right] \cdot \dots \cdot \left[\frac{d^3 \vec{P}_n}{(2\pi)^3 2E_n} \right] \cdot (2\pi)^4 \delta^4(\vec{q} + \vec{P} - \vec{P}_4 - \dots - \vec{P}_n)$$

If the energy is large enough so that $E \gg m_e$, and considering E and E' the energies of the incoming and outgoing leptons that hit a stationary proton of mass M , then the differential cross-section can be written as:

$$\frac{d\sigma}{dE' d\Omega} = \left[\frac{\alpha}{\vec{q}^2} \right]^2 \frac{E'}{E} W_{\mu\nu} L^{\mu\nu}$$

It is interesting to note that the energy of the outgoing lepton is no longer constrained by the initial energy and the scattering angle in the inelastic case.

To build up the second rank tensor $W_{\mu\nu}$ we follow the same procedure as the one described in detail in Section 6.2:

$$W_{\mu\nu} = -W_1 g_{\mu\nu} + \frac{W_2}{M^2} \vec{P}_\mu \vec{P}_\nu + \frac{W_4}{M^2} \vec{q}_\mu \vec{q}_\nu + \frac{W_5}{M^2} (\vec{P}_\mu \vec{q}_\nu + \vec{P}_\nu \vec{q}_\mu)$$

It follows that this time the functions W_i depend not on one variable as in the case of the elastic interaction but on two i.e. on \vec{q}^2 and on $\vec{q}\vec{P} \equiv qP$. It can be shown again that $\vec{q}_\nu W^{\mu\nu} = 0$, from where it follows that:

$$W_4 = \frac{M^2}{\vec{q}^2} W_1 + \left(\frac{qP}{\vec{q}^2}\right)^2 W_2,$$

$$W_5 = -\frac{qP}{\vec{q}^2} W_2,$$

which means that $W_{\mu\nu}$ can be written as a function of two structure functions W_1 and W_2 :

$$W_{\mu\nu} = \left[-g_{\mu\nu} + \frac{\vec{q}_\mu \vec{q}_\nu}{\vec{q}^2} \right] W_1 + \left[\vec{P}_\mu - \left(\frac{qP}{\vec{q}^2}\right) \vec{q}_\mu \right] \cdot \left[\vec{P}_\nu - \left(\frac{qP}{\vec{q}^2}\right) \vec{q}_\nu \right] W_2$$

The differential cross-section can thus be written as:

$$\frac{d\sigma}{dE' d\Omega} = \left[\frac{\alpha}{2E \sin^2(\theta/2)} \right]^2 \cdot \left[2W_1 \sin^2(\theta/2) + W_2 \cos^2(\theta/2) \right] \quad (7.1.2)$$

7.1.1 Kinematics of DIS

The diagram of fig. 7.2 shows the kinematics of deep inelastic scattering as commonly used.

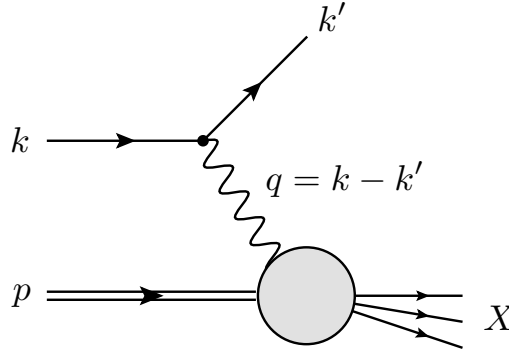


Fig. 7.2: Another form of the DIS diagram.

In this figure, $k =$ and $k' =$ are the incoming and outgoing lepton momenta, respectively, $p =$ is the incoming proton, $X =$ is the hadronic final state, while $q = k - k'$ is what is usually referred to as the momentum transfer. The interaction between the exchanged photon (or W in case of $\nu p \rightarrow \ell X$ neutrino scattering) and the proton depends on p and q , from which we can build the two Lorentz scalars:

$$\boxed{Q^2 = -q^2 \quad \text{and} \quad x = \frac{Q^2}{2p \cdot q}}$$

Other scalars that are often used to characterise the event are:

- $M^2 = p^2$ is the proton mass squared,

- $s = (p+k)^2$ is the centre of mass energy squared,
- $W^2 = (p+q)^2$ is what is usually referred to as the invariant mass of X squared,
- $y = (p \cdot q)/(p \cdot k)$ is the fractional energy transfer in the lab,
- $\nu = (p \cdot q)/M$ is the energy transfer in the lab system.

Since all kinematic variables are Lorentz invariants, it is often useful to calculate them in frames which are convenient:

- $q^2 < 0$ (hence the minus sign in the definition of Q^2): In the rest frame of the incoming electron with the outgoing electron along the z axis we have $k = (m, 0, 0, 0)$ and $k' = (E', 0, 0, k')$ so that:

$$q^2 = (m - E', 0, 0, -k')^2 = m^2 - 2mE' + E'^2 - k'^2 = m^2 - 2mE' + m^2 = 2m(m - E') < 0.$$

- $0 \leq x \leq 1$: Obviously $x = 0$ when $Q^2 = 0$. For the other limit we can set $W^2 = M^2$. This gives:

$$W^2 = (p+q)^2 = p^2 + 2p \cdot q + q^2 = M^2 + 2p \cdot q - Q^2 = M^2 \quad \rightarrow \quad Q^2 = 2p \cdot q \quad \rightarrow \quad x = 1.$$

- $0 \leq y < 1$: For the limits on y it is easiest to work in the lab frame where the proton is at rest and the electron comes in at the z direction. We then have $k = (E, 0, 0, k)$, $p = (M, 0, 0, 0)$ and $q = (E - E', q_x, q_y, q_z)$ so that $p \cdot k = ME$ and $p \cdot q = M(E - E')$. Therefore:

$$y = \frac{p \cdot q}{p \cdot k} = \frac{E - E'}{E} \quad \text{with} \quad m_e \leq E' \leq E.$$

From this it immediately follows that $0 \leq y < 1$.

- $W^2 = M^2 + Q^2(1-x)/x \geq M^2$: With $x = Q^2/(2p \cdot q)$ we find

$$W^2 = (p+q)^2 = p^2 + 2p \cdot q + q^2 = M^2 + Q^2/x - Q^2 = M^2 + Q^2(1-x)/x.$$

It is convenient to plot the allowed kinematical region in the y - Q^2 plane as indicated in fig. 7.3.

7.1.2 Bjorken scaling

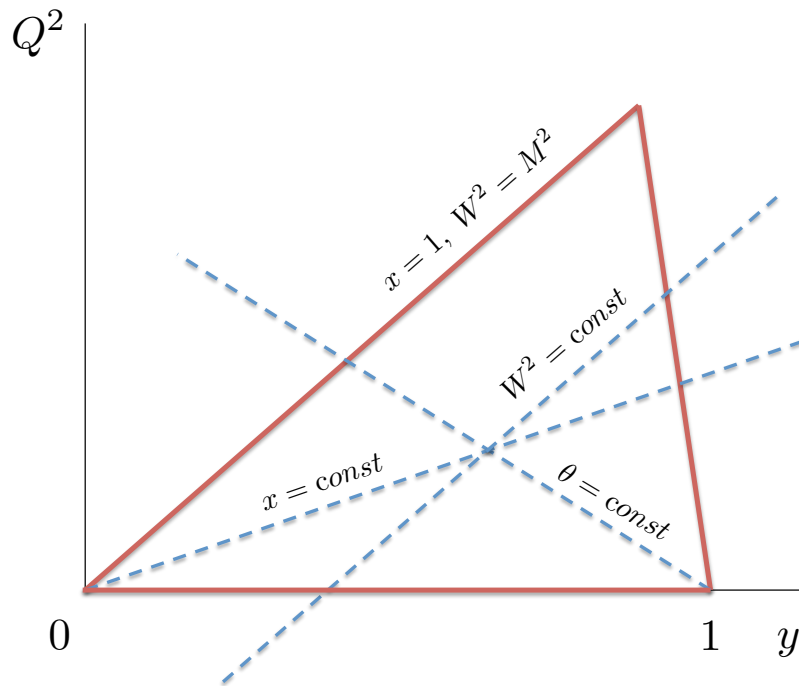
As indicated before the two structure functions depend on two quantities i.e. \vec{q}^2 and qP . However, one can define another variable that we will find quite convenient when we will be discussing the Bjorken scaling:

$$x \equiv \frac{\vec{q}^2}{2qP},$$

so that $W_1 = W_1(q^2, x)$ and $W_2 = W_2(q^2, x)$.

At very large values of q^2 , the two structure functions do not depend anymore on both q^2 and x but rather the first dependence fades out. This was predicted by Bjorken and confirmed experimentally by DIS experiments at SLAC. The prediction can be followed by the simple argumentation that the wavelength of the virtual photon, which is inversely proportional to the momentum transfer $\lambda \approx 1/Q$ is connected to the resolution (or better the resolving power of an internal structure)². The higher the energy of the interaction between the electron and the proton, the higher the momentum transfer and thus the smaller the resolution. Hence, by cranking up the energy we are slowly able to distinguish the internal structure of the proton, which is the reason why at modest energies there is a dependence of the structure functions on both q^2 and x . Above a given energy though, the virtual photon interacts with a point-like constituent, the parton (or better

² To better understand this, one can make the parallelism to a typical microscope.



$$\begin{aligned}
 Q^2 &= 2MEy + M^2 - W^2 \\
 &= 2MExy \\
 &= 4(1-y)E^2 \sin^2 \theta / 2
 \end{aligned}$$

Fig. 7.3: The triangle is the allowed kinematic region for $e + p \rightarrow e + X$.

the quark), which has no internal structure (at least to visible at these energies). This means that no matter how much Q^2 increases, the photon still 'sees' the quark and interacts with it, hence the independence of W_1 and W_2 from Q^2 . The structure functions are now written as

$$MW_1(q^2, x) \rightarrow F_1(x) \frac{-q^2}{2Mx} W_2(q^2, x) \rightarrow F_2(x) \quad (7.1.3)$$

Equation 7.1.3 is better known as **Bjorken scaling** and can be illustrated in fig. 7.4.

At a later stage, Callan and Gross suggested that the two structure functions are connected via Eq. 7.1.4. This was also confirmed experimentally to hold above a given value of x (i.e. for $x > 0.2$) as can be clearly seen in fig. 7.5.

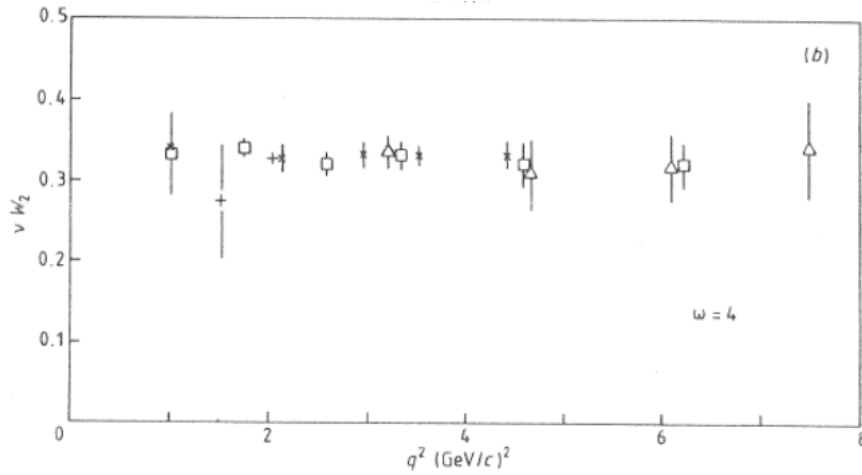


Fig. 7.4: The scaling behaviour of the structure function W_2 as a function of q^2 at $x = 0.25$.

$$2xF_1(x) = F_2(x) \tag{7.1.4}$$

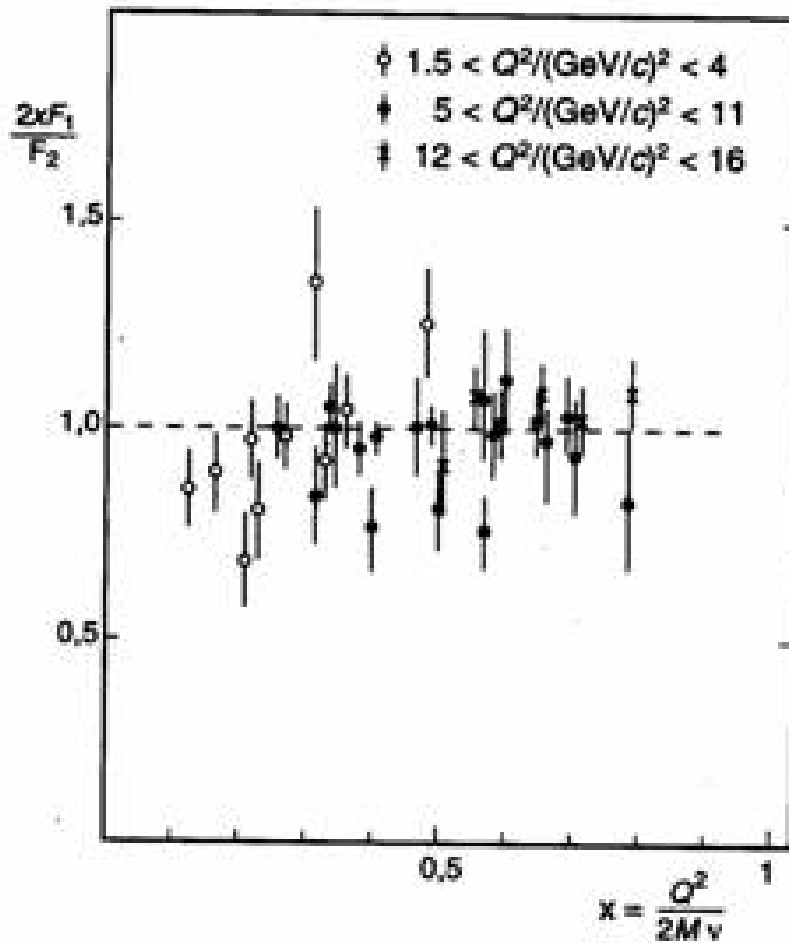


Fig. 7.5: The x -dependence of the ration $2xF_1/F_2$, as a test of the Callan-Gross equation.

7.2 The parton model

When a highly energetic virtual photon interacts with the proton, it probes its constituents i.e. the quarks and the gluons. However since the gluons do not interact with the photon, we can safely say that we mainly probe the quarks. Now, there are more than one type of such particles inside the proton. Each such quark, can carry a different fraction of the proton's momentum and energy. This is schematically depicted in fig. 7.6.

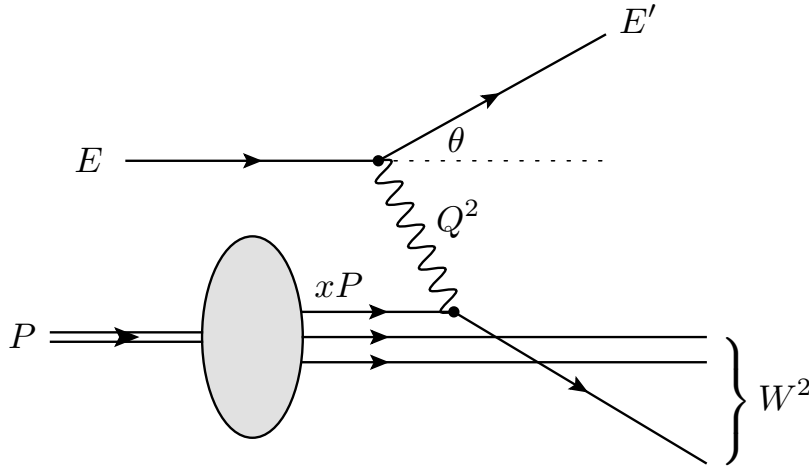


Fig. 7.6: The interaction of a highly energetic virtual photon with the quark of the initial proton that carries a fraction x of its momentum.

We now introduce the parton distribution function $f_i(x)$ which gives the probability that the struck parton carries a fraction x of the proton's momentum P . All the fractions have to add up to unity such that:

$$\sum_i \int x f_i(x) dx = 1,$$

where the index i includes also the partons that do not interact with the virtual photon. Note that in a dynamical picture, inside the proton there are also gluons from the QCD splitting $q \rightarrow qg$ and quark-antiquark pairs from the splitting $g \rightarrow q\bar{q}$. What is true is that there is a net excess of three quarks that carry the quantum numbers of the proton. A schematic picture of the QCD proton structure is given in fig. 7.7. The uud that carry the quantum numbers of the proton enter the diagram on the left, and they are called the **valence quarks**. This corresponds to a low-resolution 3-quark picture of the proton that only accounts for its quantum numbers. At the right of the diagram we see a high-resolution picture (at large Q^2) of the proton where the valence quarks are dressed with gluons and a **sea** of $q\bar{q}$ pairs. Note that the valence quarks can zig-zag through the diagram but will never disappear so that the proton quantum numbers are the same in both the low- and high-resolution pictures.

We will now try to calculate the relevant DIS cross-section. To do this, we usually first move to a frame where the masses (i.e. electrons, quarks and proton) can be neglected and we then use the so-called Mandelstam variables. Because the virtual photon is space-like ($q^2 < 0$) it follows that we can boost the photon along its direction of propagation (which points to the proton) such that q^0 vanishes. This is called **the Breit frame** or **infinite momentum frame**, since the proton then moves with very large momentum towards the virtual photon. In this frame the incoming quark moves with a 3-momentum ξp_z along the z axis, where ξ is the fraction of the proton 3-momentum p_z . The virtual photon moves with a 3-momentum Q along $-z$. The new frame is given in fig. 7.8.

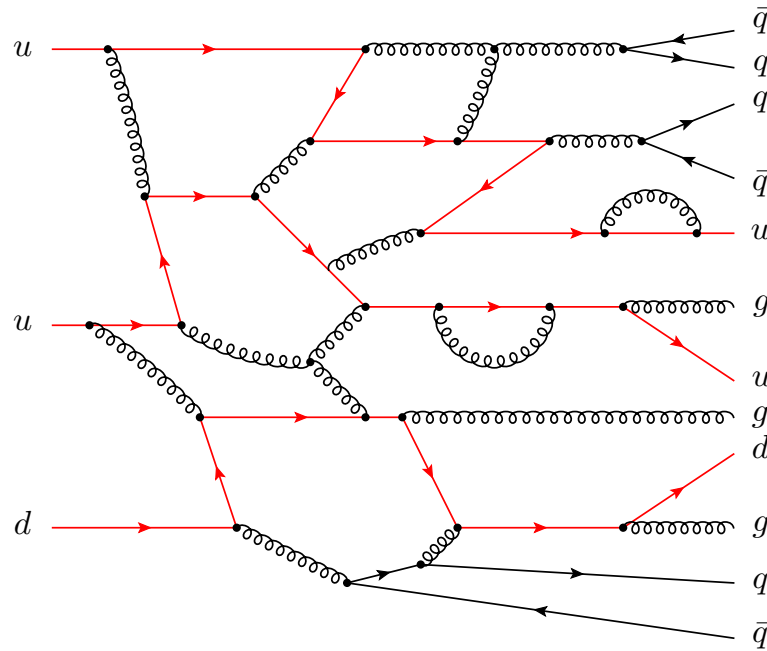


Fig. 7.7: The dynamical picture of the proton, with the valence and sea quarks and the gluons.

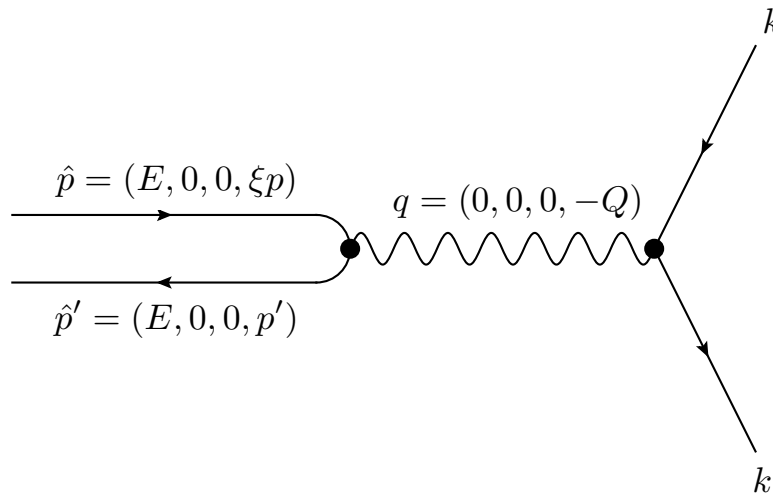


Fig. 7.8: The interaction between the photon and the quark in the Breit frame.

We take the incoming quark to be point-like, so that the scattering is necessarily elastic:³

$$\hat{p}^2 = (\hat{p} + q)^2 \rightarrow \hat{p}^2 = \hat{p}^2 + 2\hat{p} \cdot q - Q^2 \rightarrow Q^2 = 2\hat{p} \cdot q$$

If we denote the proton 4-momentum by p then, in the Breit frame,

$$\begin{aligned}\hat{p} \cdot q &= (E, 0, 0, \xi p_z) \cdot (0, 0, 0, -Q) = \xi p_z Q \\ \xi p \cdot q &= \xi (E_p, 0, 0, p_z) \cdot (0, 0, 0, -Q) = \xi p_z Q\end{aligned}$$

Thus $\hat{p} \cdot q = \xi p \cdot q$ but remember that this is only true in the Breit frame where the virtual photon does not transfer energy.

The elastic scattering condition now becomes

$$Q^2 = 2\hat{p} \cdot q = 2\xi p \cdot q \rightarrow \xi = \frac{Q^2}{2p \cdot q} = x$$

which means that we can identify the Bjorken- x variable as the 3-momentum fraction of the struck quark in the Breit frame. Note that in the Breit frame the proton moves very fast towards the photon, and is therefore Lorentz contracted to a kind of pancake. The interaction then takes place on the very short time scale when the photon passes that pancake. On the other hand, in the rest frame of the proton, the inter-quark interactions take place on time scales of the order of r_p/c but because of time dilatation these interactions are like ‘frozen’ in the Breit frame. During the short interaction time, the struck quark thus does not interact with the spectator quarks and can be regarded as a free parton.

Let’s now move to the usage of the Mandelstam variables:

$$\begin{aligned}s &= (p_1 + p_2)^2 \approx 2p_1 \cdot p_2 \\ t &= (p_1 - p_3)^2 = (p_4 - p_2)^2 \approx -2p_1 \cdot p_3 \approx -2p_2 \cdot p_4 \\ u &= (p_1 - p_4)^2 = (p_3 - p_2)^2 \approx -2p_1 \cdot p_4 \approx -2p_3 \cdot p_2\end{aligned}$$

According to the parton model of Feynman, Bjorken and others, the cross-section is the incoherent sum of partonic cross-sections, as calculated with free partons.⁴ Hence it can be written as:

$$d\sigma = \sum_i d\hat{\sigma}(\hat{s}, \hat{t}, \hat{u}) f_i(x) dx$$

Here we have introduced the parton kinematic variables

$$\hat{s} \approx 2xp \cdot k = xs, \quad \hat{t} = (k - k')^2 = t, \quad \hat{u} \approx -2xp \cdot k' = xu$$

For the partonic cross section we just take $\sigma(e\mu \rightarrow e\mu)$ with the muon charge replaced by the quark charge. The $e\text{-}\mu$ cross section is calculated as

$$\left(\frac{d\sigma}{d\Omega} \right)_{\text{cm}} = \frac{\alpha^2}{2s} \left(\frac{s^2 + u^2}{t^2} \right)$$

with momentum k_1 along x and scattering angle θ

$$\begin{aligned}k_1 &= (k, k, 0, 0) & k_3 &= (k, k \cos \theta, k \sin \theta, 0) \\ k_2 &= (k, -k, 0, 0) & k_4 &= (k, -k \cos \theta, -k \sin \theta, 0) \\ s &= 4k^2, \quad t = -2k^2(1 - \cos \theta), \quad u = -2k^2(1 + \cos \theta)\end{aligned}$$

³ We indicate the unobservable partonic kinematic variables by a hat, like \hat{p} for a partonic 4-momentum.

⁴ By ‘incoherent sum’ we mean that cross-sections are added, instead of amplitudes.

The cross-section can thus be written as:

$$\frac{d\sigma}{d\Omega} = \frac{d\sigma}{\sin\theta d\theta d\phi} = \frac{d\sigma}{\sin\theta d\phi dt} \left| \frac{dt}{d\theta} \right| = 2k^2 \frac{d\sigma}{d\phi dt} = \frac{s}{2} \frac{d\sigma}{d\phi dt}$$

Integrating over ϕ then gives

$$\frac{d\sigma}{dt} = \frac{4\pi}{s} \frac{d\sigma}{d\Omega} = \frac{2\pi\alpha^2}{s^2} \left(\frac{s^2 + u^2}{t^2} \right)$$

Using the partonic variables, and multiplying the charge at the muon vertex by the fractional quark charge e_i , we get the partonic cross section:

$$\frac{d\hat{\sigma}_i}{d\hat{t}} = \frac{2\pi\alpha^2 e_i^2}{\hat{s}^2} \left(\frac{\hat{s}^2 + \hat{u}^2}{\hat{t}^2} \right)$$

It is a simple matter to re-write this in terms of the DIS kinematic variables. We can now combine the partonic cross-sections with the parton distribution function to obtain DIS cross-section:

$$\frac{d\sigma}{dQ^2} = \sum_i \frac{2\pi\alpha^2 e_i^2}{Q^4} [1 + (1-y)^2] f_i(x) dx$$

or

$$\frac{d^2\sigma}{dx dQ^2} = \frac{2\pi\alpha^2}{Q^4} [1 + (1-y)^2] \sum_i e_i^2 f_i(x)$$

The F_2 structure function is defined as the charge weighted sum of the parton **momentum densities** $x f_i(x)$:

$$F_2(x) = \sum_i e_i^2 x f_i(x) \quad (7.2.1)$$

so that the DIS cross section can be written as⁵

$$\frac{d^2\sigma}{dx dQ^2} = \frac{4\pi\alpha^2}{Q^4} \frac{[1 + (1-y)^2]}{2x} F_2(x) \quad (7.2.2)$$

7.3 Probing the quark and gluon distributions in protons

As indicated before, the proton has a more dynamical picture than the static one where only the valence quarks, that carry the quantum numbers, are prominent. There are not only gluons but also what is usually referred to as sea quarks. We will focus on the three lightest quark flavours i.e. u, d, s since the remaining heavy flavour quarks (i.e. c, b, t) are subject to threshold effects for their production in the sea. Under these considerations, Eq. 7.2.1 can be written as:

$$\frac{1}{x} F_2^p(x) = \left(\frac{2}{3}\right)^2 [u^p(x) + \bar{u}^p(x)] + \left(\frac{1}{3}\right)^2 [d^p(x) + \bar{d}^p(x)] + \left(\frac{1}{3}\right)^2 [s^p(x) + \bar{s}^p(x)],$$

where e.g. $u(x)$ and $\bar{u}(x)$ are the probability distributions of u and \bar{u} quarks within the proton. This structure function has obviously six unknown quantities. To overcome this one relies on the fact that the proton and the neutron are members of an isospin doublet and thus their quark content is related. The inelastic neutron structure functions can be constrained by scattering of electrons off a deuterium target:

⁵ One can think of the y dependence as being an angular dependence through the relation $1 - y = \frac{1}{2}(1 + \cos\theta^*)$.

$$\frac{1}{x}F_2^n(x) = \left(\frac{2}{3}\right)^2 [u^n(x) + \bar{u}^n(x)] + \left(\frac{1}{3}\right)^2 [d^n(x) + \bar{d}^n(x)] + \left(\frac{1}{3}\right)^2 [s^n(x) + \bar{s}^n(x)],$$

The quark contents between the proton and the neutron are the same if one reverses u for d (and vice-versa). This means that:

$$u^p(x) = d^n(x) \equiv u(x)$$

$$d^p(x) = u^n(x) \equiv d(x)$$

$$s^p(x) = s^n(x) \equiv s(x)$$

Another constrain for the currently unknown quantities comes from the fact that the quantum numbers of the proton are carried by the valence quarks. In addition, if we consider the dynamical picture of the proton, schematically introduced in fig. 7.7, one can assume that the sea quarks which are radiated by the valence quarks occur to first order at the same rate and have similar momentum distributions (please note that we still consider the three lightest flavours). It is convenient to define the valence and the sea quark distributions as:

$$\begin{aligned} u_v &= u - \bar{u}, & d_v &= d - \bar{d}, & s_v &= s - \bar{s} = 0, & \dots \\ u_s &= 2\bar{u}, & d_s &= 2\bar{d}, & s_s &= 2\bar{s}, & \dots \end{aligned}$$

so that $u + \bar{u} = u_v + u_s$, etc.

Summing over all contributing partons, we should recover the quantum number of the proton and thus we have the following counting rules:

$$\int_0^1 u_v(x) dx = 2 \quad \text{and} \quad \int_0^1 d_v(x) dx = 1$$

As a result the proton and neutron structure functions can be written as:

$$\frac{1}{x}F_2^p = \frac{1}{9}[4u_v + d_v] + \frac{4}{3}S$$

$$\frac{1}{x}F_2^n = \frac{1}{9}[u_v + 4d_v] + \frac{4}{3}S,$$

where $S(x)$ is the sea quark distribution ($u_s(x) \approx \bar{u}_s(x) \approx d_s(x) \approx \bar{d}_s(x) \approx s_s(x) \approx \bar{s}_s(x) \equiv S(x)$). When studying the small momentum part of the proton (i.e. at $x \approx 0$) one probes the low momentum sea quarks. On the other side of the spectrum, at high momenta (i.e. at $x \approx 1$), the high momentum valence quarks leave little unoccupied room for the sea quarks and thus one probes the valence quarks mainly. This is experimentally illustrated in fig. 7.9, where obviously depending on the value of x one can probe either the valence and sea quarks (i.e. at high values of x) or the sea quarks (i.e. at low values of x).

Finally integrating the quark distributions obtained from deep inelastic charged lepton and neutrino scattering gives

$$\sum_i \int_0^1 x f_i(x) dx \approx 0.5$$

The missing momentum turns out that is carried by gluons. Introducing a gluon momentum distribution $xg(x)$, the correct momentum sum rule is

$$\sum_i \int_0^1 x f_i(x) dx + \int_0^1 xg(x) dx = 1$$

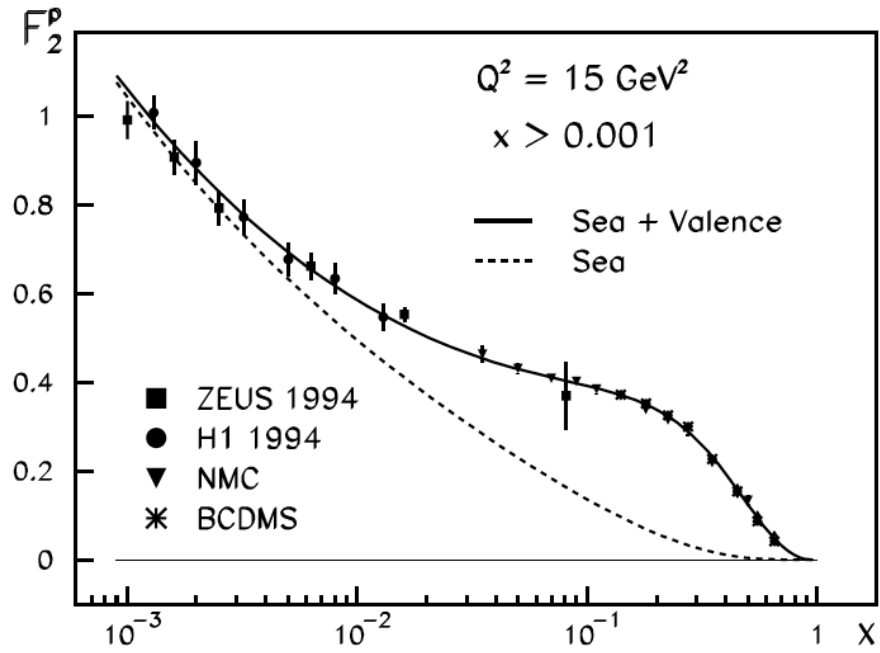


Fig. 7.9: The proton structure function as measured experimentally as a function of Bjorken- x . At different values of x one probes either the sea or the valence and sea quarks.

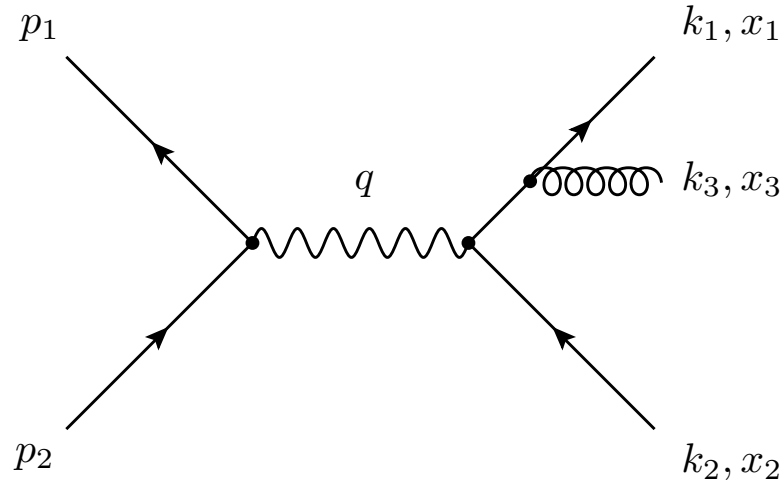
Chapter 8

Soft and Collinear Singularities

8.1 Can perturbative QCD predict anything?

- We have seen that asymptotic freedom allows us to use perturbation theory to calculate quark and gluon interactions at short distances. But is this enough to arrive at predictions for experimental observables?
- The answer is ‘no’, because the detectors in an experiment can only observe hadrons and not the constituent quarks and gluons.
- We will see that we need two more things, if we want to make the connection between theory and experiment:
 1. either infrared safety,
 2. or factorisation.
- These concepts are intimately related to the separation of the short and long distance aspects of the strong interaction.
 - **Infrared Safety:** There is a class of observables that do not depend on long distance physics and are therefore calculable in perturbative QCD.
 - **Factorisation:** There is a wide class of processes that can be factorised in a universal long distance, nonperturbative but process independent piece, and a short distance piece that is calculable in perturbative QCD.
- To understand these ideas we will, in this section, study the lowest order QCD correction to the process $e^+e^- \rightarrow q\bar{q}$.

8.1.1 The process $e^+e^- \rightarrow q\bar{q}g$



- Consider the process $e^+e^- \rightarrow q\bar{q}g$. We have the following kinematic variables:
 1. The four-momentum $q = p_1 + p_2$ of the virtual photon. The square of the centre-of-mass energy is $s = q^2 = q^\mu q_\mu$.
 2. The outgoing four-momenta k_1, k_2 and k_3 . The energies of the outgoing partons¹ in the centre-of-mass frame are $E_i = k_i^0$.
- We define the energy fractions by

$$x_i = \frac{E_i}{\sqrt{s}/2} = \frac{2q \cdot k_i}{s}$$

To show that $\sum_i x_i = 2$, we make use of the fact that $k_i \cdot q$ is Lorentz invariant so that we can calculate it in any convenient frame. We use the centre of mass frame where, by definition, $q = (\sqrt{s}, 0, 0, 0)$. Then

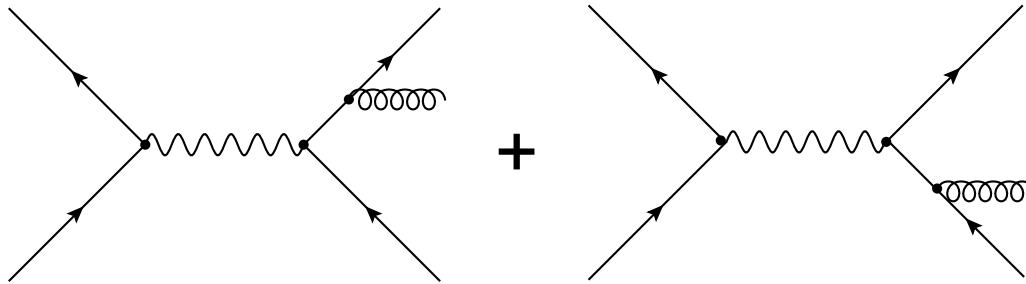
$$q \cdot k_i = E_i \sqrt{s} \quad \text{and} \quad \frac{2q \cdot k_i}{s} = \frac{2E_i}{\sqrt{s}} \equiv x_i.$$

Energy conservation gives $\sqrt{s} = E_1 + E_2 + E_3$ so that $x_1 + x_2 + x_3 = 2$.

From $\sum_i x_i = 2$ it follows that only two of the x_i are independent.

¹ We use the name ‘parton’ for both quark and gluon.

8.1.2 Singularities in the cross section



- To calculate the cross section $\sigma(e^+e^- \rightarrow q\bar{q}g)$ two Feynman graphs have to be taken into account, one where the gluon is radiated from the quark and another where it is radiated from the antiquark. The calculation of the cross section is rather lengthy so we will not give it here; you can find it in H&M Section 11.5.
- The result is

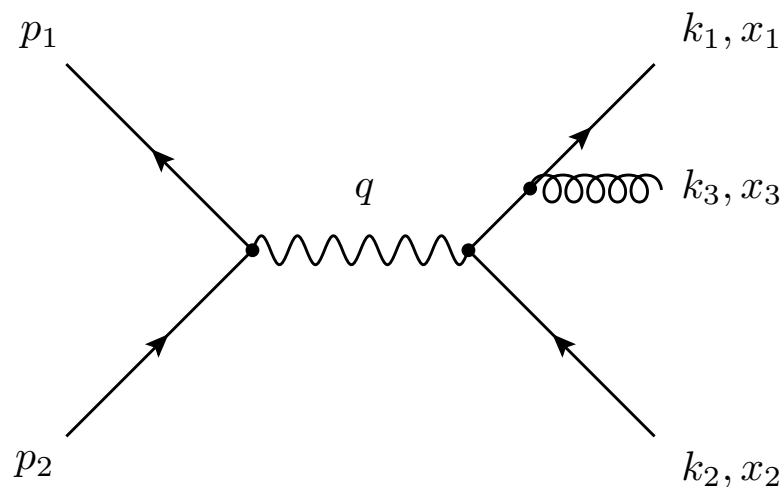
$$\frac{d^2\sigma}{dx_1 dx_2} = \sigma_0 \frac{2\alpha_s}{3\pi} \frac{x_1^2 + x_2^2}{(1-x_1)(1-x_2)}$$

Here $\sigma_0 = \sigma(e^+e^- \rightarrow \text{hadrons}) = (4\pi\alpha^2/s) \sum e_i^2$.

- There are three singularities in this cross section
 - $(1-x_1) = 0$
 - $(1-x_2) = 0$
 - $(1-x_1) = (1-x_2) = 0$

We will now have a look where these singularities come from.

8.1.3 More kinematics



- In the following we will neglect the quark masses ($k_i^2 = 0$) so that

$$(k_i + k_j)^2 = k_i^2 + k_j^2 + 2k_i \cdot k_j = 2k_i \cdot k_j$$

- Denote by θ_{ij} the angle between the momenta of partons i and j . Then we can relate these angles to the energy fractions as follows

$$2k_1 \cdot k_2 = (k_1 + k_2)^2 = (q - k_3)^2 = s - 2q \cdot k_3 \rightarrow$$

$$2E_1 E_2 (1 - \cos \theta_{12}) = s(1 - x_3)$$

To show that $k_i \cdot k_j = E_i E_j (1 - \cos \theta_{ij})$, one has to consider that $E_i = |k_i|$ for massless particles, so that

$$k_i \cdot k_j = (E_i, k_i) \cdot (E_j, k_j) = E_i E_j - |k_i| |k_j| \cos \theta_{ij} = E_i E_j (1 - \cos \theta_{ij}),$$

- Dividing by $s/2$ and repeating the above for the angles between other pairs of particles gives

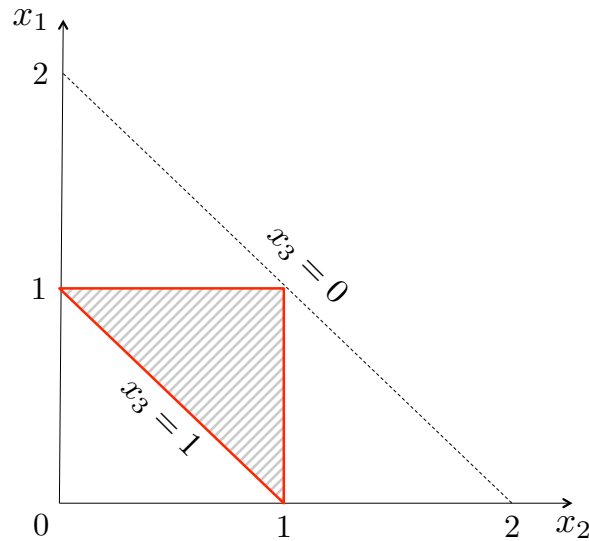
$$x_1 x_2 (1 - \cos \theta_{12}) = 2(1 - x_3)$$

$$x_2 x_3 (1 - \cos \theta_{23}) = 2(1 - x_1)$$

$$x_3 x_1 (1 - \cos \theta_{31}) = 2(1 - x_2)$$

8.1.4 Phase space

- From the above it follows that $0 \leq x \leq 1$. Together with the constraint $x_3 = 2 - x_1 - x_2$ this implies that the allowed region for (x_1, x_2) is the triangle shown below.



- From

$$x_1 x_2 (1 - \cos \theta_{12}) = 2(1 - x_3)$$

$$x_2 x_3 (1 - \cos \theta_{23}) = 2(1 - x_1)$$

$$x_3 x_1 (1 - \cos \theta_{31}) = 2(1 - x_2)$$

we find that the collinear configurations are related to the x_i by

$$\theta_{12} \rightarrow 0 \Leftrightarrow x_3 \rightarrow 1$$

$$\theta_{23} \rightarrow 0 \Leftrightarrow x_1 \rightarrow 1$$

$$\theta_{31} \rightarrow 0 \Leftrightarrow x_2 \rightarrow 1$$

Thus when $x_i \rightarrow 1$ then $\theta_{jk} \rightarrow 0$, that is, j and k are collinear.

We can show that when $x_i \rightarrow 1$ then i is back-to-back with both j and k . In addition, we can also show that $x_i \rightarrow 0$ implies $E_i \rightarrow 0$: particle i becomes soft.

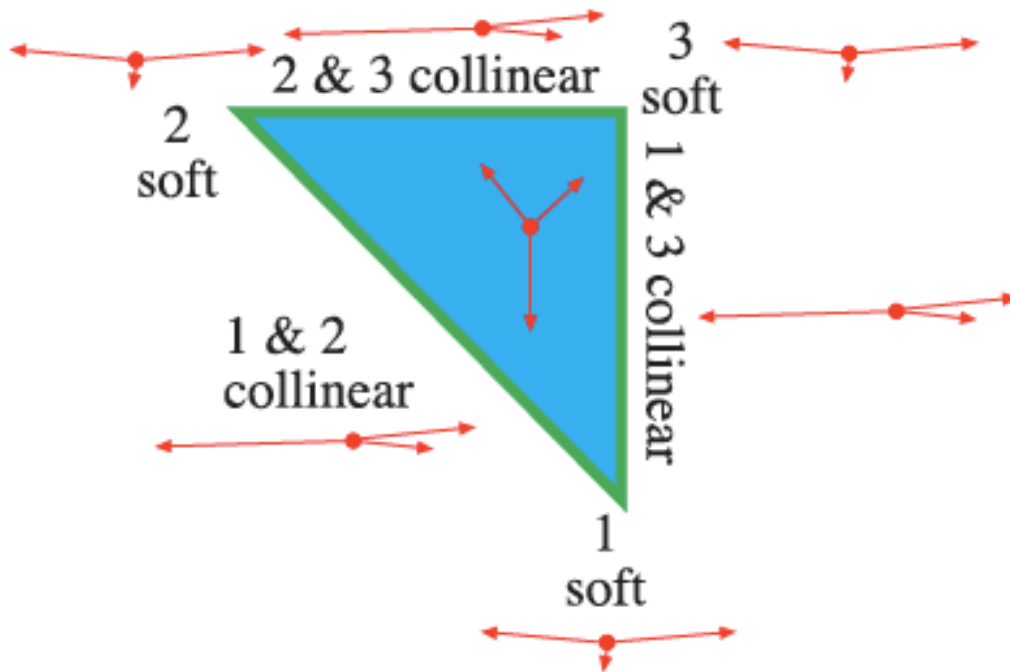
For definiteness take the case $x_3 = 1$ so that $\theta_{12} = 0$ and, because $x_1 + x_2 + x_3 = 2$, we also have $x_1 + x_2 = 1$. Then

$$x_2 x_3 (1 - \cos \theta_{23}) = 2(1 - x_1) \rightarrow x_2(1 - \cos \theta_{23}) = 2x_2 \rightarrow \cos \theta_{23} = -1 \rightarrow \theta_{23} = \pi$$

From the definition $x_i = 2E_i/\sqrt{s}$ it follows immediately that $E_i \rightarrow 0$ when $x_i \rightarrow 0$. Also from the kinematic diagram it is seen that $x_j = x_k = 1$ when $x_i = 0$ so that j and k must be back-to-back.

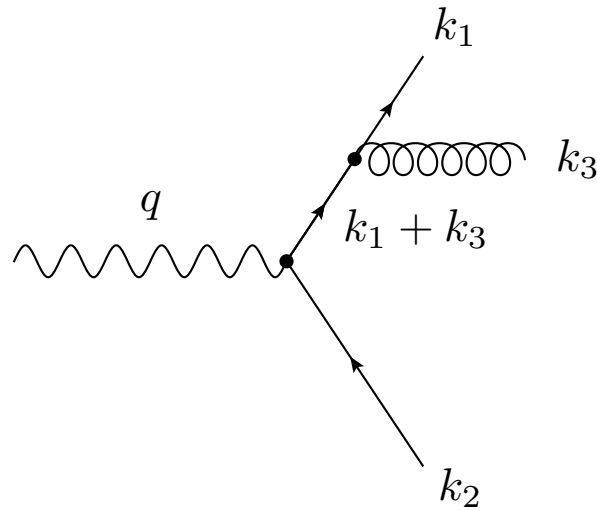
8.1.5 Three-parton configurations

- This plot shows the three-parton configurations at the boundaries of phase space.



- Edges: two partons collinear: $\theta_{ij} \rightarrow 0 \Leftrightarrow x_k \rightarrow 1$.
- Corners: one parton soft $x_i \rightarrow 0 \Leftrightarrow E_i \rightarrow 0$ (other two partons are back-to-back).
- Note that at the boundaries of phase space $2 \rightarrow 3$ kinematics goes over to $2 \rightarrow 2$ kinematics.

8.1.6 Origin of the singularities



- Where do the singularities actually come from? This is easy to see by noting that internal quark momentum is $(k_1 + k_3)$, giving a propagator term $\sim 1/(k_1 + k_3)^2$ in the cross section. Now

$$(k_1 + k_3)^2 = 2k_1 \cdot k_3 = 2E_1 E_3 (1 - \cos \theta_{31})$$

so that the propagator term evidently is singular when $\theta_{31} \rightarrow 0$ and when $E_3 \rightarrow 0$.

- The collinear singularity at $\theta_{31} \rightarrow 0$ and $E_3 \rightarrow 0$ can be made explicit by rewriting the cross section as

$$\frac{d\sigma}{dE_3 d\cos \theta_{31}} = \sigma_0 \frac{2\alpha_s}{3\pi} \frac{f(E_3, \theta_{31})}{E_3 (1 - \cos \theta_{31})}.$$

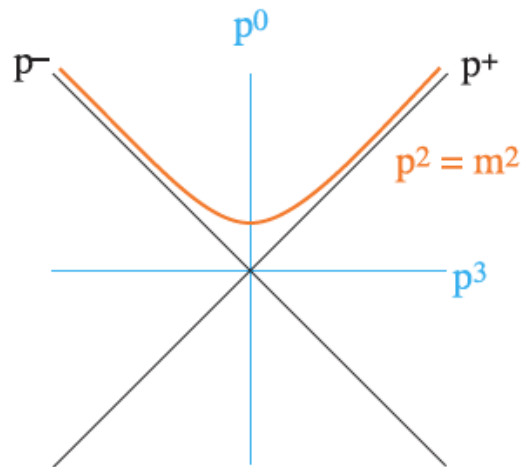
Here $f(E_3, \theta_{31})$ is a rather complicated function that turns out to be finite when $E_3 \rightarrow 0$ or $\theta_{31} \rightarrow 0$.

- Clearly we get a logarithmic divergence when we attempt to integrate over θ_{31} with E_3 kept fixed or over E_3 with θ_{31} kept fixed.

8.1.7 Infrared singularities

- Are we seeing here a breakdown of perturbative QCD? The answer is no: the problem is that we are trying to work with cross sections on the parton level that are not **infrared safe**.
- These infrared problems always show up when $2 \rightarrow 3$ kinematics becomes $2 \rightarrow 2$ kinematics. We have seen that this happens at the edges of phase space when two partons become collinear or one parton becomes soft. Another way of stating this is that the internal propagator goes on shell: $(k_1 + k_3)^2 \rightarrow 0$.
- Please note that infrared divergences are omnipresent in QCD (and also in QED) and are by no means limited to $e^+e^- \rightarrow q\bar{q}g$.
- It is useful to get a space-time picture with the help of **light cone coordinates**. We will then see that the divergences are caused by long distance interactions.

8.1.8 Light cone coordinates



- The light cone components of a four-vector a are defined by

$$a^{\pm} = (a^0 \pm a^3)/\sqrt{2}$$

The vector is then be written as $a = (a^+, a^-, a^1, a^2) = (a^+, a^-, a_T)$.²

- Exercise 1.1:** [1.0] Show that

$$a \cdot b = a^+ b^- + a^- b^+ - a_T \cdot b_T, \quad \text{and} \quad a^2 = 2a^+ a^- - a_T^2$$

Show that the vector transforms under boosts along the z axis like

$$a'^+ = a^+ e^{\psi}, \quad a'^- = a^- e^{-\psi}, \quad a'_T = a_T$$

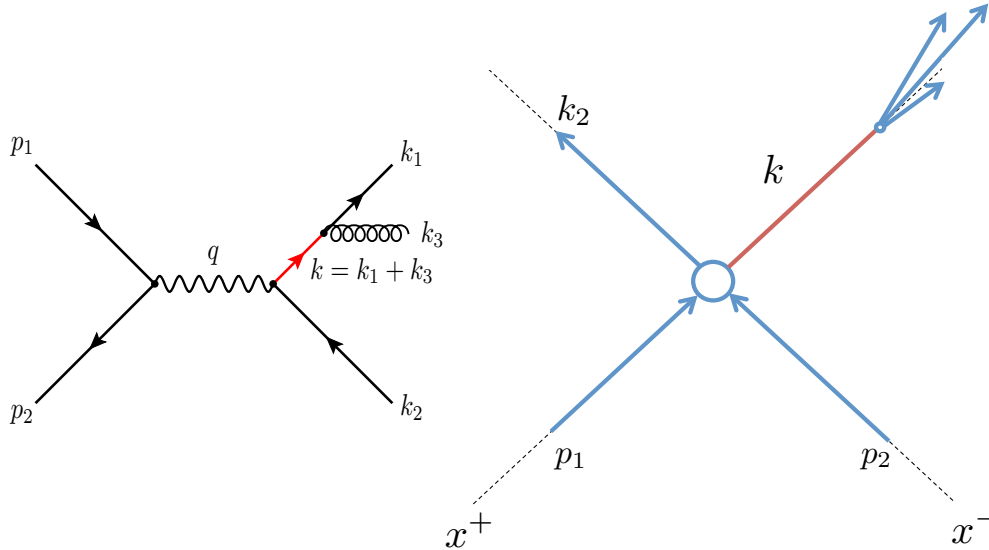
with $\psi = \frac{1}{2} \ln[(1 - \beta)/(1 + \beta)]$. How does a transform under two successive boosts β_1 and β_2 ?

- One often chooses the z axis such that, perhaps after a boost, a particle or a group of particles have large momenta along that axis. For these particles p^+ is large and (since they are on the mass shell)

$$p^- = \frac{m^2 + p_T^2}{2p^+} \quad \text{is small.}$$

² Note that a^+ and a^- are *not* 4-vector components.

8.1.9 Space-time picture of the singularities



- To see what happens when $k^2 = (k_1 + k_3)^2$ becomes small (goes on-shell), we choose the z axis along k with k^+ large and $k_T = 0$. Thus $k^2 = 2k^+k^- \rightarrow 0$ when k^- becomes small.
- In QFT, the Green functions (propagators) in momentum space are related to those in coordinate space by a Fourier transform:

$$\begin{aligned} S_F(x) &= \int d^4k \exp(-ikx) S_F(k) \\ &= \int d^4x \exp[-i(k^+x^- + k^-x^+ - k_T \cdot x_T)] S_F(k) \end{aligned}$$

Because k^+ is large and k^- is small, the contributing values of x have small x^- and large x^+ . This means that the quark propagates a long distance in the x^+ direction before decaying in a quark-gluon pair, as is indicated in the space-time diagram above.

- It follows that the singularities that can lead to divergent perturbative cross-sections arise from interactions that happen a long time after the creation of a quark-antiquark pair.

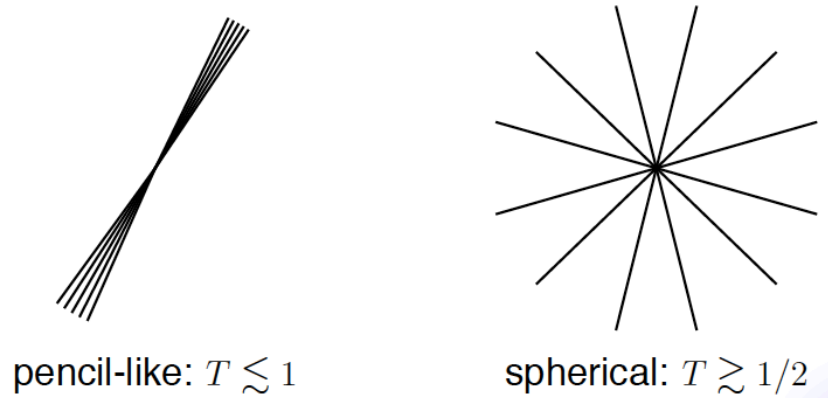
8.1.10 Infrared safe observables

- We have seen that soft/collinear singularities arise from interactions that happen a long time after the creation of the quark-antiquark pair and that perturbation theory cannot handle this long-time physics. But a detector is a long distance away from the interaction so we must somehow take long-time physics into account in our theory.
- Fortunately there are measurements that are *insensitive* to long-time physics. These are called **infrared safe** observables. We have seen that soft/collinear singularities appear when $2 \rightarrow 3$ kinematics reduces to $2 \rightarrow 2$ kinematics at the boundaries of phase space. Therefore a meaningful infrared safe observable must be insensitive to the indistinguishable $2 \rightarrow 2$, $2 \rightarrow 3$ origin of the long-distance interactions.
- The most well known example of an infrared safe observable is the total cross section $\sigma(e^+e^- \rightarrow \text{hadrons})$. This cross section is infrared safe because it is a totally *inclusive* quantity (we sum over all particles in the final state and don't

care how many there are) and the transition from partons to the hadronic final state in a given event always occurs with unit probability, whatever the details of the long-time hadronisation process.

- As an example of another infrared safe variable used in the analysis of e^+e^- collisions, we mention the thrust event shape variable.

8.1.10.1 Thrust



- Thrust is an event shape variable, used to discriminate between pencil-like and spherical events.
- Thrust is defined by

$$T = \max_{\hat{u}} \frac{\sum_i |p_i \cdot \hat{u}|}{\sum_i |p_i|}$$

Here the sum runs over all particles i in the event, and the unit vector \hat{u} is varied to maximise the sum of the projections of the 3-momenta p_i on \hat{u} .




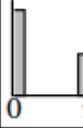
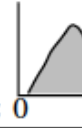
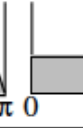
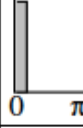
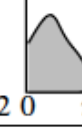
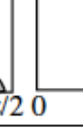
- So why is thrust infrared safe?
 1. Zero-momentum particles do not contribute to T .
 2. A collinear splitting does not change the thrust:

$$|(1-\lambda)p_i \cdot \hat{u}| + |\lambda p_i \cdot \hat{u}| = |p_i \cdot \hat{u}|$$

$$|(1-\lambda)p_i| + |\lambda p_i| = |p_i|$$

IR safe observables used in e^+e^- physics

Here is a list of more infrared safe observables.

Name of Observable	Definition	Typical Value for:			QCD calculation
					
Thrust	$T = \max_{\vec{n}} \left(\frac{\sum_i \vec{p}_i \cdot \vec{n} }{\sum_i \vec{p}_i } \right)$	1	$\geq 2/3$	$\geq 1/2$	(resummed) $O(\alpha_s^2)$
Thrust major	Like T, however T_{maj} and \vec{n}_{maj} in plane $\perp \vec{n}_T$	0	$\leq 1/3$	$\leq 1/\sqrt{2}$	$O(\alpha_s^2)$
Thrust minor	Like T, however T_{min} and \vec{n}_{min} in direction \perp to \vec{n}_T and \vec{n}_{maj}	0	0	$\leq 1/2$	$O(\alpha_s^2)$
Oblateness	$O = T_{\text{maj}} - T_{\text{min}}$	0	$\leq 1/3$	0	$O(\alpha_s^2)$
Sphericity	$S = 1.5 (Q_1 + Q_2)$; $Q_1 \leq \dots \leq Q_3$ are Eigenvalues of $S^{\alpha\beta} = \frac{\sum_i p_i^\alpha p_i^\beta}{\sum_i p_i^2}$	0	$\leq 3/4$	≤ 1	none (not infrared safe)
Aplanarity	$A = 1.5 Q_1$	0	0	$\leq 1/2$	none (not infrared safe)
Jet (Hemisphere) masses	$M_{\pm}^2 = \left(\sum_{i \in S_{\pm}} E_i^2 - \sum_i \vec{p}_i^2 \right)_{i \in S_{\pm}}$ (S_{\pm} : Hemispheres \perp to \vec{n}_T) $M_H^2 = \max(M_+^2, M_-^2)$ $M_D^2 = M_+^2 - M_-^2 $	0	$\leq 1/3$	$\leq 1/2$	(resummed) $O(\alpha_s^2)$
Jet broadening	$B_{\pm} = \frac{\sum_{i \in S_{\pm}} \vec{p}_i \times \vec{n}_T }{2 \sum_i \vec{p}_i }$; $B_T = B_+ + B_-$ $B_w = \max(B_+, B_-)$	0	$\leq 1/(2\sqrt{3})$	$\leq 1/(2\sqrt{2})$	(resummed) $O(\alpha_s^2)$
Energy-Energy Correlations	$EEC(\chi) = \sum_{\text{events}} \sum_{i,j} \frac{E_i E_j}{E_{\text{vis}}^2} \int_{z+\frac{\Delta z}{2}}^{z+\frac{\Delta z}{2}} \delta(\chi - \chi_{ij})$				(resummed) $O(\alpha_s^2)$
Asymmetry of EEC	$AEEC(\chi) = EEC(\pi - \chi) - EEC(\chi)$				$O(\alpha_s^2)$
Differential 2-jet rate	$D_2(y) = \frac{R_2(y - \Delta y) - R_2(y)}{\Delta y}$				(resummed) $O(\alpha_s^2)$

8.2 The QCD improved Parton Model

8.2.1 The QCD factorisation theorem

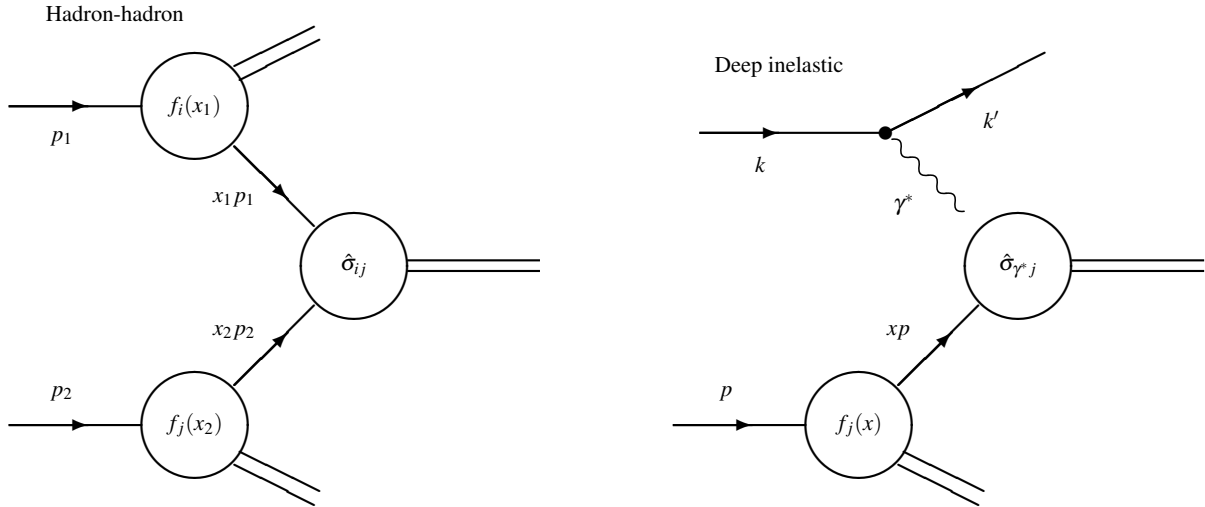
- In Section 7 we have seen that QCD suffers from infrared singularities when two daughter partons cannot be resolved because they become collinear, or because one of them becomes soft. We have also seen that these singularities are associated with ‘long-distance’ physics which takes place a long time after the initial hard scattering. So-called infrared-safe observables are still calculable in perturbative QCD, but since this is quite restrictive we have to look for ways to extend the predictive power of the theory. This way-out is provided by the **QCD factorisation theorem**.
- For hadron-hadron scattering the factorisation theorem states that the singular long-distance pieces can be removed from the partonic cross section and factored into the parton distributions of the incoming hadrons, and that this can be done consistently at all orders in the perturbative expansion.
- The partonic cross section is then calculable in perturbation theory, and does not depend on the type of incoming hadron.
- The parton distributions, on the other hand, are a property of the incoming hadrons but are universal in the sense that they do not depend on the hard scattering process. Parton distributions are nonperturbative and have to be obtained from experiment.
- Factorisation is a fundamental property of QCD. It turns perturbative QCD into a reliable calculation tool, unlike the naive parton model that does not take the parton dynamics into account.

8.2.2 Hadron-hadron cross sections I

- Schematically, a hadron-hadron cross section can be written as

$$\sigma^{\text{h-h}} = \sum_{i,j} \int dx_1 dx_2 f_i(x_1, \mu^2) f_j(x_2, \mu^2) \hat{\sigma}_{ij}(x_1, x_2, Q^2/\mu^2, \dots)$$

and can be depicted by (left diagram):



- Here the (arbitrary) **factorisation scale** μ can be thought of as the scale which separates the long and short-distance physics. Roughly speaking, a parton with a transverse momentum less than μ is then considered to be part of the hadron structure and is absorbed in the parton distribution. Partons with larger transverse momenta participate in the hard scattering process with a short-distance partonic cross-section $\hat{\sigma}$.

8.2.3 Hadron-hadron cross sections II

- What is taken for the hard scale Q^2 depends on the scattering process we are interested in. In jet production, for instance, one usually takes the transverse momentum of the jet as the hard scale, in deep inelastic scattering one takes the square of the four momentum transfer from the electron to the proton, and in e^+e^- scattering one takes the centre-of-mass energy, and so on. Often the simplifying assumption is made that the factorisation scale is equal to the hard scale: $\mu^2 = Q^2$.
- The factorisation theorem also applies to deep inelastic scattering, with one of the parton distributions replaced by an $ee'\gamma^*$ vertex as is shown in the right-hand side diagram on the previous diagram:

$$\sigma^{\text{DIS}} = \sum_j \int dx f_j(x, \mu^2) \hat{\sigma}_{\gamma^*j}(x, Q^2/\mu^2, \dots)$$

- We will use DIS to show how the infrared singularities are absorbed in the parton distributions. The QCD evolution equations of the parton densities are then derived from the **renormalisation group equation**.

8.2.4 Recap of the F_2 structure function

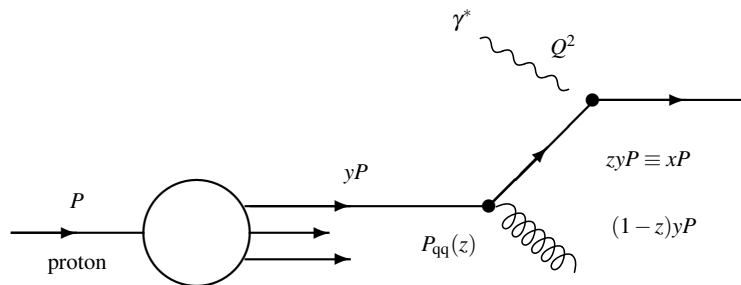
- We have seen that the F_2 structure function measured in deep inelastic electron-proton scattering is, to first order, independent of Q^2 , the negative square of the momentum transfer from the electron to the proton. This implies that DIS does not depend on the resolution $1/Q$ with which the proton is probed. This is explained in the naive parton model by assuming that the electron scatters incoherently off *pointlike* quarks in the proton. The F_2 structure function can then be written as the charge weighted sum of quark momentum distributions

$$F_2^{\text{ep}}(x) = \sum_i e_i^2 x f_i(x).$$

Here e_i is the charge of the quark, and $f_i(x)dx$ is the number of quarks that carry a fraction between x and $x + dx$ of the proton momentum. The probability that the parton carries a momentum fraction x is then given by $x f_i(x)$. The index i denotes the quark flavour $d, u, s, \dots, \bar{d}, \bar{u}, \bar{s}, \dots$

- Although gluons show up in the naive parton model as missing momentum, they are not treated as dynamical entities. We will now incorporate the effect of gluon radiation by quarks, which leads to the so-called **QCD improved parton model**.

8.2.5 Scaling violation I



- Consider a quark that carries a fraction y of the proton momentum and radiates a gluon with a fraction $1 - z$ of its momentum. After radiating the gluon, the quark with momentum fraction zy scatters off the virtual photon. The momentum fraction seen by the photon is thus $x = zy$ which implies that $z = x/y$.
- Taking gluon radiation into account, the F_2 structure function is found to be (see H&M Section 10.1–5 for a lengthy derivation):

$$\frac{F_2(x, Q^2)}{x} = \sum_i e_i^2 \int_x^1 \frac{dy}{y} f_i(y) \left[\delta \left(1 - \frac{x}{y} \right) + \frac{\alpha_s}{2\pi} P_{\text{qq}} \left(\frac{x}{y} \right) \ln \frac{Q^2}{m^2} \right]$$

Here m^2 is a lower transverse momentum cut-off to regularise the divergence when the gluon becomes collinear with the quark.

- In the above, the **splitting function** P_{qq} is given by

$$P_{qq}(z) = \frac{4}{3} \left(\frac{1+z^2}{1-z} \right).$$

It represents the probability that a parent quark emits a gluon with the daughter quark retaining a fraction z of the parent momentum. Note that an infrared divergence shows up when $(1-z) \rightarrow 0$ where the gluon becomes soft so that daughter and parent cannot be resolved anymore.

8.2.6 Scaling violation II

$$\boxed{\frac{F_2(x, Q^2)}{x} = e^2 \int_x^1 \frac{dy}{y} f(y) \left[\delta \left(1 - \frac{x}{y} \right) + \frac{\alpha_s}{2\pi} P_{qq} \left(\frac{x}{y} \right) \ln \frac{Q^2}{m^2} \right]}$$

- **Exercise 2.1:** [1.0] Carry out the integral on the first term and check that it corresponds to the parton model expression for F_2 , as is given by the DIS cross-section (note that for clarity we have suppressed the flavour index i and the summation over flavours).
- The expression above depends on the cutoff parameter m and diverges when $m \rightarrow 0$. To simplify the notation we set

$$I_{qq}(x) = \frac{\alpha_s}{2\pi} \int_x^1 \frac{dy}{y} f(y) P_{qq} \left(\frac{x}{y} \right)$$

and write

$$\frac{F_2(x, Q^2)}{x} = e^2 \underbrace{\left[\underbrace{f(x) + I_{qq}(x) \ln \frac{\mu^2}{m^2}}_{f(x, \mu^2)} + I_{qq}(x) \ln \frac{Q^2}{\mu^2} \right]}_{f(x, Q^2)}$$

- Here we have defined the *renormalised* quark distribution $f(x, \mu^2)$ at the so-called **factorisation scale** μ where we separate the singular factor, which depends on m but not on Q^2 , from the calculable factor which depends on Q^2 but not on m .
- If we substitute the renormalised distribution for the bare distribution in I_{qq} we obtain, neglecting terms beyond $O(\alpha_s)$,

$$f(x, Q^2) = f(x, \mu^2) + \frac{\alpha_s}{2\pi} \int_x^1 \frac{dy}{y} f(y, \mu^2) P_{qq} \left(\frac{x}{y} \right) \ln \frac{Q^2}{\mu^2} + \mathcal{O}(\alpha_s^2)$$

8.2.7 DGLAP evolution

- The expression for F_2 now becomes, up to $\mathcal{O}(\alpha_s^2)$,

$$\frac{F_2(x, Q^2)}{x} = e^2 \left[f(x, \mu^2) + \frac{\alpha_s}{2\pi} \int_x^1 \frac{dy}{y} f(y, \mu^2) P_{qq} \left(\frac{x}{y} \right) \ln \frac{Q^2}{\mu^2} \right]$$

- Clearly F_2 should not depend on the choice of factorisation scale which leads to the following renormalisation group equation:

$$\begin{aligned} \frac{1}{e^2 x} \frac{\partial F_2(x, Q^2)}{\partial \ln \mu^2} &= \frac{\partial f(x, \mu^2)}{\partial \ln \mu^2} + \\ &\frac{\alpha_s}{2\pi} \int_x^1 \frac{dy}{y} \left[\frac{\partial f(y, \mu^2)}{\partial \ln \mu^2} \ln \left(\frac{Q^2}{\mu^2} \right) - f(y, \mu^2) \right] P_{qq} \left(\frac{x}{y} \right) = 0 \end{aligned}$$

- From this equation it is seen that $(\partial f / \partial \ln \mu^2)$ is of order α_s so that the first term in the integral above is of order α_s^2 . Neglecting this term we obtain an evolution equation for the quark distribution³

$$\boxed{\frac{\partial f(x, \mu^2)}{\partial \ln \mu^2} = \frac{\alpha_s}{2\pi} \int_x^1 \frac{dy}{y} f(y, \mu^2) P_{qq} \left(\frac{x}{y} \right) + \mathcal{O}(\alpha_s^2)}$$

This is, together with the evolution equation for α_s , the most famous equation in QCD. It describes the evolution of a quark distribution due to gluon radiation and is called the **DGLAP evolution equation** after several authors who claim eternal fame: Dokshitzer, Gribov, Lipatov, Altarelli and Parisi.

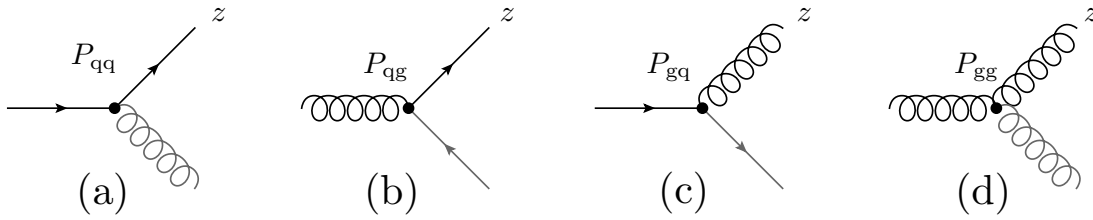
- This equation can be solved (numerically) once $f(x, \mu_0^2)$ is given as an input at some starting scale μ_0^2 . This is similar to the running coupling constant α_s where also an input has to be given at some scale (usually taken to be m_Z^2 , as we have seen).

8.2.8 Quark and gluon evolution

³ In our derivation we have assumed that α_s is a constant. Taking the running of α_s into account is somewhat subtle, but leads to the same evolution equation; see the comment in H&M exercise 10.7 on page 218.

$$\frac{\partial f(x, \mu^2)}{\partial \ln \mu^2} = \frac{\alpha_s}{2\pi} \int_x^1 \frac{dy}{y} f(y, \mu^2) P_{qq} \left(\frac{x}{y} \right) + \mathcal{O}(\alpha_s^2)$$

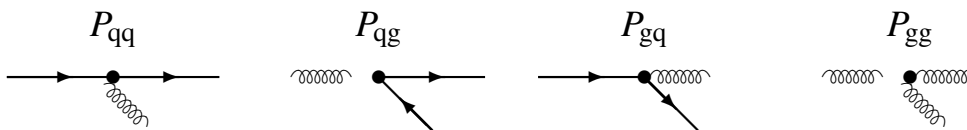
- We have seen the DGLAP evolution of quark distributions with splitting function P_{qq} but when we introduce the gluon distribution, more splitting graphs have to be included.



- (a) A daughter quark from the splitting of a parent quark into a quark and a gluon. When the gluon becomes soft $(1 - z) \rightarrow 0$, the distinction between daughter and parent vanishes, and a singularity develops.
- (b) A daughter quark from a parent gluon which splits into a quark-antiquark pair. Here no singularity develops since daughter and parent can always be distinguished.
- (c) A daughter gluon from a quark parent. Also here no singularity.
- (d) A daughter gluon from a parent gluon. Like in $q \rightarrow qg$ a singularity develops in the soft limit $(1 - z) \rightarrow 0$.

8.2.9 The leading order splitting functions

- Here are the leading order splitting functions



$$\begin{aligned}
P_{qq}^{(0)}(z) &= \frac{4}{3} \left[\frac{1+z^2}{(1-z)_+} + \frac{3}{2} \delta(1-z) \right] \\
P_{qg}^{(0)}(z) &= \frac{1}{2} [z^2 + (1-z)^2] \\
P_{gq}^{(0)}(z) &= \frac{4}{3} \left[\frac{1+(1-z)^2}{z} \right] \\
P_{gg}^{(0)}(z) &= 6 \left[\frac{z}{(1-z)_+} + \frac{1-z}{z} + z(1-z) + \left(\frac{11}{12} - \frac{n_f}{18} \right) \delta(1-z) \right]
\end{aligned}$$

- The singularities showing up in P_{qq} and P_{gg} at $(1-z) \rightarrow 0$ are regulated by a so-called ‘plus’ prescription which guarantees that the integral \int_x^1 exists of the splitting function multiplied by a parton density function (provided that the pdf $\rightarrow 0$ when $x \rightarrow 1$).
- For reference, we give here the definition of the plus prescription

$$[f(x)]_+ = f(x) - \delta(1-x) \int_0^1 f(z) dz$$

or, equivalently,

$$\int_x^1 f(z)[g(z)]_+ dz = \int_x^1 [f(z) - f(1)] g(z) dz - f(1) \int_0^x g(z) dz.$$

8.2.10 The coupled DGLAP equations

- The qq , qg , gq and gg transitions lead to a set of $2n_f + 1$ coupled evolution equations that can be written as⁴

$$\frac{\partial f_i(x, \mu^2)}{\partial \ln \mu^2} = \sum_{j=-n_f}^{n_f} \frac{\alpha_s}{2\pi} \int_x^1 \frac{dy}{y} P_{ij} \left(\frac{x}{y} \right) f_j(y, \mu^2),$$

where the splitting function $P_{ij}(z)$ represents the probability that a daughter parton i with momentum fraction z splits from a parent parton j .⁵ Here the indexing is as follows

$$i, j = \begin{cases} -1, \dots, -n_f & \text{antiquarks} \\ 0 & \text{gluon} \\ 1, \dots, n_f & \text{quarks} \end{cases}$$

⁴ Here n_f is the number of ‘active’ quark flavours. Usually a quark species is considered to be active (*i.e.* it participates in the QCD dynamics) when its mass $m < \mu$.

⁵ The conventional index notation for splitting functions is thus $P_{\text{daughter-parent}}$.

- To simplify the expressions for the evolution equations we write the Mellin convolution in short-hand notation as

$$P \otimes f \equiv \int_x^1 \frac{dy}{y} P\left(\frac{x}{y}\right) f(y, \mu^2)$$

With this notation the set of coupled equations reads

$$\frac{\partial f_i}{\partial \ln \mu^2} = \sum_{j=-n_f}^{n_f} \frac{\alpha_s}{2\pi} P_{ij} \otimes f_j$$

- In leading order QCD we can write for the splitting functions:⁶

$$P_{\bar{q}_i \bar{q}_j} = P_{q_i q_j} \equiv P_{qq} \delta_{ij}, \quad P_{\bar{q}_i g} = P_{q_i g} \equiv P_{qg}, \quad P_{g \bar{q}_i} = P_{g q_i} \equiv P_{gq}$$

8.2.11 Singlet/gluon and non-singlet evolution

- Exploiting the symmetries in the splitting functions (previous page), the set of $2n_f + 1$ coupled equations can to a large extent be decoupled by defining the **singlet distribution** q_s , which is the sum over all flavours of the quark and antiquark distributions,

$$q_s \equiv \sum_{i=1}^{n_f} (q_i + \bar{q}_i)$$

- It is easy to show that the evolution of this distribution is coupled to that of the gluon

$$\begin{aligned} \frac{\partial q_s}{\partial \ln \mu^2} &= \frac{\alpha_s}{2\pi} [P_{qq} \otimes q_s + 2n_f P_{qg} \otimes g] \\ \frac{\partial g}{\partial \ln \mu^2} &= \frac{\alpha_s}{2\pi} [P_{gq} \otimes q_s + P_{gg} \otimes g] \end{aligned}$$

In compact matrix notation, this is often written as

$$\frac{\partial}{\partial \ln \mu^2} \begin{pmatrix} q_s \\ g \end{pmatrix} = \frac{\alpha_s}{2\pi} \begin{pmatrix} P_{qq} & 2n_f P_{qg} \\ P_{gq} & P_{gg} \end{pmatrix} \otimes \begin{pmatrix} q_s \\ g \end{pmatrix}$$

- Likewise it is easy to show that **non-singlet distributions**

$$q_{ns} \equiv \sum_{i=1}^{n_f} (C_i q_i + D_i \bar{q}_i) \quad \text{with} \quad \sum_{i=1}^{n_f} (C_i + D_i) = 0$$

⁶ The splitting functions are flavour independent since the strong interaction is flavour independent. Furthermore, leading order splitting cannot change the flavour of a quark, as is expressed by the delta function.

evolve independent from the gluon and from each other:

$$\frac{\partial q_{\text{ns}}}{\partial \ln \mu^2} = \frac{\alpha_s}{2\pi} P_{\text{qq}} \otimes q_{\text{ns}}$$

An example of a non-singlet is the valence distribution $q_i - \bar{q}_i$.

- Thus, in practice we do not evolve the quark distributions $u, \bar{u}, d, \bar{d}, \dots$ but, instead, the singlet distribution (coupled to the gluon) and a well chosen set of $2n_f - 1$ non-singlet distributions.

8.2.12 Higher orders ...

Divergences for $x \rightarrow 1$ are understood in the sense of $+$ -distributions.

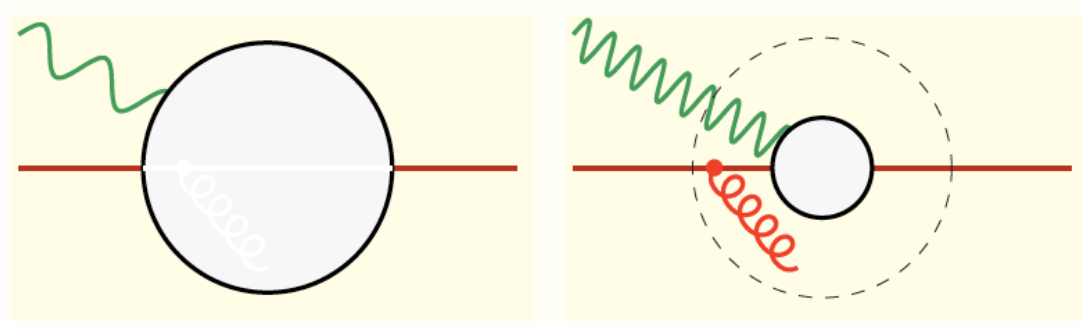
The third-order pure-singlet contribution to the quark-quark splitting function (2.4), corresponding to the anomalous dimension (3.10), is given by

$$P_{ij}^{(3)}(x) = 16C_A C_F n_f \left(\frac{4}{3} + x^2 \right) \left[\frac{13}{3} H_{1,0} - \frac{14}{9} H_{0,0} + \frac{1}{2} H_{1,1} \zeta_2 - H_{1,1,0} - 2H_{1,0} \right. \\ \left. - H_{1,2} \right] + \frac{2}{3} (1-x^2) \left[\frac{16}{3} \zeta_2 + H_{2,1} + 9 \zeta_4 + \frac{9761}{54} H_{3,1} + \frac{10}{3} H_{2,0} + H_{1,1} \zeta_2 - \frac{11}{6} H_{1,1} \right. \\ \left. - 3H_{1,0} + 2H_{1,1,0} + 2H_{1,1,1} \right] + (1-x) \left[\frac{182}{9} H_1 + \frac{158}{3} H_0 - \frac{13}{2} H_{2,0} + 3H_{0,0,0} \right. \\ \left. + \frac{13}{2} H_{1,0} + 3H_{1,1,0} + H_{3,0} + H_{2,0} \zeta_2 + 2H_{2,1,0} + 3H_{2,0,0} + \frac{1}{2} H_{0,0} \zeta_2 + \frac{1}{2} H_{1,1} \zeta_2 - \frac{1}{2} H_{1,0,0} \right. \\ \left. + \frac{3}{2} H_{1,1} + H_{1,1,0} + H_{1,1,1} \right] + (1+x) \left[\frac{7}{12} H_{0,0} \zeta_2 + \frac{31}{6} \zeta_4 + \frac{91}{18} H_{2,1} + \frac{71}{18} H_{1,1} + \frac{113}{18} \zeta_2 + \frac{826}{27} H_0 \right. \\ \left. + \frac{5}{12} H_{2,0} + \frac{5}{3} H_{1,0} + 6H_{1,1,0} + \frac{31}{6} H_{0,0,0} - \frac{1}{6} H_{2,1} + \frac{117}{20} \zeta_2^2 + 9H_{1,1} \zeta_2 + \frac{5}{2} H_{1,1} \zeta_2 + 2H_{2,1,0} \right. \\ \left. + \frac{1}{2} H_{1,0,0} - 2H_{1,2} + H_{2,0} \zeta_2 + \frac{7}{2} H_{2,0,0} + H_{1,1,0} + 2H_{2,1,1} + H_{3,1} + \frac{1}{2} H_{1,1} \right] + 5H_{2,0} + H_{2,1} \\ + H_{0,0,0,0} - \frac{1}{2} \zeta_2^2 + 4H_{3,0} + 4H_{0,0} - \frac{1}{2} H_{0,0} - \frac{1}{12} H_{0,0} - \frac{1}{12} H_{1,1} \zeta_2 - \frac{511}{12} H_{1,1} + \frac{33}{2} H_2 - H_3 \\ - \frac{11}{2} H_{0,0} + \frac{11}{2} \zeta_2 - \frac{3}{2} H_{2,0} - 10H_{0,0,0} + \frac{2}{3} \left[\frac{83}{4} H_{0,0} + \frac{243}{4} H_0 + 10\zeta_2 + \frac{511}{8} H_1 + \frac{97}{8} H_2 - \frac{4}{3} H_3 \right. \\ \left. - 6\zeta_2 - H_{0,0} + H_3 + H_{2,0} - 6H_{2,0} \right] + 16C_F n_f \left(\frac{2}{3} H_0 - 2 - H_2 + \zeta_2 + \frac{5}{2} \zeta_1^2 \right) \left[H_2 - \zeta_2 + 3 \right. \\ \left. + H_{0,0,0,0} + \frac{1}{9} (1-x^2) \left[H_{1,1} + \frac{5}{3} H_1 + \frac{2}{3} \right] + (1-x) \left[\frac{1}{2} H_{1,1} + \frac{7}{6} H_1 + 4H_2 + \frac{32}{3} H_3 + \frac{185}{24} \right] \right. \\ \left. + \frac{1}{2} (1+x) \left[\frac{4}{3} H_2 - \frac{4}{3} \zeta_2 + \zeta_1 + H_{2,1} - 2H_3 + 2H_{0,0} + \frac{29}{6} H_{0,0} + H_{0,0,0} \right] + 16C_F n_f \left(\frac{85}{12} H_1 \right. \right. \\ \left. \left. - \frac{25}{12} H_{0,0} + H_{0,0,0} + \frac{283}{12} H_0 + \frac{101}{9} \zeta_2 - \frac{23}{4} \zeta_1 + \frac{5}{2} H_{2,0} - H_{2,1} - H_{0,0} + \frac{5}{2} \zeta_1^2 + \frac{67}{12} H_2 - \zeta_2 + 3 \right. \right. \\ \left. \left. + \frac{85}{12} H_3 - \frac{22}{3} H_{0,0} + \frac{109}{3} H_{1,1} + \frac{28}{9} H_2 + \frac{28}{9} H_3 - \frac{16}{3} H_{0,0} \zeta_2 + \frac{16}{3} H_1 + 4H_{2,0} + \frac{4}{3} H_{1,1} - \frac{26}{3} \zeta_2 \right. \right. \\ \left. \left. + \frac{12}{12} H_3 + \frac{4}{3} (1-x^2) \left[\frac{3}{2} H_{1,0} - \frac{124}{3} H_{1,1} - 3\zeta_2 + \frac{5}{3} H_{1,1} + H_{1,1,0} - H_{1,1,1} \right] \right. \right. \\ \left. \left. + (1-x) \left[\frac{1}{2} H_{1,0,0} + \frac{7}{12} H_{1,1} + \frac{2743}{72} H_{0,0} - \frac{53}{12} H_{0,0,0} + \frac{25}{12} H_{1,1} + \frac{5}{4} \zeta_2 + \frac{5}{4} H_2 - \frac{3}{2} H_{1,0} + 3H_{1,0} \right. \right. \right. \\ \left. \left. + 3H_{0,0} - 2H_3 - H_{1,1,0} - H_{1,1,1} \right] + (1+x) \left[\frac{1669}{216} H_0 + \frac{5}{2} H_{0,0,0} + 4H_{2,1} + 7H_{2,0} + 10\zeta_2 - \frac{37}{10} \zeta_2^2 \right. \right. \\ \left. \left. - 7H_{0,0} + 8H_{0,0} \zeta_2 - 4H_{0,0,0} + H_{2,0} - 2H_{2,1} - 4H_{0,0} - H_{3,1} - 6H_1 \right] \right]. \quad (4.12)$$

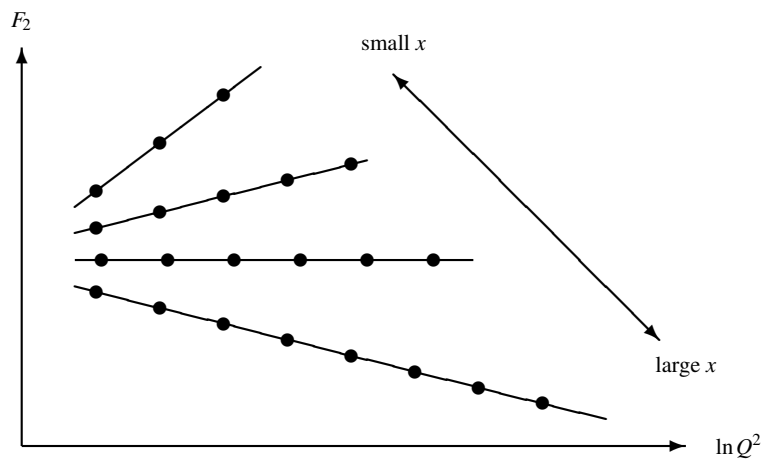
Due to Eqs. (3.11) and (3.12) the three-loop photon-quark and quark-quark splitting functions read

$$P_{ij}^{(3)}(x) = 16C_A C_F n_f \left(P_{ij}(x) \left[\frac{39}{2} H_{1,1} \zeta_2 - 4H_{1,1,1} + 3H_{2,0,0} - \frac{15}{2} H_{1,2} + \frac{9}{2} H_{1,1,0} + 3H_{2,1,0} \right. \right. \\ \left. \left. + H_{0,0} \zeta_2 - 2H_{1,1,1} + 4H_{2,0} - \frac{173}{12} H_{0,0} \zeta_2 - \frac{551}{72} H_{0,0} + \frac{64}{3} \zeta_2 - \frac{49}{4} H_1 - \frac{3}{2} H_{1,0,0} + \frac{1}{3} H_{1,1,0} \right. \right. \\ \left. \left. + 6H_{1,1,1,0} - 2H_{1,1,2} + 2H_{1,2,1} \right] + \left(\frac{1}{2} - x^2 \right) \left[\frac{32}{3} H_{2,1} + \frac{32}{3} \zeta_2 - 2H_{0,0,0} + \frac{4}{3} H_{1,1,0} - \frac{10}{9} H_{1,1} \right. \right. \\ \left. \left. - \frac{8}{9} H_{1,0,0} + \frac{3}{2} H_{1,0} + 6\zeta_2 + \frac{161}{36} H_1 - \frac{2351}{108} \right] + \frac{2}{3} (1+x^2) \left[\frac{16}{9} H_{1,0} - \frac{28}{9} H_2 - 2H_{1,1,0} \right. \right. \\ \left. \left. - 2H_{1,2} + H_{1,1} \zeta_2 + H_{1,1,1} \right] + \frac{161}{108} H_{1,1} + \frac{2351}{108} \right] + (1-x) \left[15H_{0,0,0,0} - 5H_{0,0} - \frac{65}{6} \zeta_2 + \frac{11}{6} H_{1,1,1} \right. \\ \left. - \frac{3}{2} H_{1,0} + \frac{5}{2} H_{0,0,0} + H_{1,1,0} - \frac{31}{12} H_{2,0} + \frac{17}{12} H_{1,0} - \frac{113}{4} H_{0,0,0} - \frac{113}{4} H_2 + \frac{18691}{4} H_3 + \frac{18691}{4} H_0 \right. \\ \left. + \frac{2243}{24} H_{1,0} + \frac{2243}{6} H_{2,0} + 19H_{2,1} + \frac{1}{12} H_{1,1} + \frac{23}{2} H_{2,0} - \frac{497}{2} \zeta_2 + \frac{29}{6} H_{1,1} \zeta_2 + \frac{143}{12} H_{1,1} \right. \\ \left. + \frac{11}{6} H_{1,1,1} - \frac{19}{12} H_{0,0} \zeta_2 + \frac{1223}{72} H_1 + \frac{43}{6} H_{0,0,0} - \frac{3011}{36} H_{0,0} \right] + (1+x) \left[8H_{2,1,0} - 4H_{1,2} \right. \\ \left. + 7H_{1,1,0} - \frac{35}{3} H_{1,1,1} - 5H_{2,0} - 11H_{2,0,0} + \frac{15}{2} H_{1,0} + \frac{15}{2} H_{1,1} \zeta_2 + 6H_{1,1,0} - 10H_{2,1,0} \right. \\ \left. + 5H_{2,0} + 4H_{2,1,1} - H_{3,0} + 34H_{0,0} \zeta_2 - 5H_{2,0} \zeta_2 \right] + 2H_{1,2} + 6H_{1,1,0} - 6H_{1,1,0} - 3H_{2,1,1} \\ - 11H_{0,0,0,0} - 5H_{1,1} + \frac{25}{4} H_{1,1,1} + \frac{13}{4} H_{2,0} + \frac{27}{4} H_{2,0,0} + \frac{11}{2} H_{2,1,0} + \frac{13}{4} H_{2,0} \zeta_2 + \frac{17}{4} H_{1,0,0} \\ + 13H_{2,1,0} - \frac{11}{12} H_{1,1,1,0} - \frac{3}{2} H_{2,1} - \frac{1}{2} H_{0,0} \zeta_2 + H_{1,2} + \frac{11}{2} H_{1,1,0} + \frac{79}{6} H_{1,0} + \frac{67}{6} H_{1,0} + \frac{263}{6} \zeta_2^2 \\ + \frac{119}{3} \zeta_2 + \frac{967}{45} H_{1,1} - \frac{205}{12} H_{1,0} - 24H_{0,0} \zeta_2 + H_{1,1} \zeta_2 + \frac{13375}{18} H_{0,0} + \frac{1889}{18} 3H_{1,0,0} + \frac{21}{2} H_{2,1} \\ - \frac{79}{3} H_{2,0} - \frac{217}{12} H_{2,1,0} - \frac{7}{2} H_{2,0,0} + \frac{4}{3} H_{1,1} \zeta_2 + \frac{17}{12} H_{1,1,0} + \frac{17}{12} H_{0,0} \zeta_2 + \frac{31}{18} H_{1,1} + 3H_{0,0,0} \\ + \frac{148}{12} H_{1,1} + \frac{1553}{24} H_{0,0} \right] + 16C_F n_f \left(\frac{7}{6} H_{0,0,0} + \frac{11}{36} H_1 - \frac{96}{24} H_0 + \frac{7}{24} H_{0,0} + 2H_{0,0,0,0} \right. \\ \left. - \frac{6}{5} H_{1,1} + \frac{5}{18} H_{1,0} + \frac{5}{9} \zeta_2 + \frac{5}{9} P_{ij}(x) \left[H_{2,1} + \frac{91}{2} H_2 + \frac{22}{3} H_{0,0} + H_{1,1,1} + 6H_{0,0,0} \right. \right. \\ \left. \left. - \zeta_2 - 2H_{0,0,0} + \frac{5}{2} H_1 \right] + \frac{1}{2} (1-x^2) \left[\frac{9463}{432} 4H_{0,0,0,0} - \frac{10}{3} 4H_{1,1} \right. \right. \\ \left. \left. + \frac{7}{6} H_{1,1} + \frac{8}{9} H_{1,0} + \frac{7}{9} \zeta_2 \right] - (1-x) \left[\frac{2475}{216} H_0 + \frac{103}{12} H_{0,0} \right] \right) + 16C_F n_f \left(P_{ij}(x) \left[7H_{1,3} + 7H_4 \right. \right. \\ \left. \left. - 2H_{1,3,0} - 7H_4 + 5H_{2,3} + 6H_{3,3} + 6H_{3,1} + H_{2,1,0} + 4H_{2,0,0} + 3H_{2,1} + 2H_{1,1,1} + \frac{5}{2} H_{2,0} \right. \right. \\ \left. \left. + 61 H_2 - \frac{61}{8} H_3 + \frac{87}{8} H_4 + \frac{11}{2} H_{1,2} + \frac{61}{8} H_{1,1} + \frac{17}{8} H_{1,0} - 7H_{0,0} \zeta_2 + \frac{2}{3} H_{1,0,0} + \frac{5}{2} H_{1,1,0} - \frac{19}{2} \zeta_2 \right. \right. \\ \left. \left. + \frac{81}{32} H_{1,1} - \frac{11}{32} H_{0,0} \zeta_2 - \frac{2}{32} H_{1,1} \zeta_2 + \frac{1}{2} H_{0,0,0} + \frac{6}{7} H_0 + \frac{11}{2} \zeta_2 + 3H_{1,1,1} - 5H_{2,0} - 7H_{0,0} \right. \right. \\ \left. \left. + 11H_{0,0} - 2H_{1,2,0} - 7H_{1,1,0} + 3H_{1,0,0,0} - 5H_{1,1} \zeta_2 + 4H_{1,0,0} + H_{1,1,1,0} + 2H_{1,1,1,1} + 5H_{1,1,2} \right. \right. \\ \left. \left. + 6H_{1,2,0} - 6H_{1,2,1} \right] + 4P_{ij}(x) \left[4H_{0,0,0,0} - H_{2,0} + H_{1,1,0} - H_{2,0,0} + \frac{1}{2} H_{1,1,0} - \frac{2,0}{8} H_{1,1,0} \right. \right. \\ \left. \left. - \frac{5}{4} H_{1,0} - \frac{1}{2} H_{2,0} + \frac{1}{2} H_{1,1} \zeta_2 + H_{1,1,0} - \frac{1}{2} H_{1,0,0,0} \right] + 2(1-x) \left[H_{2,1,0} - H_{2,0,0} - H_{2,2} \right. \right. \\ \left. \left. - H_{3,1} - 2H_{3,0} - 2H_{1,1} \zeta_2 + H_{1,2} - H_{1,0,0} - H_{1,1,0} + H_{2,0} \zeta_2^2 + \frac{43}{8} H_2 + \frac{13}{8} H_{1,1} \right. \right. \\ \left. \left. + 6H_{1,1,1} - 2H_{1,1,2} + 2H_{1,2,1} \right] + \left(\frac{1}{2} - x^2 \right) \left[\frac{32}{3} H_{2,1} + \frac{32}{3} \zeta_2 - 2H_{0,0,0} + \frac{4}{3} H_{1,1,0} - \frac{10}{9} H_{1,1} \right. \right. \\ \left. \left. - \frac{8}{9} H_{1,0,0} + \frac{3}{2} H_{1,0} + 6\zeta_2 + \frac{161}{36} H_1 - \frac{2351}{108} \right] + \frac{2}{3} (1+x^2) \left[\frac{16}{9} H_{1,0} - \frac{28}{9} H_2 - 2H_{1,1,0} \right. \right. \\ \left. \left. - 2H_{1,2} + H_{1,1} \zeta_2 + H_{1,1,1} \right] + \frac{161}{108} H_{1,1} + \frac{2351}{108} \right] + (1-x) \left[15H_{0,0,0,0} - 5H_{0,0} - \frac{65}{6} \zeta_2 + \frac{11}{6} H_{1,1,1} \right. \\ \left. - \frac{3}{2} H_{1,0} + \frac{5}{2} H_{0,0,0} + H_{1,1,0} - \frac{31}{12} H_{2,0} + \frac{17}{12} H_{1,0} - \frac{113}{4} H_{0,0,0} - \frac{113}{4} H_2 + \frac{18691}{4} H_3 + \frac{18691}{4} H_0 \right. \\ \left. + \frac{2243}{24} H_{1,0} + \frac{2243}{6} H_{2,0} + 19H_{2,1} + \frac{1}{12} H_{1,1} + \frac{23}{2} H_{2,0} - \frac{497}{2} \zeta_2 + \frac{29}{6} H_{1,1} \zeta_2 + \frac{143}{12} H_{1,1} \right. \\ \left. + \frac{11}{6} H_{1,1,1} - \frac{19}{12} H_{0,0} \zeta_2 + \frac{1223}{72} H_1 + \frac{43}{6} H_{0,0,0} - \frac{3011}{36} H_{0,0} \right] + (1+x) \left[8H_{2,1,0} - 4H_{1,2} \right. \\ \left. + 7H_{1,1,0} - \frac{35}{3} H_{1,1,1} - 5H_{2,0} - 11H_{2,0,0} + \frac{15}{2} H_{1,0} + \frac{15}{2} H_{1,1} \zeta_2 + 6H_{1,1,0} - 10H_{2,1,0} \right. \\ \left. + 5H_{2,0} + 4H_{2,1,1} - H_{3,0} + 34H_{0,0} \zeta_2 - 5H_{2,0} \zeta_2 \right] + 2H_{1,2} + 6H_{1,1,0} - 6H_{1,1,0} - 3H_{2,1,1} \\ - 11H_{0,0,0,0} - 5H_{1,1} + \frac{25}{4} H_{1,1,1} + \frac{13}{4} H_{2,0} + \frac{27}{4} H_{2,0,0} + \frac{11}{2} H_{2,1,0} + \frac{13}{4} H_{2,0} \zeta_2 + \frac{17}{4} H_{1,0,0} \\ + 13H_{2,1,0} - \frac{11}{12} H_{1,1,1,0} - \frac{3}{2} H_{2,1} - \frac{1}{2} H_{0,0} \zeta_2 + H_{1,2} + \frac{11}{2} H_{1,1,0} + \frac{79}{6} H_{1,0} + \frac{67}{6} H_{1,0} + \frac{263}{6} \zeta_2^2 \\ + \frac{119}{3} \zeta_2 + \frac{967}{45} H_{1,1} - \frac{205}{12} H_{1,0} - 24H_{0,0} \zeta_2 + H_{1,1} \zeta_2 + \frac{13375}{18} H_{0,0} + \frac{1889}{18} 3H_{1,0,0} + \frac{21}{2} H_{2,1} \\ - \frac{79}{3} H_{2,0} - \frac{217}{12} H_{2,1,0} - \frac{7}{2} H_{2,0,0} + \frac{4}{3} H_{1,1} \zeta_2 + \frac{17}{12} H_{1,1,0} + \frac{17}{12} H_{0,0} \zeta_2 + \frac{31}{18} H_{1,1} + 3H_{0,0,0} \\ + \frac{148}{12} H_{1,1} + \frac{1553}{24} H_{0,0} \right] + 16C_F n_f \left(\frac{7}{6} H_{0,0,0} + \frac{11}{36} H_1 - \frac{96}{24} H_0 + \frac{7}{24} H_{0,0} + 2H_{0,0,0,0} \right. \\ \left. - \frac{6}{5} H_{1,1} + \frac{5}{18} H_{1,0} + \frac{5}{9} \zeta_2 + \frac{5}{9} P_{ij}(x) \left[H_{2,1} + \frac{91}{2} H_2 + \frac{22}{3} H_{0,0} + H_{1,1,1} + 6H_{0,0,0} \right. \right. \\ \left. \left. - \zeta_2 - 2H_{0,0,0} + \frac{5}{2} H_1 \right] + \frac{1}{2} (1-x^2) \left[\frac{9463}{432} 4H_{0,0,0,0} - \frac{10}{3} 4H_{1,1} \right. \right. \\ \left. \left. + \frac{7}{6} H_{1,1} + \frac{8}{9} H_{1,0} + \frac{7}{9} \zeta_2 \right] - (1-x) \left[\frac{2475}{216} H_0 + \frac{103}{12} H_{0,0} \right] \right) + 16C_F n_f \left(P_{ij}(x) \left[7H_{1,3} + 7H_4 \right. \right. \\ \left. \left. - 2H_{1,3,0} - 7H_4 + 5H_{2,3} + 6H_{3,3} + 6H_{3,1} + H_{2,1,0} + 4H_{2,0,0} + 3H_{2,1} + 2H_{1,1,1} + \frac{5}{2} H_{2,0} \right. \right. \\ \left. \left. + 61 H_2 - \frac{61}{8} H_3 + \frac{87}{8} H_4 + \frac{11}{2} H_{1,2} + \frac{61}{8} H_{1,1} + \frac{17}{8} H_{1,0} - 7H_{0,0} \zeta_2 + \frac{2}{3} H_{1,0,0} + \frac{5}{2} H_{1,1,0} - \frac{19}{2} \zeta_2 \right. \right. \\ \left. \left. + \frac{81}{32} H_{1,1} - \frac{11}{32} H_{0,0} \zeta_2 - \frac{2}{32} H_{1,1} \zeta_2 + \frac{1}{2} H_{0,0,0} + \frac{6}{7} H_0 + \frac{11}{2} \zeta_2 + 3H_{1,1,1} - 5H_{2,0} - 7H_{0,0} \right. \right. \\ \left. \left. + 11H_{0,0} - 2H_{1,2,0} - 7H_{1,1,0} + 3H_{1,0,0,0} - 5H_{1,1} \zeta_2 + 4H_{1,0,0} + H_{1,1,1,0} + 2H_{1,1,1,1} + 5H_{1,1,2} \right. \right. \\ \left. \left. + 6H_{1,2,0} - 6H_{1,2,1} \right] + 4P_{ij}(x) \left[4H_{0,0,0,0} - H_{2,0} + H_{1,1,0} - H_{2,0,0} + \frac{1}{2} H_{1,1,0} - \frac{2,0}{8} H_{1,1,0} \right. \right. \\ \left. \left. - \frac{5}{4} H_{1,0} - \frac{1}{2} H_{2,0} + \frac{1}{2} H_{1,1} \zeta_2 + H_{1,1,0} - \frac{1}{2} H_{1,0,0,0} \right] + 2(1-x) \left[H_{2,1,0} - H_{2,0,0} - H_{2,2} \right. \right. \\ \left. \left. - H_{3,1} - 2H_{3,0} - 2H_{1,1} \zeta_2 + H_{1,2} - H_{1,0,0} - H_{1,1,0} + H_{2,0} \zeta_2^2 + \frac{43}{8} H_2 + \frac{13}{8} H_{1,1} \right. \right. \\ \left. \left. + 6H_{1,1,1} - 2H_{1,1,2} + 2H_{1,2,1} \right] + \left(\frac{1}{2} - x^2 \right) \left[\frac{32}{3} H_{2,1} + \frac{32}{3} \zeta_2 - 2H_{0,0,0} + \frac{4}{3} H_{1,1,0} - \frac{10}{9} H_{1,1} \right. \right. \\ \left. \left. - \frac{8}{9} H_{1,0,0} + \frac{3}{2} H_{1,0} + 6\zeta_2 + \frac{161}{36} H_1 - \frac{2351}{108} \right] + \frac{2}{3} (1+x^2) \left[\frac{16}{9} H_{1,0} - \frac{28}{9} H_2 - 2H_{1,1,0} \right. \right. \\ \left. \left. - 2H_{1,2} + H_{1,1} \zeta_2 + H_{1,1,1} \right] + \frac{161}{108} H_{1,1} + \frac{2351}{108} \right] + (1-x) \left[15H_{0,0,0,0} - 5H_{0,0} - \frac{65}{6} \zeta_2 + \frac{11}{6} H_{1,1,1} \right. \\ \left. - \frac{3}{2} H_{1,0} + \frac{5}{2} H_{0,0,0} + H_{1,1,0} - \frac{31}{12} H_{2,0} + \frac{17}{12} H_{1,0} - \frac{113}{4} H_{0,0,0} - \frac{113}{4} H_2 + \frac{18691}{4} H_3 + \frac{18691}{4} H_0 \right. \\ \left. + \frac{2243}{24} H_{1,0} + \frac{2243}{6} H_{2,0} + 19H_{2,1} + \frac{1}{12} H_{1,1} + \frac{23}{2} H_{2,0} - \frac{497}{2} \zeta_2 + \frac{29}{6} H_{1,1} \zeta_2 + \frac{143}{12} H_{1,1} \right. \\ \left. + \frac{11}{6} H_{1,1,1} - \frac{19}{12} H_{0,0} \zeta_2 + \frac{1223}{72} H_1 + \frac{43}{6} H_{0,0,0} - \frac{3011}{36} H_{0,0} \right] + (1+x) \left[8H_{2,1,0} - 4H_{1,2} \right. \\ \left. + 7H_{1,1,0} - \frac{35}{3} H_{1,1,1} - 5H_{2,0} - 11H_{2,0,0} + \frac{15}{2} H_{1,0} + \frac{15}{2} H_{1,1} \zeta_2 + 6H_{1,1,0} - 10H_{2,1,0} \right. \\ \left. + 5H_{2,0} + 4H_{2,1,1} - H_{3,0} + 34H_{0,0} \zeta_2 - 5H_{2,0} \zeta_2 \right] + 2H_{1,2} + 6H_{1,1,0} - 6H_{1,1,0} - 3H_{2,1,1} \\ - 11H_{0,0,0,0} - 5H_{1,1} + \frac{25}{4} H_{1,1,1} + \frac{13}{4} H_{2,0} + \frac{27}{4} H_{2,0,0} + \frac{11}{2} H_{2,1,0} + \frac{13}{4} H_{2,0} \zeta_2 + \frac{17}{4} H_{1,0,0} \\ + 13H_{2,1,0} - \frac{11}{12} H_{1,1,1,0} - \frac{3}{2} H_{2,1} - \frac{1}{2} H_{0,0} \zeta_2 + H_{1,2} + \frac{11}{2} H_{1,1,0} + \frac{79}{6} H_{1,0} + \frac{67}{6} H_{1,0} + \frac{263}{6} \zeta_2^2 \\ + \frac{119}{3} \zeta_2 + \frac{967}{45} H_{1,1} - \frac{205}{12} H_{1,0} - 24H_{0,0} \zeta_2 + H_{1,1} \zeta_2 + \frac{13375}{18} H_{0,0} + \frac{1889}{18} 3H_{1,0,0} + \frac{21}{2} H_{2,1} \\ - \frac{79}{3} H_{2,0} - \frac{217}{12} H_{2,1,0} - \frac{7}{2} H_{2,0,0} + \frac{4}{3} H_{1,1} \zeta_2 + \frac{17}{12} H_{1,1,0} + \frac{17}{12} H_{0,0} \zeta_2 + \frac{31}{18} H_{1,1} + 3H_{0,0,0} \\ + \frac{148}{12} H_{1,1} + \frac{1553}{24} H_{0,0} \right] + 16C_F n_f \left(\frac{7}{6} H_{0,0,0} + \frac{11}{36} H_1 - \frac{96}{24} H_0 + \frac{7}{24} H_{0,0} + 2H_{0,0,0,0} \right. \\ \left. - \frac{6}{5} H_{1,1} + \frac{5}{18} H_{1,0} + \frac{5}{9} \zeta_2 + \frac{5}{9} P_{ij}(x) \left[H_{2,1} + \frac{91}{2} H_2 + \frac{22}{3} H_{0,0} + H_{1,1,1} + 6H_{0,0,0} \right. \right. \\ \left. \left. - \zeta_2 - 2H_{0,0,0} + \frac{5}{2} H_1 \right] + \frac{1}{2} (1-x^2) \left[\frac{9463}{432} 4H_{0,0,0,0} - \frac{10}{3} 4H_{1,1} \right. \right. \\ \left. \left. + \frac{7}{6} H_{1,1} + \frac{8}{9} H_{1,0} + \frac{7}{9} \zeta_2 \right] - (1-x) \left[\frac{2475}{216} H_0 + \frac{103}{12} H_{0,0} \right] \right) + 16C_F n_f \left(P_{ij}(x) \left[7H_{1,3} + 7H_4 \right. \right. \\ \left. \left. - 2H_{1,3,0} - 7H_4 + 5H_{2,3} + 6H_{3,3} + 6H_{3,1} + H_{2,1,0} + 4H_{2,0,0} + 3H_{2,1} + 2H_{1,1,1} + \frac{5}{2} H_{2,0} \right. \right. \\ \left. \left. + 61 H_2 - \frac{61}{8} H_3 + \frac{87}{8} H_4 + \frac{11}{2} H_{1,2} + \frac{61}{8} H_{1,1} + \frac{17}{8} H_{1,0} - 7H_{0,0} \zeta_2 + \frac{2}{3} H_{1,0,0} + \frac{5}{2} H_{1,1,0} - \frac{19}{2} \zeta_2 \right. \right. \\ \left. \left. + \frac{81}{32} H_{1,1} - \frac{11}{32} H_{0,0} \zeta_2 - \frac{2}{32} H_{1,1} \zeta_2 + \frac{1}{2} H_{0,0,0} + \frac{6}{7} H_0 + \frac{11}{2} \zeta_2 + 3H_{1,1,1} - 5H_{2,0} - 7H_{0,0} \right. \right. \\ \left. \left. + 11H_{0,0} - 2H_{1,2,0} - 7H_{1,1,0} + 3H_{1,0,0,0} - 5H_{1,1} \zeta_2 + 4H_{1,0,0} + H_{1,1,1,0} + 2H_{1,1,1,1} + 5H_{1,1,2} \right. \right. \\ \left. \left. + 6H_{1,2,0} - 6H_{1,2,1} \right] + 4P_{ij}(x) \left[4H_{0,0,0,0} - H_{2,0} + H_{1,1,0} - H_{2,0,0} + \frac{1}{2} H_{1,1,0} - \frac{2,0}{8} H_{1,1,0} \right. \right. \\ \left. \left. - \frac{5}{4} H_{1,0} - \frac{1}{2} H_{2,0} + \frac{1}{2} H_{1,1} \zeta_2 + H_{1,1,0} - \frac{1}{2} H_{1,0,0,0} \right] + 2(1-x) \left[H_{2,1,0} - H_{2,0,0} - H_{2,2} \right. \right. \\ \left. \left. - H_{3,1} - 2H_{3,0} - 2H_{1,1} \zeta_2 + H_{1,2} - H_{1,0,0} - H_{1,1,0} + H_{2,0} \zeta_2^2 + \frac{43}{8} H_2 + \frac{13}{8} H_{1,1} \right. \right. \\ \left. \left. + 6H_{1,1,1} - 2H_{1,1,2} + 2H_{1,2,1} \right] + \left(\frac{1}{2} - x^2 \right) \left[\frac{32}{3} H_{2,1} + \frac{32}{3} \zeta_2 - 2H_{0,0,0} + \frac{4}{3} H_{1,1,0} - \frac{10}{9} H_{1,1} \right. \right. \\ \left. \left. - \frac{8}{9} H_{1,0,0} + \frac{3}{2} H_{1,0} + 6\zeta_2 + \frac{161}{36} H_1 - \frac{2351}{108} \right] + \frac{2}{3} (1+x^2) \left[\frac{16}{9} H_{1,0} - \frac{28}{9} H_2 - 2H_{1,1,0} \right. \right. \\ \left. \left. - 2H_{1,2} + H_{1,1} \zeta_2 + H_{1,1,1} \right] + \frac{161}{108} H_{1,1} + \frac{2351}{108} \right] + (1-x) \left[15H_{0,0,0,0} - 5H_{0,0} - \frac{65}{6} \zeta_2 + \frac{11}{6} H_{1,1,1} \right. \\ \left. - \frac{3}{2} H_{1,0} + \frac{5}{2} H_{0,0,0} + H_{1,1,0} - \frac{31}{12} H_{2,0} + \frac{17}{12} H_{1,0} - \frac{113}{4} H_{0,0,0} - \frac{113}{4} H_2 + \frac{18691}{4} H_3 + \frac{18691}{4} H_0 \right. \\ \left. + \frac{2243}{24} H_{1,0} + \frac{2243}{6} H_{2,0} + 19H_{2,1} + \frac{1}{12} H_{1,1} + \frac{23}{2} H_{2,0} - \frac{497}{2} \zeta_2 + \frac{29}{6} H_{1,$$

8.2.13 Intuitive picture

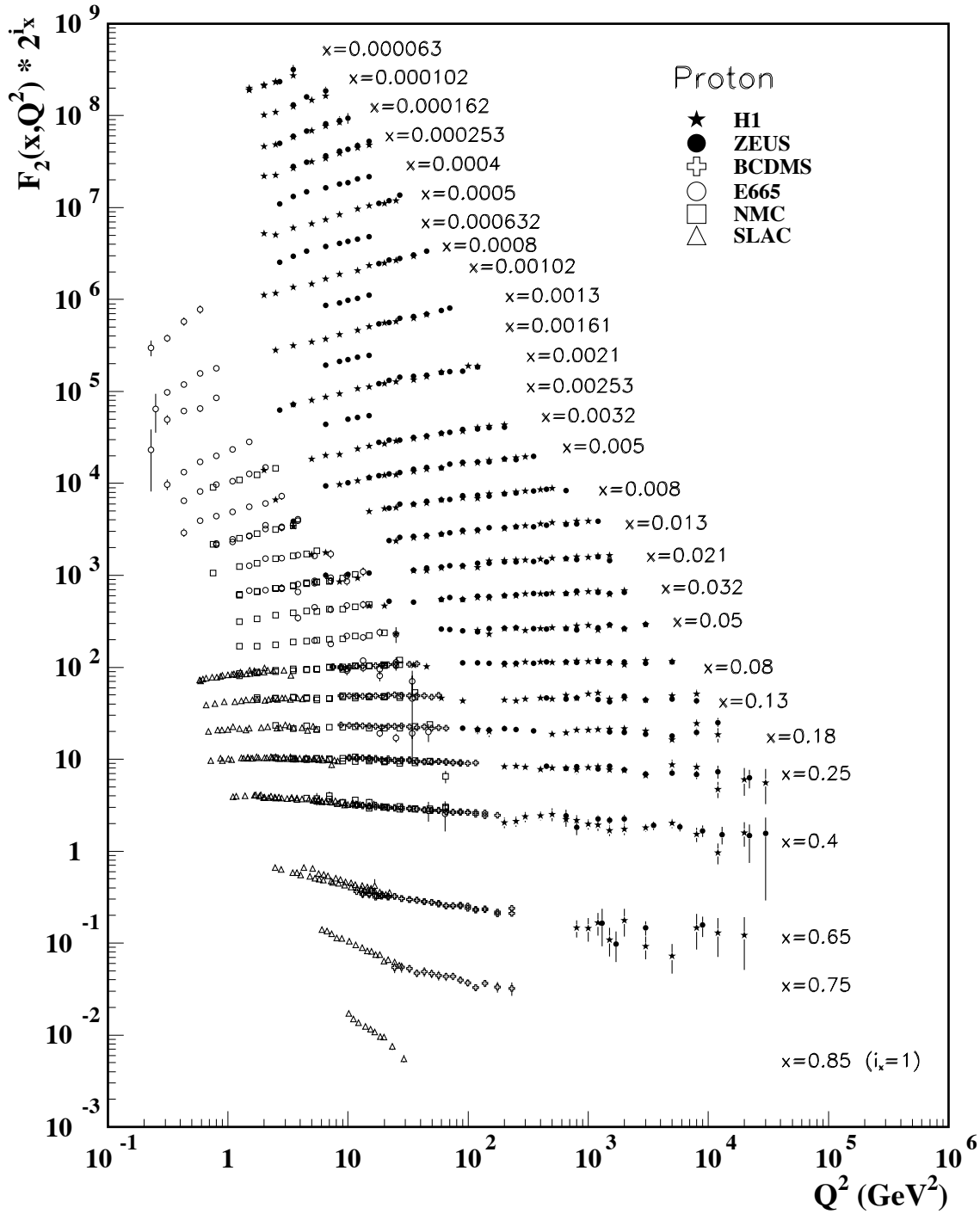


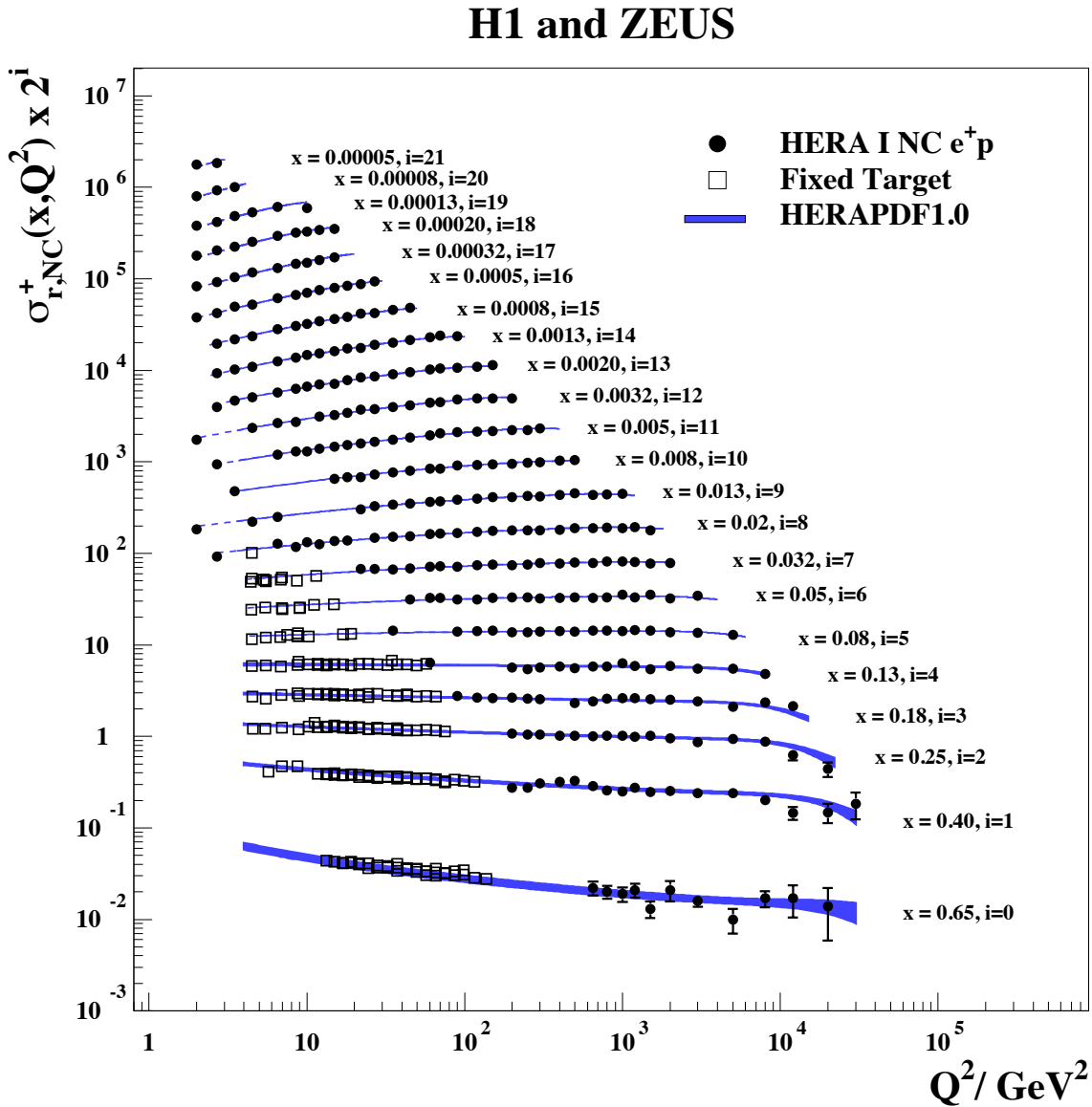
- The gross features of the evolution can be easily understood as follows. In the left plot above we indicate by the blob the resolution $1/Q$ of a photon with virtuality Q^2 . Increasing Q^2 will resolve a quark into a quark-gluon pair of lower momentum (right plot). Thus when Q^2 increases, more and more quarks are seen that have split into low momentum quarks. As a consequence, the quark distribution will shift to lower values of x with increasing Q^2 . This results in the characteristic scale breaking pattern of F_2 , when plotted versus Q^2 for several values of x .



8.2.14 Scale breaking pattern of the F_2 structure function

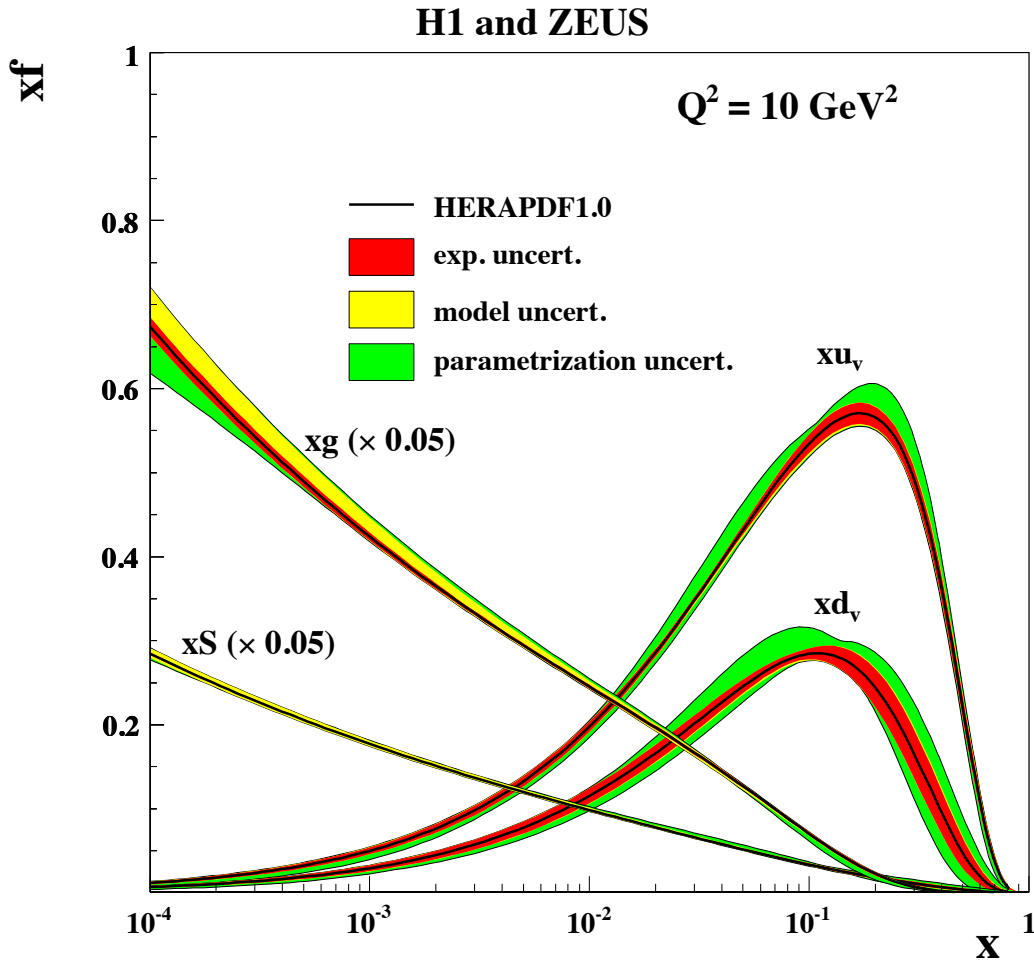
As expected!



8.2.15 Comparison of the F_2 data with the QCD prediction

- This plot shows a recent QCD analysis (up to third order) of HERA F_2 structure function data. In such an analysis the quark and the gluon distributions are parameterised at an input scale of about 2 GeV^2 and evolved over the whole Q^2 range. The parameters of the input distributions are then obtained from a least squares fit. There is an impressive agreement between data and theory.

8.2.16 The pdf set from the HERA QCD analysis



- Parton distributions obtained from the HERA QCD analysis. The sea ($xS = 2x\bar{q}(x)$) and the gluon are divided by a factor of 20. The parton distributions are parameterised at an input scale of $\mu_0^2 = 1.9 \text{ GeV}^2$ and evolved to 10 GeV^2 for this plot. The bands indicate various sources of uncertainty.
- In DIS the electrons only scatter off the charged quarks in the proton and not off the gluons. However, we still have *indirect* access to the gluon distribution via the coupled singlet/gluon evolution.

8.2.17 Scale dependence

- At this point we have introduced *three* different scales:

1. The factorization scale μ_F^2 where we have separated the short and long distance physics, and on which the pdfs evolve.
 2. The renormalisation scale μ_R^2 (called Q^2 in Section 6) on which the strong coupling constant α_s evolves.
 3. The hard scattering scale Q^2 which, in DIS, is the square of the 4-momentum transfer from the electron to the proton.
- Exposing the different scales, we write the (non-singlet) evolution equation, and the leading order expression for F_2 as

$$\frac{\partial q_{\text{ns}}(x, \mu_F^2)}{\partial \ln \mu_F^2} = \frac{\alpha_s(\mu_R^2)}{2\pi} \int_x^1 \frac{dy}{y} P_{\text{qq}}\left(\frac{x}{y}\right) q_{\text{ns}}(y, \mu_F^2)$$

$$F_2(x, Q^2) = \sum_{i=1}^{n_f} e_i^2 x [q_i(x, \mu_F^2) + \bar{q}_i(x, \mu_F^2)] + \mathcal{O}(\alpha_s)$$

- Usually one sets $\mu_R^2 = \mu_F^2 = Q^2$. The sensitivity to this choice is then quantified by varying the scales in the range, typically,

$$\frac{1}{4}\mu_F^2 \leq \mu_R^2 \leq 4\mu_F^2 \quad \text{and} \quad \frac{1}{4}Q^2 \leq \mu_F^2 \leq 4Q^2$$

- But note, however, that $F_2(x, Q^2)$ above depends only on μ_F^2 which, for a given Q^2 , is arbitrary. It follows that the leading order perturbative stability is poor, and that LO perturbative QCD has little predictive power. This defect is remedied when higher order terms are included that are functions of both Q^2 and μ_F^2 .
- Fortunately, the scale dependence rapidly decreases when higher order corrections are included, and this is of course the motivation behind that huge effort, at Nikhef, to calculate the splitting functions and the F_2 correction terms up to NNLO.

Chapter 9

Asymptotic freedom

In QED, a charged particle like the electron is surrounded by a cloud of virtual photons and e^+e^- pairs continuously popping in and out of existence. Because of the attraction of opposite charges, the virtual positrons tend to be closer to the electron and screen the electron charge, as is indicated in fig. 9.1. This is analogous to the polarisation of a dielectric medium in the presence of a charge and is called **vacuum polarisation**.

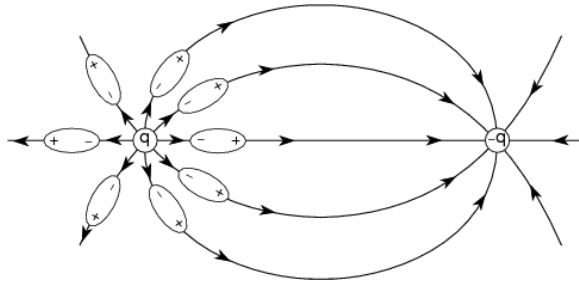


Fig. 9.1: The photon vacuum polarisation (left) generates a charge screening effect, making α smaller at larger distances.

This gives rise to the notion of an effective charge $e(r)$ that becomes smaller with larger distance. One says that the β -function is positive in QED:

$$\beta(r) \equiv -\frac{de(r)}{d\ln r}$$

Likewise, the QCD vacuum consists of virtual $q\bar{q}$ pairs, and if this would be all, the charge screening mechanism would be the same as in QED, with a positive β -function. However, due to the gluon self coupling, the vacuum will also be filled with virtual gluon pairs as is indicated in fig. 9.2. Because the gluon cloud carries colour charge, it turns out that the effective charge becomes larger with larger distance. Hence, the *beta*-function is negative. This effect is called antiscreening.¹ It turns out that the negative contribution wins over the positive contribution, so that the QCD beta function is negative, and the effective strong coupling becomes small at short distances.

¹ Antiscreening follows from the calculation of vacuum polarisation in QCD, which is non-trivial and beyond the scope of these lectures; unfortunately it is not so easy to intuitively understand the antiscreening effect.

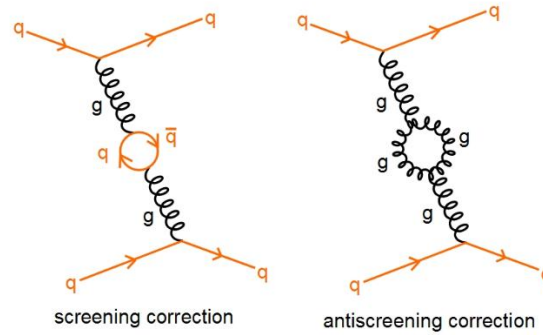


Fig. 9.2: The photon vacuum polarisation (left) generates a charge screening effect, making α smaller at larger distances.

Charge screening in QED (screening) and QCD (antiscreening) leads to the concept of a running coupling. In QED the coupling becomes large at (very) short distance but its effect is small. In QCD, the antiscreening effect causes the strong coupling to become small at short distance (large momentum transfer). This causes the quarks inside hadrons to behave more or less as free particles, when probed at large enough energies. This property of the strong interaction is called asymptotic freedom. Asymptotic freedom allows us to use perturbation theory, and by this arrive at quantitative predictions for hard scattering cross sections in hadronic interactions. On the other hand, at increasing distance the coupling becomes so strong that it is impossible to isolate a quark from a hadron (it becomes cheaper to create a quark-antiquark pair). This mechanism is called confinement. Confinement is verified in Lattice QCD calculations but, since it is non-perturbative, not mathematically proven from first principles.²

The discovery of asymptotic freedom (1973) was a major breakthrough for QCD as the theory of the strong interaction, and was awarded the Nobel prize in 2004 to Gross, Politzer and Wilczek.³ To get a more quantitative insight into asymptotic freedom, we will now first discuss the higher order corrections and the running coupling in QED.

9.1 Higher order corrections on $e - \mu$ scattering

Let us first consider the process $e^- + \mu^- \rightarrow e^- + \mu^-$. The Feynman diagram for this process can be seen in the left plot of fig. 9.3, which actually constitutes the lower order diagram. The matrix element was calculated in Section 4.2.3 and in particular in Eq. 4.2.1 (repeated below for our convenience).

$$M_{if} = \frac{-g_e^2}{q^2} \left[\bar{u}(\vec{P}_3) \gamma^\mu u(\vec{P}_1) \bar{u}(\vec{P}_4) \gamma_\mu u(\vec{P}_2) \right]$$

² A mathematical proof will gain you a \$1M millennium prize from the Clay Mathematics Institute.

³ The Nobel lecture of Frank Wilczek can be downloaded from <http://www.nobelprize.org> and makes highly recommended reading, both as an exposé of the basic ideas, and as a record of the hard struggle.

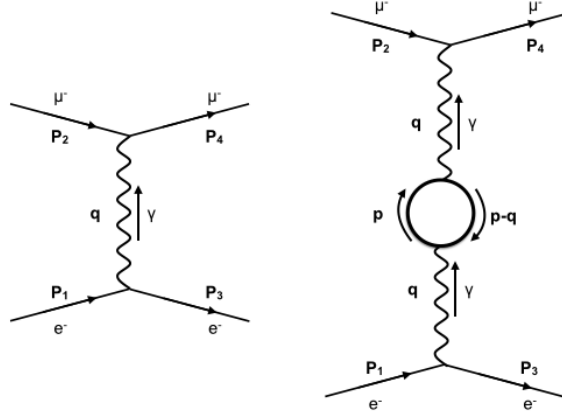


Fig. 9.3: The one loop correction to the Feynman diagram describing the scattering of an electron off a charge.

This leads to the relevant cross-section whose accuracy is good up to $O(\alpha^2)$ and is therefore an approximate perturbative result. To improve further the accuracy though, one needs to include higher order diagrams, an example of which is given in the right plot of fig. 9.3. In this diagram, it is seen that the virtual photon spends some time as a virtual e^+e^- pair. Let us now try to evaluate the matrix element for this process, which is quite similar to the one for the lower order diagram indicated above, with the only part that changes being the one that is related to the loop.

$$\begin{aligned}
 M_{if} = & -(-1)^1 g_e^2 [\bar{u}(\vec{P}_3) \gamma^\mu u(\vec{P}_1)] \left(-i \frac{g_{\mu\mu'}}{q^2} \right) \times \\
 & \int \frac{d^4 p}{(2\pi)^4} \left[(i g_e \gamma^{\mu'})_{\kappa\lambda} \frac{i(\not{p} + m)_{\lambda\rho}}{p^2 - m^2} (i g_e \gamma^{\nu'})_{\rho\tau} \frac{i(\not{p} - \not{q} + m)_{\tau\kappa}}{(p - q)^2 - m^2} \times \right. \\
 & \left. \left(-i \frac{g_{\nu\nu'}}{q^2} \right) [\bar{u}(\vec{P}_4) \gamma^\nu u(\vec{P}_2)] \right]
 \end{aligned}$$

These higher order Feynman diagrams involve, among other things, a factor of $(-1)^n$, where n is the number of fermion loops. In addition, it contains the integral over $d^4 p$ which is attributed to the existence of this higher order correction. At the loop, the four-momentum p is unrestricted and can take any value (i.e. its magnitude can take any value from 0 to infinity), although at the vertices the four-momenta are conserved. Since p is not observed, we need to integrate it out.

This addition can be considered as a modification of the initial, lowest order, propagator:

$$-i \frac{g_{\mu\nu}}{q^2} \rightarrow -i \frac{g_{\mu\nu}}{q^2} + \left(-i \frac{g_{\mu\mu'}}{q^2} \right) I^{\mu' \nu'} \left(-i \frac{g_{\nu\nu'}}{q^2} \right) =$$

$$-i\frac{g_{\mu\nu}}{q^2} + \frac{(-i)}{q^2}I_{\mu\nu}\frac{(-i)}{q^2} = -i\frac{g_{\mu\nu}}{q^2} + (-i)^2\frac{I_{\mu\nu}}{q^4}$$

where

$$I_{\mu\nu} = (-1)^1 \int \frac{d^4p}{(2\pi)^4} \text{Tr} \left[(ig_e\gamma_\mu) \frac{i(\not{p} + m)}{p^2 - m^2} (ig_e\gamma_\nu) \frac{i(\not{p} - \not{q} + m)}{(p - q)^2 - m^2} \right]$$

The previous formula indicates that $I_{\mu\nu}$ is a function of q^2 . In fact the integral contains terms of the form $\int |p|^3 d|p|/|p|^2$. These terms go to infinity for $p \rightarrow \infty$ and thus the correction diverges.

Because, after integration, the tensor $I_{\mu\nu}$ only depends on q_μ it must be some linear combination of $g_{\mu\nu}$ and $q_\mu q_\nu$, since these are the only tensors at our disposal. We can thus parameterise $I_{\mu\nu}$ as,

$$I_{\mu\nu} = -ig_{\mu\nu}q^2 I(q^2) + q_\mu q_\nu J(q^2),$$

where $I(q^2)$ and $J(q^2)$ are some functions of q^2 . It can be shown that the term $q_\mu q_\nu J(q^2)$ does not contribute to the matrix element M_{if} . Thus only the first term needs to be considered, and the function $I(q^2)$ is found to be, after a lengthy calculation,

$$I(q^2) = \frac{g_e^2}{12\pi^2} \left\{ \int_{m_e^2}^{\infty} \frac{dz}{z} - 6 \int_0^1 dz z(1-z) \ln \left[1 - \frac{q^2}{m_e^2} z(1-z) \right] \right\}.$$

Indeed, the first integral is logarithmically divergent, while all non-divergent contributions are collected in the second integral.

9.1.1 Renormalisation

Because $q^2 < 0$ we define $Q^2 \equiv -q^2$ and write:

$$I(q^2) = \frac{g_e^2}{12\pi^2} \left[\int_{m_e^2}^{\infty} \frac{dz}{z} - f\left(\frac{Q^2}{m_e^2}\right) \right]$$

$$f\left(\frac{Q^2}{m_e^2}\right) \equiv 6 \int_0^1 dz z(1-z) \ln \left[1 + \frac{Q^2}{m_e^2} z(1-z) \right]$$

We now impose a cutoff M so that first integral becomes finite

$$\int_{m_e^2}^{\infty} \frac{dz}{z} \rightarrow \int_{m_e^2}^{M^2} \frac{dz}{z} = \ln \left(\frac{M^2}{m_e^2} \right)$$

so that we obtain

$$I(q^2) = \frac{g_e^2}{12\pi^2} \left\{ \ln \left(\frac{M^2}{m_e^2} \right) - f \left(\frac{Q^2}{m_e^2} \right) \right\}.$$

The modification of the propagator can now be written as:

$$\frac{g_{\mu\nu}}{q^2} \rightarrow \frac{g_{\mu\nu}}{q^2} - \frac{iI_{\mu\nu}}{q^4} = \frac{g_{\mu\nu}}{q^2} [1 - I(q^2)]$$

Because the propagator is always accompanied by the factor g_e^2 , its modification can be interpreted as a loop correction to the ‘bare’ electron charge g_e :

$$g_e^2 \rightarrow g_e^2 [1 - I(q^2)] = g_e^2 \left\{ 1 - \frac{g_e^2}{12\pi^2} \left[\ln \left(\frac{M^2}{m_e^2} \right) - f \left(\frac{Q^2}{m_e^2} \right) \right] \right\}$$

9.1.2 The running coupling constant of QED

The Q^2 evolution of the bare coupling constant is thus given by

$$g_e^2 \rightarrow g_e^2 \left\{ 1 - \frac{g_e^2}{12\pi^2} \left[\ln \left(\frac{M^2}{m_e^2} \right) - f \left(\frac{Q^2}{m_e^2} \right) \right] \right\}$$

The first term is called the renormalised coupling constant

$$g_0^2 = g_e^2 \left[1 - \frac{g_e^2}{12\pi^2} \ln \left(\frac{M^2}{m_e^2} \right) \right]$$

so that we may write

$$g_e^2 \rightarrow g_0^2 + \frac{g_e^4}{12\pi^2} f \left(\frac{Q^2}{m_e^2} \right) = g_0^2 \left\{ 1 + \frac{1}{12\pi^2} \frac{g_e^4}{g_0^2} f \left(\frac{Q^2}{m_e^2} \right) \right\}$$

Up to terms $O(g_e^4)$ we may set $g_e^4 = g_0^4$ inside the braces, so that

$$g_e^2 \rightarrow g_0^2 \left\{ 1 + \frac{g_0^2}{12\pi^2} f\left(\frac{Q^2}{m_e^2}\right) + \mathcal{O}(g_0^4) \right\} \equiv g_R^2(Q^2)$$

Here $g_R^2(Q^2)$ is called the **running coupling constant**. Because $f(0) = 0$ we can set $g_0^2 = g_R^2(0)$ and thus:

$$g_R^2(Q^2) = g_R^2(0) \left\{ 1 + \frac{g_R^2(0)}{12\pi^2} f\left(\frac{Q^2}{m_e^2}\right) + \mathcal{O}(g_R^4) \right\}$$

The cutoff M has now disappeared from view since it is absorbed in $g_R^2(0)$ which becomes infinitely large when we let $M \rightarrow \infty$. The mathematical technique to isolate the singularities in a perturbative calculation is called regularisation, cut-off regularisation in our case.

In terms of $\alpha = g_e^2/4\pi$, the running coupling becomes

$$\alpha(Q^2) = \alpha(0) \left\{ 1 + \frac{\alpha(0)}{3\pi} f\left(\frac{Q^2}{m_e^2}\right) + \mathcal{O}(\alpha^2) \right\}$$

The next step is to admit that our theory cannot describe physics at asymptotically small distances so that we must replace the singular part of the calculation by measurement. This is called renormalisation. In fact 't Hooft and Veltman showed that this can be done consistently to all orders, without spoiling gauge invariance: they proved in general that gauge theories are renormalisable. They received for this work the Nobel prize in 1999. In QED it means that $\alpha(0)$ is replaced by the fine structure constant $\alpha = 1/137$, as measured at large distances of the order of the nuclear scale. There remains a finite correction term $f(Q^2)$ which causes the coupling to run with Q^2 . This is a consequence of vacuum polarisation, as we have already discussed before. It turns out that the effect of the running QED coupling constant is really small and can safely be neglected at atomic or nuclear scales. Even at large momentum transfers of $Q^2 \sim 1000 \text{ GeV}^2$ at the HERA collider, the correction to α is only about 1–2%.

Figure 9.4-a presents the vacuum polarisation graph discussed before. Apart from this graph there are three more divergent graphs to consider also shown in the same figure. The vertex correction (b) modifies the electron magnetic moment while the graphs (c) renormalise the electron mass. The three graphs (b) and (c) also contribute to the renormalisation of the electron charge. However, it turns out that these contributions cancel each other so that our previous calculation, based on diagram (a) alone, remains valid. This cancellation is called a Ward identity and is quite fortunate: without it, the graphs (c) would cause the coupling constant to be dependent on the lepton mass, and we would have different renormalisation for the electron and the muon electric charge.

For $Q^2 \gg m_e^2$ the one-loop corrected coupling constant is given by

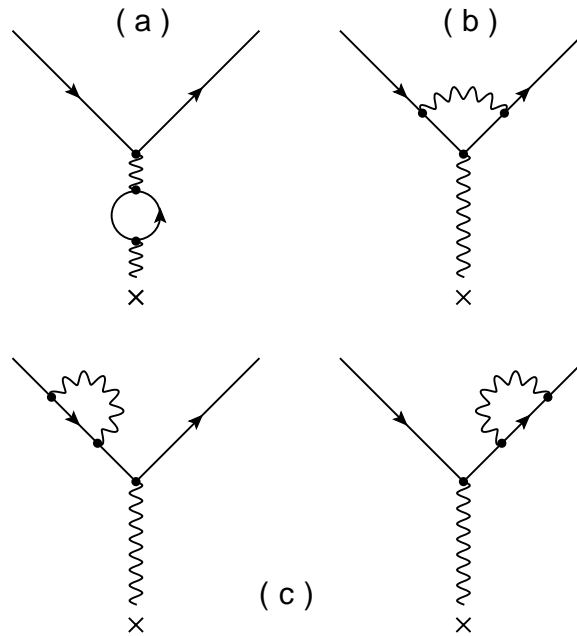


Fig. 9.4: A complete set of $O(\alpha^2)$ Feynman graphs.

$$\alpha(Q^2) = \alpha(0) \left\{ 1 + \frac{\alpha(0)}{3\pi} \ln \left(\frac{Q^2}{m_e^2} \right) + O(\alpha^2) \right\}.$$

Because of the Ward identities, only propagator loops will contribute at higher orders. A set of them is presented in fig. 9.5:

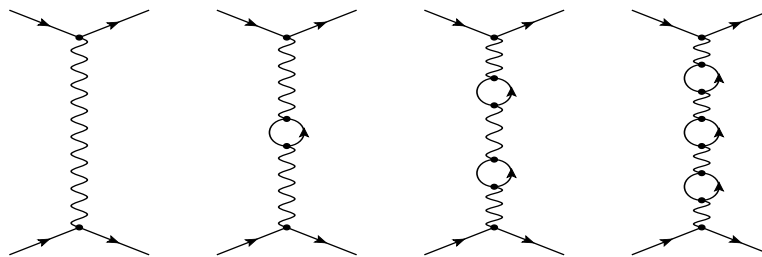


Fig. 9.5: A set of higher order correction diagrams.

This induces a series

$$1 + X + X^2 + X^3 + \dots = \frac{1}{1 - X}$$

and indeed, from a full calculation one gets⁴

$$\alpha(Q^2) = \frac{\alpha(0)}{1 - [\alpha(0)/3\pi] \ln(Q^2/m_e^2)} \quad \text{for } m_e^2 \ll Q^2 < Q_{\max}^2$$

⁴ This is an example of resummation where terms in a perturbative calculation are arranged in a geometric series which is then summed up to all orders.

The expression blows up when $\ln(Q^2/m_e^2) = 3\pi/\alpha(0)$, which occurs at an astronomical scale of $Q_{\max}^2 = 10^{280} \text{ MeV}^2$. Although the loops are summed to all orders, there are still more complicated propagator diagrams (like multi-photon exchange between loops), which are ignored. The result given above is thus not exact, and is known as the leading log approximation.

We have seen that the running QED coupling constant decreases with decreasing Q^2 (increasing distance) to the asymptotic value $\alpha(0) = 1/137$ at $Q^2 = 0$. However, we could also have specified an input value $\alpha(\mu^2)$ at some arbitrary reference scale μ^2 . We will now derive the formula for the coupling constant running from $Q^2 = \mu^2$, instead of from $Q^2 = 0$. This is useful because, as we will see, the reference scale $Q^2 = 0$ cannot be used in QCD.

From

$$\alpha(Q^2) = \frac{\alpha(0)}{1 - [\alpha(0)/3\pi] \ln(Q^2/m_e^2)}$$

we have

$$\frac{1}{\alpha(Q^2)} = \frac{1}{\alpha_0} - \frac{1}{3\pi} \ln\left(\frac{Q^2}{m_e^2}\right)$$

and

$$\frac{1}{\alpha(\mu^2)} = \frac{1}{\alpha_0} - \frac{1}{3\pi} \ln\left(\frac{\mu^2}{m_e^2}\right).$$

A simple subtraction gives

$$\frac{1}{\alpha(Q^2)} - \frac{1}{\alpha(\mu^2)} = -\frac{1}{3\pi} \left[\ln\left(\frac{Q^2}{m_e^2}\right) - \ln\left(\frac{\mu^2}{m_e^2}\right) \right] = -\frac{1}{3\pi} \ln\left(\frac{Q^2}{\mu^2}\right)$$

and thus

$$\alpha(Q^2) = \frac{\alpha(\mu^2)}{1 - [\alpha(\mu^2)/3\pi] \ln(Q^2/\mu^2)} \quad \text{for } m_e^2 \ll Q^2 < Q_{\max}^2$$

The reference scale μ^2 where we wish to specify our input value of α is called the renormalisation scale. Obviously, the value of $\alpha(Q^2)$ does not depend on what renormalisation scale μ^2 we chose.

The running coupling can now be written as:

$$\frac{1}{\alpha(Q^2)} = \frac{1}{\alpha(\mu^2)} - \frac{1}{3\pi} \ln\left(\frac{Q^2}{\mu^2}\right)$$

Differentiation to $t = \ln Q^2$ gives

$$\frac{d}{dt} \left(\frac{1}{\alpha} \right) = -\frac{1}{\alpha^2} \frac{d\alpha}{dt} = -\frac{1}{3\pi} \quad \text{or} \quad \frac{d\alpha}{dt} \equiv \beta(\alpha) = \frac{1}{3\pi} \alpha^2$$

In the above, we have introduced the so-called β -function:

$$\frac{d\alpha(Q^2)}{d\ln(Q^2)} \equiv \beta(\alpha) = -(\beta_0 \alpha^2 + \beta_1 \alpha^3 + \beta_2 \alpha^4 + \dots)$$

Here we have written this function as a series expansion in powers of the coupling constant,⁵ where the first term corresponds to the leading log approximation. It is an important task of perturbative QED and QCD to calculate the coefficients in this expansion.⁶ The QED one-loop beta function is $\beta = \alpha^2/3\pi > 0$. This means that the coupling constant increases with increasing Q^2 (decreasing distance). For QCD it turns out that $\beta < 0$, as we will see. The one-loop QED coupling constant can now be written as:

$$\alpha(Q^2) = \frac{\alpha(\mu^2)}{1 + \beta_0 \alpha(\mu^2) \ln(Q^2/\mu^2)} \quad \text{with} \quad \beta_0 = -\frac{1}{3\pi}$$

9.2 The running coupling constant of QCD

Let's now turn to the strong coupling constant α_s . Note that α_s is large, compared to the electromagnetic coupling constant $\alpha = 1/137$: strong interactions are indeed strong. The running is also strong, compared to a few percent effect at large Q^2 in QED. The running of α_s is beautifully confirmed by experiment. For $Q^2 \sim 1$, $\alpha_s \sim 1$ and perturbative QCD breaks down. Usually $Q^2 \sim 5\text{--}10 \text{ GeV}^2$ is considered to be reasonable lower bound for perturbation theory to apply.

$$\alpha_s(Q^2) = \frac{\alpha_s(\mu^2)}{1 + \beta_0 \alpha_s(\mu^2) \ln(Q^2/\mu^2)} \quad \text{with} \quad \beta_0 = \frac{11N_c - 2n_f}{12\pi}$$

Because $\beta_0 > 0$ we find that $\alpha_s \rightarrow 0$ for $Q^2 \rightarrow \infty$. This vanishing coupling is called asymptotic freedom and is responsible for the fact that quarks behave like free particles

⁵ The minus sign in front of the series expansion is a matter of convention.

⁶ This is an explosive business: for QCD the 4-loop coefficient β_3 has been calculated (at Nikhef!) by evaluating 50.000 Feynman diagrams, using sophisticated symbolic algebra programs (also developed at Nikhef).

at short distances (large momentum transfers) as is observed in deep inelastic scattering experiments. The expression for the running coupling constant can be simplified when we define the QCD scale parameter Λ as follows:

$$\frac{1}{\alpha_s(Q^2)} = \frac{1}{\alpha_s(\mu^2)} + \beta_0 \ln\left(\frac{Q^2}{\mu^2}\right) \equiv \beta_0 \ln\left(\frac{Q^2}{\Lambda^2}\right)$$

The parameter Λ is thus equal to the scale where the first term on the right-hand side vanishes, that is, the scale where $\alpha_s(\mu^2)$ becomes infinite. Now we may write

$$\alpha_s(Q^2) = \frac{1}{\beta_0 \ln(Q^2/\Lambda^2)}$$

Experimentally, the value of Λ is found to be about 300 MeV, but the scale parameter is nowadays out of fashion because it cannot be defined unambiguously beyond 1-loop order. Instead, it is now common practise to not quote a value for Λ , but a value for α_s at the mass of the Z. This is unambiguous at all orders. At Q^2 values close to Λ , the coupling constant becomes large and perturbative QCD breaks down.

9.2.1 Numerical results of α_s

Beside the quark masses, the only free parameter in the QCD Lagrangian is the strong coupling constant α_s . The coupling constant in itself is not a physical observable, but rather a quantity defined in the context of perturbation theory, which enters predictions for experimentally measurable observables, such as R in Eq. 6.1.6.

Many experimental observables are used to determine α_s . The simplest observables in QCD are those that do not involve initial-state hadrons and that are fully inclusive with respect to details of the final state. One example is the total cross section for e^+e^- hadrons at center-of-mass energy Q , for which one can write:

$$R = \frac{\sigma(e^- + e^+ \rightarrow \text{hadrons})}{\sigma(e^- + e^+ \rightarrow \mu^- + \mu^+)} = R_{EW}(Q) \left[1 + \delta_{QCD}(Q) \right] \quad (9.2.1)$$

where $R_{EW}(Q)$ is the purely electroweak prediction for the ratio and $\delta_{QCD}(Q)$ is the correction due to QCD effects. To keep the discussion simple, we can restrict our attention to energies $Q \ll M_Z$, where the process is dominated by photon exchange ($R_{EW} = 3 \sum_q e_q^2$, neglecting finite-quark-mass corrections, where the e_q are the electric charges of the quarks):

$$\delta_{QCD}(Q) = \sum_{n=1}^{\infty} c_n \left[\frac{\alpha_s(Q^2)}{\pi} \right]^n + \mathcal{O}\left(\frac{\Lambda^4}{Q^4}\right)$$

Considerations in such determinations include:

- The observable's sensitivity to α_s as compared to the experimental precision. For example, for the e^+e^- cross section to hadrons, QCD effects are only a small correction, since the perturbative series starts at order α_s^0 ; 3-jet production or event shapes in e^+e^- annihilations are directly sensitive to α_s since they start at order α_s ; the hadronic decay width of heavy quarkonia, $\Gamma(\Upsilon \rightarrow \text{hadrons})$, is very sensitive to α_s since its leading order term is $\approx \alpha_s^3$.
- The accuracy of the perturbative prediction, or equivalently of the relation between α_s and the value of the observable. The minimal requirement is generally considered to be an NLO prediction. Some observables are predicted to NNLO (many inclusive observables, 3-jet rates and event shapes in e^+e^- collisions) or even N³LO (e^+e^- hadronic cross section and Υ branching fraction to hadrons). In certain cases, fixed-order predictions are supplemented with resummation.
- The size of uncontrolled non-perturbative effects. Sufficiently inclusive quantities, like the e^+e^- cross section to hadrons, have small non-perturbative uncertainties $\approx \Lambda/Q^4$.

9.2.1.1 Results from DIS

New measurements of α_s from inclusive jet cross sections in γp interactions at HERA are available from the ZEUS collaboration. Jet cross sections and values of α_s are presented as a function of the jet transverse energy, E_T^{jet} , for jets with $E_T^{jet} > 17$ GeV. The resulting values of $\alpha_s(E_T^{jet})$, based on NLO QCD calculations, are in good agreement with the running of α_s , as expected by QCD, and average to:

$$\begin{aligned} \alpha_s(M_{Z^0}) &= 0.1224 \pm 0.0001 \text{ (stat.)} \\ &\quad +0.0022 \text{ (exp.)} \\ &\quad -0.0019 \text{ (theo.),} \\ &\quad +0.0054 \text{ (theo.),} \\ &\quad -0.0042 \end{aligned} \tag{9.2.2}$$

if evolved to the energy scale of M_{Z^0} using the QCD β function in two-loop approximation. Averaging all measurements of α_s from jet production at HERA results in:

$$\begin{aligned} \alpha_s(M_{Z^0}) &= 0.120 \pm 0.002 \text{ (exp.)} \\ &\quad \pm 0.004 \text{ (theo.),} \end{aligned} \tag{9.2.3}$$

A new global analysis using all available precision data of deep inelastic and related hard scattering processes includes recent measurements of structure functions from HERA and of the inclusive jet cross sections at the Tevatron. After analysis of experimental and theoretical uncertainties the authors obtain

$$\alpha_s(M_{Z^0}) = 0.1165 \pm 0.002 \text{ (exp.)} \\ \pm 0.003 \text{ (theo.)} , \quad (9.2.4)$$

in NLO QCD. Using NNLO QCD calculations wherever available, the same fit gives:

$$\alpha_s(M_{Z^0}) = 0.1153 \pm 0.002 \text{ (exp.)} \\ \pm 0.003 \text{ (theo.)} . \quad (9.2.5)$$

The latter result, however, does not relate to complete NNLO since predictions of jet production cross sections and parts of the DIS structure functions are only available in NLO so far.

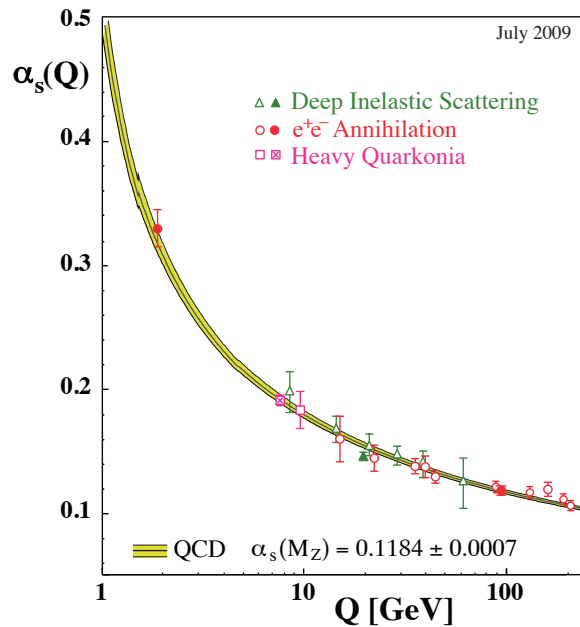


Fig. 9.6: The Q dependence of the strong coupling constant α_s .

The wealth of available results provides a rather precise and stable world average value of $\alpha_s(M_Z)$, as well as a clear signature and proof of the energy dependence of α_s , in full agreement with the QCD prediction of asymptotic freedom. This is demonstrated in fig. 9.6, where results of $\alpha_s(Q)$ obtained at discrete energy scales Q , now also including those based just on NLO QCD, are summarized. Thanks to the results from the Tevatron

and from the LHC, the energy scales at which α_s is determined now extend to several hundred GeV up to 1 TeV.

Chapter 10

Heavy-ion physics

One of the most remarkable predictions of the Standard Model of particle physics is that, at sufficiently high densities and temperatures, the protons and neutrons of ordinary matter should melt into a plasma where the quark and gluon degrees of freedom are not anymore confined, but can extend over large distances. This hot and dense primordial state of matter is called a Quark-Gluon plasma (QGP) and should have existed in the expanding universe up to a few microseconds after the Big-Bang, when the phase transition to hadronic matter of confined quarks and gluons took place. Temperatures and energy densities similar to the ones in the very early universe can be created in collisions of heavy ions at ultra-relativistic energies in particle accelerators. An integral part of the Standard Model is Quantum Chromo Dynamics (QCD), which is the theory that describes the physics of the strong interaction. According to QCD, the phase transition from deconfined QGP to hadronic matter should occur at a critical temperature of about 170 MeV, corresponding to a critical energy density ε of about 1 GeV/fm³. In ultra-relativistic heavy-ion collisions at the energies of the Large Hadron Collider (LHC) we attain values of $\varepsilon = 14$ GeV/fm³ that exceed by far the critical energy density. This makes the QCD phase transition the only one within reach of laboratory experiments, contrary to the electro-weak phase transition which is also predicted by the Standard Model, but at much higher temperatures and densities.

10.1 The Bag model

At very high-temperature such that the particles have energy much larger than their rest mass, we may describe them using relativistic kinematics and ignore their masses. Thus these energetic weakly interacting particles form a system that is, to an excellent approximation, a hot relativistic free gas. Since particles and antiparticles can be created and annihilated easily in such an environment, their densities are much higher than their differences. Therefore the chemical potential μ can be neglected. The number densities of the partons (species i) are then described by the quantum distribution functions

$$n_i = \int \frac{d^3 p_i}{(2\pi)^3} \frac{1}{e^{\beta E_i} \pm 1},$$

where $\beta = 1/k_B T$ and the $-$ sign is for bosons and the $+$ is for fermions. For relativistic particles, $p_i = E_i$. For $E_i \beta < 1$, the exponential factor is small and there is a large difference between fermions and bosons. For $E_i \beta \geq 1$ the ± 1 becomes increasingly unimportant, and the distributions become similar. Integrating over the phase space, one finds:

$$n_i = \zeta(3)/\pi^2 T^3 (\text{boson})$$

$$n_i = \frac{3}{4} \zeta(3)/\pi^2 T^3 (\text{fermion}),$$

where $\zeta(3) = 1.20206\dots$ is a Riemann zeta function. The T^3 dependence follows simply from dimensional analysis.

The energy density for a free gas can be computed from the same quantum distribution functions:

$$\varepsilon_i = \int \frac{d^3 p_i}{(2\pi)^3} \frac{1}{e^{\beta E_i} \pm 1} \Leftrightarrow$$

$$n_i = \frac{\pi^2}{30} T^4 (\text{boson}),$$

It is seen that the fermion energy density is 7/8 of that of boson. These expressions are valid for each spin/flavor/charge/color state of each particle. For a system of fermions and bosons, we need to include separate degeneracy factors for the various particles:

$$\varepsilon = \sum_i g_i \varepsilon_i = g \frac{\pi^2}{30} (k_B T)^4,$$

where $g = (g_b + 7g_f/8)$ with g_b and g_f the degeneracy factors for bosons and fermions, respectively. Each of these degeneracy factors counts the total number of degrees of freedom, summed over the spins, flavours, charge (particle-antiparticle) and colours of particles. When some species are thermally decoupled from others due to the absence of interactions (such as neutrinos at present epoch), they no longer contribute to the degeneracy factor. For example, at temperature above 100 GeV, all particles of the standard model are present. At lower temperatures, the W and Z bosons, top, bottom, and charm quarks freeze out and g decreases. Therefore g is generally a decreasing function of temperature. We can now calculate the contribution to the energy density

from the quark-gluon plasma as a relativistic free parton gas. For a gluon, there are 2 helicity states and 8 choices of colour so we have a total degeneracy of $g_b = 16$. For each quark flavour, there are 3 colours, 2 spin states, and 2 charge states (corresponding to quarks and antiquarks). At temperatures below $k_B T \approx 1$ GeV, there are 3 active flavours (up, down and strange) so we expect the fermion degeneracy to be a large number like $g_f \approx 36$ in this case. Thus we expect for the QGP:

$$\varepsilon_{QGP} \approx 47.5 \frac{\pi^2}{30} (k_B T)^4$$

With two quark flavours, the pre-factor is $g = 37$. The pressure of the free gas can be calculated just like the case of black-body radiation. For relativistic species:

$$p = \frac{1}{3} \varepsilon$$

which is the equation of state.

To calculate the entropy of the relativistic gas, we consider the thermodynamics relation, $dE = TdS - pdV$. At constant volume we would have just $dE = TdS$, or $d\varepsilon = Tds$ where ε and s are the energy and entropy per unit volume. Since $\varepsilon \approx \alpha T^4$, we can easily find that:

$$s = \frac{4}{3} \frac{\varepsilon}{T}$$

For an isolated system of relativistic particles, we expect the total entropy to be conserved.

Until this point we have been treating the quarks and gluons in the QGP as free particles without interactions. Of course, in a high-temperature QGP we expect QCD perturbative theory to be applicable due to asymptotic freedom. One important additional consequence is that chiral symmetry is now a good symmetry, and the chiral condensate must vanish in the plasma:

$$\langle QGP | \bar{\psi} \psi | QGP \rangle = 0$$

where strictly-speaking the QGP ?state? is actually the thermal average over the excited states of the QCD vacuum when the baryon number density is ignored. Another important feature of the QGP is colour deconfinement. In QCD perturbation theory, the quarks and gluons are free particles that can be described by plane waves. Asymptotic freedom will guarantee that high momentum transfer interactions are weak. Small momentum transfer scattering involves long distance interactions which are screened by the plasma (although this is only strictly true in the colour electric sector). As such, the charged quarks and gluons can move freely inside the plasma without being confined

to a local region. This remarkable property is radically different from the low energy limit of QCD where all charges are permanently confined to the interior of hadrons a scale about 1 fm. Consider a colour charge in midst of a colour-neutral plasma. The other particles in the plasma will act to screen it, and as a consequence the interaction between colour charges is damped exponentially. To calculate the screening length, one can start from a colour charge and calculate its induced colour fields. The result is a correlation function of gluon fields. This function can be calculated in perturbation theory at high-temperature, and the result for the screening mass is

$$m_D^2 = g^2 T^2$$

to leading order in the strong coupling expansion. The so-called Debye screening length is simply $1/m_D$ or $1/gT$, which is very short at high-temperature. When the colour charges are screened in a plasma, it has a finite energy and therefore in this sense, the colour charges are now liberated. Unfortunately, the magnetic interaction is only weakly screened; it has a screening mass of order $g^2 T$. Absence of the magnetic screening means that the magnetic sector of the QCD remains non-perturbative even at high-temperature. Fortunately, at high-temperature this non-perturbative part contributes to physical observables only at higher-order in QCD coupling, so the free gas behaviour is dominant. Another important feature of the plasma is the plasma frequency. In a QED plasma, light cannot propagate below the plasma frequency, $\omega_{pl} = (ne^2/m)^{1/2}$, but will be reflected from the surface, like in a silver-plated mirror. The physics of the QGP is similar: gluons cannot propagate as a free field in the plasma if its energy is too low. In fact, the gluons acquire an effective mass which is effectively the plasma frequency. Perturbative calculations confirms this behaviour, and to leading order in perturbation theory the plasma frequency is:

$$\omega_{pl} = \frac{1}{3} \sqrt{\frac{N_c + N_f}{2}} gT$$

where $N_c = 3$ is the number of colour and N_f is the number of fermion flavour.

The low (i.e. close to zero) temperature ground state of QCD is strikingly different from the high-temperature QGP: colour charges are confined to the interior of individual hadrons and chiral symmetry is broken spontaneously. Therefore, as the plasma cools in the universe, some rapid changes in thermodynamic observables must occur from the high-temperature QGP phase to the low-temperature confining and chiral-symmetry breaking phase, where the quarks and gluons combine to form colourless states of hadronic matter. It is possible to estimate the transition temperature by comparing the QGP gas pressure with that of hadronic gas. The lightest hadrons are pions, and for $T < 1$ GeV, we might expect a gas of relativistic pions. This is a system with only 3 degrees of freedom, $g = 3$, so the energy density and pressure of the system can be written as:

$$\rho_\pi = \frac{3\pi^2}{30} T^4$$

$$P_\pi = \frac{3\pi^2}{90} T^4$$

This, however, is not the full story. Pions are collective excitations of the non-perturbative QCD vacuum. This true ground state of the QCD vacuum has a lower-energy B than the perturbative QCD vacuum. Lorentz invariance requires that the energy-momentum density is of form $T^{\mu\nu} = Bg^{\mu\nu}$. Thus the non-perturbative QCD vacuum has a positive pressure as well. Therefore, the total pressure of the hadronic phase is:

$$P_{low} = B + \frac{3\pi^2}{90} T^4$$

On the other hand, we have seen before that the pressure of the QGP phase with 2 quark flavours is, $P_{QGP} = 37\pi^2 T^4/90$. Equating the two pressures, we find the transition temperature:

$$T_c = \left(\frac{45B}{17\pi^2} \right)^{1/4} \approx 180 \text{ MeV}$$

where we have used the MIT bag constant $B = 200 \text{ MeV}$ as determined by fits to the masses of physical hadrons.

10.2 Lattice QCD calculations

Quantum Chromodynamics (QCD) is the underlying theory of the strong force. Although its fundamental degrees of freedom (quarks and gluons) cannot be observed as free particles the QCD Lagrangian is well established. One of the key features of QCD is the self coupling of the gauge bosons (gluons) which cause the coupling constant to increase with decreasing momentum transfer. This running of the coupling constant gives rise to asymptotic freedom and confinement at large and small momentum transfers, respectively. At small momentum transfer non-perturbative corrections, which are notoriously hard to calculate, become important. For this reason two important non-perturbative properties of QCD, confinement and chiral symmetry breaking, are still poorly understood from first principles.

One of the fundamental questions in QCD phenomenology is what the properties of matter are at the extreme densities and temperatures where the quarks and gluons are in a deconfined state, the so-called Quark Gluon Plasma (QGP). Basic arguments allow us to estimate the energy density $\varepsilon \sim 1 \text{ GeV/fm}^3$ and temperature $T \sim 170 \text{ MeV}$ at

which the strong phase transition takes place. These values imply that the transition occurs in a regime where the coupling constant is large so that we can not rely anymore on perturbative QCD. Better understanding of the non-perturbative domain comes from lattice QCD, where the field equations are solved numerically on a discrete space-time grid. Lattice QCD provides quantitative information on the QCD phase transition and the Equation of State (EOS) of the deconfined state. At extreme temperatures (large momenta) we expect that the quarks and gluons are weakly interacting and that the QGP would behave as an ideal gas. For an ideal massless gas the Equation of State (EoS) is given by:

$$P = \frac{1}{3}\varepsilon, \quad \varepsilon = g \frac{\pi^2}{30} T^4, \quad (10.2.1)$$

where P is the pressure, ε the energy density, T the temperature and g is the effective number of degrees of freedom. Each bosonic degree of freedom contributes 1 unit to g , whereas each fermionic degree of freedom contributes $\frac{7}{8}$. The value of $g = 47.5$ for a three flavor QGP which is an order of magnitude larger than that of a pion gas where $g \sim 3$.

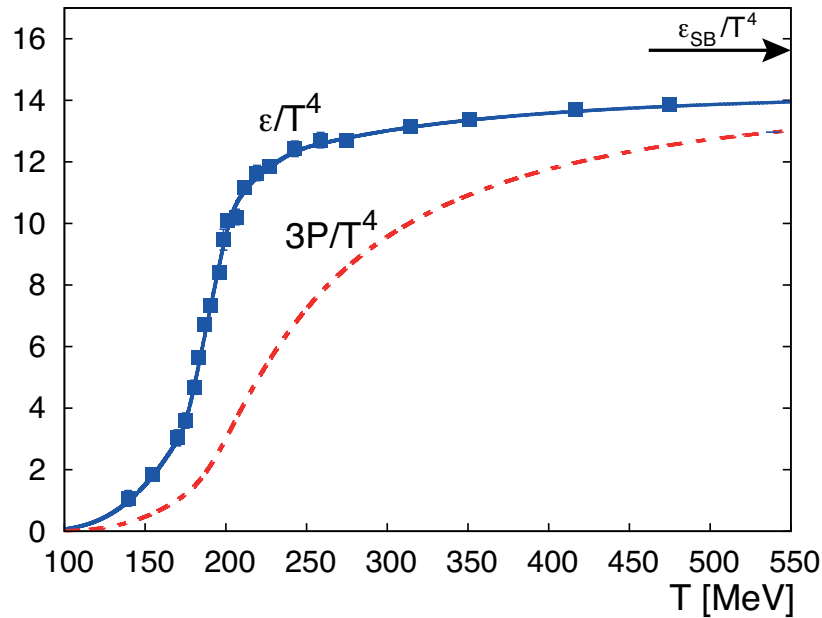


Fig. 10.1: Energy density ε/T^4 (full curve) and pressure $3P/T^4$ (dashed curve) as a function of temperature T from lattice calculations [?]. The arrow indicates the Stefan Boltzmann limit of the energy density.

Figure 10.1 shows the temperature dependence of the energy density as calculated from lattice QCD. It is seen that the energy density changes rapidly around $T \sim 190$ MeV, which is due to the rapid increase in the effective degrees of freedom (lattice calculations show that the transition is a crossover). Also shown in Fig. 10.1 is the pressure which changes slowly compared to the rapid increase of the energy density around

$T = 190$ MeV. It follows that the speed of sound, $c_s = \sqrt{\partial P / \partial \epsilon}$, is reduced during the strong phase transition. At large temperature the energy density reaches a significant fraction (~ 0.9) of the ideal massless gas limit (Stefan-Boltzmann limit).

Relativistic heavy-ion collisions are a unique tool to create and study hot QCD matter and its phase transition under controlled conditions. As in the early universe, the hot and dense system created in a heavy-ion collision will expand and cool down. During this evolution the system probes a range of energy densities and temperatures, and possibly different phases. Provided that the quarks and gluons undergo multiple interactions the system will thermalize and form the QGP which subsequently undergoes a collective expansion and eventually becomes so dilute that it hadronizes.

10.3 Probing the Quark-Gluon Plasma (QGP)

For composite hadrons, with finite spatial extension, concept of hadronic matter appears to lose its meaning at sufficiently high density. Once we have a system of mutually interpenetrating hadrons, each quark will find in its vicinity, at a distance less than the hadron radius, a number of quarks. The situation is shown schematically in fig. 10.2. At low density, a particular quark in a hadron knows in partner quarks. However, at high density, when the hadrons starts to interpenetrate each other, a particular quark will not be able to identify the quark which was its partner at lower density. Similar phenomena can happen at high temperature. As the temperature of a nuclear matter is increased, more and more low mass hadrons (mostly pions) will be created. The system again will be dense enough and hadrons will starts to interpenetrate. The system where, hadrons interpenetrate is best considered as a Quark matter, rather than made of hadrons. It is customary to call the quark matter as Quark-Gluon-Plasma (QGP). We define QGP as a thermalised, or near to thermalised state of quarks and gluons, where quarks and gluons are free to move over a nuclear volume rather than a nucleonic volume.

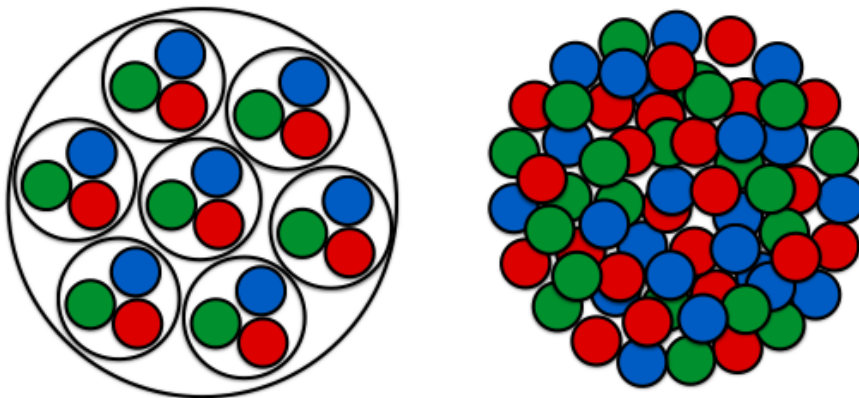


Fig. 10.2: Left panel shows a nucleus at normal density. The right panel shows the same at high density.

QGP is the deconfined state of strongly interacting matter. Since at low density or low temperature quarks are confined within the hadrons and at high density or at high temperature, quarks are deconfined, one can talk about a confinement-deconfinement phase transition. We will discuss it later, but it turns out that the confinement-deconfinement transition is not a phase transition in thermodynamic sense (in thermodynamic phase transition, free energy or its derivative have singularity at the transition point), rather it is a smooth cross-over, from confinement to deconfinement or vice-versa. The mechanism of deconfinement is provided by the screening of the colour charge. It is analogous to the Mott transition in atomic physics. In dense matter, the long range coulomb potential, which binds ions and electrons into electrically neutral atom, is partially screened due to presence of other charges, the potential become much more short range,

We believe that the QGP existed in the very early universe i.e. few μs after the Big Bang. Figure 10.3-left presents the different stages of the evolution of the universe, in the Big bang model. At the earliest time, temperatures are of the order of $T = 10^{19}$ GeV, it is the Planck scale temperature. At this stage, we believe that quantum gravity is important. Despite an enormous effort by e.g. string theorists, little is understood about this era. On the other hand, we have better understanding of the later stage of evolution, say, around temperature $T = 10^{16}$ GeV. This is what is usually referred to as the Grand unification scale. Strong and electroweak interactions are unified at this scale. The universe at this scale may also be supersymmetric. As the universe further expands and cools, strong and electroweak interactions are separated. At much lower temperature $T \approx 100$ GeV, electroweak symmetry breaking takes place. Baryon asymmetry may be produced here. Universe exists further on and for some time as QGP, the deconfined state of quarks and gluons.

Similar conditions can be achieved with ultra-relativistic heavy-ion collisions at the Relativistic Heavy Ion Collider (RHIC) and the LHC produce fireballs made of extraordinarily hot matter, at initial energy densities (at the time when the matter reaches approximate local thermal equilibrium) that exceed the energy density of atomic nuclei in their ground states by two to three orders of magnitude. Due to enormous pressure gradients between the fireball centre and the surrounding vacuum, these fireballs undergo explosive collective expansion, cooling down rapidly through several different states of matter, finally fragmenting into thousands of free-streaming hadrons whose energy and momentum distributions can be detected in the detectors set up around the collider rings. The evolution history of these “Little Bangs” has much similarity with the Big Bang that created our Universe as indicated in fig. 10.3-right. Both undergo a Hubble-like expansion, since the relative velocity between two matter elements increases roughly linearly with their relative distance, features a hierarchy of decoupling processes that are driven by the expansion dynamics. These processes start with the chemical decoupling of the finally observed particle abundances. In the Big Bang the chemical composition is frozen during the process of primordial nucleosynthesis at an age of about 3 minutes, while in the Little Bang this happens during hadro-synthesis at the quark-hadron transition at an age of about 20-30 yocto-seconds. This stage is

followed by the kinetic decoupling. In the Big Bang, the formation of neutral atoms by charge recombination at an age of about 380,000 yr makes the universe transparent to light and freezes the thermal Bose-Einstein energy distribution of the Cosmic Microwave Background radiation. When the Little Bang reaches an age of about 40-50 yocto-seconds, the final-stage hadron gas becomes so dilute that strong interactions between the hadrons cease and their energies and momenta are “frozen out”. Of course, the Big and Little Bangs are quite different in other aspects: Their expansion rates differ by about 18 orders of magnitude; the Little Bang’s expansion is 3-dimensional and driven by pressure gradients, not 4-dimensional and controlled by gravity; Little Bangs evolve on time scales of yocto-seconds, not billions of years; distances are measured in femto-meters rather than light years.

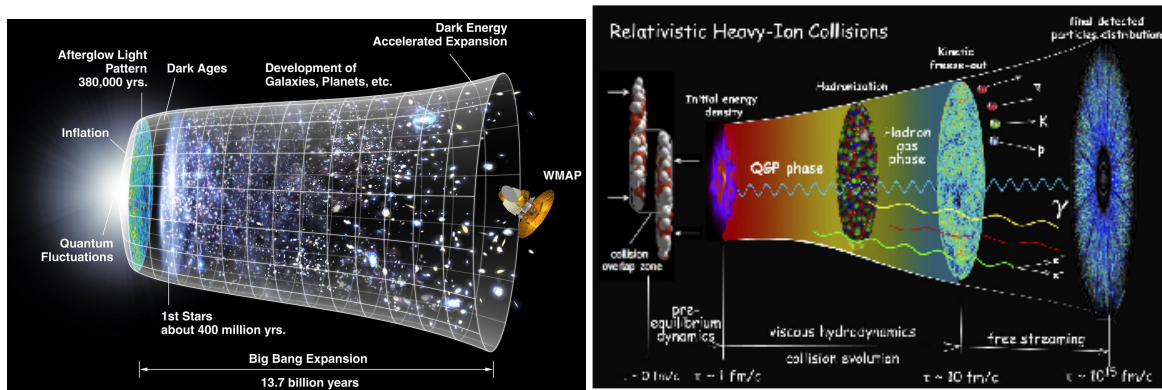


Fig. 10.3: A schematic view of the evolution of the early universe (left) and its similarity to the evolution of a heavy-ion collision (right plot).

10.4 Kinematics

For a particle emitted at an angle θ with respect to the beam axis, the pseudo-rapidity variable is,

$$\eta = -\ln\left(\tan(\theta/2)\right) = 0.5\ln\left(\frac{P + P_z}{P - P_z}\right)$$

Pseudo-rapidity is determined only angle by the emission angle θ . It is a convenient parameter for experimentalists when details of the particle, e.g. mass, momentum etc. are not known, but only the angle of emission is known (for example in emulsion experiments).

When the mass of the particle is known, then one can define the rapidity, given by

$$y = 0.5\ln\left(\frac{E + P_z}{E - P_z}\right) = \tanh^{-1}\left(\frac{P_z}{E}\right)$$

Rapidity has the advantage that it is additive under a longitudinal boost. A particle with rapidity y in a given inertial frame has rapidity $y + dy$ in a frame which moves relative to the first frame with rapidity dy in the z direction. One can see this from the addition formula of relativistic velocity β_1 and β_2 . The resultant velocity is:

$$\beta = \frac{\beta_1 + \beta_2}{1 + \beta_1\beta_2}$$

is also the addition formula for hyperbolic tangents,

$$\tanh(y_1 + y_2) = \frac{\tanh(y_1) + \tanh(y_2)}{1 + \tanh(y_1)\tanh(y_2)}$$

10.5 Centrality

The nucleus, unlike the proton, is an extended object. Accordingly, depending upon the impact parameter of the collision, several types of collision can be defined, e.g. central collision when two nuclei collide head on, peripheral collision when only glancing interaction occur between the two nuclei. System created in a central collision can be qualitatively as well as quantitatively different from the system created in a peripheral collision. Different aspects of reaction dynamics can be understood if heavy ion collisions are studied as a function of impact parameter. Impact parameter of a collision can not be measured experimentally. However, one can have one to one correspondence between impact parameter of the collision and some experimental observable. e.g. particle multiplicity. For example, one can safely assume that multiplicity or transverse energy is a monotonic function of the impact parameter. High multiplicity or transverse energy events are from central collisions and low multiplicity or low transverse energy events are from peripheral collisions. One can then group the collisions according to multiplicity or transverse energy. It can be done quantitatively. Define a minimum bias collision where all possible collisions are allowed. In Fig.6 charged particles multiplicity (N_{ch}) in a minimum bias collision is shown schematically. Minimum bias yield can be cut into successive intervals starting from maximum value of multiplicity. First 5% of the high N_{ch} events corresponds to top 5% or 0-5% collision centrality. Similarly, first 10% of the high N_{ch} corresponds to 0-10% centrality. The overlap region between 0-5% and 0-10% corresponds to 5-10% centrality and so on. Similarly, centrality class can be defined by measuring the transverse energy. Instead of impact parameter, one often defines centrality in terms of number of participating nucleons (the nucleons that undergo at least one inelastic collision) or in terms of binary nucleon collision number. These measures have one to one relationship with impact parameter and can be calculated in a Glauber model.

Glauber model views AA collisions in terms of the individual interactions of constituent nucleons. It is assumed that at sufficient high energy, nucleons carry enough momentum and are undeflected as the nuclei pass through each other. It is also assumed that the nucleons move independently in the nucleus and size is large compared to NN interaction range. The hypothesis of independent linear trajectories of nucleons made it possible to obtain simple analytical expression for nuclear cross section, number of binary collisions, participant nucleons etc. Details of Glauber modelling of heavy ion collisions can be found in [10]. Below, salient features of the model are described. In Fig.7 collisions of two heavy nuclei at impact parameter b is shown. Consider the two flux tubes, (i) located at a displacement s from the centre of target nucleus and (ii) located at a displacement $s-b$ from the centre of the projectile nucleus. During the collision, these two flux tube overlap. Now, for most of the nuclei, density distribution can be conveniently parameterised by a three parameter Fermi function,

$$\rho(r) = \rho_0 \frac{1 + w(r/R)^2}{1 + e^{(r^2/R)/a}}$$

where ρ_0 is the nucleon density, R the radius, a the skin thickness. The parameter w measures the deviation from a spherical shape. In the previous equation, $\rho(r)$ normalised to unity, can be interpreted as the probability to find a given nucleon at a position $r(= x, y, z)$. It follows that

$$T_A(s) = \int dz \rho_A(s, z)$$

is the probability that a given nucleon in the nucleus A (say projectile) is at a transverse distance s . Similarly,

$$T_B(s?b) = \int dz \rho(s - b, z)$$

is the probability that a given nucleon in the target nucleus B is at a transverse distance $(s ? b)$. Then $T_A(s)T_B(s?b)$ is the joint probability that in an impact parameter b collision, two nucleons in target and projectile are in the overlap region. One then defines an overlap function, at impact parameter b as

$$T_{AB}(b) = \int d^2s T_A(s)T_B(s?b)$$

The overlap function is in unit of inverse area and can interpreted as the effective area with which a specific nucleon in A interact with a given nucleon at B. If σ_{NN} is the inelastic cross section, then probability of an inelastic interaction is $\sigma_{NN}T_{AB}(b)$. Now there can be AB interactions between nucleus A and B. The probability that at an impact parameter b there is an interaction can then be written as:

$$P(n, b) = (AB n) (\sigma_{NN} T_{AB}(b))^n (1 - \sigma_{NN} T_{AB}(b))^{AB-n}$$

The first term is the number of combinations for finding n collisions out of AB collisions, the second term is the probability for having n collisions and the third term is the probability that $AB-n$ collisions do not occur. The total probability of an interaction between A and B is then:

$$\frac{d\sigma}{db^2} = \sum_i^{AB} P(n, AB) = 1 - [1 - \sigma_{NN} T_{AB}(b)]^{AB}$$

The total inelastic cross-section is,

$$\sigma_{inel} = \int_0^{\text{inf}} 2\pi b db [1 - (1 - \sigma_{NN} T_{AB}(b))^{AB}] \approx \int_0^{\text{inf}} 2\pi b db [1 - e^{-\sigma_{NN} T_{AB}(b)}]$$

One can then Total number of binary collisions is:

$$N_{coll}(b) = \sum n P(n, b) = (AB) T_{AB}(b) \sigma_{NN}$$

The number of nucleons in projectile and target that interacts is called participant nucleons or the wounded nucleons. One obtains:

$$N_{part}(b) = A \int d^2s T_A(s) [1 - (1 - \sigma_{NN} T_B(b-s))^B] + B \int d^2s T_B(b-s) [1 - (1 - \sigma_{NN} T_A(s))^A]$$

Glauber model calculation of binary collision number or participant number is energy dependent through the inelastic NN cross section σ_{NN} .

In Monte-Carlo Glauber model, individual nucleons are stochastically distributed event-by-event and collision properties are calculated averaging over many events. Optical Glauber model and Monte-Carlo Glauber model give very close results for average quantities like binary collision number or participant numbers. However, in the quantities where fluctuations are important, e.g. participant eccentricity, the results are different. Monte-Carlo Glauber model calculations proceed as follows: (i) nucleons in the colliding nuclei are distributed randomly following the probability distribution $\rho(r)$, (ii) an impact parameter is selected randomly from a distribution $dN/db \approx b$, (iii) assuming the nuclei are moving in the straight line, two nuclei are collided, (iv) if the transverse separation between two colliding nucleons are less than the ball diameter $D = \sqrt{\sigma_{NN}/\pi}$, they are tagged as interacted, and a register, keeping the coordinates of the colliding nucleons is updated.

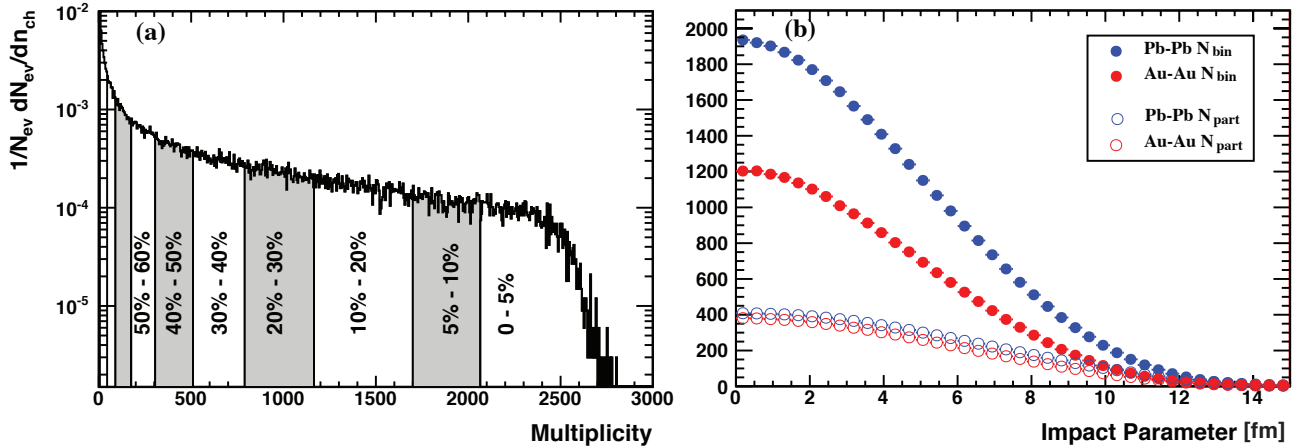


Fig. 10.4: a) Charged particle distribution from Pb-Pb collisions at $\sqrt{s_{NN}} = 2.76$ TeV measured with ALICE, showing a classification in centrality percentiles (from [?]). b) Number of participating nucleons N_{part} and binary collisions N_{bin} versus impact parameter for Pb-Pb and Au-Au collisions at $\sqrt{s_{NN}} = 2.76$ and 0.2 TeV, respectively.

Experimentally, the collision centrality can be inferred from the measured particle multiplicities, given the assumption that the multiplicity is a monotonic function of b . The centrality is then characterised by the fraction, $\pi b^2 / \pi (2R_A)^2$, of the geometrical cross-section with R_A the nuclear radius (see Fig. 10.4-a). Instead of by impact parameter, the centrality is also often characterised by the number of participating nucleons (nucleons that undergo at least one inelastic collision) or by the number of equivalent binary collisions. Phenomenologically it is found that the total particle production scales with the number of participating nucleons whereas hard processes scale with the number of binary collisions. These measures can be related to the impact parameter b using a realistic description of the nuclear geometry in a Glauber calculation, as is shown in fig. 10.4-b. This Figure also shows that Pb-Pb collisions at $\sqrt{s_{NN}} = 2.76$ TeV and Au-Au at $\sqrt{s_{NN}} = 0.2$ TeV have a similar distribution of participating nucleons. The number of binary collisions increases from Au-Au to Pb-Pb by about 50% because the nucleon-nucleon inelastic cross section increases by about that amount at the respective centre of mass energies of 0.2 and 2.76 TeV. Finally, fig. 10.5 gives schematically the correlation between impact parameter and number of particles produced in a peripheral (left) or central (right) collision.

10.6 Key observables

10.6.1 Collective flow

Flow signals the presence of multiple interactions between the constituents of the medium created in the collision. More interactions usually leads to a larger magni-

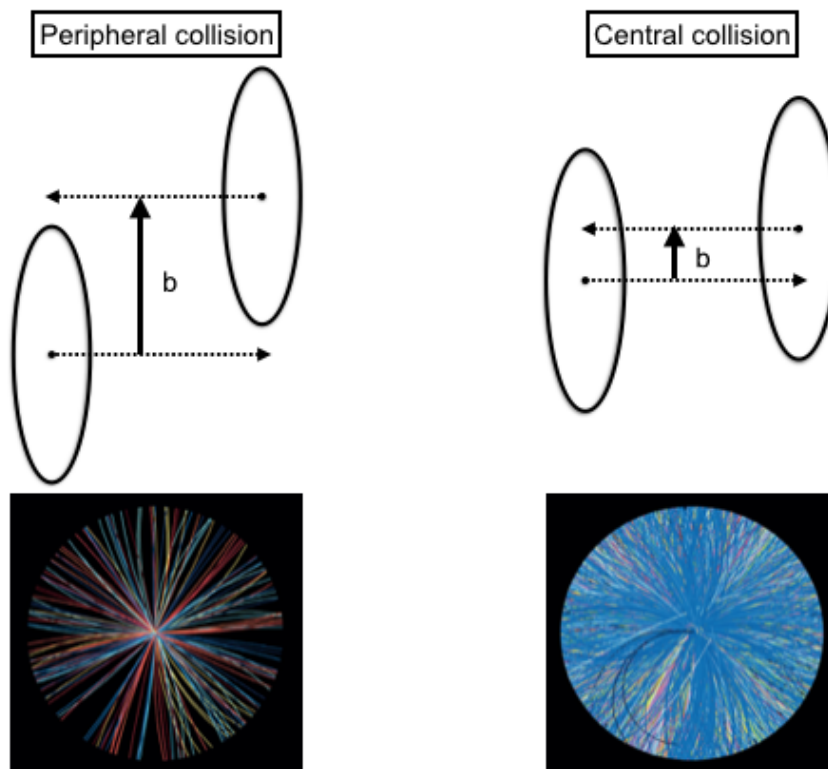


Fig. 10.5: The correlation between impact parameter and number of particles produced in a peripheral (left) or central (right) collision.

tude of the flow and brings the system closer to thermalization. The magnitude of the flow is therefore a detailed probe of the level of thermalization.

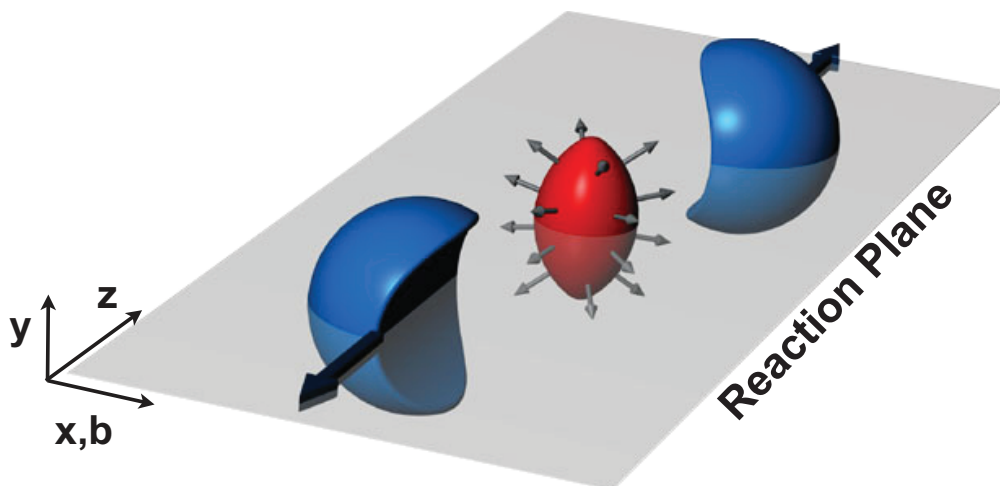


Fig. 10.6: Almond shaped interaction volume after a non-central collision of two nuclei. The spatial anisotropy with respect to the x - z plane (reaction plane) translates into a momentum anisotropy of the produced particles (anisotropic flow).

The theoretical tools to describe flow are hydrodynamics or microscopic transport (cascade) models. In the transport models flow depends on the opacity of the medium, be it partonic or hadronic. Hydrodynamics becomes applicable when the mean free path of the particles is much smaller than the system size, and allows for a description of the system in terms of macroscopic quantities. This gives a handle on the equation of state of the flowing matter and, in particular, on the value of the sound velocity c_s .

Experimentally, the most direct evidence of flow comes from the observation of anisotropic flow which is the anisotropy in particle momentum distributions correlated with the reaction plane. The reaction plane is defined by the impact parameter and the beam direction z (see Fig. 10.6). A convenient way of characterising the various patterns of anisotropic flow is to use a Fourier expansion of the invariant triple differential distributions:

$$E \frac{d^3N}{d^3\mathbf{p}} = \frac{1}{2\pi} \frac{d^2N}{p_t dp_t dy} \left(1 + 2 \sum_{n=1}^{\infty} v_n \cos[n(\varphi - \Psi_{\text{RP}})] \right), \quad (10.6.1)$$

where E is the energy of the particle, p the momentum, p_t the transverse momentum, φ the azimuthal angle, y the rapidity, and Ψ_{RP} the reaction plane angle. The sine terms in such an expansion vanish because of the reflection symmetry with respect to the reaction plane. The Fourier coefficients are p_T and y dependent and are given by

$$v_n(p_T, y) = \langle \cos[n(\varphi - \Psi_{\text{RP}})] \rangle, \quad (10.6.2)$$

where the angular brackets denote an average over the particles, summed over all events, in the (p_T, y) bin under study. In this Fourier decomposition, the coefficients v_1 and v_2 are known as directed and elliptic flow, respectively.

Recently the ALICE Collaboration presented the p_T differential v_2 (i.e. $v_2(p_T)$) of mesons (π^\pm , K^\pm , K_S^0 , ϕ) and baryons (p , Λ , Ξ^- , Ω^- , and their antiparticles) measured in Pb–Pb collisions at $\sqrt{s_{\text{NN}}} = 2.76$ TeV. The results were reported in $|y| < 0.5$, with y the rapidity of each particle, and $0.2 < p_T < 6.0$ GeV/ c . The values of v_2 were obtained with the Scalar Product method, using a pseudo-rapidity gap of $|\Delta\eta| > 0.9$ to suppress correlations not related to the common symmetry plane. The latter are known as non-flow effects and consist of correlations arising from jets or resonance decays and quantum statistics correlations.

Figure 10.7 presents the dependence of v_2 for different particle species on transverse momentum in the 10-20% centrality interval of Pb–Pb collisions at $\sqrt{s_{\text{NN}}} = 2.76$ TeV. For $p_T < 2$ GeV/ c particles are ordered according to their mass i.e. for a fixed value of p_T heavier particles exhibit lower v_2 compared to lighter particles. This ordering is induced by an interplay between radial and elliptic flow that results in a mass dependent lower v_2 . This can be understood considering that radial flow acts over the particle spectra that consist of two components i.e. the thermal part and the part that is affected

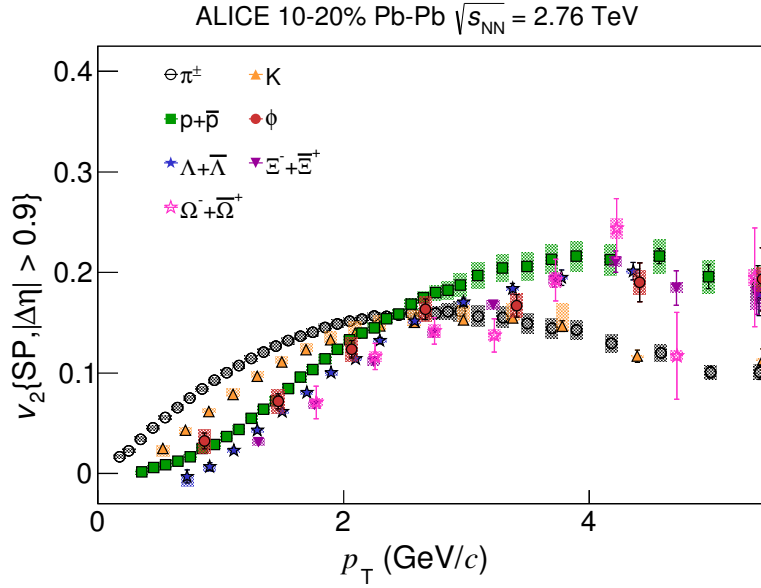


Fig. 10.7: The p_T -differential v_2 for different particle species in the 10-20% centrality interval of Pb–Pb collisions at $\sqrt{s_{NN}} = 2.76$ TeV.

by the expanding medium and is mass dependent. This mass dependent component introduces a depletion in the particle spectrum at low values of p_T , which is more pronounced for heavier particles. In an azimuthally asymmetric system, the pressure gradient and thus the expansion velocity is larger in-plane compared to the out-of-plane direction. This naturally leads to a larger depletion at low values of p_T in the direction of the symmetry plane. Since v_2 quantifies the relative difference of particle yield in-plane versus out-of-plane, this mechanism leads naturally to a reduction of the value of v_2 . When the two effects (i.e. radial flow acting on particle spectra and an azimuthally asymmetric system) are coupled then v_2 becomes lower with increasing mass for a given value of p_T .

10.6.2 Jet quenching

Among all available observables in high-energy nuclear collisions, particles with large transverse momentum and/or mass, $p_T, m \gtrsim Q_0 \gg \Lambda_{QCD}$, where $Q_0 = \mathcal{O}(1 \text{ GeV})$ and $\Lambda_{QCD} \approx 0.2 \text{ GeV}$ is the QCD scale, constitute valuable tools to study tomographically the hottest and densest phases of the reaction (Fig. 10.8). Indeed, such hard probes (i) originate from partonic scatterings with large momentum transfer Q^2 and thus are directly coupled to the fundamental QCD degrees of freedom, (ii) are produced in very short time-scales, $\tau \sim 1/p_T \ll 1/Q_0 \sim 0.1 \text{ fm/c}$, allowing them to propagate through (and be potentially affected by) the medium, and (iii) their cross sections can be theoretically predicted using the perturbative QCD (pQCD) framework.

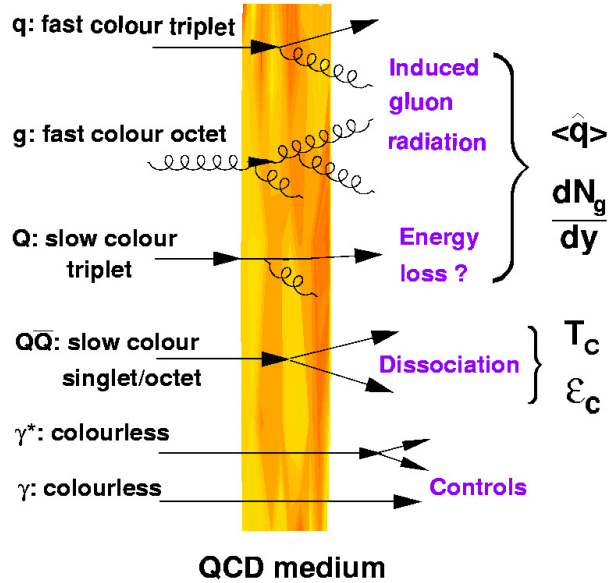


Fig. 10.8: Examples of hard probes whose modifications in high-energy A - A collisions provide direct information on properties of QCD matter such as the transport coefficient $\hat{q}t$, the initial gluon rapidity density dN_g^s/dy , and the critical temperature T_{crit} and energy density ϵ_{crit} .

Jet production in hadronic collisions is a paradigmatic hard QCD process. An elastic ($2 \rightarrow 2$) or inelastic ($2 \rightarrow 2 + X$) scattering of two partons from each one of the colliding hadrons (or nuclei) results in the production of two or more partons in the final-state. At high p_T , the outgoing partons have a large virtuality Q which they reduce by subsequently radiating gluons and/or splitting into quark-antiquark pairs. Such a parton branching evolution is governed by the QCD “radiation probabilities” given by the Dokshitzer-Gribov-Lipatov-Altarelli-Parisi (DGLAP) equations down to virtualities $\mathcal{O}(1 \text{ GeV}^2)$. At this point, the produced partons fragment non-perturbatively into a set of final-state hadrons. The characteristic collimated spray of hadrons resulting from the fragmentation of an outgoing parton is called a “jet”.

One of the first proposed “smoking guns” of QGP formation was “jet quenching” i.e. the attenuation or disappearance of the spray of hadrons resulting from the fragmentation of a parton having suffered energy loss in the dense plasma produced in the reaction (Fig. 10.9). The energy lost by a particle in a medium, ΔE , provides fundamental information on its properties. In a general way, ΔE depends both on the characteristics of the particle traversing it (energy E , mass m , and charge) and on the plasma properties (temperature T , particle-medium interaction coupling α , and thickness L), i.e. $\Delta E(E, m, T, \alpha, L)$. The following (closely related) variables are extremely useful to characterise the interactions of a particle inside a medium:

- the *mean free path* $\lambda = 1/(\rho\sigma)$, where ρ is the medium density ($\rho \propto T^3$ for an ideal gas) and σ the integrated cross section of the particle-medium interaction¹,

¹ One has $\lambda \sim (\alpha T)^{-1}$ since the QED, QCD *screened* Coulomb scatterings are $\sigma_{el} \propto \alpha/T^2$.

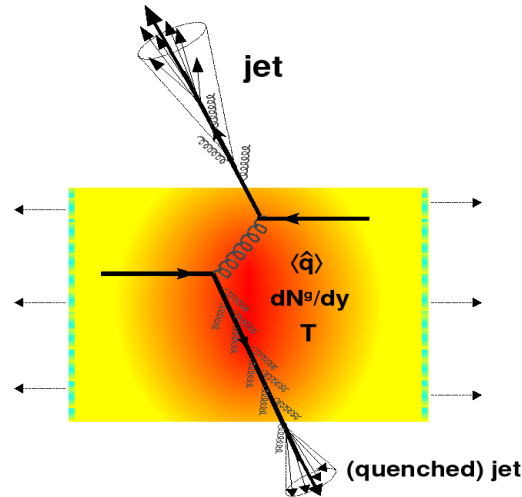


Fig. 10.9: “Jet quenching” in a head-on nucleus-nucleus collision. Two quarks suffer a hard scattering: one goes out directly to the vacuum, radiates a few gluons and hadronises, the other goes through the dense plasma created (characterised by transport coefficient \hat{q} , gluon density dN^g/dy and temperature T), suffers energy loss due to medium-induced gluonstrahlung and finally fragments outside into a (quenched) jet.

- the *opacity* $N = L/\lambda$ or number of scatterings experienced by the particle in a medium of thickness L ,
- the *Debye mass* $m_D(T) \sim gT$ (where g is the coupling parameter) is the inverse of the screening length of the (chromo)electric fields in the plasma. m_D characterises the typical momentum exchanges with the medium and also gives the order of the “thermal masses” of the plasma constituents,
- the *transport coefficient* $\hat{q} \equiv m_D^2/\lambda$ encodes the “scattering power” of the medium through the average transverse momentum squared transferred to the traversing particle per unit path-length. \hat{q} combines both thermodynamical (m_D, ρ) and dynamical (σ) properties of the medium:

$$\hat{q} \equiv m_D^2/\lambda = m_D^2 \rho \sigma . \quad (10.6.3)$$

As a numerical QCD example let us consider an equilibrated *gluon* plasma at $T = 0.4$ GeV and a strong coupling $\alpha_s \approx 0.5$. At this temperature, the particle (energy) density is $\rho_g = 16/\pi^2 \zeta(3) \cdot T^3 \approx 15 \text{ fm}^{-3}$ ($\epsilon_g = 8\pi^2/15 \cdot T^4 \approx 17 \text{ GeV/fm}^3$), i.e. 100 times denser than normal nuclear matter ($\rho = 0.15 \text{ fm}^{-3}$). At leading order (LO), the Debye mass is $m_D = (4\pi\alpha_s)^{1/2}T \approx 1$ GeV. The LO gluon-gluon cross section is $\sigma_{gg} \simeq 9\pi\alpha_s^2/(2m_D^2) \approx 1.5$ mb. The gluon mean free path in such a medium is $\lambda_g = 1/(\rho_g\sigma_{gg}) \simeq 0.45$ fm (the quark mean-free-path is $\lambda_q = C_A/C_F \lambda_g \approx 1$ fm, where $C_A/C_F = 9/4$ is the ratio of gluon-to-quark colour factors). The transport coefficient is therefore $\hat{q} \simeq m_D^2/\lambda_g \simeq 2.2 \text{ GeV}^2/\text{fm}$. Note that such a numerical value has been obtained with a LO expression in α_s for the parton-medium cross section. Higher-order scatterings (often encoded in a “ K -factor” $\approx 2 - 4$) could well result in much larger values of \hat{q} .

- the *diffusion constant* D , characterising the dynamics of *heavy* non-relativistic particles (mass M and speed v) traversing the plasma, is connected, via the Einstein relations

$$D = 2T^2/\kappa = T/(M \eta_D) \quad (10.6.4)$$

to the *momentum diffusion coefficient* κ – the average momentum squared gained by the particle per unit-time (related to the transport coefficient as $\kappa \approx \hat{q}v$) – and the *momentum drag coefficient* η_D .

In a general way, the total energy loss of a particle traversing a medium is the sum of collisional and radiative terms: $\Delta E = \Delta E_{coll} + \Delta E_{rad}$. Depending on the kinematic region, a (colour) charge can lose energy in a plasma with temperature T mainly by two mechanisms:

- **Collisional energy loss** through *elastic* scatterings with the medium constituents dominates at low particle momentum. The *average* energy loss in one scattering (with cross section $d\sigma/dt$, where $t = Q^2$ is the momentum transfer squared) in a medium of temperature T , is:

$$\langle \Delta E_{coll}^{1scat} \rangle \approx \frac{1}{\sigma T} \int_{m_D^2}^{t_{max}} t \frac{d\sigma}{dt} dt . \quad (10.6.5)$$

- **Radiative energy loss** through *inelastic* scatterings within the medium dominates at higher momenta. This loss can be determined from the corresponding single- or double-differential photon or gluon *Bremsstrahlung spectrum* ($\omega dI_{rad}/d\omega$ or $\omega d^2I_{rad}/d\omega dk_{\perp}^2$, where ω, k_{\perp} are respectively the energy and transverse momentum of the radiated photon or gluon):

$$\Delta E_{rad}^{1scat} = \int^E \omega \frac{dI_{rad}}{d\omega} d\omega , \quad \text{or} \quad \Delta E_{rad}^{1scat} = \int^E \int^{k_{T,max}} \omega \frac{d^2I_{rad}}{d\omega dk_{\perp}^2} d\omega dk_{\perp}^2 \quad (10.6.6)$$

For incoherent scatterings one has simply: $\Delta E^{tot} = N \cdot \Delta E^{1scat}$, where $N = L/\lambda$ is the medium opacity. The energy loss per unit length or *stopping power* is:

$$-\frac{dE}{dl} = \frac{\langle \Delta E^{tot} \rangle}{L} , \quad (10.6.7)$$

which for *incoherent* scatterings reduces to: $-dE/dl = \langle \Delta E^{1scat} \rangle / \lambda$.

Experimentally, direct information on the thermodynamical properties (like temperature, energy or particle densities) and transport properties (such as viscosity, diffusivity and conductivity coefficients) of the QGP can be obtained by comparing the results for

a given observable measured in nucleus-nucleus (AA, “QCD medium”) to those measured in proton-proton (pp , “QCD vacuum”) collisions as a function of centre-of-mass (c.m.) energy $\sqrt{s_{nn}}$, transverse momentum p_T , rapidity y , reaction centrality (impact parameter b), and particle type (mass m). Schematically:

$$R_{AA}(\sqrt{s_{nn}}, p_T, y, m; b) = \frac{\text{“hot/dense QCD medium”}}{\text{“QCD vacuum”}} \propto \frac{(dN/dp_T)_{AA}(\sqrt{s_{nn}}, y, m; b)}{(dN/dp_T)_{pp}(\sqrt{s}, y, m)} \quad (10.6.8)$$

Any observed *enhancement* ($R_{AA} > 1$) and/or *suppression* ($R_{AA} < 1$) in this ratio can then be linked to the properties of strongly interacting matter after accounting for a realistic (hydrodynamical) modeling of the space-time evolution of the expanding system of quarks and gluons produced in the collision.

hslash

Appendix A

Units and conversion factors

In particle physics, energy is measured in units of GeV = 10^6 eV, where 1 eV = 1.6×10^{-19} J is the change in kinetic energy of an electron when it traverses a potential difference of one volt. From the relation $E^2 = p^2c^2 + m^2c^4$ it follows that the units of momentum and mass are GeV/c and GeV/c², respectively. The dimension of \hbar is energy×time so that the unit of time is \hbar/GeV ; $\hbar c$ has dimension energy×length so that length has unit $\hbar c/\text{GeV}$.

One often works in a system of units where \hbar and c have a numerical value of one, so that these constants can be omitted in expressions, as in $E^2 = p^2 + m^2$. A disadvantage is that the dimensions carried by \hbar (energy×time) and c (length/time) also disappear but these can always be restored, if necessary, by a dimensional analysis afterward.

Here are some useful conversions.

	Conversion	$\hbar = c = 1$ units	Natural units
Mass	1 kg = 5.61×10^{26}	GeV	GeV/c ²
Length	1 m = 5.07×10^{15}	GeV ⁻¹	$\hbar c/\text{GeV}$
Time	1 s = 1.52×10^{24}	GeV ⁻¹	\hbar/GeV
Charge	$e = \sqrt{4\pi\alpha}$	dimensionless	$\sqrt{\hbar c}$

$$1 \text{ TeV} = 10^3 \text{ GeV} = 10^6 \text{ MeV} = 10^9 \text{ KeV} = 10^{12} \text{ eV}$$

$$1 \text{ fm} = 10^{-15} \text{ m} = 10^{-13} \text{ cm} = 5.07 \text{ GeV}^{-1}$$

$$1 \text{ barn} = 10^{-28} \text{ m}^2 = 10^{-24} \text{ cm}^2$$

$$1 \text{ fm}^2 = 10 \text{ mb} = 10^4 \mu\text{b} = 10^7 \text{ nb} = 10^{10} \text{ pb}$$

$$1 \text{ GeV}^{-2} = 0.389 \text{ mb}$$

$$\hbar c = 197 \text{ MeV fm}$$

$$(\hbar c)^2 = 0.389 \text{ GeV}^2 \text{ mb}$$

$$\alpha = e^2/(4\pi\hbar c) \approx 1/137$$

Appendix B

Covariant notation ($c = 1$)

- Contravariant space-time coordinate: $x^\mu = (x^0, x^1, x^2, x^3) = (t, x)$
- Covariant space-time coordinate: $x_\mu = (x_0, x_1, x_2, x_3) = (t, -x)$
- Contravariant derivative: $\partial^\mu \equiv \partial / \partial x_\mu = (\partial_t, -\nabla)$
- Covariant derivative: $\partial_\mu \equiv \partial / \partial x^\mu = (\partial_t, +\nabla)$
- Metric tensor: $g_{\mu\nu} = g^{\mu\nu} = \text{diag}(1, -1, -1, -1)$
- Index raising/lowering: $a_\mu = g_{\mu\nu} a^\nu$, $a^\mu = g^{\mu\nu} a_\nu$
- Lorentz boost along x -axis:¹ $x'^\mu = \Lambda_\nu^\mu x^\nu$ and $x'_\mu = \Lambda_\mu^\nu x_\nu$

$$\Lambda_\nu^\mu = \Lambda_\mu^\nu = \begin{pmatrix} \gamma & -\gamma\beta & 0 & 0 \\ -\gamma\beta & \gamma & 0 & 0 \\ 0 & 0 & 1 & 0 \\ 0 & 0 & 0 & 1 \end{pmatrix} \quad \gamma = \frac{1}{\sqrt{1-\beta^2}}$$

- Lorentz scalar: $a \cdot b = a^\mu b_\mu = a^0 b_0 - a \cdot b = a_\mu b^\mu$
- $a^2 > 0$ time-like 4-vector \rightarrow possible causal connection
 $a^2 = 0$ light-like 4-vector
 $a^2 < 0$ space-like 4-vector \rightarrow no causal connection
- 4-momentum: $p^\mu = (E, p)$, $p_\mu = (E, -p)$
- Invariant mass: $p^2 = p^\mu p_\mu = p_\mu p^\mu = E^2 - p^2 = m^2$
- Particle velocity: $\gamma = E/m$, $\beta = |p|/E$

¹ This is the relation between the coordinates x^μ of an event observed in a system S and the coordinates x'^μ of that *same* event observed in a system S' that moves with a velocity $+\beta$ along the x -axis of S .

Appendix C

Vector calculus

$$\nabla \times (\nabla \psi) = 0$$

$$\nabla \cdot (\nabla \times A) = 0$$

$$\nabla \times (\nabla \times A) = \nabla(\nabla \cdot A) - \nabla^2 A$$

$$\int_V \nabla \cdot A \, dV = \int_S A \cdot \hat{n} \, dS \quad (\text{Divergence theorem})$$

$$\int_V (\phi \nabla^2 \psi - \psi \nabla^2 \phi) \, dV = \int_S (\phi \nabla \psi - \psi \nabla \phi) \cdot \hat{n} \, dS \quad (\text{Green's theorem})$$

$$\int_S (\nabla \times A) \cdot \hat{n} \, dS = \oint_C A \cdot dl \quad (\text{Stokes' theorem})$$

- In the above, S is a closed surface bounding V , with \hat{n} the outward normal unit vector at the surface element dS .
- In Stokes' theorem, the direction of \hat{n} is related by the right-hand rule to the sense of the contour integral around C .

Appendix D

Maxwell's equations in vacuum

- Maxwell's equations

$$\begin{aligned}\nabla \cdot E &= \rho & \nabla \cdot B &= 0 \\ \nabla \times E + \partial B / \partial t &= 0 & \nabla \times B - \partial E / \partial t &= j\end{aligned}$$

- Continuity equation

$$\nabla \cdot j = -\frac{\partial \rho}{\partial t}$$

- The potentials V and A are defined such that the second and third of Maxwell's equations are automatically satisfied

$$\begin{aligned}B = \nabla \times A & \quad \rightarrow \quad \nabla \cdot B = 0 \\ E = -\partial A / \partial t - \nabla V & \quad \rightarrow \quad \nabla \times E = -\partial B / \partial t\end{aligned}$$

- Gauge transformations leave the E and B fields invariant

$$V' = V + \frac{\partial \lambda}{\partial t} \quad \text{and} \quad A' = A - \nabla \lambda$$

- Maxwell's equations in 4-vector notation

4-vector potential	$A^\mu = (V, A)$
4-vector current	$j^\mu = (\rho, j)$
Electromagnetic tensor	$F^{\mu\nu} = \partial^\mu A^\nu - \partial^\nu A^\mu$
Maxwell's equations	$\partial_\mu F^{\mu\nu} = j^\nu$
Continuity equation	$\partial_\mu j^\mu = 0$
Gauge transformation	$A^\mu \rightarrow A^\mu + \partial^\mu \lambda$

- Lorentz gauge and Coulomb condition

$$\begin{array}{ll} \text{Lorentz gauge} & \partial_\mu A^\mu = 0 \quad \rightarrow \quad \partial_\mu \partial^\mu A^\nu = j^\nu \\ \text{Coulomb condition} & A^0 = 0 \quad \text{or equivalently} \quad \nabla A = 0 \end{array}$$

Appendix E

The Lagrangian in classical mechanics

In classical mechanics, the Lagrangian is the difference between the kinetic and potential energy: $L(q, \dot{q}) \equiv T - V$. The coordinates $q(t) = \{q_1(t), \dots, q_N(t)\}$ fully describe the system at any given instant t . The number N of coordinates is called the **number of degrees of freedom** of the system.

Let the system move from $A(t_1)$ to $B(t_2)$ along some given path. The **action** $S[\text{path}]$ is defined by the integral of the Lagrangian along the path:

$$S[\text{path}] = \int_{t_1}^{t_2} dt L(q, \dot{q})$$

The action S assigns a number to each path and is thus a function of the path. In mathematical terms, S is called a **functional**.

The **principle of least action** states that the system will evolve along the path that minimises the action.

Let $q(t)$ be a path and $q(t) + \delta q(t)$ be some deviating path between the *same* points $A(t_1)$ and $B(t_2)$. That is, $\delta q(t_1) = \delta q(t_2) = 0$. The variation in the action is then given by

$$\delta S = \int_{t_1}^{t_2} dt \delta L(q, \dot{q}) = \int_{t_1}^{t_2} dt \left(\frac{\partial L}{\partial q} \delta q + \frac{\partial L}{\partial \dot{q}} \delta \dot{q} \right) \stackrel{\text{I want}}{=} 0.$$

Because

$$\frac{d}{dt} \left(\frac{\partial L}{\partial \dot{q}} \delta q \right) = \left(\frac{d}{dt} \frac{\partial L}{\partial \dot{q}} \right) \delta q + \left(\frac{\partial L}{\partial \dot{q}} \right) \delta \dot{q},$$

we find, by partial integration,

$$\delta S = \int_{t_1}^{t_2} dt \left(\frac{\partial L}{\partial q} - \frac{d}{dt} \frac{\partial L}{\partial \dot{q}} \right) \delta q + \int_{t_1}^{t_2} d \left(\frac{\partial L}{\partial \dot{q}} \delta q \right) \stackrel{\text{I want}}{=} 0.$$

The second integral vanishes because $\delta q(t_1) = \delta q(t_2) = 0$.

The first integral vanishes for all δq if and only if the term in brackets vanishes, leading to the **Euler-Lagrange equations**, for N degrees of freedom:

$$\frac{\delta S}{\delta q_i} = \frac{d}{dt} \left(\frac{\partial L}{\partial \dot{q}_i} \right) - \frac{\partial L}{\partial q_i} = 0 \quad i = 1, \dots, N$$

Solving the EL equations for a given Lagrangian lead to the **equations of motion** of the system.

Appendix F

The Hamiltonian in classical mechanics

If L does not explicitly depend on time we have for the time derivative

$$\frac{dL}{dt} = \frac{\partial L}{\partial \dot{q}} \ddot{q} + \frac{\partial L}{\partial q} \dot{q}$$

Substituting $\partial L / \partial q$ from the Euler-Lagrange equations gives

$$\frac{dL}{dt} = \frac{\partial L}{\partial \dot{q}} \ddot{q} + \frac{d}{dt} \left(\frac{\partial L}{\partial q} \right) \dot{q} = \frac{d}{dt} \left(\frac{\partial L}{\partial \dot{q}} \dot{q} \right) \rightarrow \frac{d}{dt} \left(\frac{\partial L}{\partial \dot{q}} \dot{q} - L \right) = 0$$

The term in brackets is the **Legendre transform** of L and is called the **Hamiltonian**:

$$H \stackrel{\text{def}}{=} \frac{\partial L}{\partial \dot{q}} \dot{q} - L = p\dot{q} - L \quad \text{with} \quad p \stackrel{\text{def}}{=} \frac{\partial L}{\partial \dot{q}},$$

where we have also introduced the **canonical momentum** p . The Hamiltonian is identified with the total energy $E = T + V$ which is thus conserved in the time evolution of the system. This is an example of a conservation law.

In the Lagrangian, the dependence on \dot{q} resides in the kinetic energy term T while the dependence on q is contained in the potential energy V . Thus if $V = 0$ (or a constant) we have in the EL equations

$$\frac{\partial L}{\partial q} = 0 \quad \rightarrow \quad \frac{d}{dt} \left(\frac{\partial L}{\partial \dot{q}} \right) = \frac{dp}{dt} = 0$$

Thus the momentum p is conserved in a system that is not under the influence of an external potential. This is another example of a conservation law.

The Hamiltonian equations of motion are

$$\dot{q} = \frac{\partial H}{\partial p} \quad \text{and} \quad \dot{p} = -\frac{\partial H}{\partial q}$$

This can be derived as follows. Consider the total differential

$$dL = \frac{\partial L}{\partial q}dq + \frac{\partial L}{\partial \dot{q}}d\dot{q}$$

Now

$$\frac{\partial L}{\partial q} = \dot{p} \text{ (from EL), } \quad \frac{\partial L}{\partial \dot{q}} = p \text{ (by definition),}$$

and thus, using $p d\dot{q} = d(p\dot{q}) - \dot{q}dp$, we obtain

$$dL = \dot{p}dq + d(p\dot{q}) - \dot{q}dp \quad \rightarrow \quad d(p\dot{q} - L) = dH = \dot{q}dp - \dot{p}dq,$$

from which the Hamiltonian equations immediately follow.

Appendix G

Dirac δ -function

- The Dirac δ -function can be defined by¹

$$\delta(x) = \begin{cases} 0, & \text{if } x \neq 0 \\ \infty, & \text{if } x = 0 \end{cases} \quad \text{with} \quad \int_{-\infty}^{\infty} \delta(x) dx = 1$$

- Generalisation to more dimensions is trivial, like $\delta(r) \equiv \delta(x)\delta(y)\delta(z)$.
- For $x \rightarrow 0$ we may write $f(x)\delta(x) = f(0)\delta(x)$ so that

$$\int_{-\infty}^{\infty} f(x)\delta(x) dx = f(0) \quad \text{and} \quad \int_{-\infty}^{\infty} f(x)\delta(x-a) dx = f(a)$$

- For a linear transformation $y = k(x-a)$ we have

$$\delta(y) = \frac{1}{|k|} \delta(x-a)$$

This is straight-forward to prove by showing that $\delta(y)$ satisfies the definition of the δ -function given above.

- Likewise, if $\{x_i\}$ is the set of points for which $f(x_i) = 0$, then it is easy to show by Taylor expansion around the x_i that

$$\delta[f(x)] = \sum_i \frac{1}{|f'(x_i)|} \delta(x-x_i)$$

- There exist many representations of the δ -function, for instance,

$$\delta(r) = \frac{1}{(2\pi)^3} \int e^{ik \cdot r} d^3k \quad \text{or} \quad \delta(x) = \frac{d\theta(x)}{dx},$$

$$\text{with} \quad \theta(x) = \begin{cases} 0, & \text{for } x < 0 \\ 1, & \text{for } x \geq 0 \end{cases} \quad (\text{Heaviside step function}).$$

¹ A more rigorous mathematical definition is usually in terms of a limiting sequence of functions.

Appendix H

Green functions

- Let Ω be some linear differential operator. A **Green function** of the operator Ω is a solution of the differential equation

$$\Omega G(r) = \delta(r)$$

These Green functions can be viewed as some potential caused by a point source at r .

- Once we have the Green function we can immediately solve the differential equation for any source density $s(r)$

$$\Omega \psi(r) = s(r)$$

By substitution it is easy to see that (ψ_0 is the solution of $\Omega \psi_0 = 0$)

$$\psi(r) = \psi_0(r) + \int G(r - r')s(r') dr'$$

Here it is clearly seen that $G(r - r')$ ‘propagates’ the contribution from the source element $s(r')dr'$ to the potential $\psi(r)$.

- A few well-known Green functions are ...

$$\begin{aligned} \nabla^2 G(r) &= \delta(r) & G(r) &= -1/(4\pi r) \\ (\nabla^2 + k^2) G(r) &= \delta(r) & G^\pm(r) &= -\exp(\pm ikr)/(4\pi r) \\ (\nabla^2 - m^2) G(r) &= \delta(r) & G(r) &= -\exp(-mr)/(4\pi r) \end{aligned}$$

- ... and here are their Fourier transforms

$$\begin{aligned} G(r) &= -1/(4\pi r) & \tilde{G}(q) &= -1/q^2 \\ G^+(r) &= -\exp(ikr)/(4\pi r) & \tilde{G}^+(q) &= 1/(k^2 - q^2 + i\epsilon) \\ G(r) &= -\exp(-mr)/(4\pi r) & \tilde{G}(q) &= -1/(q^2 + m^2) \end{aligned}$$

Appendix I

Non-relativistic scattering theory I

- Classical relation $E = p^2/2m + V$ with substitution $E \rightarrow i\partial/\partial t$ and $p = -i\nabla$ gives the Schroedinger equation

$$i\frac{\partial}{\partial t}\psi(r,t) = -\left[\frac{\nabla^2}{2m} - V(r,t)\right]\psi(r,t)$$

- Separate $\psi(r,t) = \phi(t)\psi(r)$. Dividing through by $\phi\psi$ gives

$$\frac{i\partial_t\phi(t)}{\phi(t)} = -\frac{[\nabla^2 - 2mV(r,t)]\psi(r)}{2m\psi(r)}$$

Assume now that V does not depend on t . The left and right-hand side must then be equal to a constant, say E , and we have

$$\frac{\partial\phi(t)}{\partial t} = -iE\phi(t) \quad \rightarrow \quad \phi(t) = e^{-iEt}$$

$$[\nabla^2 + k^2]\psi(r) = 2mV(r)\psi(r)$$

where we have set $k^2 = 2mE$. Using Green functions we get

$$\psi(r) = \psi_0(r) - \frac{m}{2\pi} \int \frac{e^{ik|r-r'|}}{|r-r'|} V(r')\psi(r')dr'$$

- For large $r \gg r'$ we have $|r-r'| \approx r - \hat{r}r'$ so that

$$\psi(r) = \psi_0(r) - \frac{m}{2\pi} \frac{e^{ikr}}{r} \int e^{-ik\hat{r}r'} V(r')\psi(r')dr'$$

- We set $k' \equiv k\hat{r}$ and write, formally,

$$\psi(r) = \psi_0(r) + f(k') \frac{e^{ikr}}{r} \quad \text{with} \quad f(k') \equiv -\frac{m}{2\pi} \int e^{-ik'r'} V(r')\psi(r')dr'$$

The function $f(k')$ is called the **scattering amplitude**.

Appendix J

Non-relativistic scattering theory II

- An incoming plane wave $\psi_{\text{in}} = Be^{ikz}$ describes beam particles moving along the z axis with momentum k . The wave function is normalised such that $\rho = \psi^* \psi = |B|^2$ is the particle density (number of particles per unit volume). The current density is

$$j_{\text{in}} = \frac{1}{2mi}(\psi^* \nabla \psi - \psi \nabla \psi^*) = |B|^2 \frac{k}{m} = \rho \frac{k}{m} = \rho v$$

with v the velocity of the particle. The number of beam particles passing per second through an area A is $R_{\text{in}} = \rho v A = |j_{\text{in}}| A$. Likewise, the number of scattered particles that pass per second through an area $r^2 d\Omega$ is $R_{\text{sc}} = |j_{\text{sc}}| r^2 d\Omega$.

- We now imagine a hypothetical area $d\sigma$ such that the number of beam particles that pass through that area is equal to the number of particles that scatter in the solid angle $d\Omega$. We then have, by definition, $|j_{\text{in}}| d\sigma = |j_{\text{sc}}| r^2 d\Omega$, or

$$\boxed{\frac{d\sigma}{d\Omega} = \frac{r^2 |j_{\text{sc}}|}{|j_{\text{in}}|}}$$

The quantity $d\sigma/d\Omega$ is called a **differential cross section**.

- For our scattered wave $\psi_{\text{sc}} = f(k') e^{ikr}/r$ we find

$$j_{\text{sc}} = \frac{1}{2mi} \left(\psi^* \frac{\partial \psi}{\partial r} - \psi \frac{\partial \psi^*}{\partial r} \right) = |f(k')|^2 \frac{k}{mr^2}$$

and thus

$$\boxed{\frac{d\sigma}{d\Omega} = |f(k')|^2}$$

where we have assumed $\rho = 1$ and $k_{\text{sc}} = k_{\text{in}}$ (elastic scattering).

Appendix K

Non-relativistic scattering theory III

- Recall that for scattering on a potential, the outgoing wave is

$$\psi_{\text{out}}(r) = \psi_0(r) + f(k') \frac{e^{ikr}}{r}$$

with

$$f(k') \equiv -\frac{m}{2\pi} \int e^{-ik'r'} V(r') \psi_{\text{out}}(r') dr'$$

Here k' is the momentum vector of the scattered particle.

- The problem now is that ψ_{out} occurs on both sides of the equation above. A first order approximation is achieved by setting in the scattering amplitude $\psi_{\text{out}} \approx \psi_{\text{in}} = e^{ikz} = e^{ikr}$. This gives

$$f(k, k') \equiv -\frac{m}{2\pi} \int e^{i(k-k')r'} V(r') dr' = -\frac{m}{2\pi} \int e^{-iqr'} V(r') dr'$$

where we have set the momentum transfer $q \equiv k' - k$. In this so-called **Born approximation**, the scattering amplitude $f(k, k') \equiv f(q)$ is thus the Fourier transform of the potential.

- Example: Yukawa potential $V(r) = Q_1 Q_2 e^{-ar} / r$

$$f(q) = -\frac{mQ_1Q_2}{2\pi} \int \frac{e^{-ar'}}{r'} e^{-iqr'} dr' = \dots = \frac{2mQ_1Q_2}{q^2 + a^2}$$

$$\frac{d\sigma}{d\Omega} = |f(q)|^2 = \left[\frac{2mQ_1Q_2}{q^2 + a^2} \right]^2$$

- Example: Coulomb potential $V(r) = Q_1 Q_2 / r$ set $a = 0$ above:

$$\frac{d\sigma}{d\Omega} = \left[\frac{2mQ_1Q_2}{q^2} \right]^2 = \left[\frac{Q_1Q_2}{2mv^2 \sin^2(\theta/2)} \right]^2$$

This is the famous formula for **Rutherford scattering**.

Appendix L

Dirac's bra-ket notation I

- A state vector ψ_α can be represented by a column vector of complex numbers in a Hilbert space and is denoted by the ket $|\alpha\rangle$. To each ket is associated a bra vector $\langle\alpha|$ in a dual Hilbert space. This bra is represented by the conjugate transpose ψ_α^\dagger , that is, by the row vector of complex conjugates. The operation of **Hermitian conjugation** turns a bra into a ket and *vice versa*

$$|\alpha\rangle^\dagger = \langle\alpha| \quad \text{and} \quad (c|\alpha\rangle)^\dagger = \langle\alpha|c^* \quad (c \text{ any complex number})$$

Note that the Hermitian conjugate of a c-number is the complex conjugate. The inner product $\psi_\alpha^\dagger \cdot \psi_\beta$ is denoted by $\langle\alpha|\beta\rangle$ and is a c-number so that

$$\langle\beta|\alpha\rangle \equiv \langle\alpha|\beta\rangle^\dagger = c^\dagger = c^* = \langle\alpha|\beta\rangle^*$$

- An operator O transforms a ket $|\alpha\rangle$ into another ket, say $|\gamma\rangle$. The operator and its Hermitian conjugate are then defined by

$$O|\alpha\rangle = |\gamma\rangle \quad \text{and} \quad \langle\alpha|O^\dagger = \langle\gamma|$$

Multiplying from the left with $\langle\beta|$ and from the right with $|\beta\rangle$ we find the relation between the **matrix elements** of O and O^\dagger

$$\begin{aligned} O_{\beta\alpha} &\equiv \langle\beta|O|\alpha\rangle = \langle\beta|\gamma\rangle \\ O_{\alpha\beta}^\dagger &\equiv \langle\alpha|O^\dagger|\beta\rangle = \langle\gamma|\beta\rangle = \langle\beta|\gamma\rangle^* = \langle\beta|O|\alpha\rangle^* = O_{\beta\alpha}^* \end{aligned}$$

- An operator for which $O = O^\dagger$ is called **self-adjoint** or **Hermitian**. Observable quantities are always represented by Hermitian operators. Indeed, the **expectation value** $\langle\alpha|O|\alpha\rangle$ is then real, as it should be, since

$$\langle\alpha|O|\alpha\rangle \equiv \langle\alpha|O^\dagger|\alpha\rangle = \langle\alpha|O|\alpha\rangle^*$$

Appendix M

Dirac's bra-ket notation II

- An orthonormal basis is written as $|e_i\rangle$ with $\langle e_i|e_j\rangle = \delta_{ij}$. On this basis, a state $|\alpha\rangle$ is given by the linear combination

$$|\alpha\rangle = \sum_i |e_i\rangle \langle e_i|\alpha\rangle$$

The operator $|e_i\rangle\langle e_i|$ is called a **projection operator**, for obvious reasons. The **closure relation** reads $\sum_i |e_i\rangle\langle e_i| = 1$

- We denote the wave function $\psi_\alpha(r)$ by $\langle r|\alpha\rangle$ and its Hermitian conjugate $\psi_\alpha^\dagger(r)$ by $\langle\alpha|r\rangle$. In particular, the wave function of a momentum eigenstate is $\langle r|k\rangle \propto e^{ikr}$.
- For the complete set of states $|r\rangle$ the closure relation reads

$$\int |r\rangle\langle r| dr = 1$$

From this, we nicely recover the expression for the inproduct of two wave functions

$$\langle\alpha|\beta\rangle = \int \langle\alpha|r\rangle\langle r|\beta\rangle dr = \int \psi_\alpha^*(r)\psi_\beta(r) dr$$

that of the delta function

$$\delta(k-k') = \langle k'|k\rangle = \int \langle k'|r\rangle\langle r|k\rangle dr \propto \frac{1}{(2\pi)^3} \int e^{i(k-k')r} dr$$

and also that of Fourier transforms

$$\psi(k) = \langle k|\psi\rangle = \int \langle k|r\rangle\langle r|\psi\rangle dr \propto \int e^{-ikr}\psi(r) dr$$

Appendix N

Dirac equation

- Dirac equation:

$$i\gamma^\mu \partial_\mu \psi - m\psi = 0$$

$$\underbrace{(\not{p} - m)u = 0}_{\text{particle in}}, \quad \underbrace{\bar{u}(\not{p} - m) = 0}_{\text{particle out}}, \quad \underbrace{(\not{p} + m)v = 0}_{\text{antiparticle out}}, \quad \underbrace{\bar{v}(\not{p} + m) = 0}_{\text{antiparticle in}}$$

$$\bar{\psi} = \psi^\dagger \gamma^0, \quad \not{a} = \gamma^\mu a_\mu$$

- Pauli matrices:

$$\sigma_x = \begin{pmatrix} 0 & 1 \\ 1 & 0 \end{pmatrix}, \quad \sigma_y = \begin{pmatrix} 0 & -i \\ i & 0 \end{pmatrix}, \quad \sigma_z = \begin{pmatrix} 1 & 0 \\ 0 & -1 \end{pmatrix}$$

$$\sigma_i \sigma_j = \delta_{ij} + i\epsilon_{ijk} \sigma_k, \quad \sigma_i^\dagger = \sigma_i = \sigma_i^{-1}, \quad [\sigma_i, \sigma_j] = 2\epsilon_{ijk} \sigma_k$$

$$(a \cdot \sigma)(b \cdot \sigma) = a \cdot b + i\sigma \cdot (a \times b)$$

$$\exp(i\theta \cdot \sigma) = \cos |\theta| + i(\hat{\theta} \cdot \sigma) \sin |\theta|$$

- Dirac matrices:

$$\gamma^0 = \begin{pmatrix} 1 & 0 \\ 0 & -1 \end{pmatrix}, \quad \gamma^i = \begin{pmatrix} 0 & \sigma_i \\ -\sigma_i & 0 \end{pmatrix}, \quad \gamma^5 = i\gamma^0\gamma^1\gamma^2\gamma^3 = \begin{pmatrix} 0 & 1 \\ 1 & 0 \end{pmatrix}$$

$$\gamma^{0\dagger} = \gamma^0, \quad \gamma^{i\dagger} = -\gamma^i, \quad \gamma^0 \gamma^\mu \gamma^{0\dagger} = \gamma^\mu$$

$$\{\gamma^\mu, \gamma^\nu\} = 2g^{\mu\nu}, \quad \{\gamma^\mu, \gamma^5\} = 0, \quad (\gamma^5)^2 = 1$$

Appendix O

Traces

Using Casimir's identity reduces the calculation of a complicated matrix element to a calculation of the trace of a complicated product of γ -matrices. This algebra is facilitated by a number of theorems which will be listed here for your convenience.

- For three matrices A, B, C and a is a scalar:
 - $\text{Tr}(A + B) = \text{Tr}(A) + \text{Tr}(B)$
 - $\text{Tr}(aA) = a\text{Tr}(A)$
 - $\text{Tr}(AB) = \text{Tr}(BA)$
 - $\text{Tr}(ABC) = \text{Tr}(CAB) = \text{Tr}(BCA)$
- $g_{\mu\nu}g^{\mu\nu} = 4$
- Contraction theorems
 - $\gamma_{\mu}\gamma^{\mu} = 4$
 - $\gamma_{\mu}\gamma^{\nu}\gamma^{\mu} = -2\gamma^{\nu}$
 - $\gamma_{\mu}\not{a}\gamma^{\mu} = -2\not{a}$
 - $\gamma_{\mu}\gamma^{\nu}\gamma^{\lambda}\gamma^{\mu} = 4g^{\nu\lambda}$
 - $\gamma_{\mu}\not{a}\not{b}\gamma^{\mu} = -4(ab)$
 - $\gamma_{\mu}\gamma^{\nu}\gamma^{\lambda}\gamma^{\sigma}\gamma^{\mu} = -2\gamma^{\sigma}\gamma^{\lambda}\gamma^{\nu}$
 - $\gamma_{\mu}\not{a}\not{b}\not{c}\gamma^{\mu} = -2\not{c}\not{b}\not{a}$
- Trace theorems
 - The trace of the product of odd number of γ -matrices is 0
 - $\text{Tr}(I) = 4$
 - $\text{Tr}(\gamma^{\mu}\gamma^{\nu}) = 4g^{\mu\nu}$
 - $\text{Tr}(\not{a}\not{b}) = 4(ab)$

- $\text{Tr}(\gamma^\mu \gamma^\nu \gamma^\lambda \gamma^\sigma) = 4(g^{\mu\nu} g^{\lambda\sigma} - g^{\mu\lambda} g^{\nu\sigma} + g^{\mu\sigma} g^{\nu\lambda})$
- $\text{Tr}(\not{a}\not{b}\not{c}\not{d}) = 4[(ab)(cd) - (ac)(bd) + (ad)(bc)]$
- Since $\gamma^5 = i\gamma^0\gamma^1\gamma^2\gamma^3$ i.e. the product of even number of γ -matrices, then $\text{Tr}(\gamma^5\gamma^\mu) = \text{Tr}(\gamma^5\gamma^\mu\gamma^\nu\gamma^\lambda) = 0$
 - $\text{Tr}(\gamma^5) = 0$
 - $\text{Tr}(\gamma^5\gamma^\mu\gamma^\nu) = 0$
 - $\text{Tr}(\gamma^5\not{a}\not{b}) = 0$
 - $\text{Tr}(\gamma^5\gamma^\mu\gamma^\nu\gamma^\lambda\gamma^\sigma) = 4i\varepsilon^{\mu\nu\lambda\sigma}$
 - $\text{Tr}(\gamma^5\not{a}\not{b}\not{c}\not{d}) = 4i\varepsilon^{\mu\nu\lambda\sigma}a_\mu b_\nu c_\lambda d_\sigma$

In the previous:

$$\varepsilon^{\mu\nu\lambda\sigma} = \begin{pmatrix} -1 & \text{if } \mu\nu\lambda\sigma \text{ is an even permutation of } 0123 \\ +1 & \text{if } \mu\nu\lambda\sigma \text{ is an odd permutation of } 0123 \\ 0 & \text{if any two indices are the same} \end{pmatrix}$$